PROPAGATION AND BIT ERROR RATE MEASUREMENTS IN THE MILLIMETRE WAVE BAND ABOUT 60GHz.

by

A.R. Tharek, BSc. MSc.

A thesis submitted to the University of Bristol in accordance with the requirements for the degree of Doctor of Philosophy in the Faculty of Engineering, Electrical and Electronic Department

June, 1988

TO MY PARENTS, MY WIFE NAURAH, MY DAUGHTERS ZAHIRAH, MUNIRAH, SALWA AND MUSHIRAH, AND MY SON ANAS.

ABSTRACT

This thesis describes the propagation and bit error rate measurements that have been conducted at 60GHz. The outdoor propagation measurements have been conducted in different environments to study the envelope fading distribution, the propagation power law with distance, and the obstruction and diffraction effects. Indoor propagation measurements have also been conducted in different areas within a reinforced concrete building. They include the envelope fading distribution, the propagation power law with distance, signal coverage measurements, and diffraction measurements. Also within buildings, bit error rate measurements were conducted using non-coherent FSK modulation at 240 and 480kbit/sec.

The results indicate that for a usable signal level outdoors, a line-of-sight path is required between the transmitter and receiver. This is because the reflection and diffraction losses are too high. Indoor results have indicated that communications within a room with a single radio distribution port is feasible. This is due to the shorter propagation distances and large number of reflectors which can provide a high signal level behind obstructions.

The results of the bit error rate measurements have indicated that when no line-of-sight path existed, the bit error rate closely followed the theoretical curve for Rayleigh fading. However, when a line-of-sight path existed, it departed from the theoretical curve. No irreducible error rate occurred, which indicated that time delay spreading and doppler spreading had negligible effects.

ACKNOWLEDGEMENTS

I wish to express my gratitude to my supervisor, Professor J.P. McGeehan, for his invaluable help, guidance and continuous encouragement during the course of this research.

I would like to thank John Curtis for designing the RF circuitry, the data generator/error detector and for his help throughout the project. Also, I would like to thank Geoff Reed for checking the thesis. I am grateful to the technicians in the Electronic workshop and friends and colleagues in the Communications Research Group for their help.

I would like to thank the Science and Engineering Research Council, UK, for providing a substantial Research Grant towards this work. In addition, I am most grateful to the University of Technology Malaysia and the Malaysian Government for their award of my research studentship.

Finally, I would have found this work impossible without the moral support and sacrifice of my wife and four daughters.

AUTHOR'S DECLARATION

The work described in this thesis was carried out by the author at the University of Bath, in the School of Electrical and Electronic Engineering between October 1984 and September 1985 and at the University of Bristol, in the Department of Electrical and Electronic Engineering between October 1985 and January 1988.

All work and ideas in this thesis are original unless otherwise ackowledged in the text or by reference. The work was performed by the author without collaboration.

(A. R. Tharek)

CONTENTS

ABBREVIATIONS

A/D	Analogue to Digital Converter.
AFC	Automatic Frequency Control.
AGC	Automatic Gain Control.
AM	Amplitude Modulation.
ASK	Amplitude Shift Keying
BER	Bit Error Rate
CDF	Cumulative Distribution Function.
CSO	Central Switching Office.
D/A	Digital to Anologue Converter.
dB	Decibel.
DC	Direct Current
DPSK	Differential Phase Shift Keying.
FET	Field Effect Transistor.
FM	Frequency Modulation.
FRP	Fixed Radio Port.
FSK	Frequency Shift Keying.
GaAs	Gallium Arsenide.
Hz	Hertz.
HF	High Frequency.
IF	Intermediate Frequency.
ITU	International Telecommunication Union.
LDN	Local Distribution Network.
LOS	Line-of-sight.
MIC	Microwave Integrated Circuit.
MMIC	Monolithic Microwave Integrated Circuit.
MSK	Minimum Shift Keying.

NCFSK	Non-coherent Frequency Shift Keying.
OQPSK	Offset Quadrature Phase Shift Keying.
RF	Radio Frequency.
PBX	Private Branch Exchange.
PDF	Probability Density Function.
PRBS	Pseudo Random Binary Sequence
PSK	Phase Shift Keying
PSTN	Public Switched Telephone Network.
QPSK	Quadrature Phase Shift Keying
SNR	Signal to Noise ratio.
UHF	Ultra High Frequency.
V	Volts.
VCO	Voltage Controlled Oscillator.
VHF	Very High Frequency.
WGN	White Gaussian Noise.

LIST OF SYMBOLS

A	amplitude of a single-path signal.
a_0	obstruction attenuation factor.
A_0	obstruction attenuation factor (dB)
b	average power received by an isotropic aerial
b_0	mean received signal power.
B	total bandwidth.
B_n	noise bandwidth.
c	speed of light.
d	distance between the transmitter and receiver
E	signal energy per bit.
erfc(x)	complementry error function.
E_z	electric field component.
f	frequency.
f_t,f_c	transmission frequency.
f_d	doppler shift.
f_e	bit error frequency.
f_m	maximum doppler shift.
f_p	peak frequency deviation of FSK.
f_r	received frequency.
f_s	bit rate.
F	noise figure (dB).
F(u)	field strength (relative to freespace due to diffraction).
G_r	receiver aerial gain.
G_t	transmitter aerial gain.
h_t	height of transmitter.
h_r	height of receiver.
$I_0(x)$	modified Bessel function of first kind

k	Boltzman constant (1.38×10^{-23} J/K)
K(x)	complete elliptic integral of the first kind.
k_0	oxygen attenuation (nepers/m)
K_0	oxygen attenuation (dB/km)
k_r	rain attenuation (nepers/m)
K_r	rain attenuation (dB/km)
N	number of cells per cluster
N_0	noise power spectral density in Hz.
N_r	received noise power.
N(R)	number of level crossings below R.
Pe	Probability of error.
P_n	noise power.
P_t	transmitted power.
P_r	received power.
P(x)	Cumulative distribution of x.
p(x)	probability density function of x.
R_i	distance between the centres of the closest co-channel cells.
R_0	maximum distance from cell centre to cell boundary.
R_r	received signal
r,R	signal envelope.
S	channel bandwidth.
T	bit period.
T_a	aerial noise temperature (K)
T_m	time delay spread.
t	time
u	fresnel parameter.
v	mobile speed.
λ	wavelength.

γ	instantaneous SNR
Γ	mean SNR
ω	angular frequency (rad/s).
θ	angle of arrival of incoming wave relative to direction of motion of mobile.
ϕ	angle between the incident wave and surface.
σ	standard deviation of surface irregularities.

CHAPTER ONE

INTRODUCTION

At present, land mobile radio systems are becoming popular to the extent of saturating the available frequency bands. For example, the number of mobile radios in use in 1984 was about 540,000 with a growth rate of about 10% per annum in the UK, and an estimated growth rate of up to 20% has been made for other European countries. Using these figures, there will be an estimated 1 million users by 1990 and 2.5 million users by the end of this century in the UK [1].

The demand for mobile radio services has increased rapidly over the past decade and the demand for their use has always exceeded the available system capabilities. Since the early days, as the demand increased, the solution to the spectrum congestion was to increase to higher frequencies and to reduce the channel spacing [2]. Today, there are mobile radio services operating at 800-900MHz with a channel spacing of 25kHz. However, as the demand increases, decreasing the channel spacing is soon limited.

An alternative solution is to reuse the available radio channels a number of times at different locations to enable the efficient use of the allocated spectrum. This leads to the introduction of the cellular mobile radio systems which provide the solution at least temporarily for the present problem of spectrum congestion. This system has been used in Japan since 1979, in Sweden since 1982 and in the USA and UK since 1985. However, due to the rapid acceptance of these cellular mobile radio systems, it has been predicted that the growth rate could be as high as 20% per annum in the UK which would lead to 13 million users by the year 2000 [3].

Basically, the cellular radio system is designed to work with vehicular equipment which typically transmit power levels in the order of one to several watts. It only partially satisfies portable communication needs and furthermore, it requires tall towers for the base stations to provide a wide coverage area and the number of users in a given area for a given band of frequencies is limited.

In order to provide portable communications which could be used both within buildings and outdoors, universal digital portable communication systems have been proposed at 900MHz [4]. These systems would operate using low power portable hand sets which could be carried anywhere within the service areas. The system would use fixed radio distribution ports (low power base stations) attached to a telephone network.

The popularity of the cordless telephone and cellular mobile radio clearly demonstrates the demand for cordless portable communications. Therefore, in future, due to the increase in demand for portable and mobile communications, spectrum congestion will occur again within the allocated frequency bands below 1GHz. In order to reduce the problem of spectrum congestion, research is now being concentrated on ways of improving spectral efficiency through efficient modulation techniques and systems. However, if this is achieved by the end of the century, severe spectrum congestion will occur again within the allocated frequency bands no matter what modulation is used. There will be insufficient channels to cope with the increase in the number of users, particularly if higher data rate communication links are required. Therefore, the only solution to this spectrum congestion is to use higher frequency bands above 1GHz wherever available which could provide large amounts of bandwidth.

A region of the radio spectrum is being sought which could accommodate a large number of users and wideband services especially in the usual demand 'hot spots' where most of the people spend their time such as shopping centres, city centres, public transport terminals, office blocks, factories and major road and motorway intersections. One such region is the millimetric waveband around 60GHz for providing integrated personal communications and a wide range of digital services to mobile users and data terminals. Currently, much interest has been generated concerning the use of this band for mobile communication [5] and establishing in future, local cellular radio network (LCRNs) which could provide a broad range of wideband services in both urban and suburban areas [6]. Furthermore, this band has the potential for interference-free frequency re-use at a few kilometres separation and the potential for small size moderate gain aerials. However, this frequency band is unsuitable for long range communications because of the 10 to 16db/km attenuation due to oxygen absorption. With recent advances in Gallium Arsenide (GaAs) technology and signal processing, the use of 60GHz in broadband short range point-to-point links is also the subject of much investigation at the moment[7]. There are also several other applications at 60GHz such as wideband local radio networks and intersatellite links[8].

As in other areas of communication systems, detailed knowledge of the propagation characteristics of 60GHz transmission are required before comprehensive system studies can be undertaken with any degree of confidence. At 60GHz, there is currently very little propagation data available [9,10]. The work described here, which is the subject of this thesis, is concerned with propagation measurements conducted both within buildings and outdoors in order to determine the narrowband propagation characteristics. The method of measurements were designed to simulate the type of usage expected from the integrated portable communication systems

operating at 60GHz. Also, within buildings, the bit error rate performance using FSK through a 60GHz radio link under fading and non-fading conditions was measured.

REFERENCES

[1] Matthews, P.A. "Communication on the move," Electronic and Power, July 1984, pp.513-518.

[2] Jakes, W.C., "Microwave mobile communications," John Wiley 1974.

[3] McGeehan, J.P., and Yates, K.W., "High-capacity 60GHz Microcellular Mobile Radio Systems," Telecommunication September 1986,pp 58-92.

[4] Cox, D.C., "Universal Digital Portable Radio Communications," Proc. of the IEEE, Vol. 75, No. 4, April 1987, pp.436-477.

[5] Steele, R., "Towards a high-capacity digital cellular mobile radio systems," IEE Proc. Vol. 132, Pt. F, No.5, August 1985, pp.409-415.

[6] Walke, B. and Brunchle, R., "A local cellular radio network (LCRN) for digital voice and data transmission at 60GHz," Proc. of 'Cellular and Mobile Communications Intl.' Online Publications (Pinner), 1985, pp.215-225.

[7] Blake, R.G., "The use of millimetre-waves for broadband local distribution," Conf. Proc. 17th European Microwave Conference 7th -11th September 1987.

[8] Anzic, G., "A study of 60GHz intersatellite link applications," Proc. IEEE Int. Conf. on Communications Progress CICC '83 Boston and USA, June, 1983 pp.1181-1188.

[9] Alexader, S.E. and Pugliese, G., "A 60GHz radio system for propagation studies in buildings," Proc. Int. Conf. on Antenna and Propagation, ICAP83, Norwich, UK, 1983.

[10] Chia, S.T.S., Greenwood, D.R., Rickard, D.C., Shepherd, C.A. and Steele, R., "Propagation studies for a point-to-point 60GHz microcellular system for urban environments," COMS 86, Birmingham, 1986, pp.21-32.

CHAPTER TWO

COMMUNICATIONS AT 60 GHz

Given the congestion in the mobile radio frequency bands below 1GHz, there is currently significant interest in the millimetric waveband around 60GHz for providing integrated personal communications and a wide range of digital services to mobile users and data terminals. Furthermore, with recent advances in Gallium Arsenide (GaAs) technology and signal processing, the use of 60GHz in broadband short-range point-to-point links is also the subject of much investigation at the moment.[1] However, this frequency band is unsuitable for long range communications because of the 10 to 16dB/km attenuation due to oxygen absorption. This chapter describes the millimetre wave spectrum and the possible applications at 60GHz.

2.1 MILLIMETRE-WAVE SPECTRUM

As the propagation frequency is increased above 1GHz, wider bandwidths are available, but most of the lower part of the gigahertz band is already occupied by other communication systems such as analog and digital radio relay systems [2]. Fig. 2.1 shows the frequencies already allocated to fixed and mobile communication systems by the International Telecommunication Union (ITU)[3]. In the millimetre bands more frequency spectrum is unused particularly at frequencies where high atmospheric absorption occurs. These frequency bands offer large unexploited bandwidths which could accommodate a large number of users.

At millimetre-wave frequencies, the high attenuation due to gas molecules and precipitation present in the atmosphere could restrict their use for long range terrestrial communication links. When an electromagnetic field is incident on the

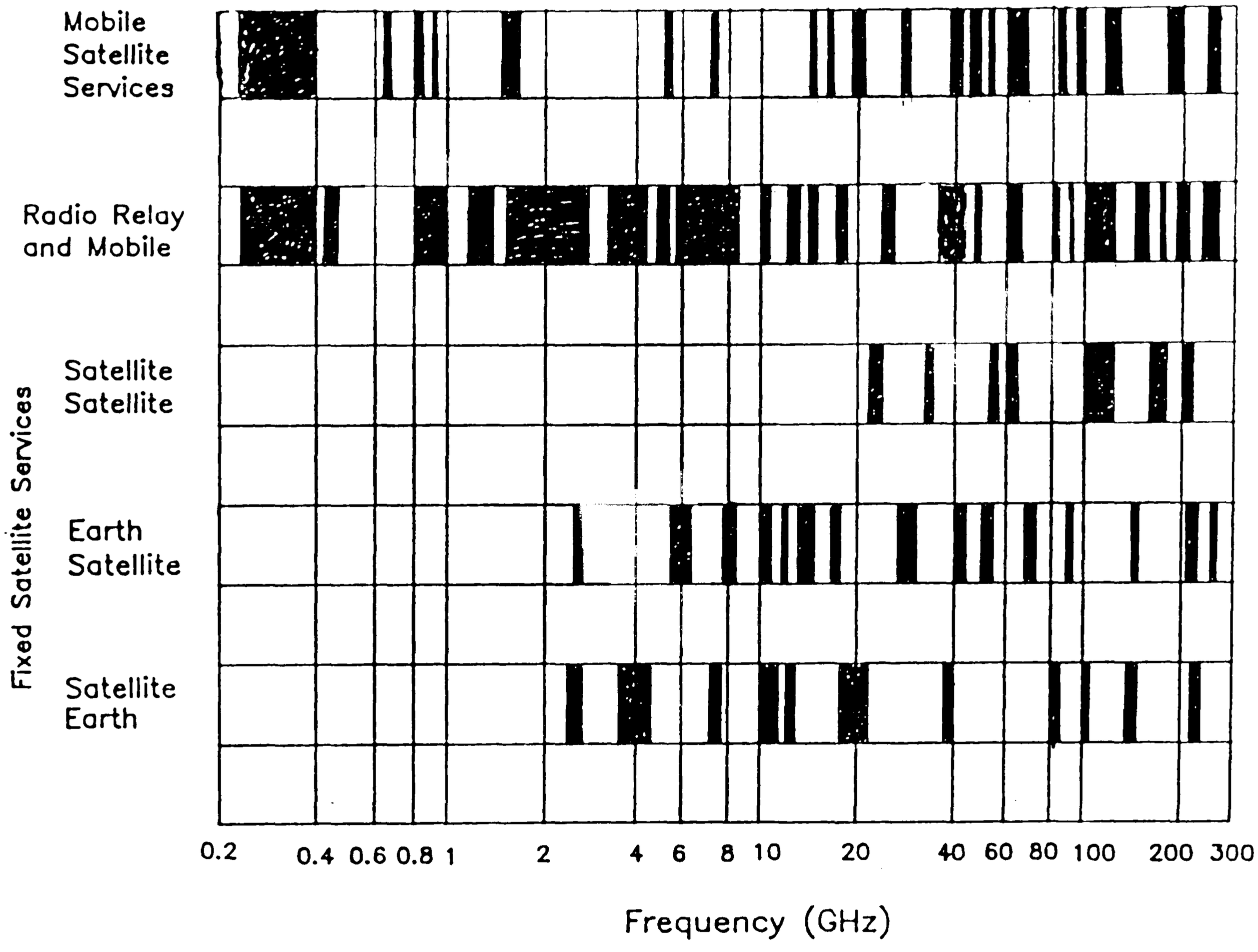

Fig.2.1 Frequency allocations for Microwave Communications Systems.

molecules of oxygen, water vapour or rain, a change in their total angular momentum causes transitions between their energy states [4]. For oxygen molecules, these transitions are found in the range from about 50 to 70GHz and result in the absorption of a broad range of frequencies centred at 60GHz (band A1) and also a narrow range centred at 118GHz (band A2). For horizontal radio paths, fig. 2.2 [5] shows the oxygen absorption at various altitudes for a standard atmosphere. At sea level, the air pressure causes all the absorption lines to merge to form a continuous absorption spectrum with the maximum absorption at the centre of the band, while at high altitudes, where the air pressure is low, the individual absorption lines are resolvable, each being a few megahertz wide. The attenuation is as high as 16dB/km at 60GHz due to oxygen absorption.

Fig. 2.3 shows the atmospheric attenuation versus frequency. For band A1, the attenuation due to oxygen absorption reaches a peak value and the attenuation due to water vapour is a minimum when compared to band A2 [6]. For a moderately humid atmosphere at the earth's surface, the attenuation due to water vapour for a horizontal radio path varies from 0.1 to 0.2dB/km for frequencies between 50 to 70GHz, which is insignificant compared to the oxygen attenuation. Therefore, band A1 is more preferable for communications systems than band A2, especially at 60GHz where peak oxygen absorption occurs. The 60GHz oxygen absorption spectrum is quite stable with time since it does not depend on weather conditions, making it a useful frequency range for applications requiring a high attenuation beyond the normal service area to reduce co-channel interference. On the other hand, bands with absorption peaks due to water vapour, which occurs at 22GHz and 200GHz, are very dependent on weather conditions, so should be avoided.

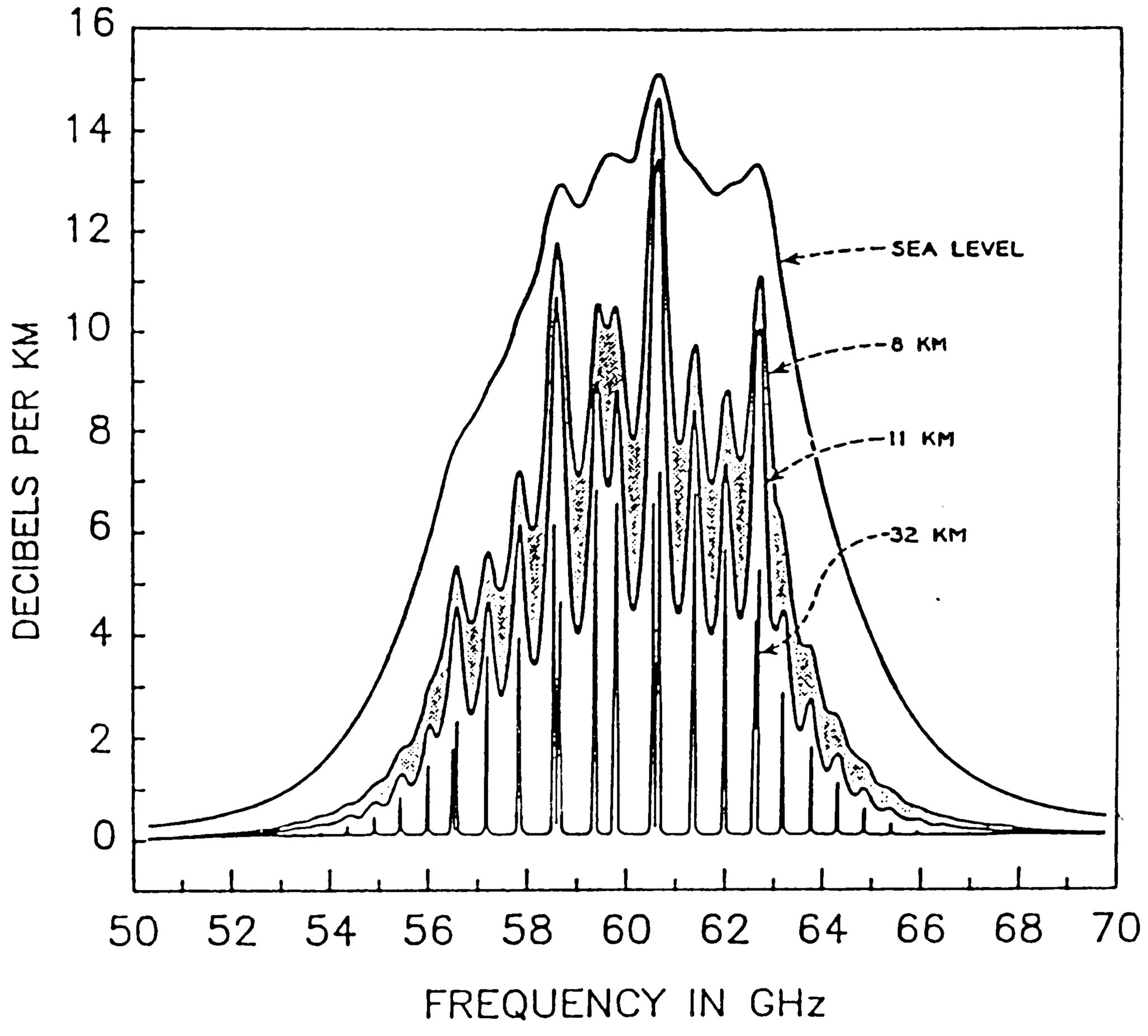

FIG. 2.2 OXYGEN ABSORPTION AT VARIOUS ALTITUDES FOR A STANDARD ATMOSPHERE

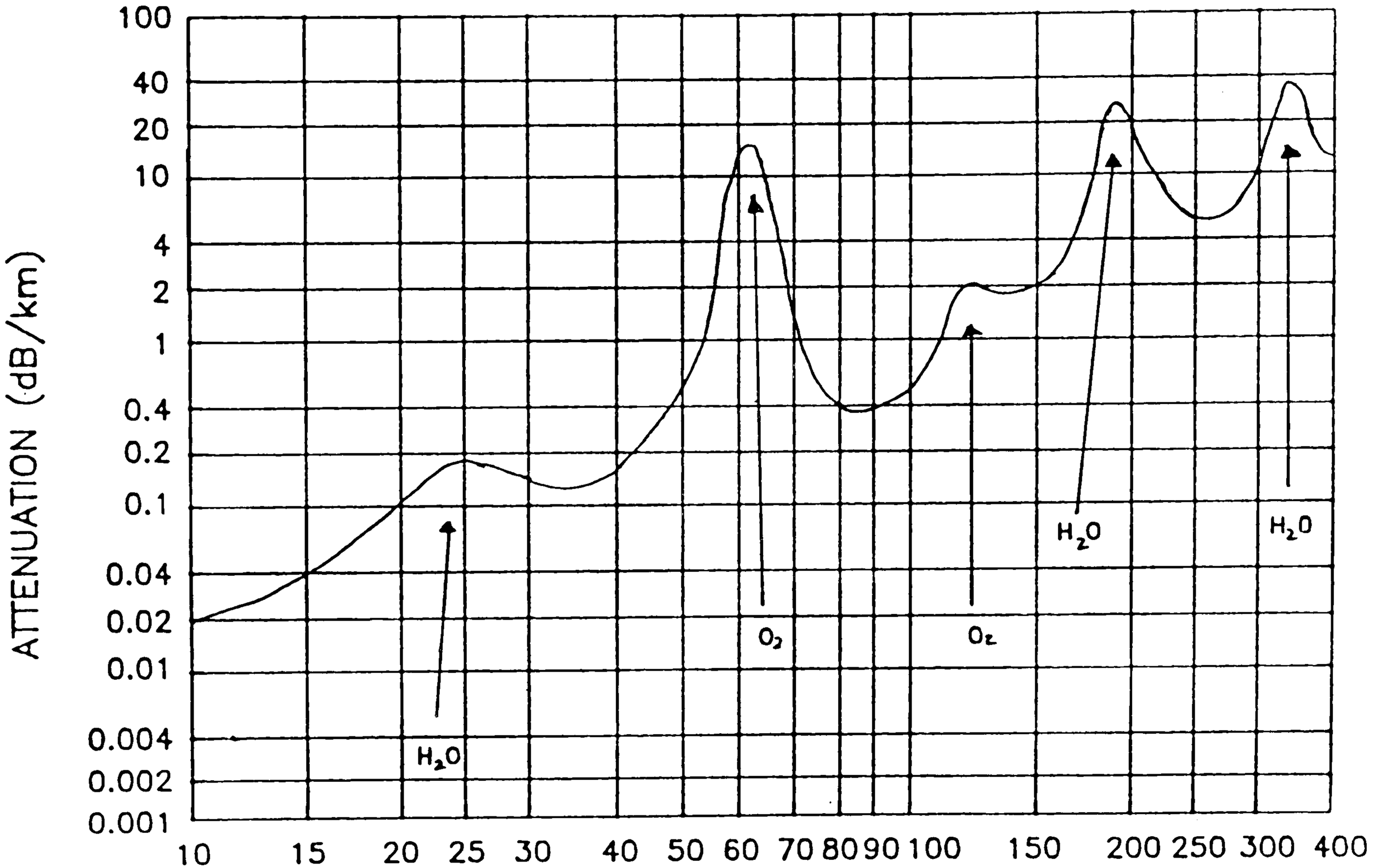

FIG. 2.3 AVERAGE ATMOSPHERIC ABSORPTION OF MILLIMETRE WAVES (HORIZONTAL PROPAGATION)

Rain attenuates and scatters radiowaves causing rapid phase and amplitude fluctuations and signal depolarisation. The estimation of rain attenuation is well documented in the literature [6,7]. At centimetre and millimetre wave frequencies, Bodtman and Ruthroff [7] have computed the rain attenuation coefficients for different rainfall rates and their results are shown in figure 2.4. From this, it can be seen that rain attenuation increases with both frequency and rain rate. This attenuation is about 10dB/km for 25mm/h of rain at 60GHz. During very heavy rain, the extra attenuation can equal or exceed the oxygen absorption at 60GHz. Also at 60GHz, Dietrich and Delango [6] have measured the rain attenuation for the year 1970 over a 1.03km long path at Holmdel, New Jersey. Their experimental results along with the computed outage time for which the rain attenuation exceeds a certain level are shown in figure 2.5. About 99.9% of the time, rain attenuation is less than or equal to 9dB. One way of combatting this extra attenuation due to rain is to simply over-design the system.

2.2 MILLIMETRE-WAVE TECHNOLOGY

Microwave and millimetre wave equipment is benefiting from higher levels of component integration in micro-strip, fin-line and semiconductor chip technologies as well as from material advances. In the millimetre region [8], alumina has been introduced as the substrate material for microwave integrated circuits (MIC's). Systems for high capacity millimetre wave transmission through a low loss waveguide are also being constructed [9].

Several significant developments have been reported on millimetre wave devices. For example, there is a continued advance of various forms of Field Effect transistors (FET's) to achieve higher gains, higher power outputs, and low noise figures at higher frequencies so that they can be successfully used as oscillators,

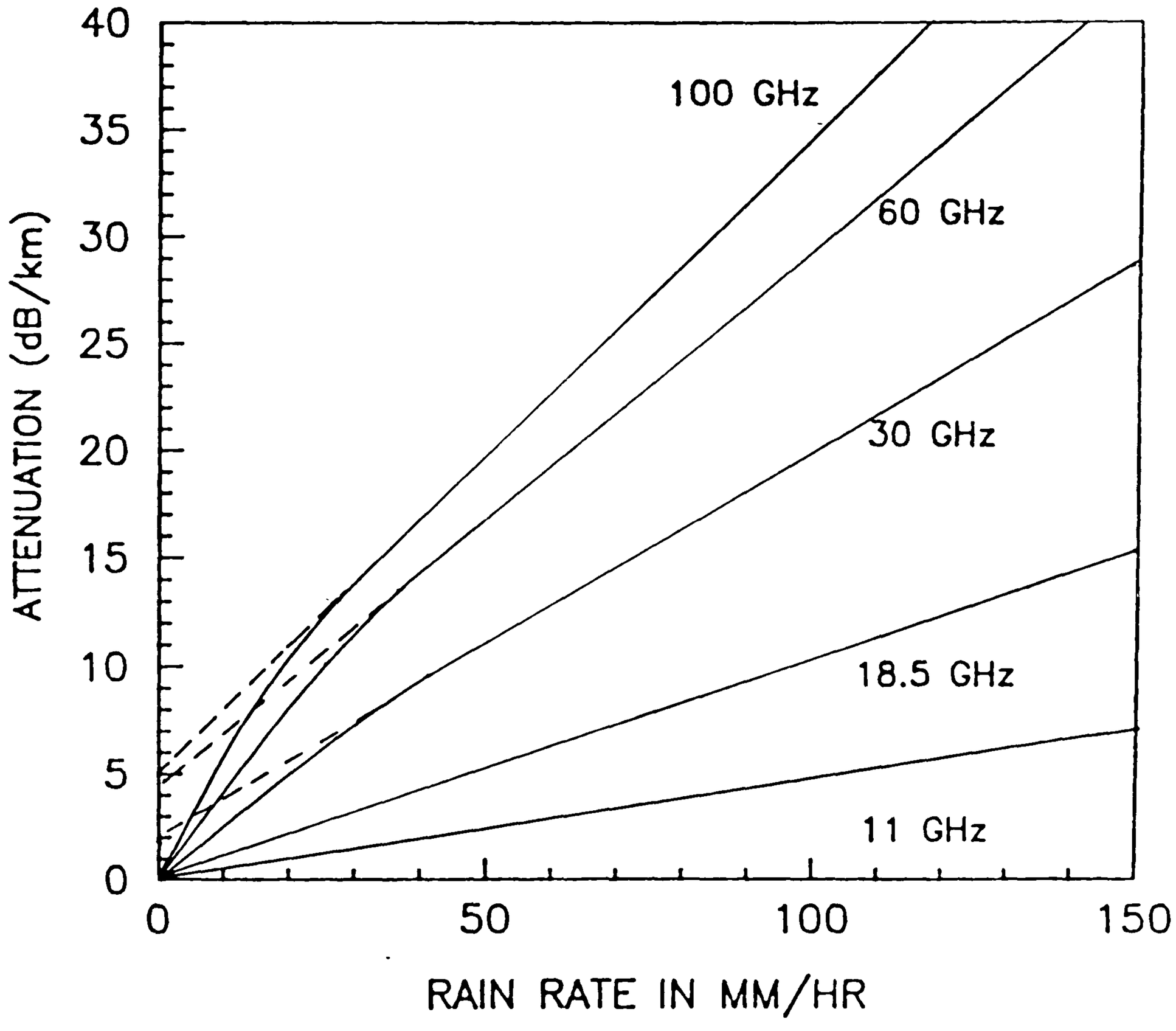

FIG. 2.4 COMPUTED ATTENUATION AS A FUNCTION OF RAIN RATE AND FREQUENCY.

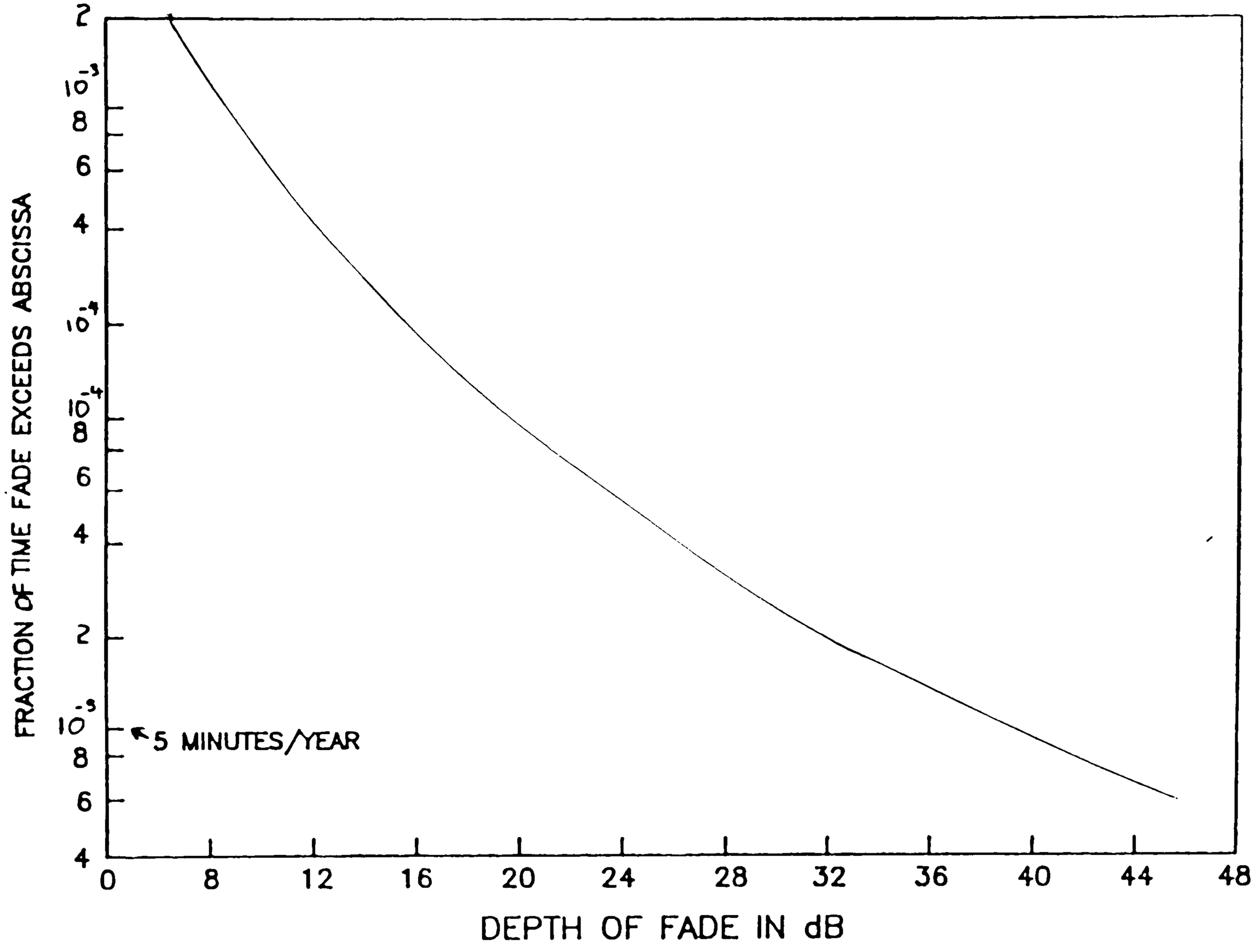

FIG. 2.5 DISTRIBUTION OF RAIN ATTENUATION (1970)

power amplifiers and low noise amplifiers. Previously, microwave oscillators and amplifiers have been based on one port devices such as Gunn or IMPATT diodes. At microwave frequencies, these generally have lower efficiencies as oscillators and power amplifiers, and higher noise figures as low noise amplifiers when compared to Gallium Arsenide Field Effect Transistors (GaAs FET's). At the moment however, GaAs FET's lose these advantages above about 30GHz, although this frequency is being continually increased with the use of smaller gate lengths. A gate length of 0.25μm has been developed which has resulted in gains of about 5dB from 55 to 62GHz with noise figures of about 7dB at 60GHz [10]. Different transistor structures and materials other than GaAs have been proposed which are believed to be able to offer even better performance. These FET advances are being incorporated into monolithic microwave integrated circuits (MMIC's) formed on semi-insulating GaAs to achieve very wide bandwidth performance [11]. Future communication systems operating at 60GHz are expected to require MMIC technology for the transmitter and receiver. Monolithic transmitters and receivers are already under development at 20 and 30GHz and in time, should be available at 60GHz.

At present, low-noise balanced mixer-preamplifiers are available for full coverage of the 40-60GHz and 50-75GHz wavebands. Improved receiver designs [12] at 55, 100 and 205GHz have achieved noise figures of 5dB, 7dB and 9.5dB with conversion losses of 2.9dB, 7.2dB and 9.5dB respectively.

Advances in technology have now permitted the construction of compact transmitting and receiving systems for communication applications. The compactness of the RF components (aerial, transmitter and receiver) at millimetre wave frequencies reduces the size and weight of the equipment. A millimetric front end transceiver could be attached, for example, to a lamp post for applications such as

outdoor portable communication systems. Equipment costs at millimetre wave frequencies are still comparatively high, although advances in solid state technology and innovative design will reduce these costs in the future [13].

2.3 DESCRIPTION OF CELLULAR RADIO

In cellular systems, the total allocated spectrum is divided into a number of channels. Each set of channnels is allocated to several users in different locations or cells, separated by a distance known as the re-use distance such that the co-channel interference is kept to a minimum. As the demand increases, the number of channels assigned to a cell becomes insufficient to provide the required grade of service. To overcome this problem, the congested cells can be subdivided into smaller cells (i.e. cell splitting), the aerial height and transmitted power of the new base station can be reduced and the channel sets can be re-allocated in a similar manner as before. As the cell size decreases, practical limitations on the overall system performance increase such as the handover rate between adjacent base stations as the mobile crosses through the cells. Also, the requirement to keep the co-channel interference to a minimum becomes a problem. The number of available channels per cell is given by [14]

$$\text{Number of channel/cell} = \frac{B}{NS} \qquad (2.1)$$

where B is the total bandwidth, N is the number of cells per cluster and S is the channel bandwidth.

Fig 2.6 demonstrates a cell pattern for N = 7 along with the set of co-channel cells assuming a hexagonal layout. If the operational range, Ro, is the maximum distance from the cell centre to the cell boundary, and the interference

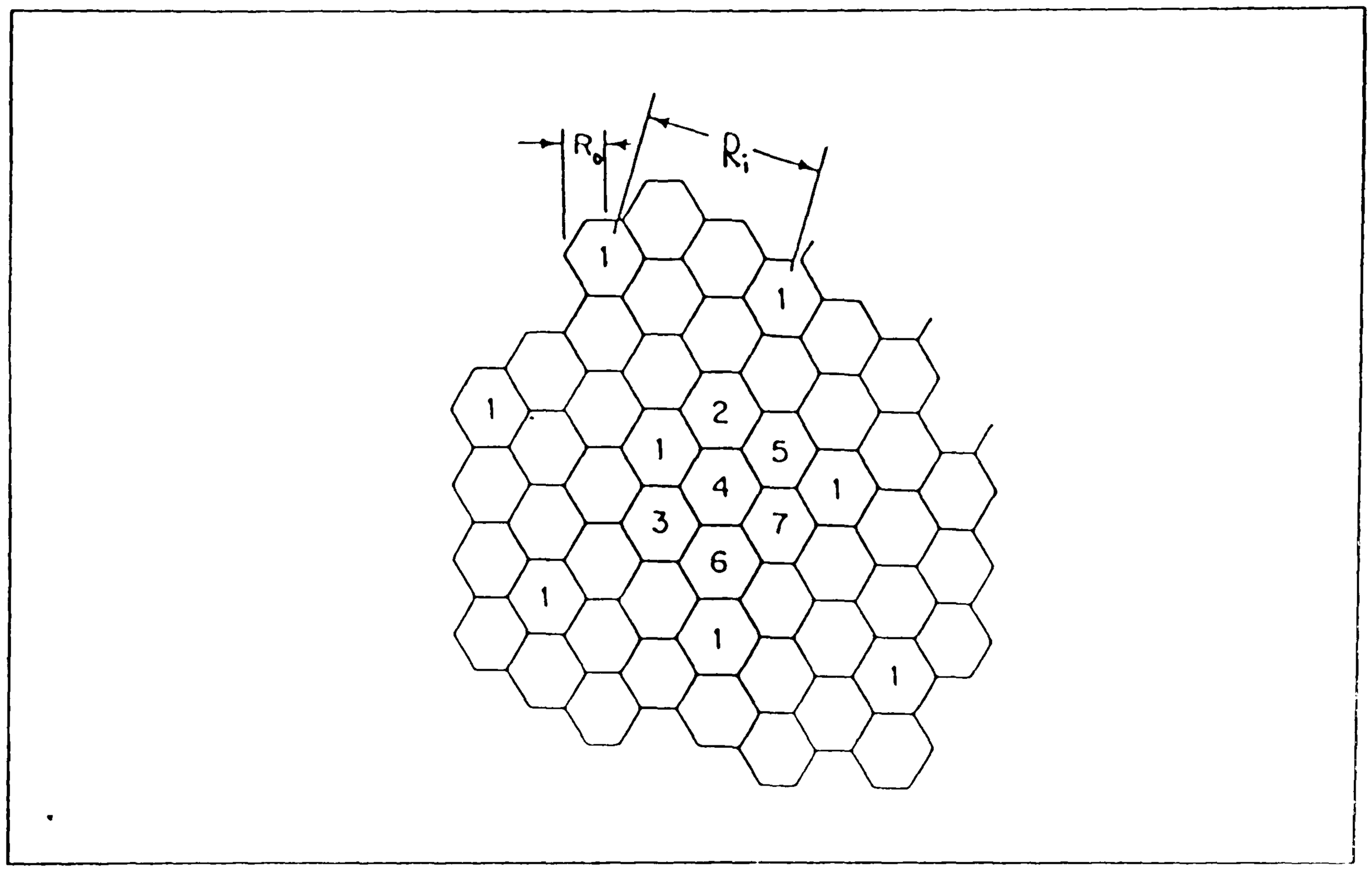

FIG. 2.6 HEXAGONAL CELL GEOMETRY WITH N=7

range, Ri, is the distance between the centres of the closest co-channel cells, then the cochannel reuse distance is given by [14]

$$\frac{R_i}{R_0} = \sqrt{3N} \qquad (2.2)$$

2.4 PORTABLE COMMUNICATION SYSTEMS

2.4.1 Introduction

Portable communication systems have been proposed in the literature at 60GHz by Steele [15], and generally by Cox [16]. In the future, integrated portable communication systems operating at 60GHz could be accomplished by using a radio link at the end of the telephone loop, so that the 60GHz mobile links would be an integrated part of the telephone distribution network. They would offer nationwide coverage, access to a Public Switched Telephone Network (PSTN) and the ability for the users to move from one place to another. This is the only effective way of communicating with people on the move for the transmission of data and speech within restricted areas both within buildings and outdoors. Every communication terminal, eg a portable telephone, a computer terminal etc, would communicate with a fixed radio port by a short distance, high capacity, low power mobile radio link. Many portable handsets and data terminals could communicate simultaneously from a single distribution port.

In this integrated portable communication system, multi-channel distribution ports need to be connected to a central switching office (CSO) for switching of voice and data and for controlling the channel allocation of the ports. Since the coverage area of the multichannel distribution ports would be small at 60GHz due to its limited transmission range, the probability of the portable users moving from one service area to another is high. Therefore, the strength of the signal in the existing

service area would have to be constantly monitored over the channels by the central switching office and compared with the standard level of the signal strength. If the signal gets weaker and goes below the standard, the central switching office would transfer the call to a vacant channel that would give a better signal either in the same service area or the adjacent service area. At the same time, the fixed radio port in that service area would direct the portable users handsets to switch to a newly assigned channel. This would be done by the portable handset automatically and the CSO would check to see that the switch had taken place. This process is called handover.

The switching equipment also needs to be able to communicate rapidly with switching equipment in adjacent service areas in order to coordinate handover of moving portable from one service area to another when necessary. Fig. 2.7 illustrates several multi-channel distribution ports both within buildings and outdoors connected to central switching office equipment and PSTN's. Each central switching office would be connected and controlled from the PSTN in order to allow connection to national and international subscribers. The connection between two central switching offices in the network would support the incoming call to be routed to another user wherever located. The ports should be completely compatible both within buildings and outdoors so that the same portable set could be used in both environments. These radio ports would allow wideband coverage of locations such as shopping centres, travel terminals, offices, factories, domestic buildings and major roads and motorways.

In the future, inexpensive miniature millimetre-wave portable handsets would become available. The users might have hand-held portables which resemble a folding wallet which can be placed in their pockets. Each user would be assigned a

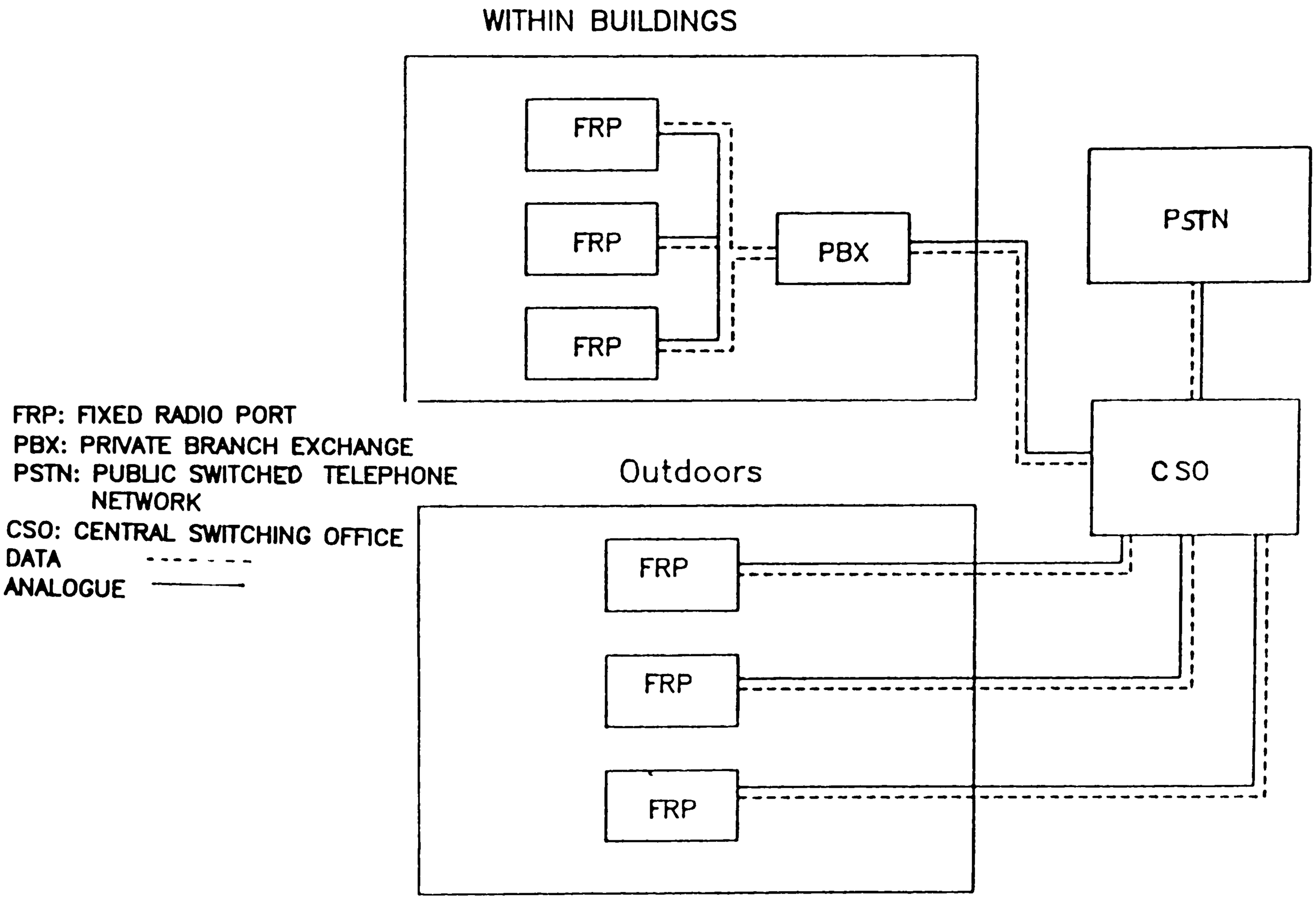

FIG. 2.7 DISTRIBUTION OF RADIO PORTS.

special identification number when they have purchased a portable set. Therefore the user must have a more complex multichannel handset than is available for current cordless telephone. This new system would provide cordless portable communications to people moving about, no matter where they are located within the service area. However, this system requires to identify people who move from one radio coverage area to another rather than identify places as with the present telephone network. The concept would be similar to the present cellular systems [14].

In future, wideband optical fibre distribution networks could be used to replace the existing telephone networks, since they can transmit at a rate of over a gigabit per sec. This would require the installation of optical fibres in every building where people reside.

Outdoors, the radiation could be from street lamp elevation while within buildings, the radiation could be from fixed radio ports attached to the ceiling within office rooms and corridors. The coverage of fixed radio ports is determined by the radiated power and the propagation exponent. Service areas would overlap, and the small coverage area would increase frequency reuse and handover between service areas. Since power is radiated over relatively short distances compared to the present cellular system, the delay spread should be small, allowing high data rates without problems due to intersymbol interference, and the received envelope is expected to have a Rician PDF.

The fixed radio port must be configured to reuse radio frequencies efficiently. Each radio port would use a group of frequencies sufficiently different from the frequencies in use in the adjacent radio port to avoid interference. The strength of radio signals generally decreases as the distance between transmitter and

receiver increases so that the frequencies can be reused for radio ports having sufficient separation. Therefore the reuse of radio frequencies throughout the service area is necessary to ensure the efficient use of radio spectrum. At 60GHz, the radiated energy is strongly attenuated by oxygen molecules, and, for the low transmitted power levels and small coverage areas that are being considered, the radiated signals are unlikely to propagate into different service areas using the same frequency, so co-channel interference should be significantly decreased compared to other frequencies where atmospheric absorption is negligible. However, frequency reuse in the portable communications environment is complicated by large variations in signal level both within buildings and outdoors. This occurs because the transmitted signals are attenuated by the materials in the walls and ceilings within buildings and experience multipath propagation between the radio ports and portable sets. The coverage area needs to be shaped to suit the local geography and a wide variety of environments need to be considered. This can be done by using suitable types of aerials, correct location of the radio ports and control of the radiated power level. Space diversity can also be used without making the hand-held transmitter cumbersome since the aerials have to be separated by a distance greater than half the carrier wavelength, and at 60GHz the carrier wavelength is only 5mm.

2.4.2 System Configuration within Buildings

At certain times, the density of users within some buildings, especially in city areas, may be much higher than the density outdoors, except for rush hour periods. Many users move around multi storey buildings and therefore, there is a need for personal portable communications throughout buildings. However, all telecommunication facilities used in offices, are still dependent upon a cable to connect them to the network system. Even though cordless telephones have become popular for use at home, they are not part of an integrated portable communication

system. Cordless telephone sets consist of two separate units, a base unit and a handset. Communication between the handset and base unit, which is connected to a telephone line, is by a low powered two way duplex radio link. There are several limitations on the present cordless telephone systems, for example limited user density, excessive co-channel interference, a very limited service area of a few hundred metres radius because of the low powered handset and limitations on data handling. These limitations are no longer true for the proposed integrated portable radio network because when users move out of the buildings, they can communicate through the fixed radio ports outdoors.

Distribution networks located outside buildings do not appear feasible at 60GHz due to the large attenuation of the radio waves through walls and other partitions because the exterior and interior building walls act as shields. This requires the fixed distribution network to be placed inside buildings.

One important application within buildings is office communications using the Private Branch Exchange (PBX) system. The PBX would be connected to multi-channel fixed radio ports radiating 60GHz signals to various devices such as portable handsets or computer terminals. At the PBX, the digital switching network uses a control processor to provide switching connections between any pair of devices, with voice or data circuit switched. It also uses a control processor to set calls, switch signals, and control peripheral equipments.

These fixed radio ports could be distributed throughout buildings as shown in Fig. 2.8. Radio ports may be required in each room or floor depending on the type of partitions used. Each individual would be able to move about the building and never be out of range of the telephone. Moving an office or a desk would not

FRP: FIXED RADIO PORT
PBX: PRIVATE BRANCH EXCHANGE
PSTN: PUBLIC SWITCHED TELEPHONE NETWORK
CSO: CENTRAL SWITCHING OFFICE

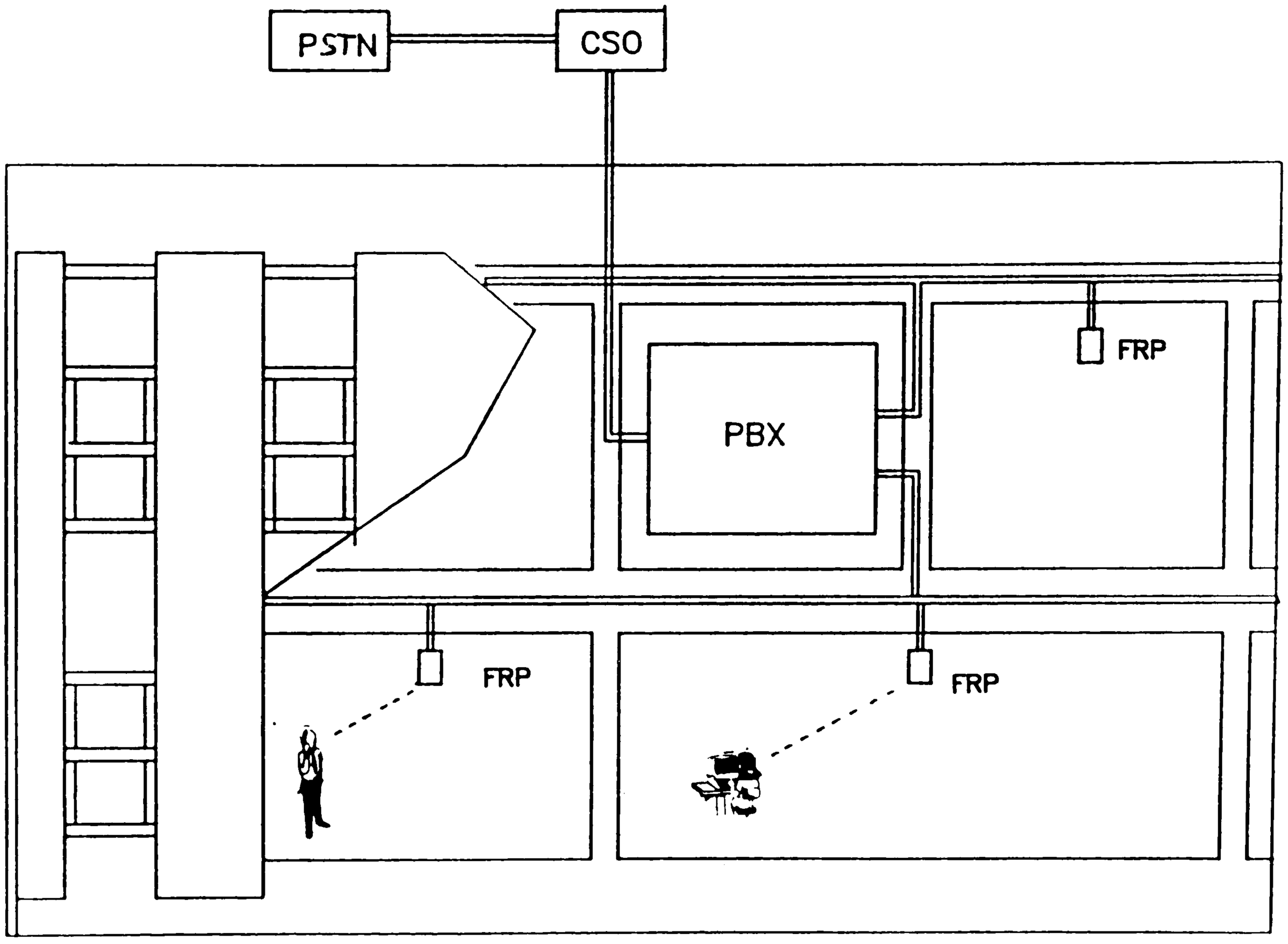

FIG. 2.8 DISTRIBUTION OF RADIO PORTS WITHIN BUILDINGS.

involve moving a telephone connection or waiting for a new telephone number to be assigned. For new buildings, the telecommunications facilities can be built in, along with the plumbing and electricity, while construction is under way. Fig. 2.8 also illustrates the portable hand sets and data terminals communicating by short radio links through fixed multi-channel radio ports hanging from the ceiling using an omnidirectional aerial. Communications between distribution ports and the portable handsets or data terminals are accomplished by radio links operating at 60GHz as indicated by the dotted line.

Distributing radio ports throughout a building would permit frequency reuse, which would significantly increase the user density due to the smaller coverage area. One radio port could serve an area as small as an office or as large as one or more floors.

2.4.3 System Configuration Outdoors.

When the users move out from the building, with the portable communication scheme, they can communicate with the outside radio ports using the same portable handsets or data terminals. The outside ports would require the aerial to be mounted at the height of street lights or traffic signals. The height of street lights is lowest in suburban areas and highest along motorways. The radio coverage area around the port would be approximately circular if omnidirectional aerials are used provided that there is no obstruction between the port and the portable unit. 60GHz signal do not propagate significantly around obstacles such as buildings.

Within urban areas with a high density of buildings, the radio signals within the streets will be substantially limited. A possible arrangement of the distribution ports in the streets between the buildings is shown in figure 2.9. Frequency reuse

A,B,C,D AND E
ARE RADIO DISTRIBUTION
PORTS WITH DIFFERENT
FREQUENCY ALLOCATIONS.

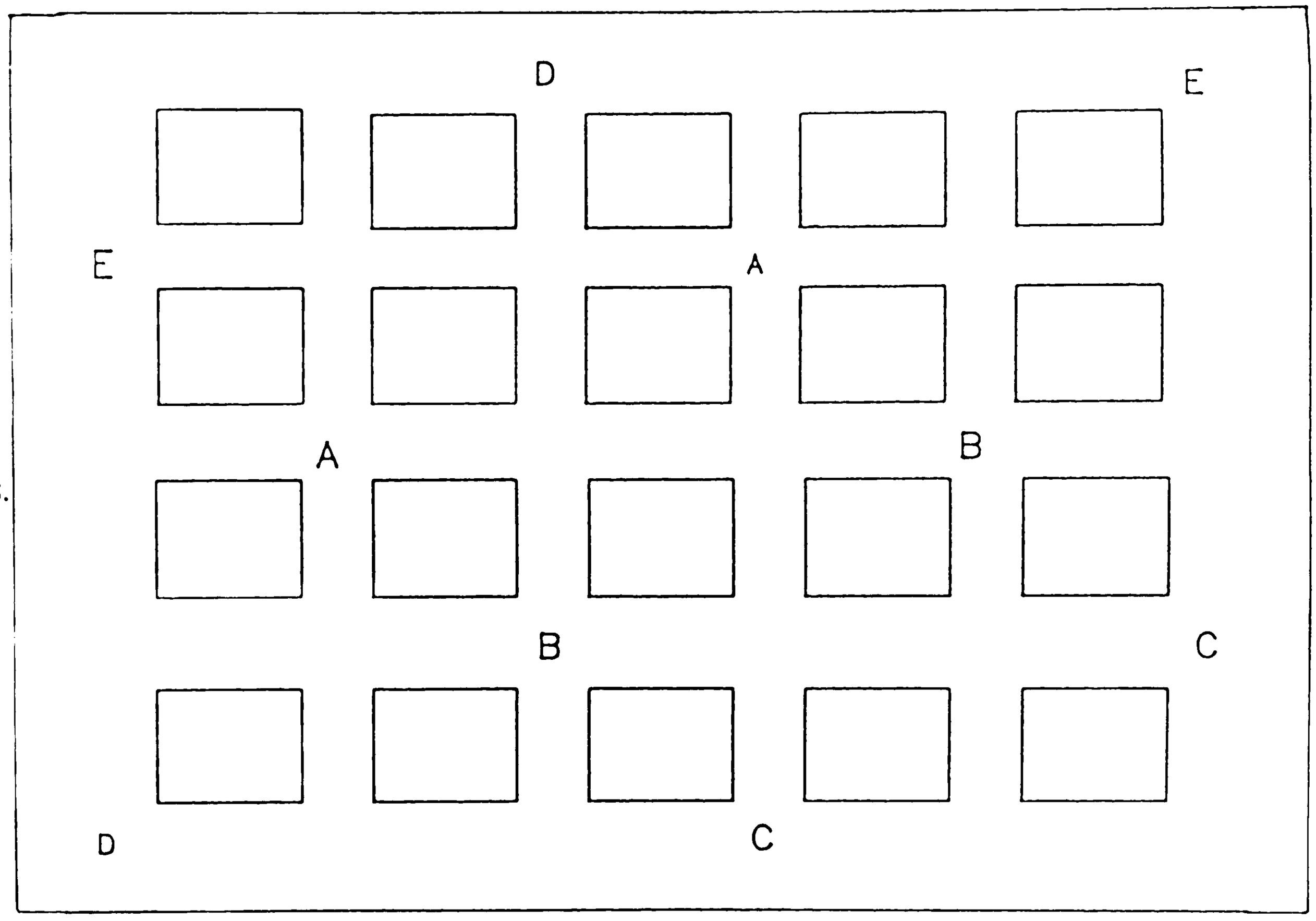

FIG. 2.9 AN ARRANGEMENT OF RADIO PORTS ALONG STREETS BETWEEN BUILDINGS

within buildings can be combined with frequency reuse in the streets and the overall system would be controlled by the central switching office.

Possible distribution networks along roads are shown in Fig. 2.10, where directional aerials are used.[17] These would limit the total radiated power, and help to reduce the multipath fading and would lower co-channel inteference. The beamwidth of the directional aerial should not be too narrow otherwise a misalignment of the radio port and portable set can occur. The radio signals are then radiated from fixed radio ports distributed along the roads at lamp post heights. By using this configuration, the distance between two fixed radio ports becomes farther apart and the radiated area stretches out along the road, thereby reducing co-channel interference. In addition, the interference from forward ports is small due to the radiation in one direction. Furthermore, the transmissions are more likely to have a strong line-of-sight radiated component and shadow fading is likely to have less impact on system performance unless a lorry or a van blocks the LOS path.

At road junctions, radio ports using omnidirectional aerials can be used as illustrated in figure 2.11. In order to provide a service within tunnels at 60GHz, the fixed radio ports could be placed at various points along the roof of the tunnels, although some would be required to radiate at the openings. Directional aerials could be used at the radio ports.

2.5 OTHER APPLICATIONS AT 60GHz.

Other applications are also possible at 60GHz. The large amount of available bandwidth and the reduced co-channel interference [18] make the 60GHz band suitable for short distance line-of-sight links, such as wideband temporary links or local distribution networks. These include the distribution from nodes of optical

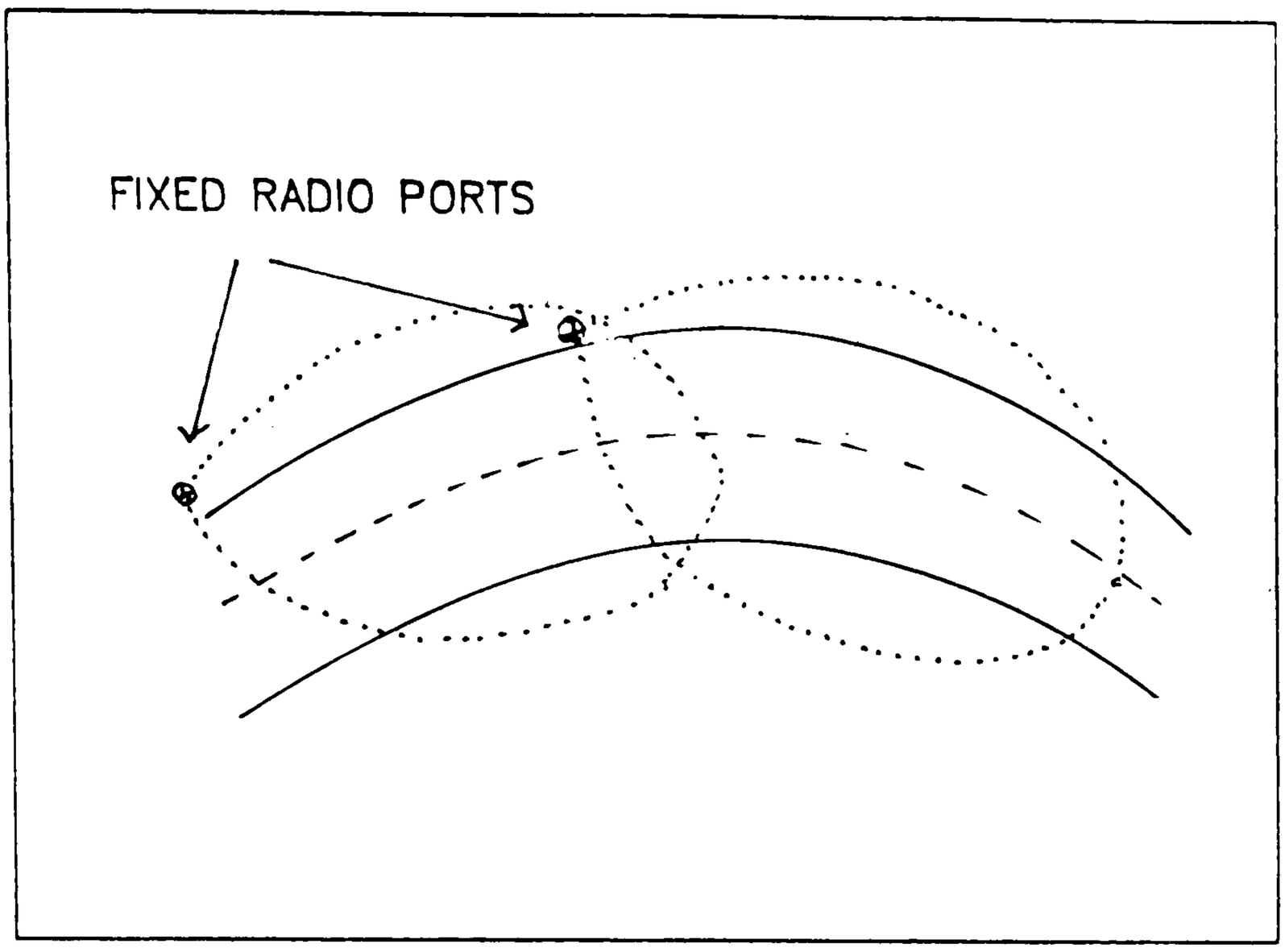

FIG. 2.10 DISTRIBUTION OF FIXED RADIO PORTS ALONG A ROAD

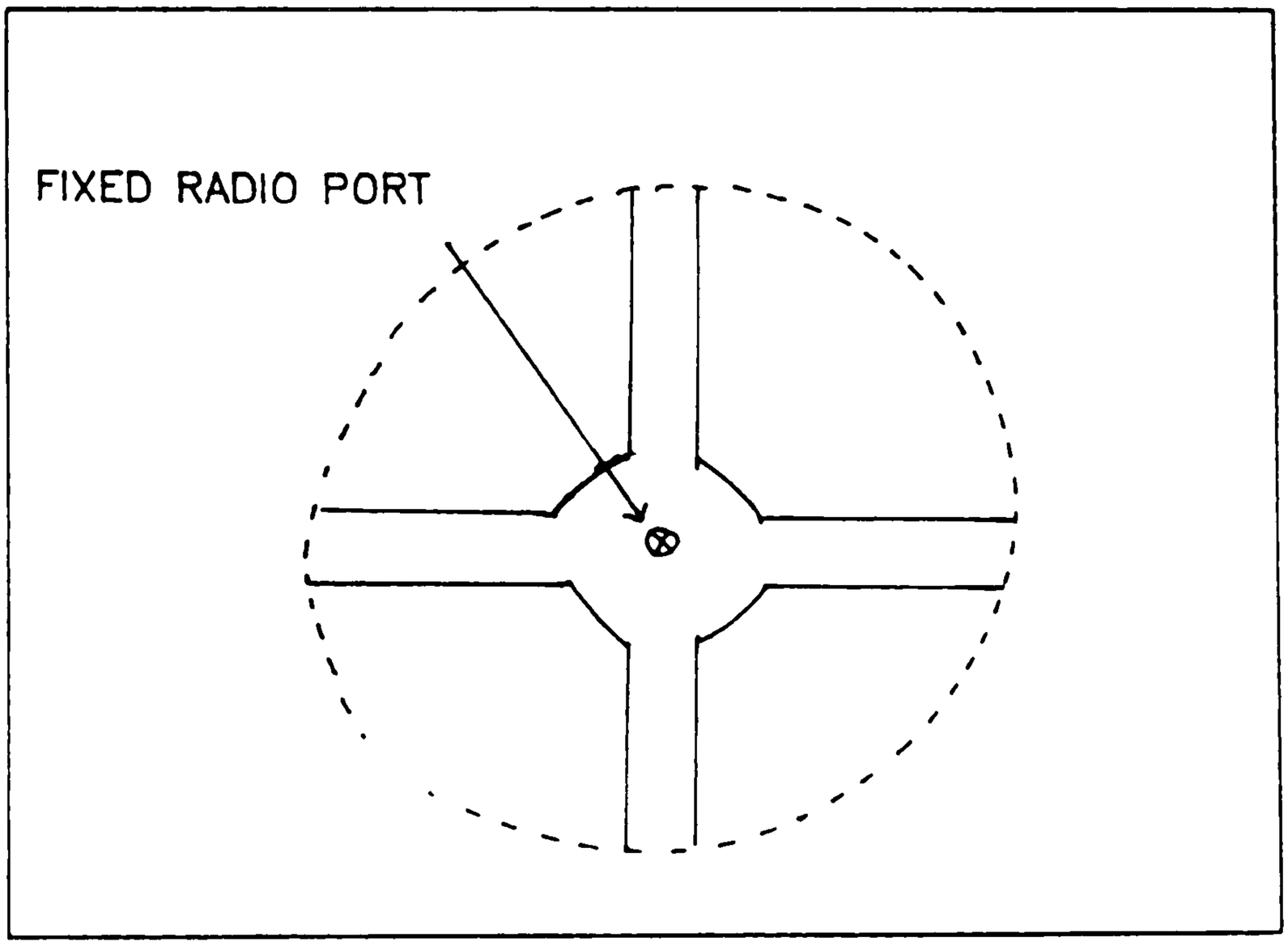

FIG. 2.11 FIXED RADIO PORTS AT THE INTERSECTION OF BUSY ROADS.

fibre and trunk systems, and local area communication systems for industrial estates, harbours, airports etc. Intersatellite communications have also been proposed at 60GHz [19] which have the advantage of the earth's atmosphere acting as a natural shield against interferences between intersatellite and terrestrial communication systems.

For point-to-point communication links, the equipment could easily be mounted on a flat roof, or could even be allowed to radiate through a window for temporary links. At 60GHz, a small aerial provides high gain and a narrow beamwidth, and the equipment will be compact.

Wideband services would be required mainly in city centres, commercial areas and industrial areas. The possible form of Local Distribution Networks (LDN) is shown in figure 2.12. The distribution network would be a link to a PSTN by optical fibre. The system must be installed on a tall building having a flat roof suitable for accommodating several transceivers simultaneously. The line-of-sight path must not be obstructed between the transceivers. Because of oxygen absorption, frequencies could be reused a few kilometres away without interference so the spectrum can be utilised efficiently. Point-to-point communication links could be realized by employing high directivity aerials installed on tall buildings so that interference to and from portable communication users would be minimal.

As mentioned in section 2-1, at high altitudes, the individual oxygen absorptions lines are resolvable at 60GHz causing absorption windows to appear. These absorption windows can be used for inter-satellite links which shield against interference from ground users such as portable and point-to-point communication systems. Compared to lower frequency links, 60GHz offers reasonable aerial size,

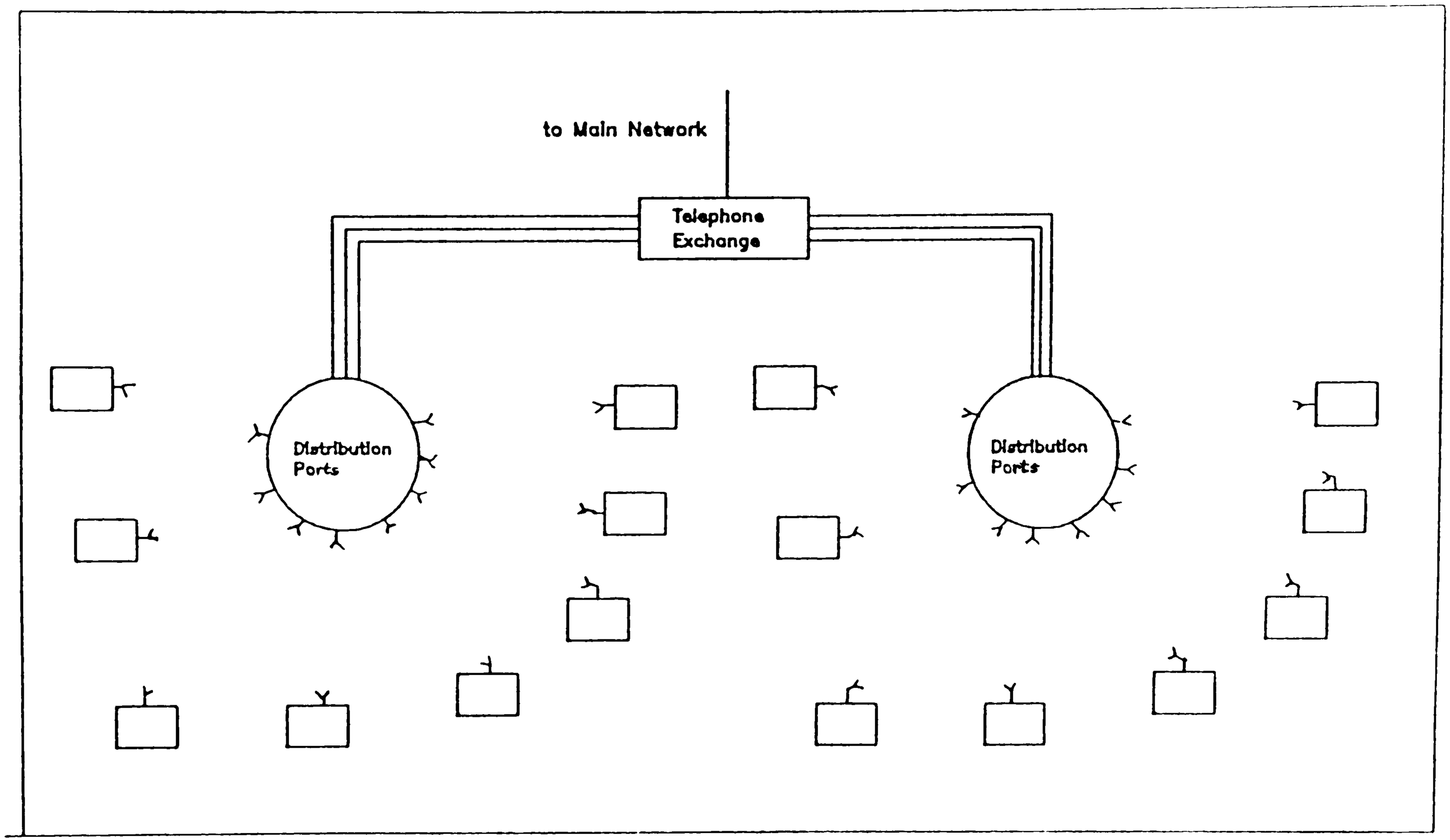

FIG. 2.12 LOCAL DISTRIBUTION NETWORKS OF 60 GHz LINKS

large available bandwidth, and freedom from interference from other users. Approximately 9GHz of bandwidth, near 60GHz, are currently allocated for inter-satellite link applications [16]. It is expected that 60GHz inter-satellite links will have a significant role in future satellite communication applications. At present, the applications of inter-satellite links have been primarily experimental, involving relatively short distances and low data rates.

REFERENCES

[1] Blake, R.G., "The use of millimetre-waves for broadband local distribution," Conf. Proc. 17th European Microwave Conference, 7th - 11th, September 1987.

[2] Gerst, H.G., et al "New Generation Analog Radio Relay Equipment for 2 GHz, 4 GHz, and 6 GHz Bands," IEE Proc. NTC 81 p.E.6.6.1 - E.6.6.5, 1981.

[3] Rupp, H., "Microwave Systems for fixed and mobile services," Standard Elektrik Lorenz Ag, Ostendstr 3, D-7530 Pforzhein, West Germany, pp.44 - 53.

[4] Reber,E.E, Mitchell, R.L., and Carter, C.J., "Attenuation of the 5 mm wavelength band in a variable Atmosphere," IEEE Trans on Antennas and Propagation, Vol. Ap-18, No. 4, July 1970, pp.472 - 479.

[5] Crawford, A. B., and Hogg, D.C., "Measurements of atmospheric attenuation at millimetre wavelengths," Bell Syst. Tech. J., No.4, July 1956, pp.907 - 916.

[6] De Lange, O.E., Dietrich, A.F., and Hogg, D.C., "An experiment on propagation of 60GHz waves through rain," Bell Syst. Tech. J., 1975, Vol.54, pp 165-176.

[7] Bodtmann and Ruthroff, C.L., "Rain attenuation on short radio paths: Theory, Experiment, and Design," Bell Syst. Tech. J., Sept. 1974, Vol. 53, no.7.

[8] Tokumitsu,Y., Ishizaki, M., Iwakuni, M. and Saito, T., "50 GHz I.C components using Alumina substrates," IEEE Trans. Microwave Theory and Tech., Vol. MTT-31, pp.121-128, Feb. 1983.

[9] Miyanchi, K., "W-404 guided millimeter wave transmission system," 1975 International Microwave Symposium.

[10] Skillman, W.A., "Microwave technology - key to AWAC's success," in 1983 Int. Microwave Symp. Digest (Boston,MA)

[11] Spielman, B.E., "Technologies Summaries for microwave theory and techniques - 1983." IEEE Trans on Microwave Theory and Techniques, Vol. MTT 32. No. 1 October 1984 pp. 1372 - 1378.

[12] IEEE MTT-S Int. Microwave Symposium (Boaston,MA) May 1983, Digest Papers, U4, I2, C4.

[13] Dupuis, P., Mayer, S and Guana, J., " Millimeter wave subscriber loops," IEEE Journal on selected areas in communication Vol. Sac, No.4 Sept. 1983, pp 623-631.

[14] MacDonald, V. H., "Advance Mobile Phone Services: The cellular Concept," The Bell System Technical Technical Journal, Vol. 58, No.1, January 1979, pp.15 - 41.

[15] Steele,R., "Towards a high-capacity digital cellular mobile radio system," IEE Proc., Vol. 132, Pt. F , No. 5, August 1985, pp.405 - 415.

[16] Cox,D.C., "Universal Digital Portable Radio Communications," Proc. of the IEEE, Vol. 75, No. 4, April 1987,pp.436-477.

[17] Steele,R. and Prabhu,V.K., "High-user-density digital cellular mobile radio systems," IEE Proc., Vol. 132, Pt. F, No.5, August 1985, pp.396 - 404.

[18] Steffes, P.G. and Meck, R.A., "Prototype Secure Millimeter Communications," MSN, october 1980, pp.59 - 68.

[19] Anzic,G., "A study of 60GHz intersatellite link applications," Proc. IEEE INT. CONF. on communications progress. CICC '83 Boston MA. USA June 1983, pp.1181-1188.

CHAPTER 3

PORTABLE MOBILE RADIO PROPAGATION ENVIRONMENT.

The portable mobile radio environment is qualitatively similar to the cellular mobile radio environment. The difference is that in the portable radio environment, the aerials are located both within buildings and outdoors. Furthermore, the aerial heights are lower and the distance between the transmitter and receiver is shorter than for the cellular mobile radio case. Because of the high attenuation due to obstructions, the coverage distance of fixed radio ports at 60GHz is likely to be less than 30m within buildings and less than 200m outdoors. Outdoors, the radio ports could be at lamp post height (about 8m) and indoors, they could be at ceiling height (about 3m).

3.1 MOBILE RADIO ENVIRONMENT.

In the portable radio environment, the signal would be transmitted or received from fixed radio ports to portable handsets or data terminals. Objects that have dimensions which are much greater than a wavelength become scatterers, which create reflected waves. The reflected waves come from different directions and result in many propagation paths existing between the fixed radio port and the portable handset with different time delays and different attenuations. The received signal is the vector addition of the direct wave and the many reflected waves. When the mobile handset is in motion, the relative phases of the direct wave and the reflected waves vary, so the magnitude of their vector addition fluctuates. Since fades tend to occur every half wavelength of travelled distance, these fluctuations are very rapid, so this phenomenon is called 'short term fading' or 'fast fading'. Superimposed on this short term fading is fading which is mainly cause by changes in the parameters of the environment, which cause changes in diffraction losses

around obstacles. Since appreciable changes in signal power occur after movements of many wavelengths, this type of fading is called 'long term fading' or 'slow fading'

There will be quite a lot of difference between systems operating within buildings and outdoors. The outdoors environment will have fast moving vehicles, and the difference in path lengths is likely to be longer. Within buildings, it may be expected that applications such as integrated portable communications, where there is a significant number of mobile users, will create high traffic densities. The spacing between reflectors such as partition walls will be in the order of three to twenty metres. The users and the furniture will provide additional reflectors, creating a multipath environment.

The received signal power can be represented as a function of distance or time. A typical plot of the received signal power as the mobile receiver moves away from the fixed transmitter is shown in figure 3.1. The fluctuations which occur about the mean signal power are caused by constructive and destructive interference of the direct and many reflected waves as the mobile moves. When the operating frequency is increased, the fluctuations become more rapid.

Propagation is also dominated by the effects of shadowing where the mean signal power varies slowly and is apparent over distances large compared to a wavelength. The average received signal power also decreases as the mobile receiver moves away from the fixed transmitter. The decrease in average signal power with distance is one of the major parameters of interest in the analysis of radio wave propagation for mobile communications.

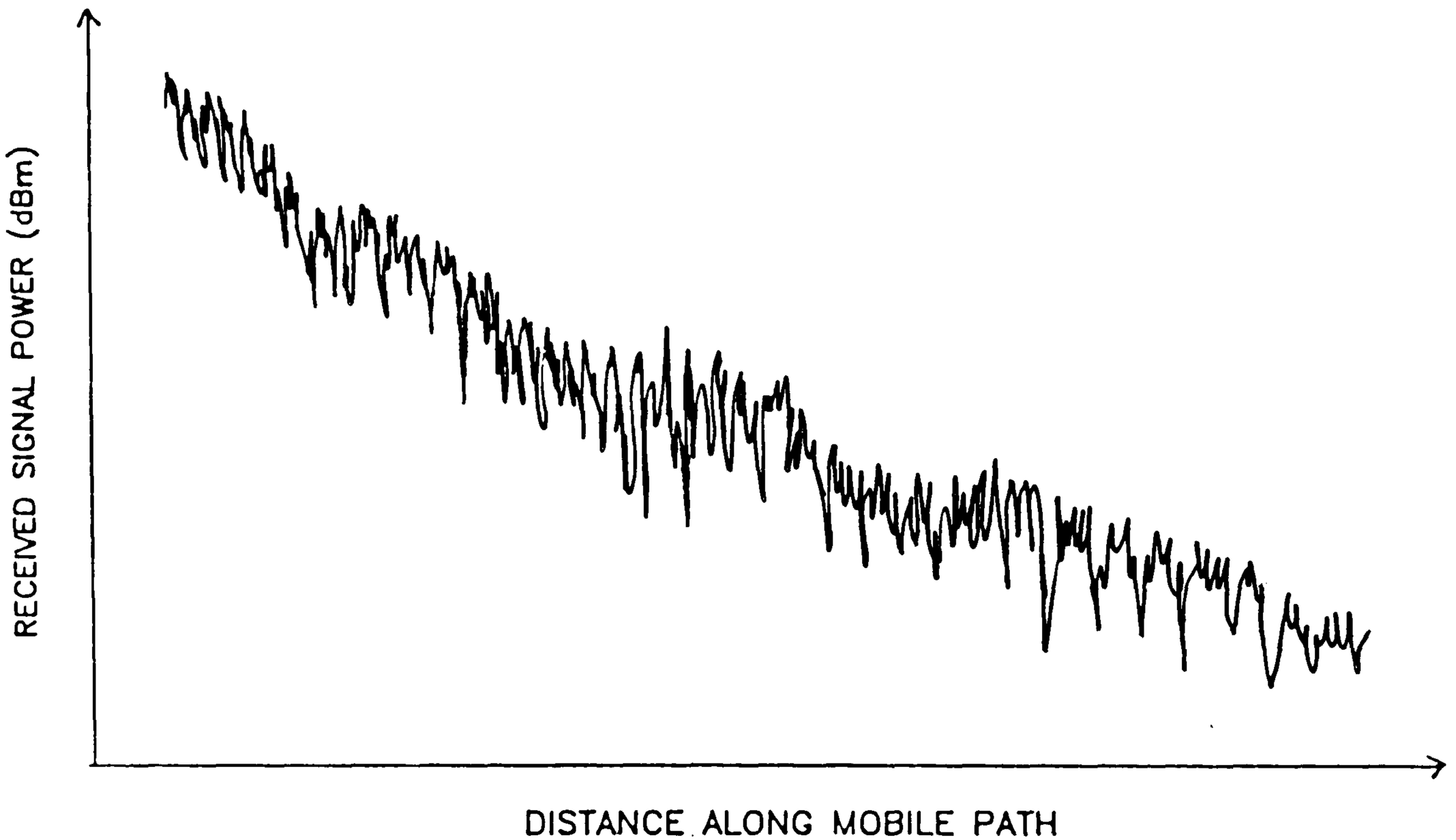

FIG. 3.1 THE VARIATION OF THE RECEIVED SIGNAL POWER WITH DISTANCE AS THE MOBILE RECEIVER MOVES AWAY FROM THE FIXED TRANSMITTER.

If the signal bandwidth is restricted to being much less than 1/(delay spread), then narrowband signal description and statistics are all that is required. These can be determined from measurements at a single frequency within the signal bandwidth, because the multipath fading is virtually frequency independent over this bandwidth.

3.2 MULTIPATH FADING.

3.2.1 Causes of Multipath Fading.

Multipath fading is caused by multiple reflections of a transmitted wave by local scatterers such as furniture, ceilings, walls, and buildings surrounding the mobile unit. In order to illustrate the causes of multipath fading, a fixed transmitter and a mobile receiver will be assumed. If the mobile receiver is surrounded by many moving objects, the received signal will experience fading depending on the distance between the object and the receiver as illustrated in figure 3.2.

If the receiver is moving at a velocity of v with no scatterers (figure 3.3) around the receiver, the received signal, R_r, can be represented as

$$R_r = A.\exp[j2\pi(f_t - \frac{v}{\lambda}\cos\theta)t] \qquad (3.1)$$

where A is the amplitude of the received signal, f_t is the transmission frequency, λ is the wavelength and θ is the angle of arrival of the incoming wave relative to the direction of motion of the mobile. However, if there is a perfect reflector ahead close to the moving receiver (figure 3.4) and the angle of arrival of the incoming wave is 0^0 and the angle of arrival of the reflected wave is 180^0, the resultant received signal is the sum of two waves, which is given by

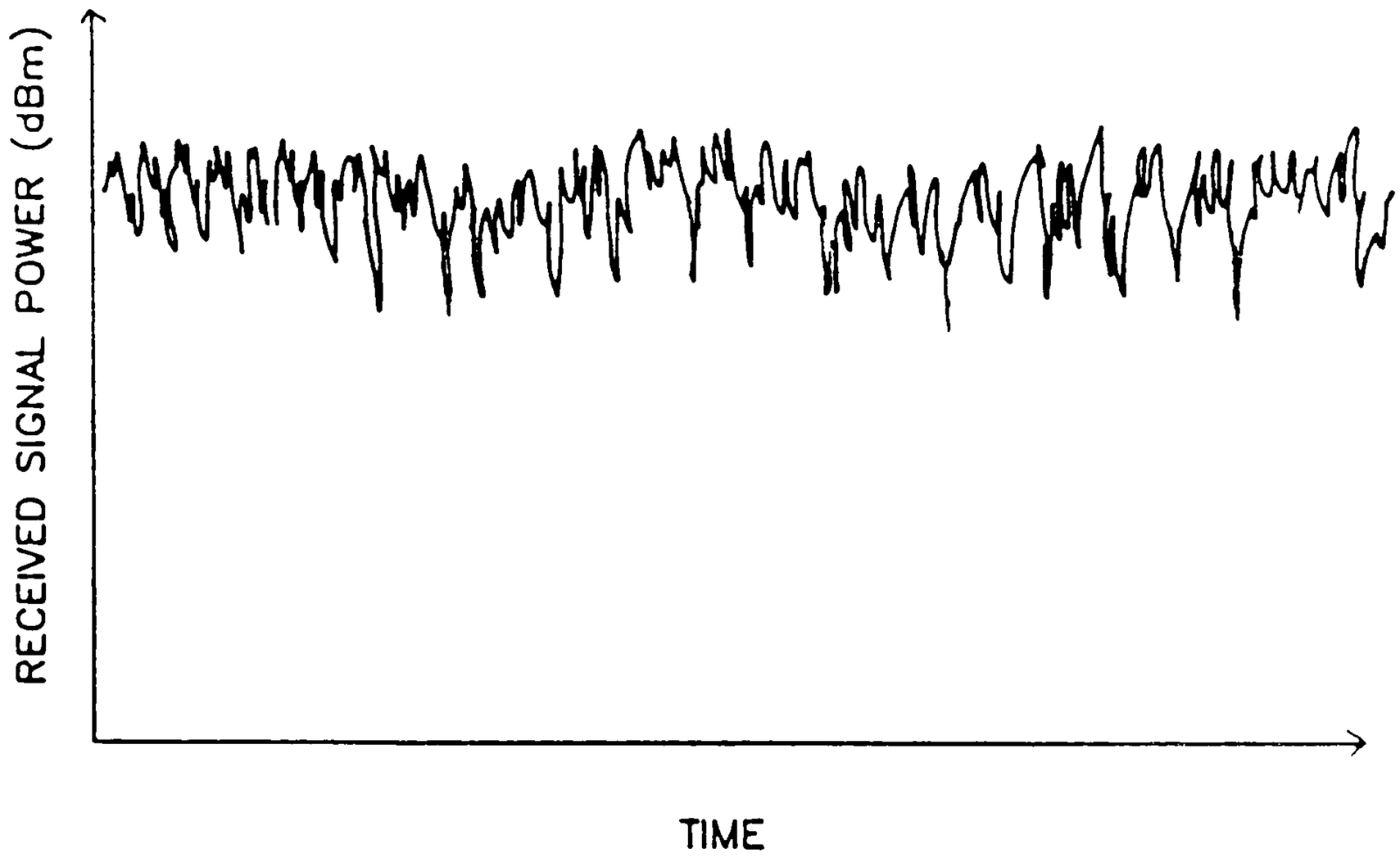

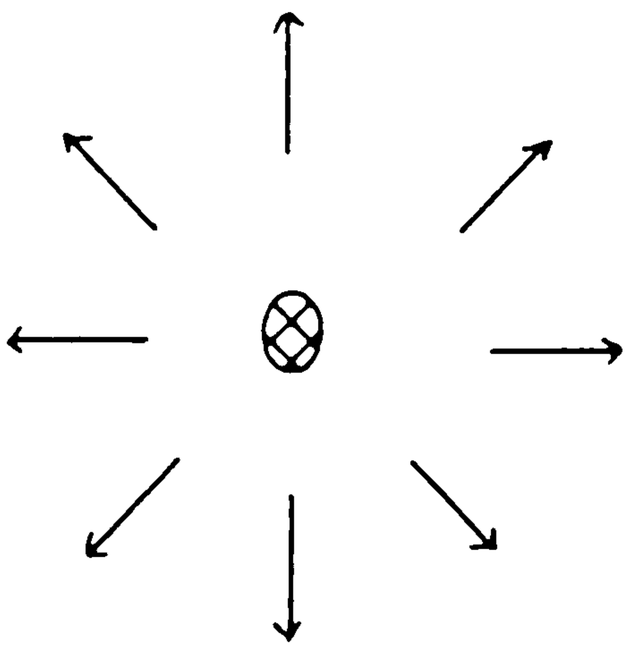

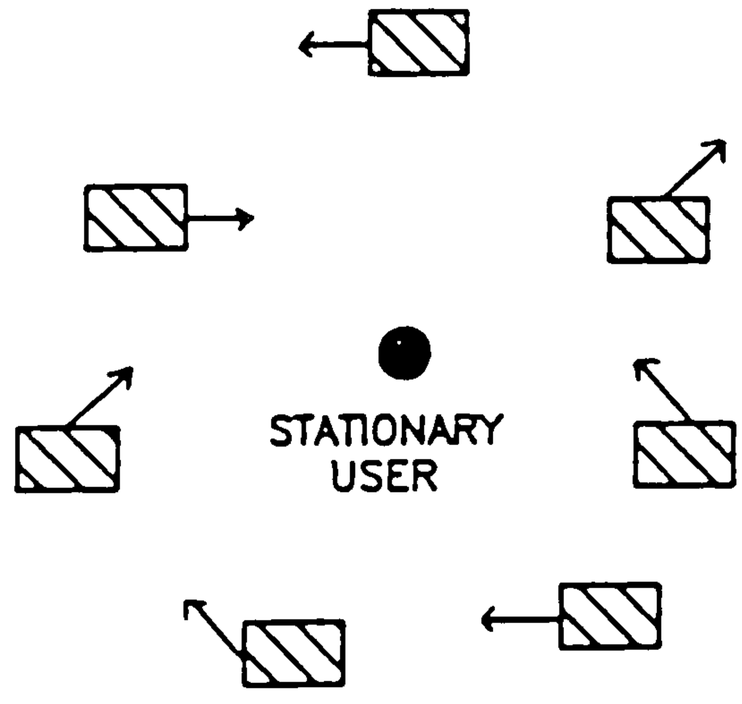

FIG. 3.2 MULTIPATH FADING PHENOMENA WHEN THE STATIONARY USER IS SURROUNDED BY MOVING OBJECTS.

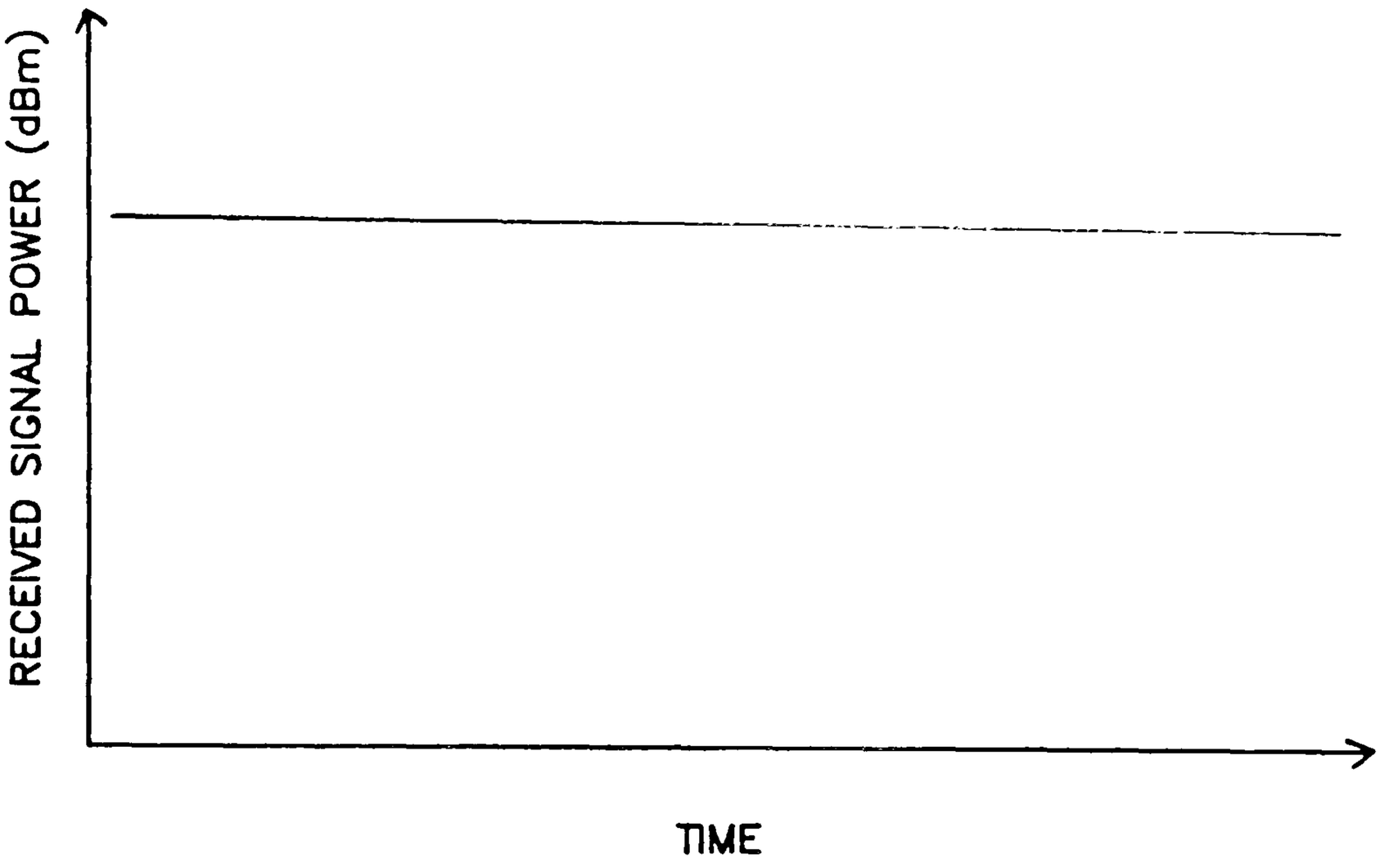

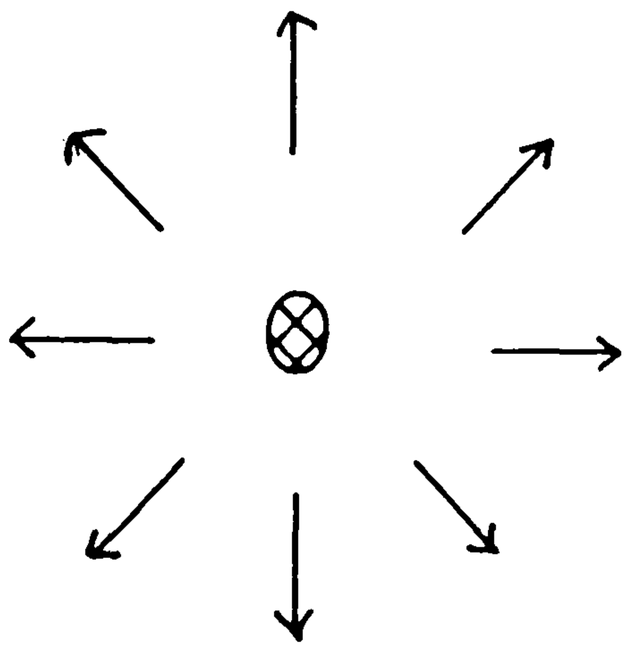

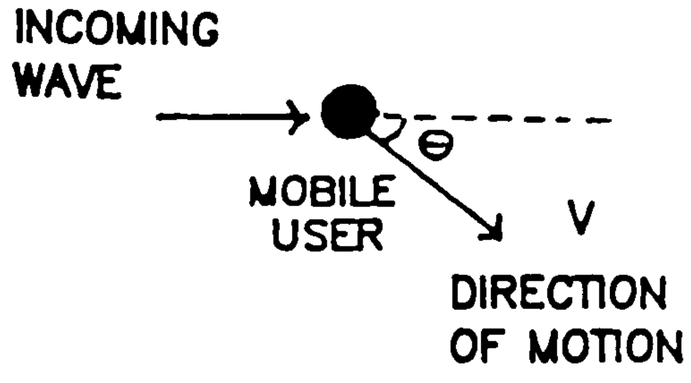

FIG. 3.3 MULTIPATH FADING PHENOMENA WHEN THE MOBILE USER IS MOVING AT VELOCITY V WITH NO SCATTERERS

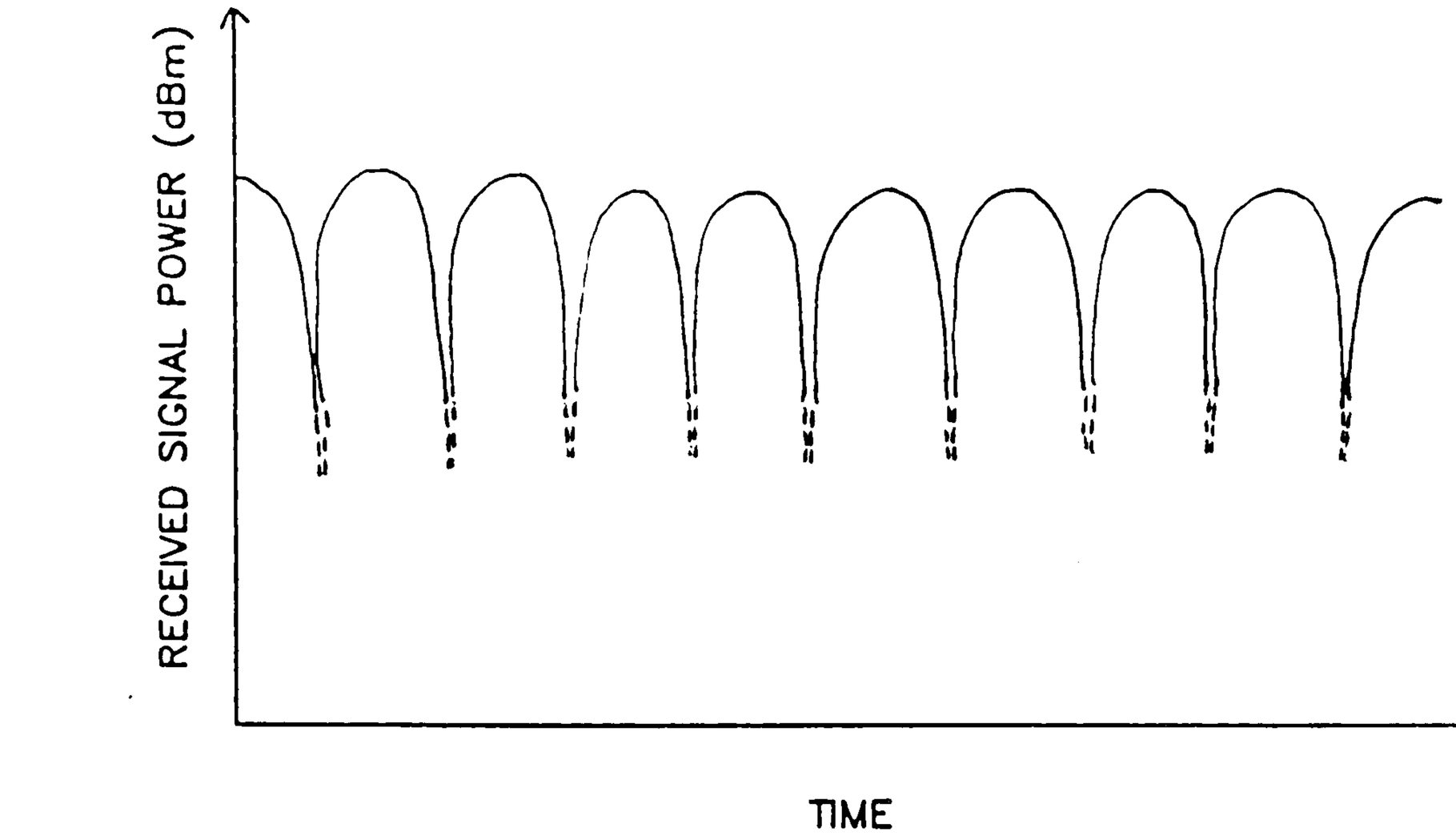

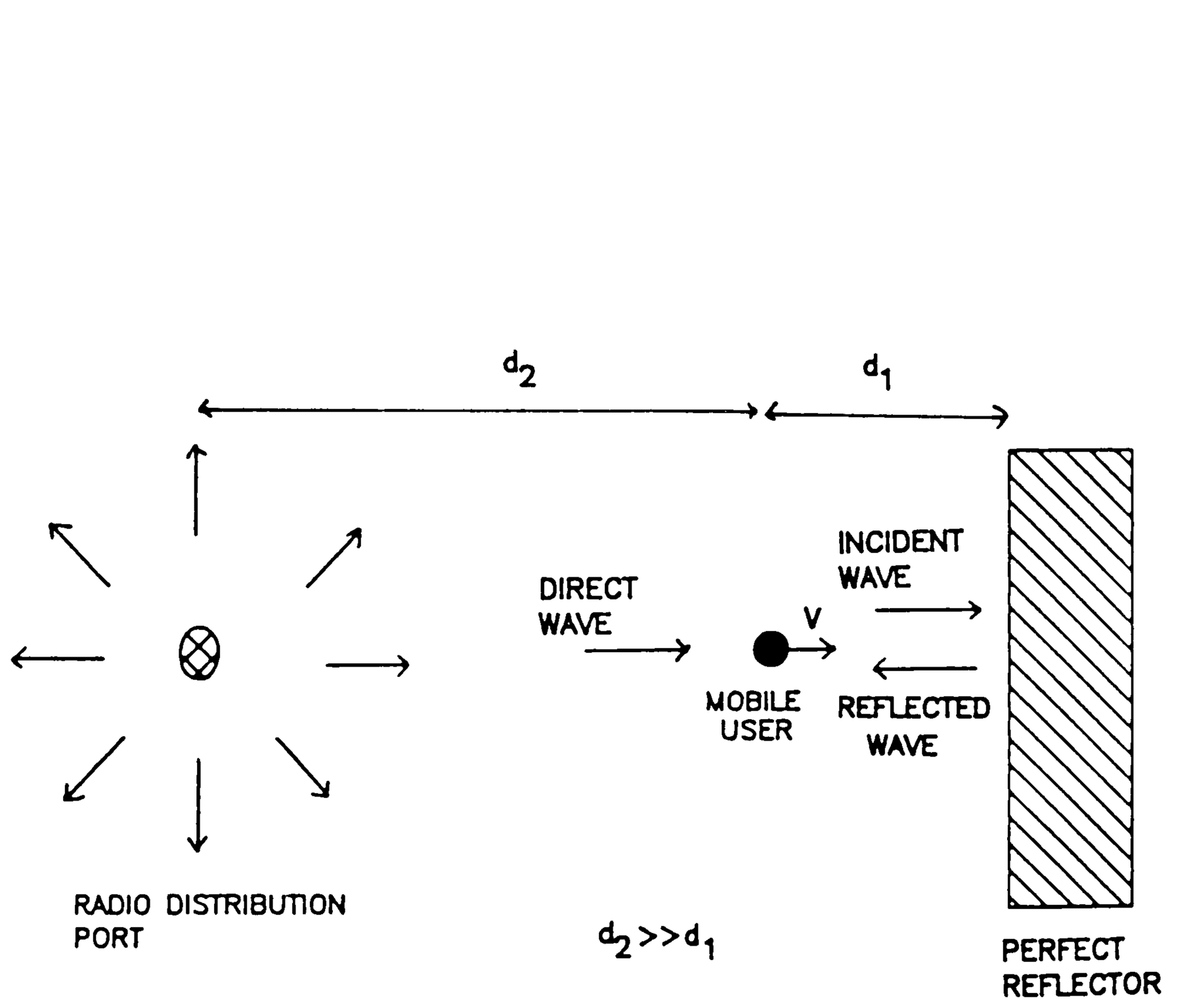

FIG. 3.4 MULTIPATH FADING PHENOMENA WHEN THE MOBILE USER IS MOVING AT VELOCITY V WITH ONE SCATTERER.

$$R_r = \left[A.\exp\left(\frac{-j2\pi vt}{\lambda}\right) + A.\exp\left(\frac{j2\pi vt}{\lambda}\right)\right]\exp\left(j2\pi f_t t\right) \qquad (3.2)$$

The envelope of the received signal becomes

$$|R_r| = 2A.\cos\left[\frac{2\pi vt}{\lambda}\right] \qquad (3.3)$$

This results in the standing wave pattern as shown in figure 3.4.

Now if there is no direct wave, but there are N reflected waves coming from N different directions and arriving at angles which are evenly distributed around the receiver as shown in fig. 3.5, the received signal will become

$$R_r = \sum_{i=1}^{N} A_i \exp(j2\pi f_t t).\exp\left[\frac{-j2\pi vt\cos\theta_i}{\lambda}\right] \qquad (3.4)$$

where A_i is the amplitude of the i'th wave, and θ_i is the angle of arrival of the i'th wave which is randomly distributed from 0 to 2π.

The resultant received signal is itself a random quantity and varies rapidly when the mobile receiver moves a few wavelengths, which results in multipath fading. The rate of variation of the multipath fading is directly related to the mobile speed. In moving through this environment, the mobile receiver experiences fading with amplitude variations of typically 20dB and usually ranging from 10 to 35dB [1], the actual amount being dependent on the environment. Minima in the standing wave pattern tend to occur at a separation of about half a wavelength. The fading pattern for this condition is shown in figure 3.5 and is found to have a Rayleigh distribution at VHF and UHF [1,2]. However, when a LOS path is present between

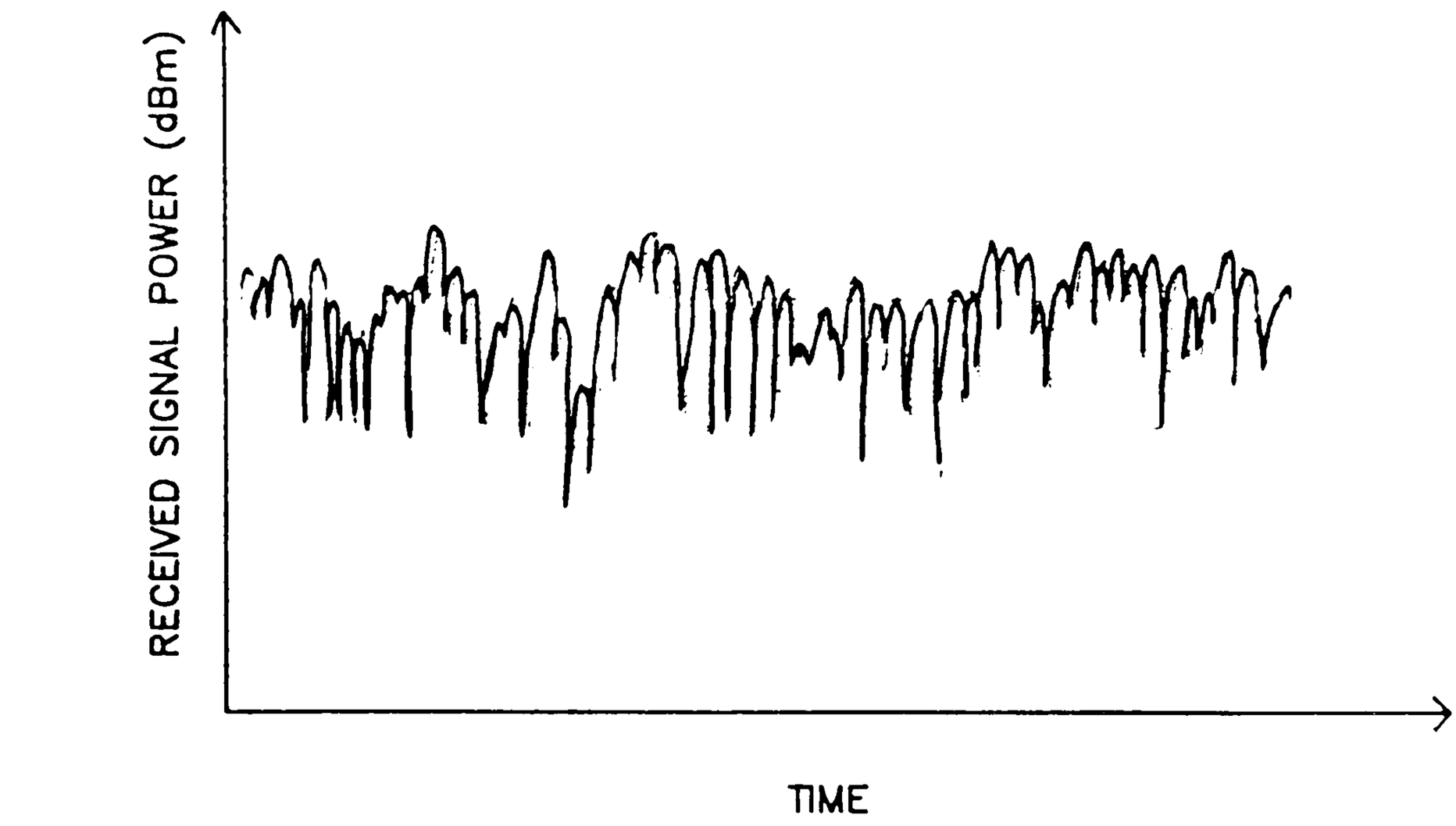

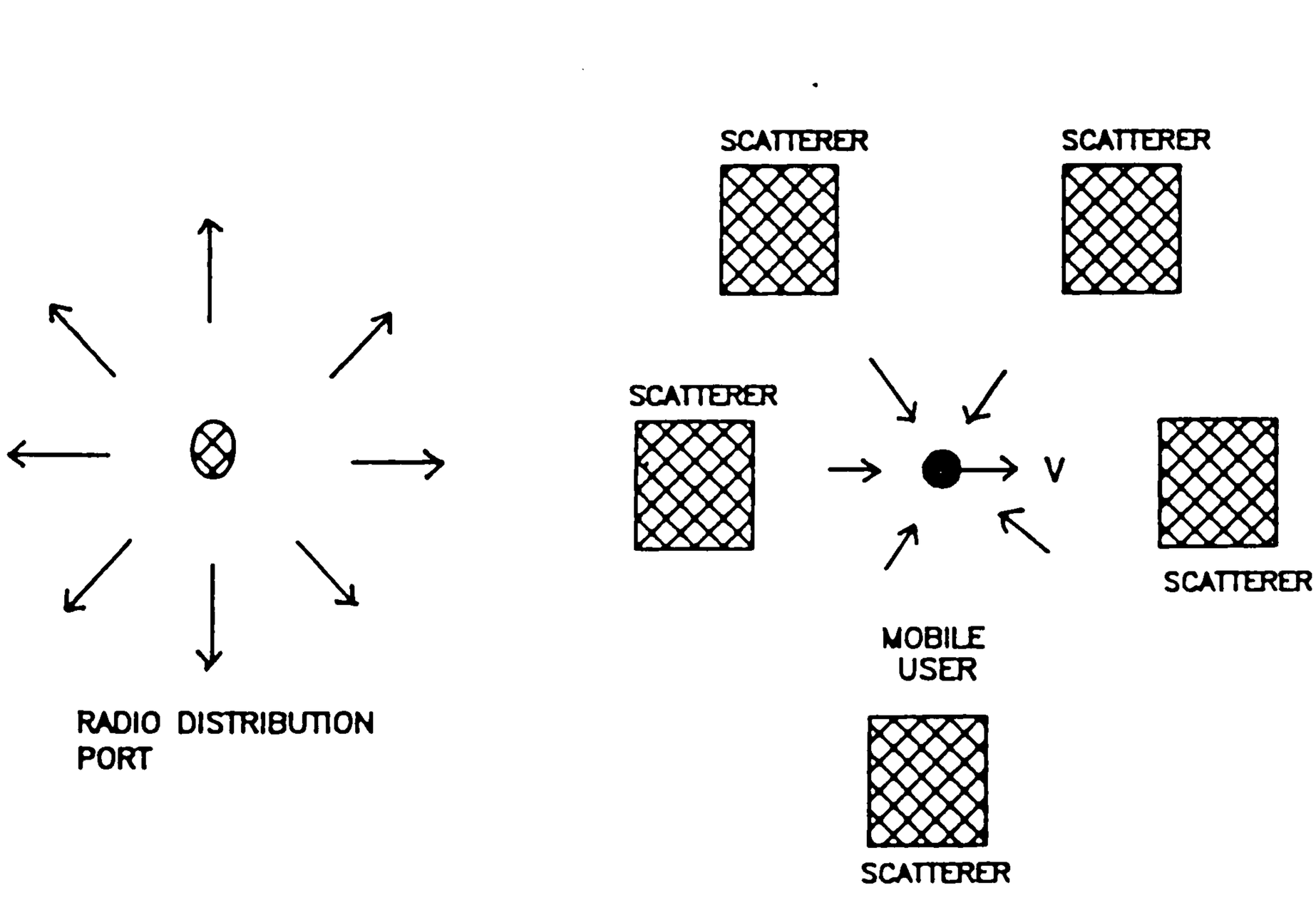

FIG. 3.5 MULTIPATH FADING PHENOMENA WHEN THE MOBILE USER IS MOVING AT VELOCITY V WITH N REFLECTED WAVES AND NO DIRECT WAVE.

the transmitter and receiver, then the envelope of the received signal has been shown to follow a Rician distribution [5].

3.2.2 Doppler Frequency Shift.

Associated with the multipath fading is a Doppler frequency shift due to the motion of the mobile. The magnitude of the doppler shift depends upon the carrier frequency, the mobile velocity and the angle of arrival of the direct or reflected waves relative to the direction of motion of the mobile. From equation 3.1, the doppler shift is given by

$$f_d = \frac{v.\cos\theta}{\lambda} \qquad (3.5)$$

The received frequency, f_r, is offset from the transmitted frequency, f_t, by the doppler frequency, f_d, as the mobile unit moves. The received frequency is given by

$$f_r = f_t - f_d \qquad (3.6)$$

When the mobile unit is moving away from the transmitter (fig 3.6) at $\theta = 0^0$, the received frequency is $f_r = f_t - v/\lambda$. When the mobile unit is circling around the transmitter, $\theta = 90^0$, so there is no doppler shift and therefore $f_r = f_t$. When the mobile unit is moving towards the transmitter, then $\theta = 180^0$, so $f_r = f_t + v/\lambda$. A table of the maximum doppler shift (Hz) at 60GHz for various speeds is given in Figure 3.7.

3.2.3 Envelope Properties of the Multipath Fading.

Since multipath fading is difficult to predict, statistical data on the time variation of the received signal is required. The envelope of the received signal

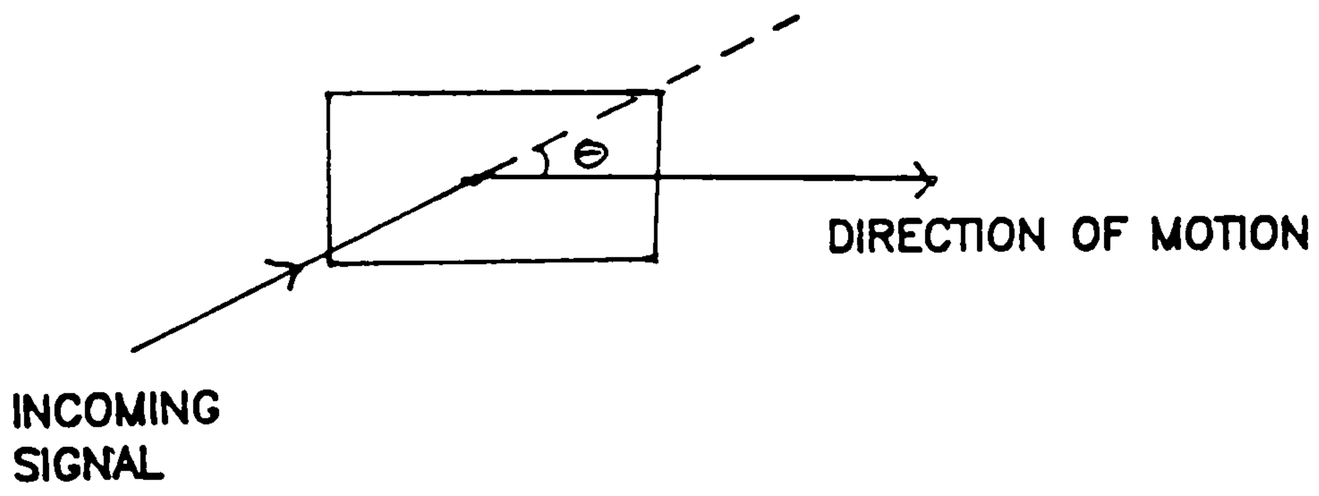

FIG. 3.6 THE ANGLE OF ARRIVAL OF THE INCOMING SIGNAL.

Speed m/s	0.5	1	1.5	2	2.5	3	3.5	4	5
Doppler Shift (Hz)	100	200	300	400	500	600	700	800	1000

FIG. 3.7 MAXIMUM DOPPLER SHIFT (Hz) AT 60GHz FOR VARIOUS MOBILE SPEEDS.

when there is no line-of-sight (LOS) path between the transmitter and receiver is Rayleigh distributed [3,4] with a probability density function given by

$$p(r) = \frac{r}{b_o} \exp\left(\frac{-r^2}{2b_o}\right) \qquad \text{for } r \geq 0$$

$$p(r) = 0 \qquad \text{for } r < 0 \tag{3.7}$$

where r is the signal envelope and b_0 is the mean signal power. The Rayleigh distribution describes the first order statistics of the envelope. From equation 3.7, the cumulative distribution function (CDF), i.e. the probability that the envelope is below any specified value, R, can be derived as [3]

$$P(R) = \text{prob}\ (r<R) = 1 - \exp\left(\frac{-R^2}{2b_o}\right) \tag{3.8}$$

A plot of P(R) plotted on Rayleigh paper produces a straight line as shown in figure 3.8. From this, it is possible to find the overall fraction of time for which the signal envelope is less than any specific value.

If the mobile receiver is in direct line-of-sight with the fixed transmitter, the received signal will consist of a relatively strong direct component plus much weaker reflected components, and the PDF can be obtained by the application of the theory developed by Rice [5] for a sine wave accompanied by narrowband Gaussian noise.

The PDF of the signal envelope is then known as a Rician distribution and may be expressed as [5]

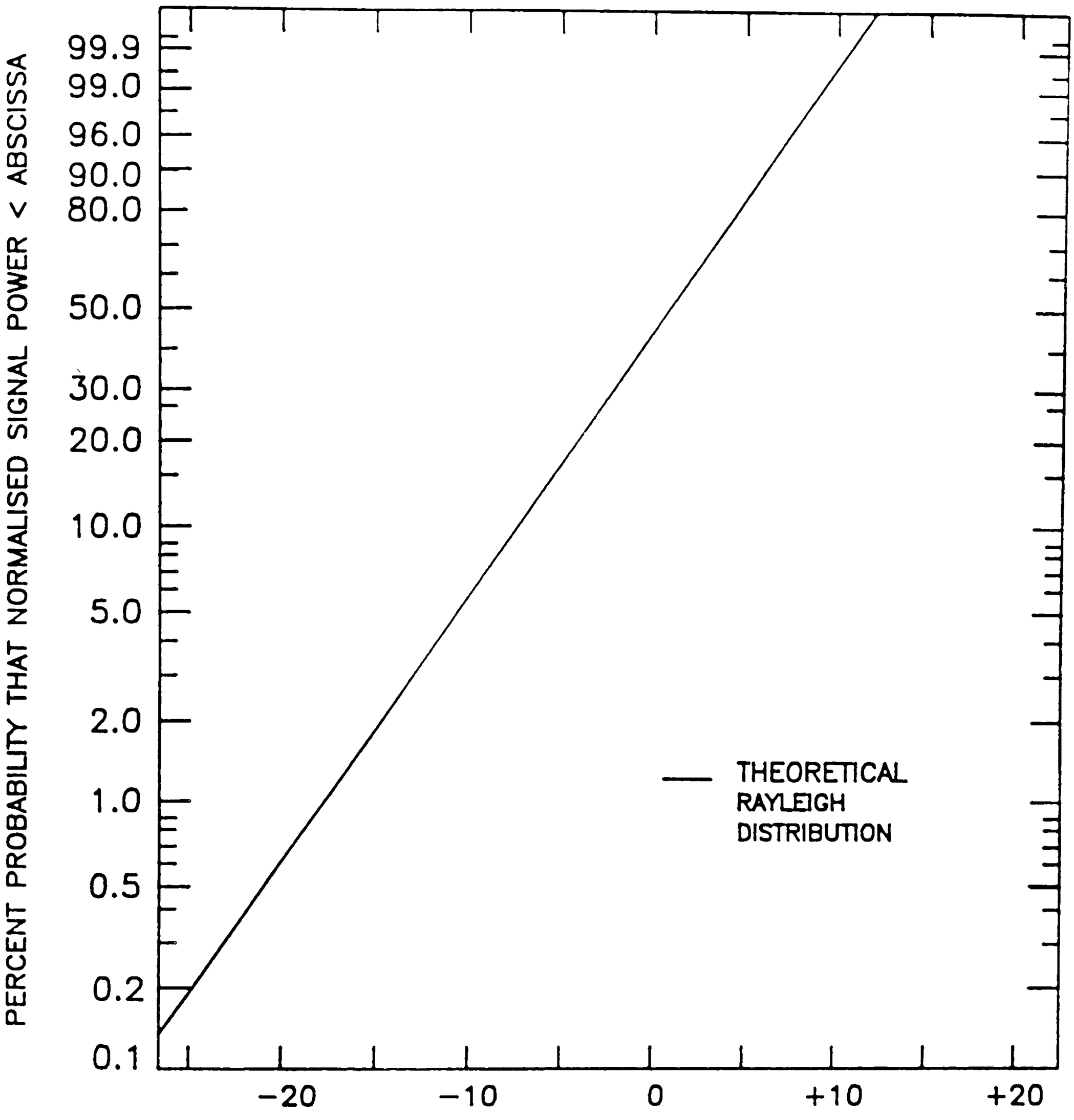

FIG. 3.8 CDF OF THE RECEIVED SIGNAL POWER PLOTTED ON RAYLEIGH PAPER

$$p(r) = \frac{r}{b_o} \exp\left[\frac{-r^2 + Q^2}{2b_o}\right] I_o\left[\frac{rQ}{b_o}\right] \qquad (3.9)$$

where r is the envelope of the fading signal, b_o is the average power of the fading signal, Q is the amplitude of the direct wave, and $I_o(x)$ is the modified Bessel function of zero order.

Fig. 3.9 is a graph of the Rician PDF of a fading envelope. When Q is large (graph C), $Q^2/2b_o >> 1$, equation 3.9 becomes a Gaussian distribution and when the direct line-of-sight path does not exist (graph B), Q becomes zero and equation 3.9 becomes the Rayleigh PDF.

Practically, the statistical distribution of the received signal envelope can be determined from the digitised recorded data. A typical plot of the multipath fading of a digitised recorded signal is shown in figure 3.10, with N sample points. The vertical axis is in dB which is equally divided into 1dB intervals. In order to obtain the PDF, the number of data in each interval is counted and plotted against the corresponding level. The percentage of the signal within a particular interval can be calculated by dividing the number of samples in that interval by the total number of samples. The PDF generated from experimental data in dB needs to be converted to linear values before it can be compared with the theoretical distribution.

In order to determine the CDF of the received signal envelope, the number of samples, N, can be counted below each level. These levels can be plotted on Rayleigh paper which produces a straight line for the Rayleigh distribution.

Rician Distribution: $P(r) = r/b_o \exp[(-r^2 + Q^2)/2b_o] \, I_o(rQ/b_o)$

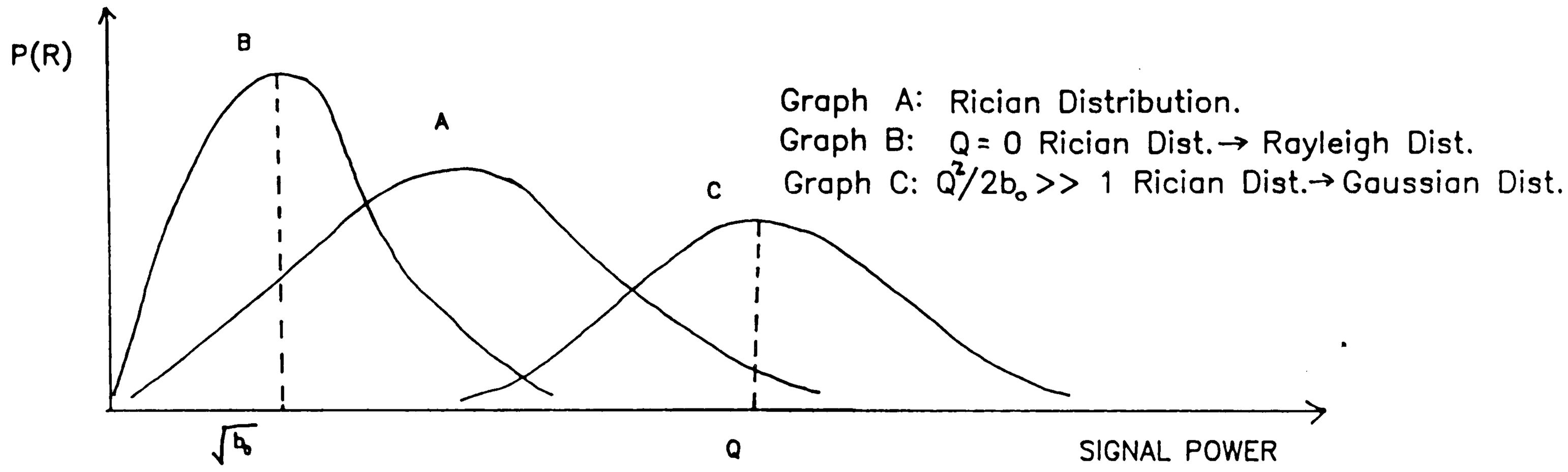

Graph A: Rician Distribution.
Graph B: $Q = 0$ Rician Dist. → Rayleigh Dist.
Graph C: $Q^2/2b_o >> 1$ Rician Dist. → Gaussian Dist.

FIG. 3.9 RICIAN DISTRIBUTION.

3.2.4 Level Crossing Rate and Duration of Fades.

The PDF and CDF are both first order statistics and by definition are not functions of time. The PDF and CDF of the Rayleigh distribution are related to non-direct wave components whereas for the Rician distribution, they are related to non-direct waves plus a direct component. Second order statistics are functions of time, and examples are the level crossing rate and the average duration of fades. For the mobile radio situation in which waves are assumed to arrive from all directions with equal probability, and for Rayleigh fading, it can be shown that the level crossing rate of the electric field component is given by [3]

$$N(R) = \sqrt{\frac{\pi}{b_0}}\, f_m R. \exp\left[\frac{-R^2}{2b_0}\right] \qquad (3.10)$$

From equation 3.10, it can be seen that the number of crossings per second depends on the mobile speed due to the presence of the Doppler Shift, f_m. For the same mobile speed, the level crossing rate is directly proportional to the carrier frequency.

By dividing the cumulative distribution (i.e. the total fraction of time that the envelope r is below a given level) by the crossing rate, N(R), the average fade duration is obtained. Therefore the average duration of a fade below R is P(R)/N(R)

$$= \frac{1 - \exp\left(-\frac{R^2}{2b_0}\right)}{N(R)} \qquad (3.11)$$

By substituing for N(R), the average duration of fades below any level R is

$$\sqrt{\frac{b_0}{\pi}}\left[\frac{\exp\left(\frac{R^2}{2b_0}\right) - 1}{f_m R}\right] \qquad (3.12)$$

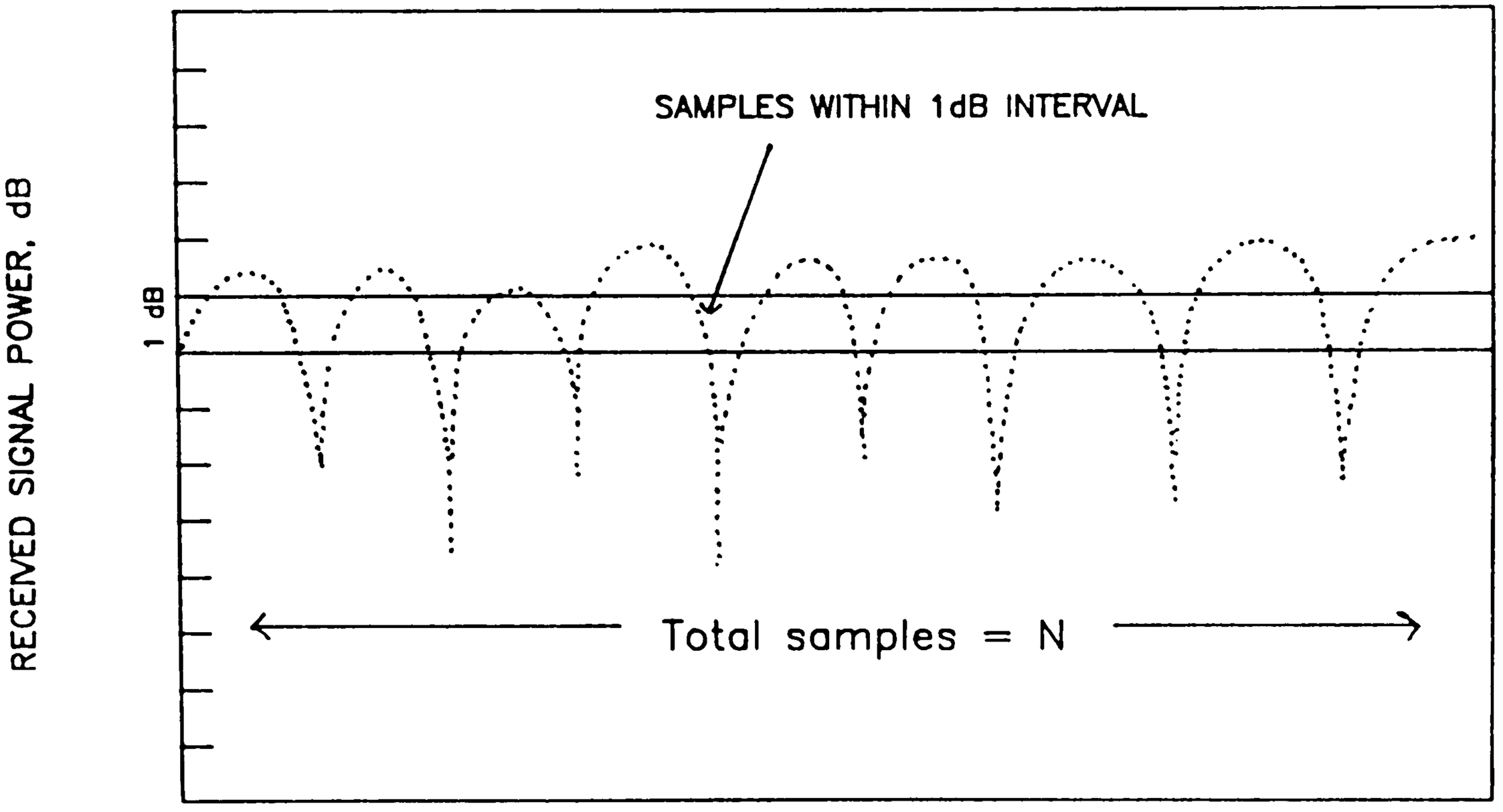

FIG. 3.10 THE TYPICAL STEPS FOR OBTAINING THE PDF AND CDF.

From equation 3.12 it can be seen that the fade duration at a constant mobile speed is inversely proportional to the carrier frequency.

3.2.5 RF and Baseband Power Spectrum of Fading Signal.

The RF power spectrum of the electric field component for vertical polarisation is theoretically given by [3]

$$S_{Ez}(f) = \frac{3b}{2\pi f_m \sqrt{1 - \left[\frac{f - f_t}{f_m}\right]^2}} \qquad (3.13)$$

where f_m is the maximum doppler shift, f_t is the transmitted frequency and b is the average power that would be received by an isotropic aerial.

The spectrum of a single frequency component received via multipath propagation is shown in figure 3.11a. It is centred at the transmitted carrier frequency and has a bandwidth of twice the maximum doppler shift. The additional presence of a direct component appears in the R.F spectrum as a single frequency (the line in figure 3.11b). The frequency of this is that of the doppler shifted transmitted frequency.

The spectrum of the received signal envelope is given by [3]

$$S_{Ez}(f) = \frac{b_o}{8\pi f_m} K\left[\sqrt{1 - \left[\frac{f}{2f_m}\right]^2}\right] \qquad (3.14)$$

where b_0 is the average power, f_m is the maximum doppler shift and K(x) is the complete elliptic integral of the first kind. This is a baseband spectrum as shown in figure 3.12a and shows that a sharp cut-off frequency exists at twice the maximum doppler frequency. This implies that the maximum doppler frequency, and therefore

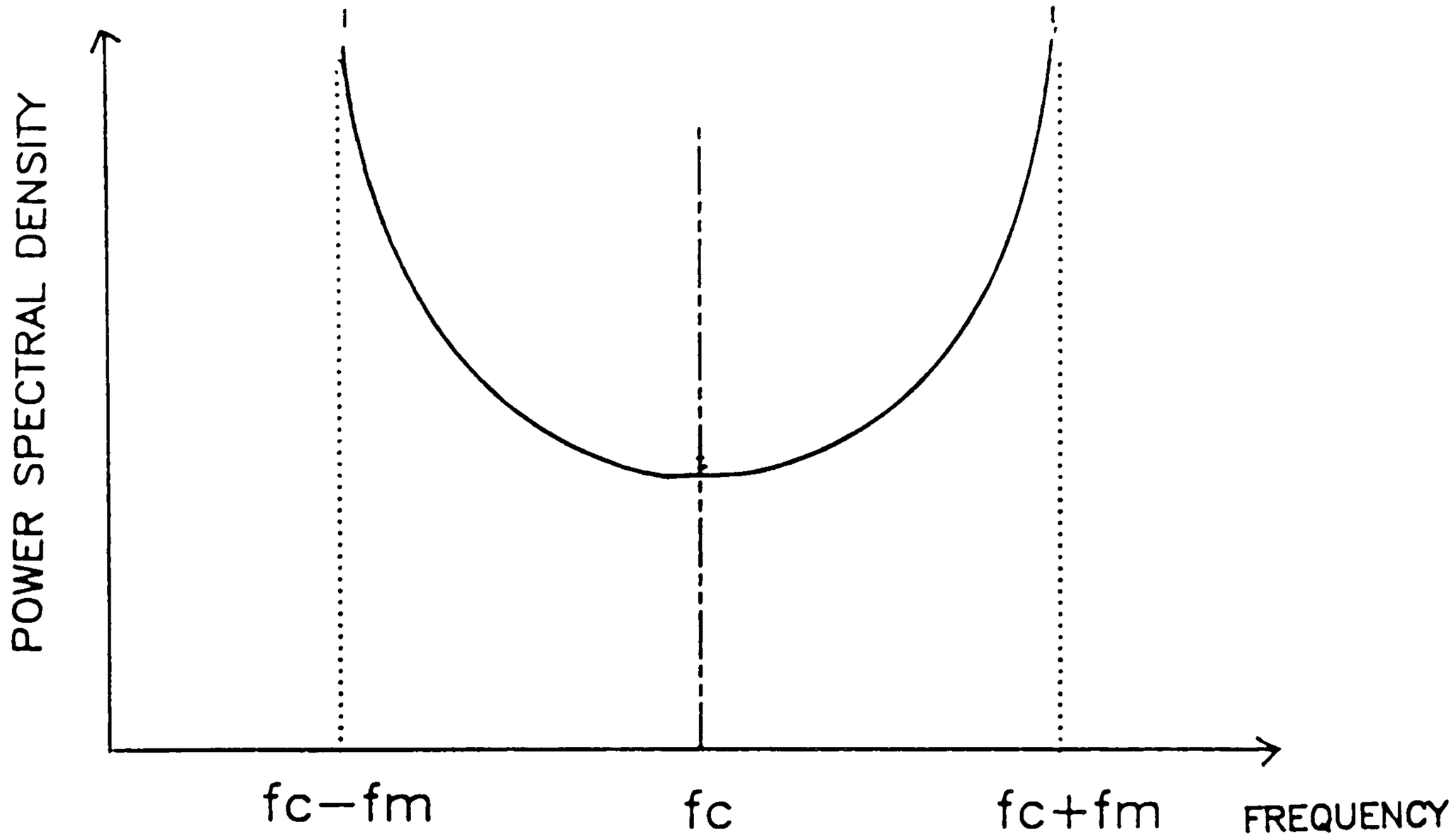

(a)

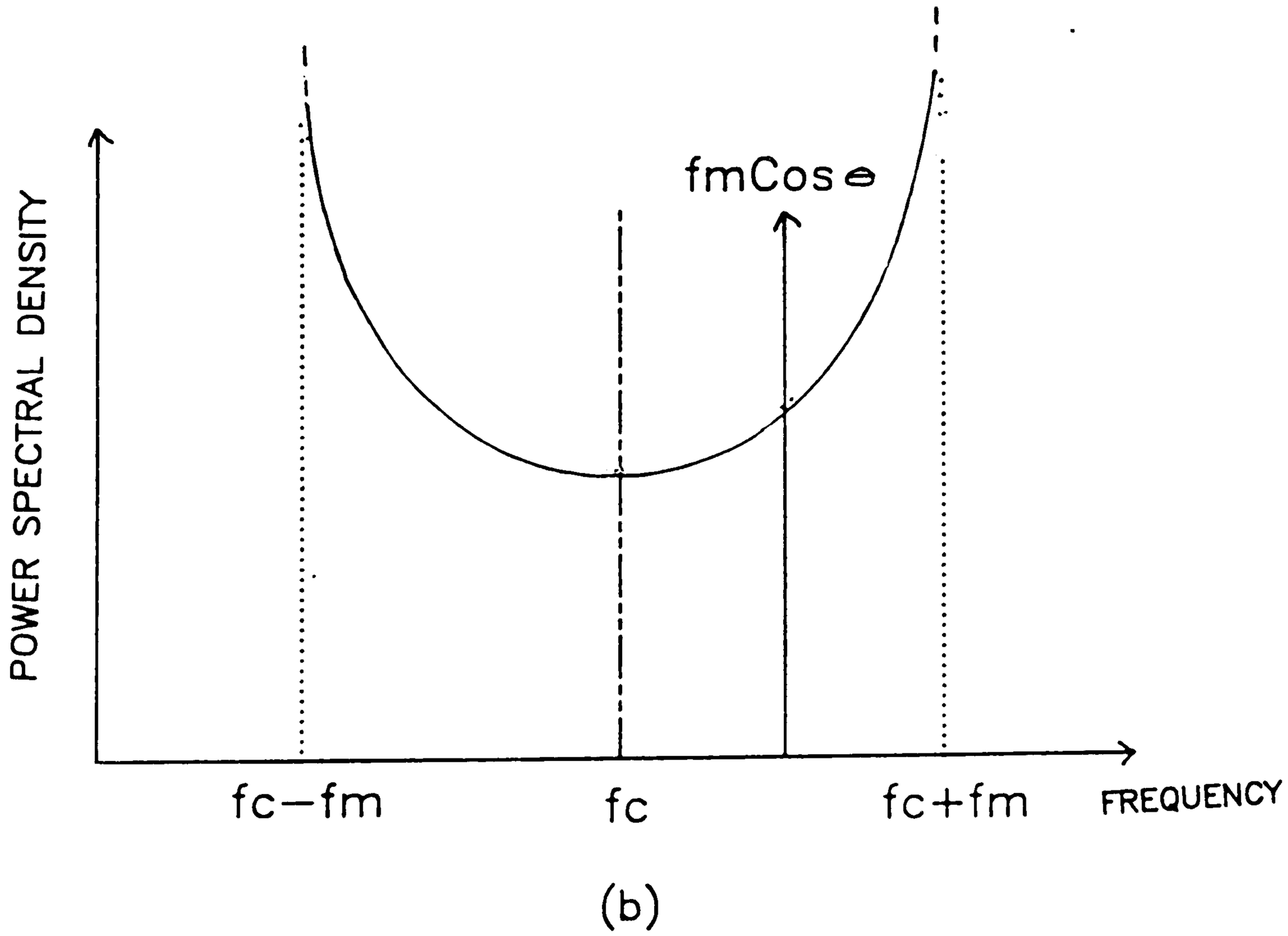

(b)

FIG. 3.11 R.F. POWER SPECTRAL DENSITY.
(a) WITH NO LOS PATH.
(b) WITH A LOS PATH.

the mobile speed, is constant. However, if the mobile speed and therefore f_m varies, the resulting spectrum will appear smeared and will not show a clearly defined cut-off frequency.

The presence of a direct component in the received signal alters the spectral shaping as shown in figure 3.12b, and results in two distinct peaks occurring at frequencies $f = f_m(1 +/- \cos\theta)$ where θ is the angle of arrival of the direct wave relative to the direction of motion of the mobile.

3.2.6 Effect of Multipath Fading.

In the fading environment, the receiver will experience difficulty in receiving information undistorted. The fast amplitude variations severely impair the quality of the signal being received. Amplitude modulated signals under fading conditions suffer multiplicative modulation by the fading waveform. This can be reduced by using AGC, which detects the amplitude of the carrier and feeds this back to change the gain of the RF and/or IF amplifiers. However, AGC is not very effective at removing fast fades, because the feedback loop tends to become unstable if the speed of the AGC is increased.

The rapid fading tends to eliminate the capture properties of frequency modulation systems. In addition, doppler shifts result in random FM, and the deeper fades usually coincide with rapid phase changes which produce demodulated frequency components greater than the theoretical maximum doppler shift. Also the fading causes a random capture of the F.M. receiver, resulting in increased baseband noise. Furthermore, the effect of multipath fading depends largely on the speed of the mobile receiver. The higher the speed, the faster the fading.

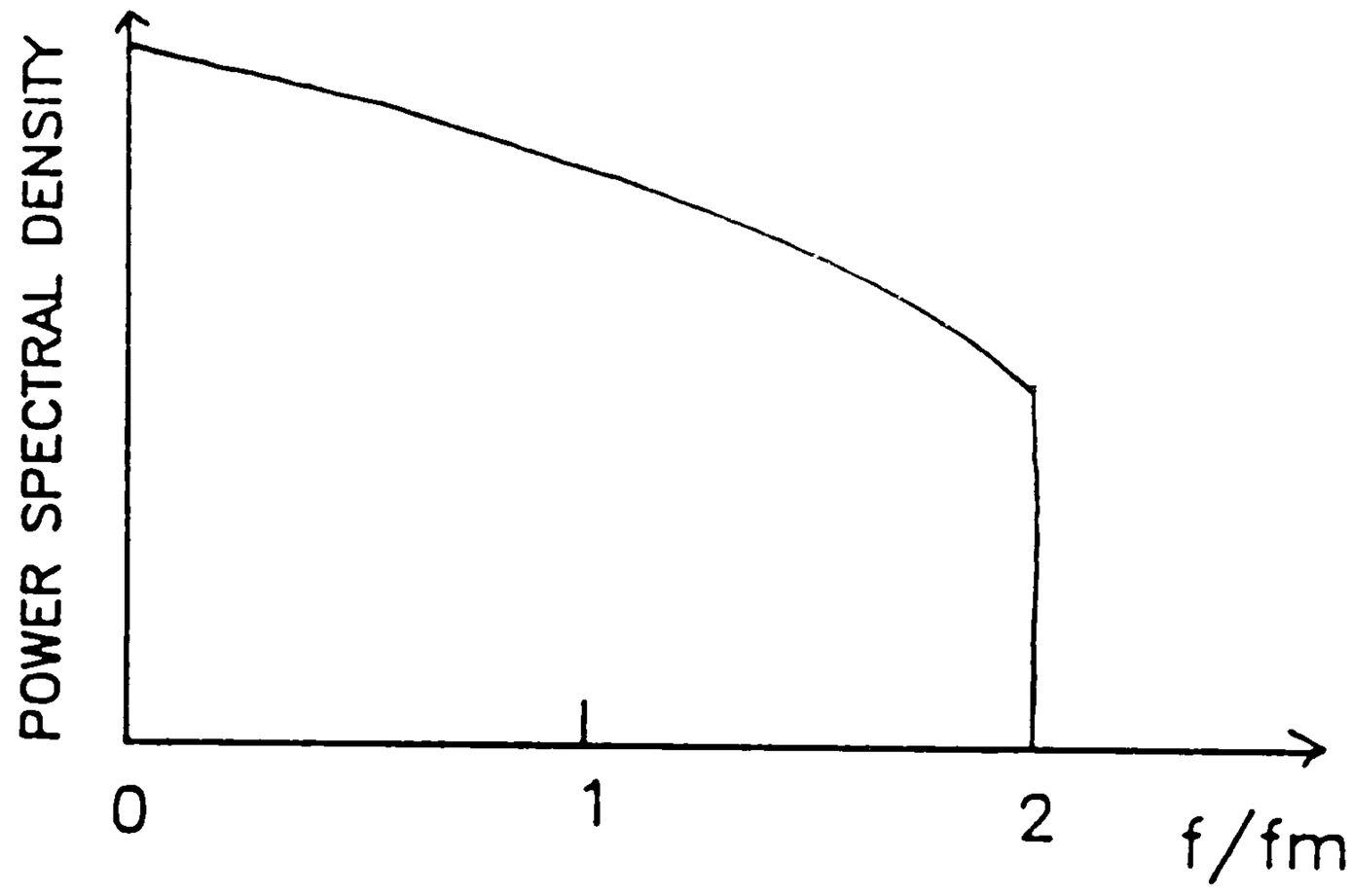

(a)

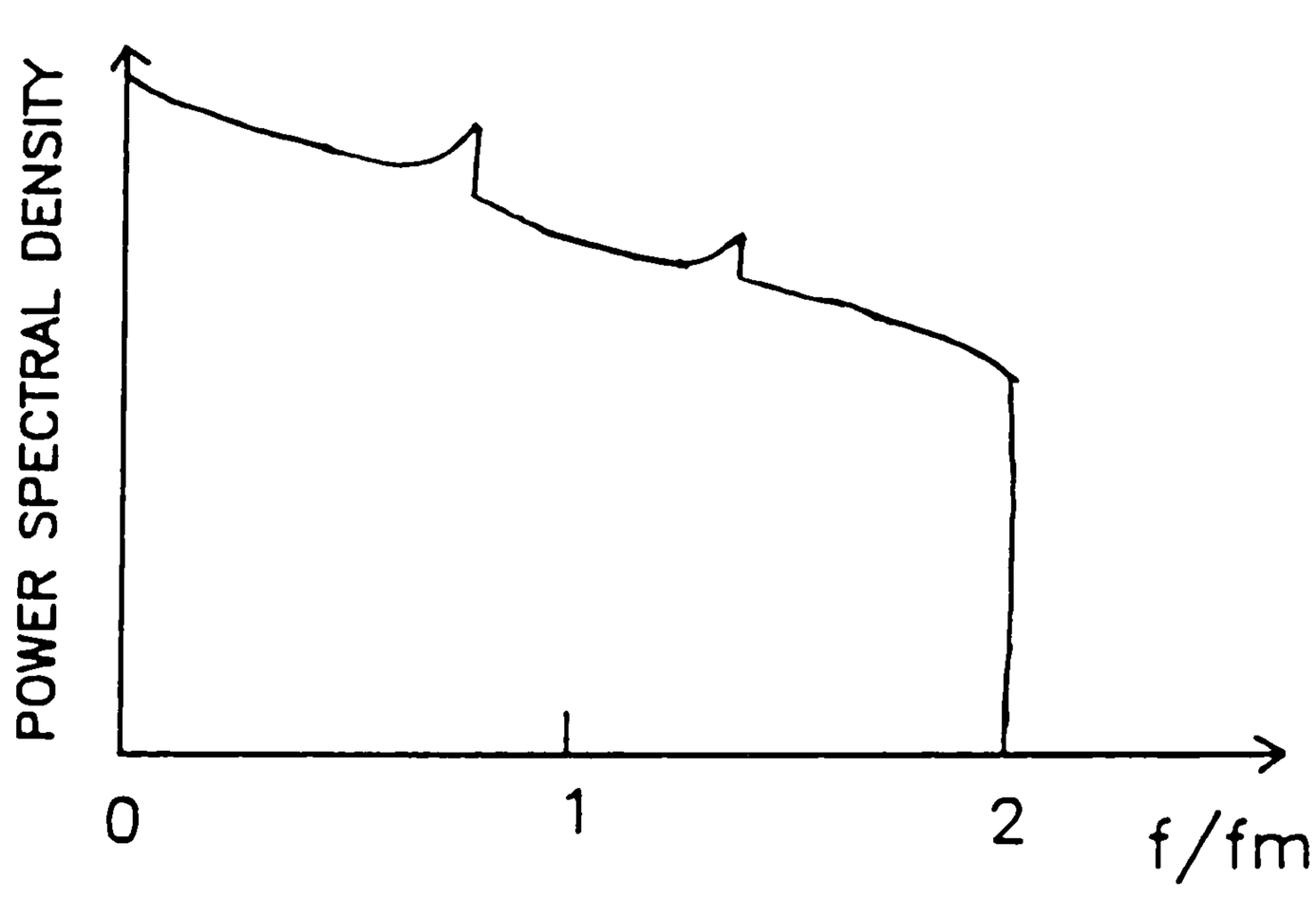

(b)

FIG. 3.12 BASEBAND POWER SPECTRUM OF THE ENVELOPE.

(a) NO DIRECT COMPONENT.
(b) WITH DIRECT COMPONENT.

3.3 PROPAGATION PATH LOSS.

3.3.1 Received Signal Power in Freespace.

In the absence of obstacles blocking the line-of-sight radio path, the power received by an aerial separated a distance d from a transmitting aerial is given by [6]

$$P_r = P_t \left[\frac{\lambda}{4\pi d}\right]^2 G_t . G_r \qquad (3.15)$$

where P_t is the transmitted power, P_r is the received power, G_t is the gain of the transmitting aerial, G_r is the gain of the receiving aerial and λ is the wavelength.

Therefore, the freespace propagation power loss experienced by a signal is proportional to the square of the frequency, and to the square of the distance. However, even in a simple idealised model of mobile propagation, the earth's surface must be taken into account. The radio waves are modified by the ground due to ground reflections, so that the propagation path loss is usually greater than would be expected in free space.

3.3.2 Received Signal Power in freespace with Ground Reflection.

Consider propagation over a flat earth with no obstructions between the transmitter and receiver, such that a direct and a reflected component of equal magnitude are present (figure 3.13). These two components interfere, so the resultant signal amplitude depends on their relative phases. This simple model will later be developed into a more representive model for 60GHz propagation.

From equation 3.15, modified to take the reflected component into account [3],

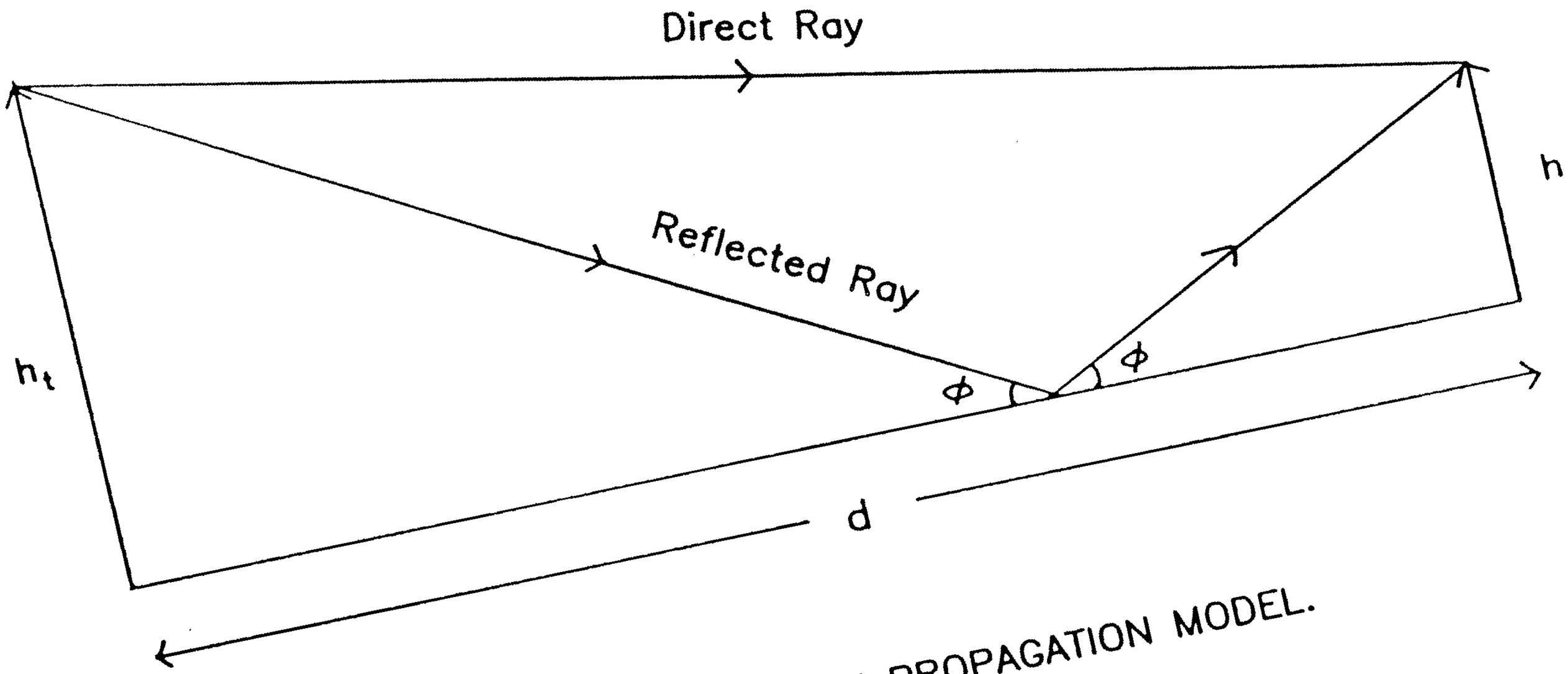

FIG. 3.13 FLAT EARTH PROPAGATION MODEL.

$$P_r = \frac{P_t . G_t . G_r}{\left(\frac{4\pi d}{\lambda}\right)^2} \cdot 4.\sin^2\left(\frac{2\pi h_t h_r}{\lambda d}\right) \qquad (3.16)$$

where h_t is the height of the transmitter and h_r is the height of the receiver.

At UHF, where a large cell radius is used, the received power is often assumed to be proportional to $1/d^4$. This can be shown to be true with the following example.

Assume that the height of the transmitting aerial (h_t) is 30m, the height of the receiving aerial (h_r) is 1.5m and the distance (d) between the transmitter and the receiver is 5km. These are typical values for a 900MHz cellular radio system. In this case the argument of the sine term of equation 3.16 is small (equal to 0.17), so

$$Sin\left(\frac{2\pi h_t h_r}{\lambda d}\right) \simeq \left(\frac{2\pi h_t h_r}{\lambda d}\right) \qquad (3.17)$$

Substituting this in equation 3.16,

$$P_r = \frac{P_t . G_r . G_t}{\left(\frac{4\pi d}{\lambda}\right)^2} . 4. \left(\frac{2\pi h_t h_r}{\lambda d}\right)^2 \propto \frac{1}{d^4} \qquad (3.18)$$

Thus, when the distance d is large, the received signal power should be proportional to $1/d^4$. Practical measurements have approximately confirmed this. Field measurements near 900MHz in three different cities made by independent workers in Kanto and Tokyo [7], New York [2], and Philadelphia [8], showed that the propagation loss was proportional to $1/d^{\alpha}$, where α was always less than 4 and greater than 2 and was dependent upon the distance d relative to the base-station aerial height. For example, Black [8] found that the median signal power tends to fall off as $1/d^3$ (i.e $\alpha = 3$) for distances greater than 1 to 2 miles from the base

station aerial. Generally, the propagation exponent is dependent on the nature of the earth and usually has a value of 3.2 to 3.8.

A comparison can be made theoretically at 60GHz with h_t equal to 8m (lamp post height), h_r equal to 1.5m, and d equal to 1km (about the maximum achievable without excessive attenuation due to oxygen). The argument of the sine term of equation 3.14 (equal to 15) is no longer small even at this large transmission distance, so the $1/d^4$ power law is not applicable at 60GHz.

A graph of received power against distance would be of the form shown in figure 3.14. The maxima are due to constructive interference between the direct and reflected components, and the minima are due to destructive interference between them. In practice, infinite attenuation does not occur at the minima because the reflection coefficient of the ground, i.e., the ratio of direct and reflected E-field components, is less than unity. At 60GHz, this is due to the surface roughness of the ground, which is appreciable compared with 5mm wavelength, and due to low ground conductivity. In order to determine whether the surface will give specular reflection, the Rayleigh criterion can be used, which is given by [3]

$$C = \frac{4\pi\sigma\phi}{\lambda} \qquad (3.19)$$

where σ is the standard deviation of the surface irregularities and ϕ is the angle in radians between the incident wave and the surface. Experimental evidence [11] suggests that if C is less than 0.1, then there is specular reflection and the surface can be considered smooth, while if C is greater than 10, the surface is considered to be rough, so the reflected wave is almost insignificant. A low reflection coefficient

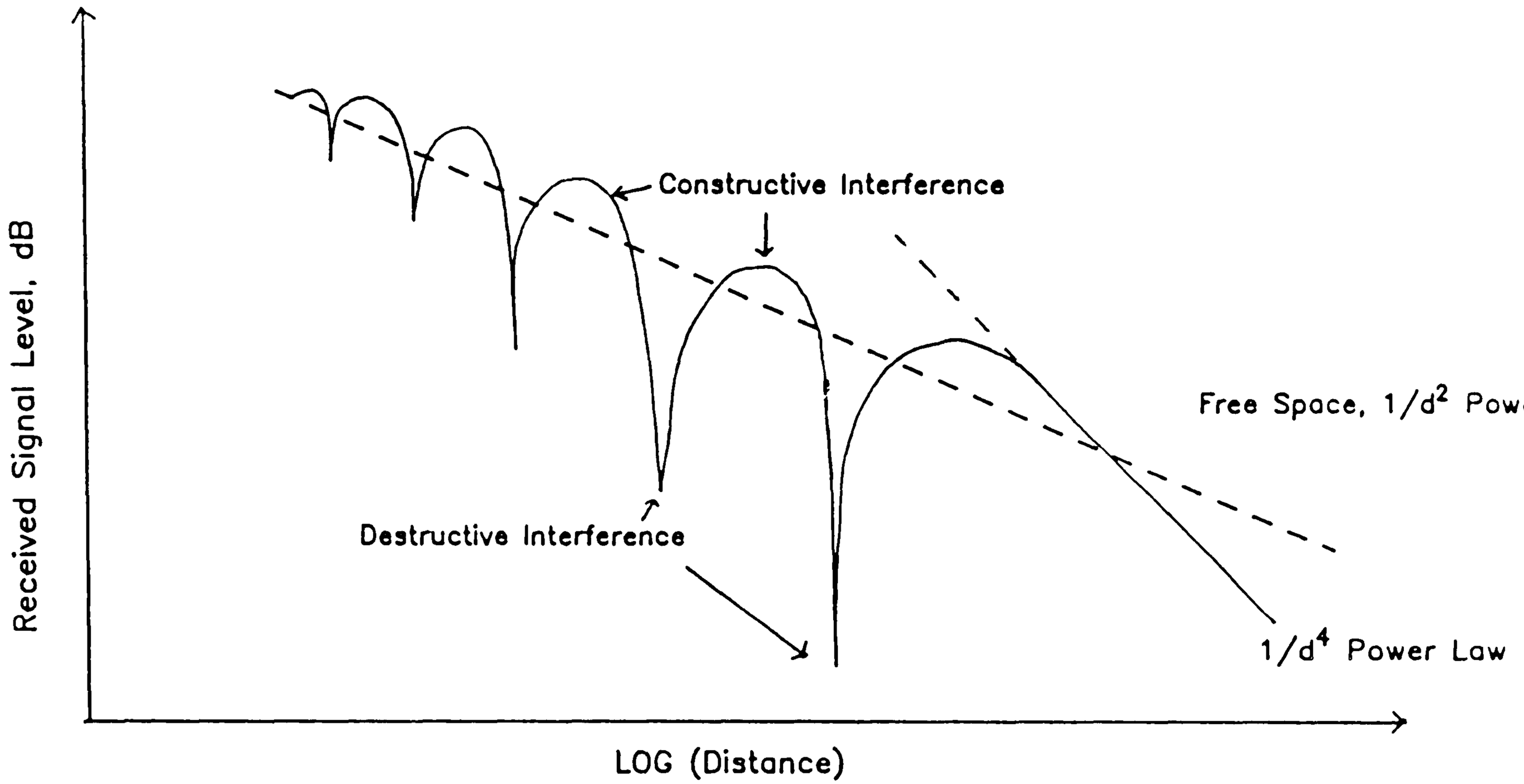

FIG. 3.14 PLOT OF RECEIVED SIGNAL POWER VS DISTANCE FOR THE FLAT EARTH PROPAGATION MODEL.

is desirable because it results in a higher received power level, hence a higher SNR, at positions of destructive interference.

3.3.3 Received Signal Power and SNR with Obstructions and Oxygen Absorption.

If the reflected component is assumed to be negligible, a $1/d^2$ power law results given by equation 3.15. If in addition to this law, the absorption due to oxygen and rain [section 2.1] is included, as well as an obstruction attenuation factor, a, the received power is given by

$$P_r = \frac{G_t . G_r . P_t}{\left(\frac{4\pi d}{\lambda}\right)^2} . \exp(-k_0 d) . \exp(-k_r d) . a \qquad (3.20)$$

where k_0 is the oxygen attenuation in nepers/m and k_r is the rain attenuation in neper/m. In dB's with λ = 5mm at 60GHz,

$$P_r = P_t(\text{dBW}) + G_r(\text{dB}) + G_t(\text{dB}) - 20\log_{10} d(\text{km}) - (K_r + K_0)(\text{dB/km})d.(\text{km}) - A(\text{dB}) - 128. \qquad (3.21)$$

where K_0 is the oxygen attenuation in dB/km, K_r is the rain attenuation in dB/km and A is the obstruction attenuation factor in dB.

To find the signal to noise ratio (SNR), the received noise power must be evaluated, which is given by [4]

$$N_r = 10\log_{10} (kT_a B) \qquad (3.22)$$

where k is Boltzman's constant (1.38×10^{-23} J/K), T_a is the aerial noise temperature (approximately 290K at 60GHz) and B_n is the noise bandwidth (Hz) of the receiver IF. Thus

$$N_r = -204 + 10\log_{10} B_n \text{ (dBW)} \qquad (3.23)$$

Taking a noise figure, F into account, the SNR is,

$$SNR = P_r - (N_r + F)$$

$$\therefore \quad SNR = P_t + G_t + G_r - 20\log d(km) - (K_r + K_0)d - A_0 - F$$
$$- 10\log_{10} B_n + 76 \qquad (3.24)$$

3.3.4 Example Calculation of the Received SNR for a Non-Phase-Locked System

In order to find the theoretical mean received signal to noise ratio as a function of distance at 60GHz under worst case conditions, the following typical figures applicable to a simple and relatively inexpensive non-phase-locked system may be assumed. P_t=-20dBW (10mW), G_t=G_r=8dB, (This results in an elevation beamwidth of approximately 20^0 from an omnidirectional aerial. A narrower beamwidth may cause problems if the mobile transceiver is held at an angle). Also, assume K_r=10dB/km (for a rainfall rate of 25mm/hr as given in section 2.1), K_o=16dB/km, F=10dB and B_n=2MHz (a smaller bandwidth would result in problems due to frequency drifting)

From equation 3.24

$$SNR = -20 + 8 + 8 - 20\log_{10} d(km) - (16 + 10)d(km)$$
$$- A_0 - 10 - 63 + 76$$

$$\therefore \quad SNR = -20\log_{10} d(km) - 26d(km) - A_0 - 1 \qquad (3.25)$$

This equation is plotted in figure 3.15 as a graph of SNR against distance. Assuming a minimum SNR of 20dB for an acceptable bit error rate (such a high value is needed because of the degradation caused by fast fading), the maximum transmission distance possible is about 70m. If the attenuation factor due to obstructions, A_0, is 30dB, the distance becomes only 3m. It can therefore be assumed that successful reception outdoors over a long distance requires a LOS or near LOS path (small angle diffraction or a strong reflection around obstacles). In order to fulfil this portable communications application in a large and crowded city with fairly randomly arranged streets for each service area, many fixed radio ports would be required, i.e., base station diversity would be necessary. Improvements could be made by increasing the transmitted power to 100mW (a 10dB improvement) reducing the noise figure to 4dB (a 6dB improvement achieved by using a low noise 60GHz amplifier which may become available with future devices) and by using phase-locked tranceivers, which would allow a smaller receiver IF bandwidth, and therefore a lower noise level to be achieved.

For LOS fixed links at 60GHz, the received signal power should be more than sufficient, especially if high gain aerials are used. A parabolic reflector aerial has a gain of 40dB for a parabola diameter of only about 20cm at 60GHz, making the system easily transportable. The transmitted power could be substantially reduced, whilst the transmission distance could be increased. The advantage of 60GHz over other frequencies for LOS links is that the 13 to 16dB/km oxygen absorption (invariant with weather conditions) minimises co-channel interference problems, even when the same frequency is reused only a few km away. [12] At frequencies where high atmospheric absorption is not present, under certain weather conditions, which create refraction and ducting effects in the atmosphere,

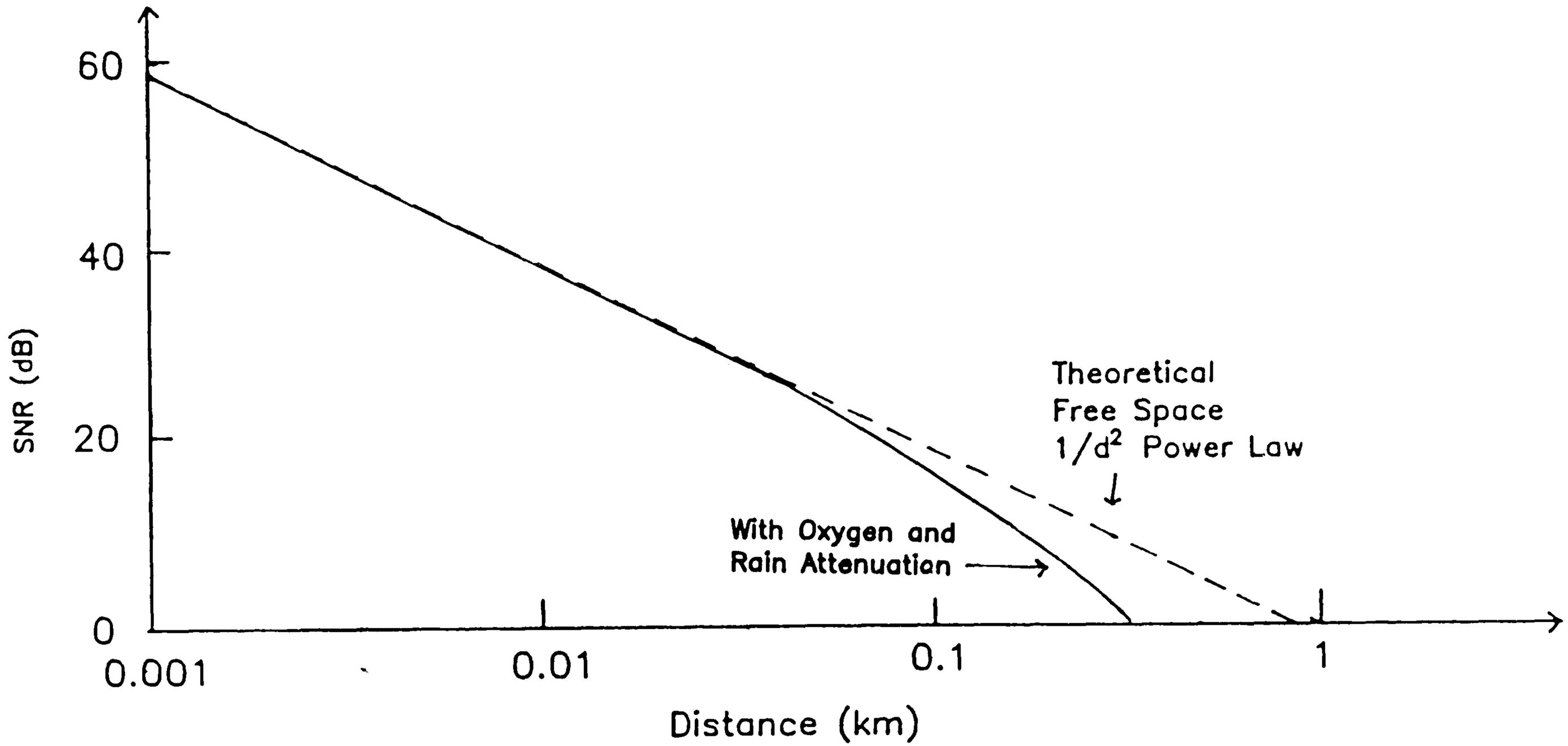

FIG. 3.15 PLOT OF SNR AGAINST DISTANCE FOR THE EXAMPLE CALCULATION

microwave signals can be strongly received from distant co-channel transmitters, which can block the wanted transmission. This cannot happen at 60GHz because beyond a few km's, the oxygen absorption loss is very high and is virtually independent of weather conditions, so the co-channel interference from distant transmitters is negligible.

3.3.5 Obtaining Mean Received Signal Power data from Measurements.

The mean received signal power can be determined by averaging the signal power data to obtain a local mean at each particular distance. The speed of the mobile must be constant so that the time axis can be linearly changed to the distance axis (distance = velocity x time). If the mobile unit does not maintain constant speed while receiving the signal, information of distance or speed versus time has to be recorded.

It has been stated earlier that the received signal envelope when the mobile is in motion consists of a fast fading signal superimposed on a slow fading component. It has been demonstrated experimentally, at VHF and UHF, that the slow fading has a log-normal distribution especially when the observation distance is greater than approximately 1km [7],[8].

The local mean of a long piece of raw data depends on many factor such as the distance from the transmitter, the nature and type of the environment, the orientation and width of the street etc. The process is non-stationary and can be considered as stationary only over a small distance of between 20λ to 40λ [9] where factors influencing the local mean remain virtually unchanged. The local mean can be obtained by averaging the received signal power over a length L which can be treated as an averaging window over the raw data as shown in figure 3.16. If the

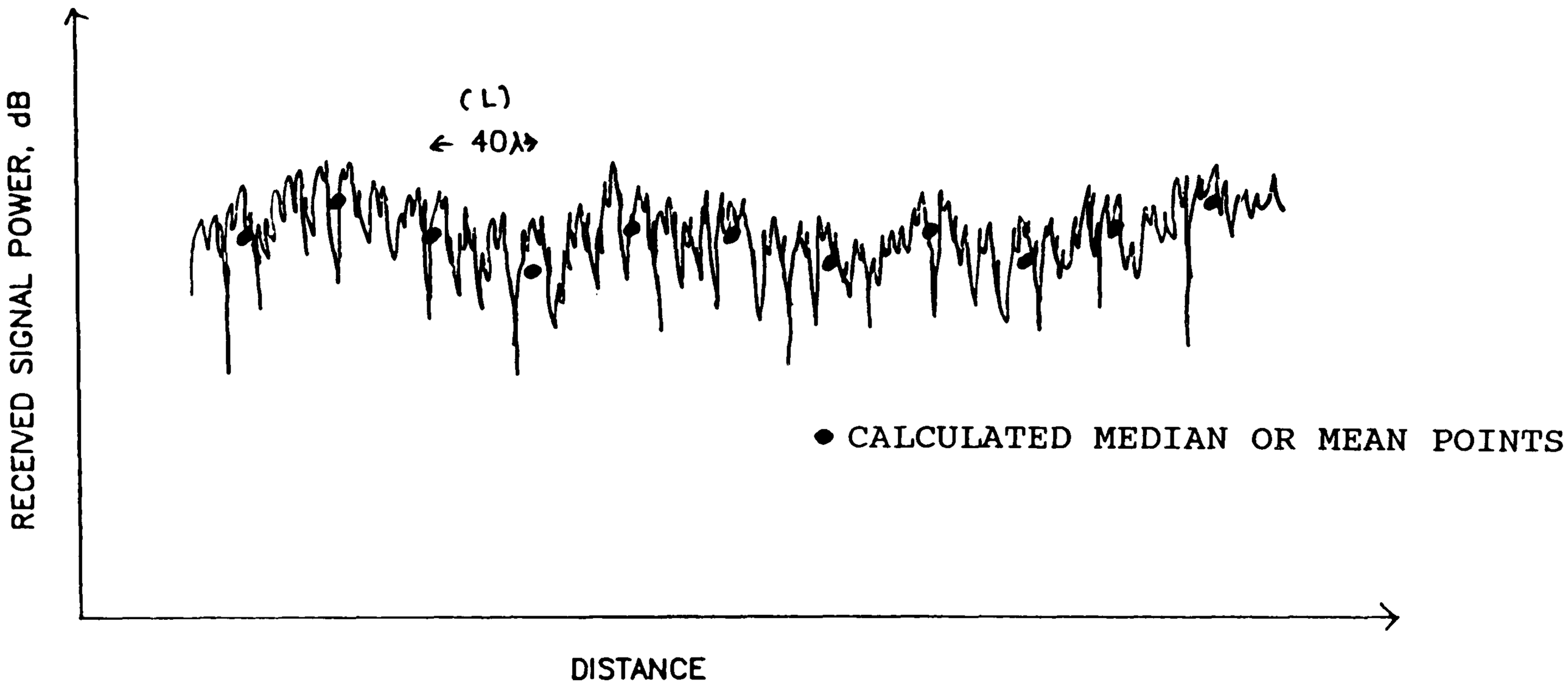

FIG. 3.16 OBTAINING THE LOCAL MEAN OR MEDIAN.

length L is too long, some of the variations of the long term fading will be smoothed out, whereas if it is too short, the short term variations will not be sufficiently smoothed out. A compromise must therefore be reached in choosing the averaging length, and [9] states that 40λ is a good choice.

Since most data processing is done digitally, it is necessary to find the number of samples required over the length of 40λ. It has been found that at least 50 samples are needed to be 90% certain of being within 1dB of the true mean [9]. If N is reduced to 36, this increases to 1.17 dB. If more samples are taken, the accuracy improves, but it is necessary to store and process more data, which can be a problem when using a small computer.

In order to determine the median propagation exponent of the received signal power, the median signal power can be computed over 40λ. If the median signal power is in dB (10logP) and is plotted against the log of distance, the propagation exponent can be found from a straight line approximation to the plot. The propagation exponent, x, (for the propagation law $1/d^x$) is given by -(slope of line)/10.

3.4 EDGE DIFFRACTION.

If electromagnetic waves hit the edge of an obstructing object, a certain amount of power is diffracted into the geometrical shadow region. Fig. 3.17 illustrates knife edge diffraction where a perfectly conducting knife edge is placed between the transmitter and receiver and all ground obstructions are ignored.

The field strength, F(u), received by an aerial placed at point P behind the knife edge is the vector sum of all the contributions from the Huygen secondary

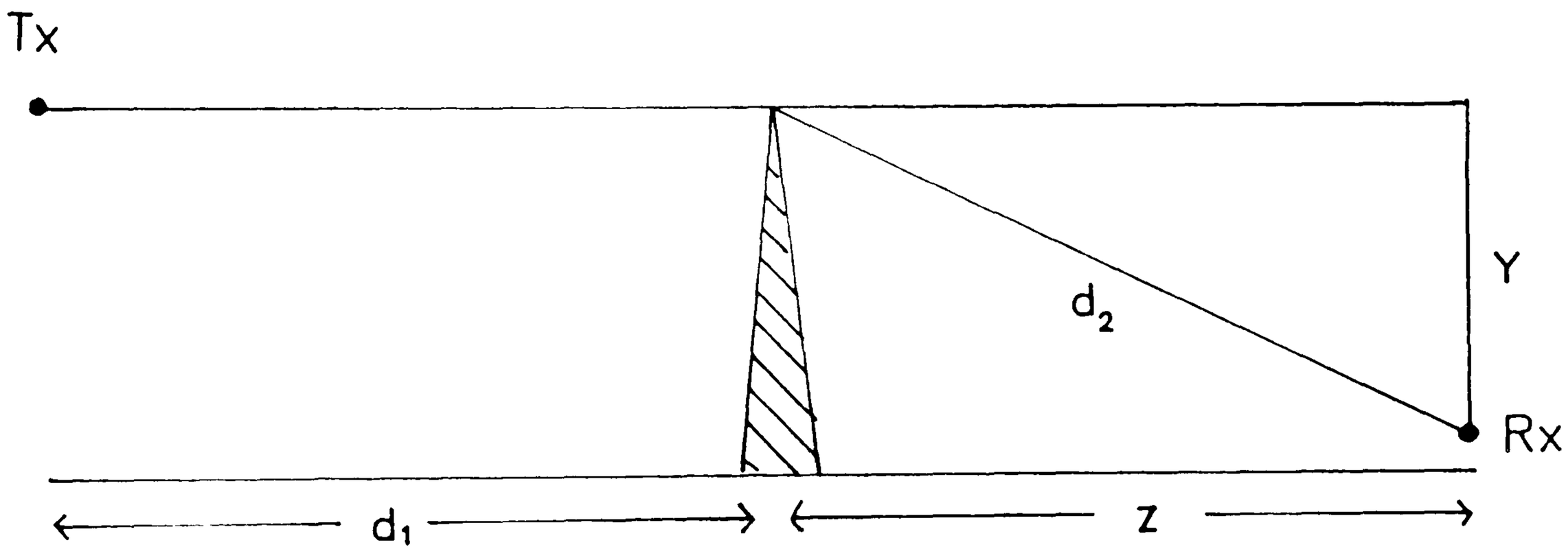

FIG. 3.17 KNIFE EDGE DIFFRACTION.

sources in the half plane above the edge. The mathematical solution to this yields the fresnel integral in terms of u, where u is the Fresnel parameter given by [13]

$$u = Y\sqrt{\frac{2d_1}{\lambda(d_1 + z)z}} \qquad (3.26)$$

Fig. 3.18 shows the graph of the solution of the integral which can be obtained by a numerical method.

When there is a LOS path between the transmitter and receiver, the edge diffraction effects have very little influence on the received signal power. As the receiver moves from LOS into the geometrical shadow region, the received signal begins to fluctuate and reaches a maximum at u =-1.25. When the obstructing edge is just in line with the transmitter and receiver (u=0), the lower half of the incident beam is blocked, and the received signal power is reduced by 6dB. As the receiving aerial is moved into the geometrical shadow region, the received signal power decreases rapidly.

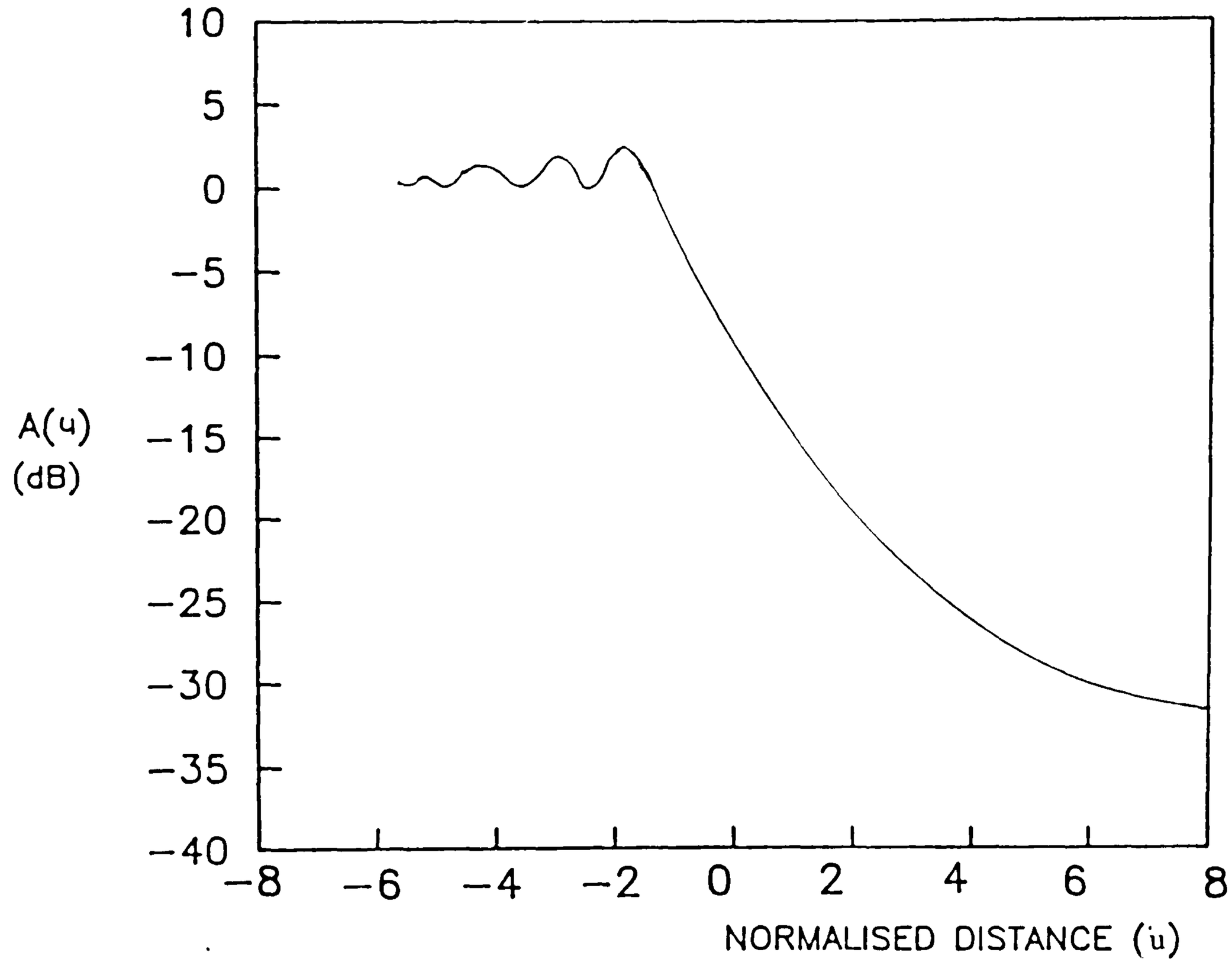

FIG. 3.18 KNIFE–EDGE DIFFRACTION LOSS.

REFERENCES.

[1]. Nylund, H.W., "Characteristics of small-area signal fading on mobile circuits in 150 MHz band," IEEE Trans. on Veh. Tech. VT-17, pp. 24-30, Oct. 1968.

[2]. Young, W.R. Jnr, "Comparison of mobile radio transmission at 150,450,900 and 3700 MHz," BSTJ, Vol 31, pp 1068-1085, Nov. 1952.

[3] Jakes, W.C., "Microwave Mobile Communications," John Wiley, 1974.

[4] Schwartz, W.R., Bennett, W.R., Stein, S. "Communication systems and techniques," New York, McGraw Hill, 1965.

[5] Rice, S.O., "Statistical properties of a sine wave plus random noise," BSTJ, Vol. 27, Jan 1948 pp.109-157

[6] Friss, H.T., "A note on a simple transmission formula," Proc IRE, 34, May 1946.

[7] Okumura, Y., Ohmori, E., Kawano, T., and Fakuda, K., "Field strangth and its variability in VHF and UHF land-mobile radio service," Elec. Communication Lab.", Vol. 16., pp 825 - 873, Sept.- oct. 1968.

[8] Black, D.M. "Some characteristics of Mobile-Radio Properties at 836 MHz in the Philadephia Area," IEEE Trans. Veh. Technol., Vol. VT-21,pp. 45 - 51, May 1972.

[9] Lee, W. C. Y. "Estimate of Local Average Power of a mobile radio signal," IEEE Trans. on Vehicular Technology, Vol. VT-34, No. 1, February 1985, pp.22 - 27.

[10] Clarke, R.H., "Statistical Theory of Mobile Radio Reception," B.S.T.J. vol. 47, no. 6, July/August 1968, pp.2935 - 2971.

[11] Bullington, K., "Radio Propagation at Frequencies above 30 megacycles," Proc. IRE, 35, October 1947, pp.1122-1136.

[12] Steffers, P.G., and Meck, R.A., "Prototype secure millimetre communications," Microwave Systems News, October 1980.

[13] Rokkos, N., Johnson, R.A., "Diffraction of millimetre wave signals into shadow regions," CORADCOM-81-1, U.S. Army Communication Research and Development Command, Forth Mormouth, NJ 07703 (1981)

CHAPTER 4

MEASURING EQUIPMENT AND EXPERIMENTAL PROCEDURE.

4.1 NON-PHASE LOCKED SYSTEM

Initially, only non-phase-locked 60GHz oscillators were available for the transmitter and receiver which had relatively poor frequency stability. All of the outdoor measurements and a few of the indoor signal power measurements were made with these. A block diagram of the non-phase-locked system is shown in Fig. 4.1.

The transmitter consisted of an Alpha CMF 910 60GHz, 20mW Gunn Oscillator. The 60GHz receiver local oscillator, shown in fig. 4.2, had an output power of about 20mW and was based on the disc resonator Gunn Oscillator design [1] which is frequently used at millimetre wavelengths. The resonator disc is supposed to have a diameter of approximately half a wavelength (2.5mm at the resonant frequency of 60GHz). Several disc resonators were tried, and the one which gave the correct operating frequency had a diameter of 2.9mm. The disc not only acts as a resonator, but also as an impedance match, so that the available power from the Gunn diode is transferred to the waveguide. The backshort reflects power back to the waveguide and also acts as an impedance match. The quarter wavelength steps improve its reflecting properties by minimising the power that leaks through the small gaps between the backshort and the waveguide walls. The backshort was anodised to insulate it from the waveguide walls in order to prevent excessive phase noise when it was moved backwards and forwards in the waveguide for tuning purposes. The choke supplies d.c power to the Gunn diode via the disc. The dc earth return is through the metal body of the diode and the body of the oscillator. The quarter wavelength steps ensure that the end is a short circuit at 60GHz, so that no

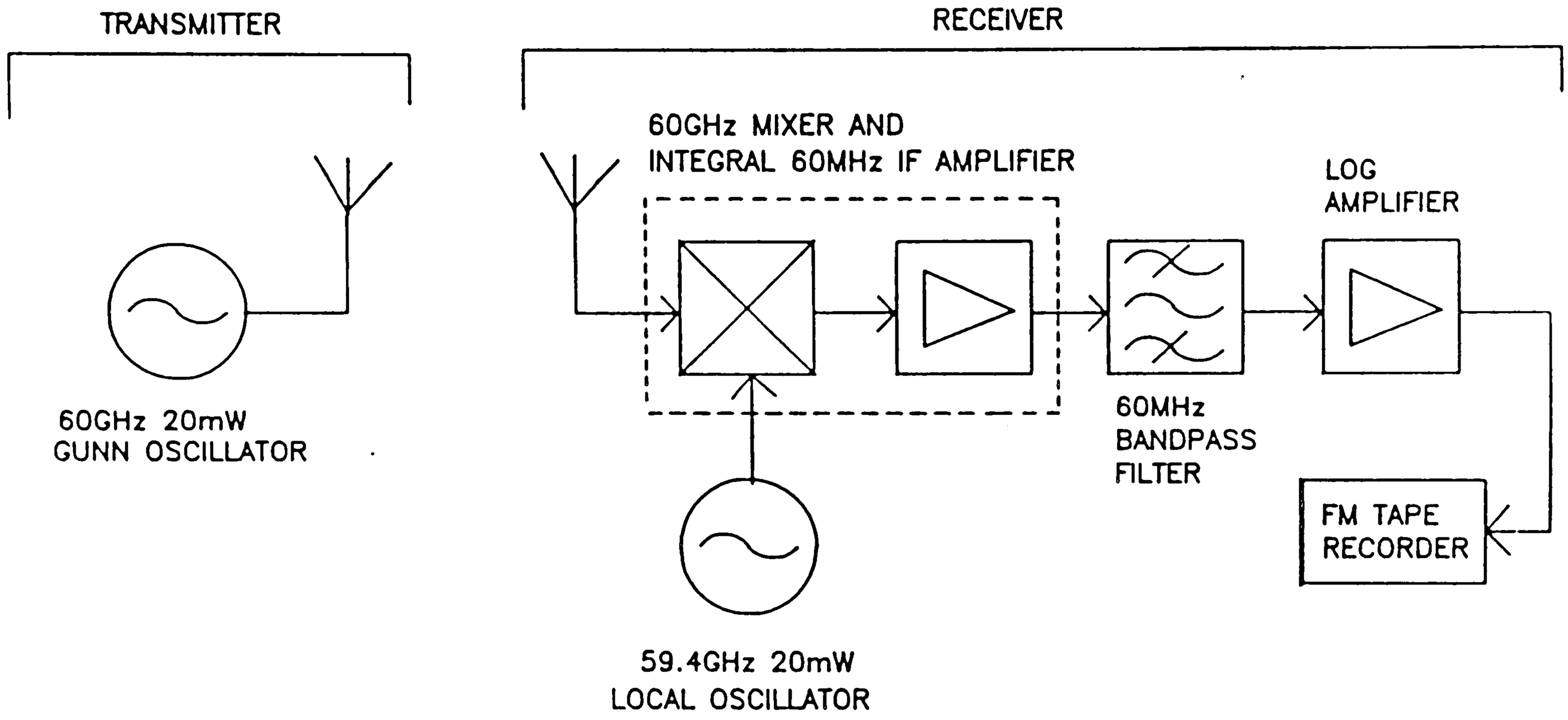

FIG. 4.1 NON–PHASE–LOCKED SYSTEM FOR PROPAGATION MEASUREMENTS.

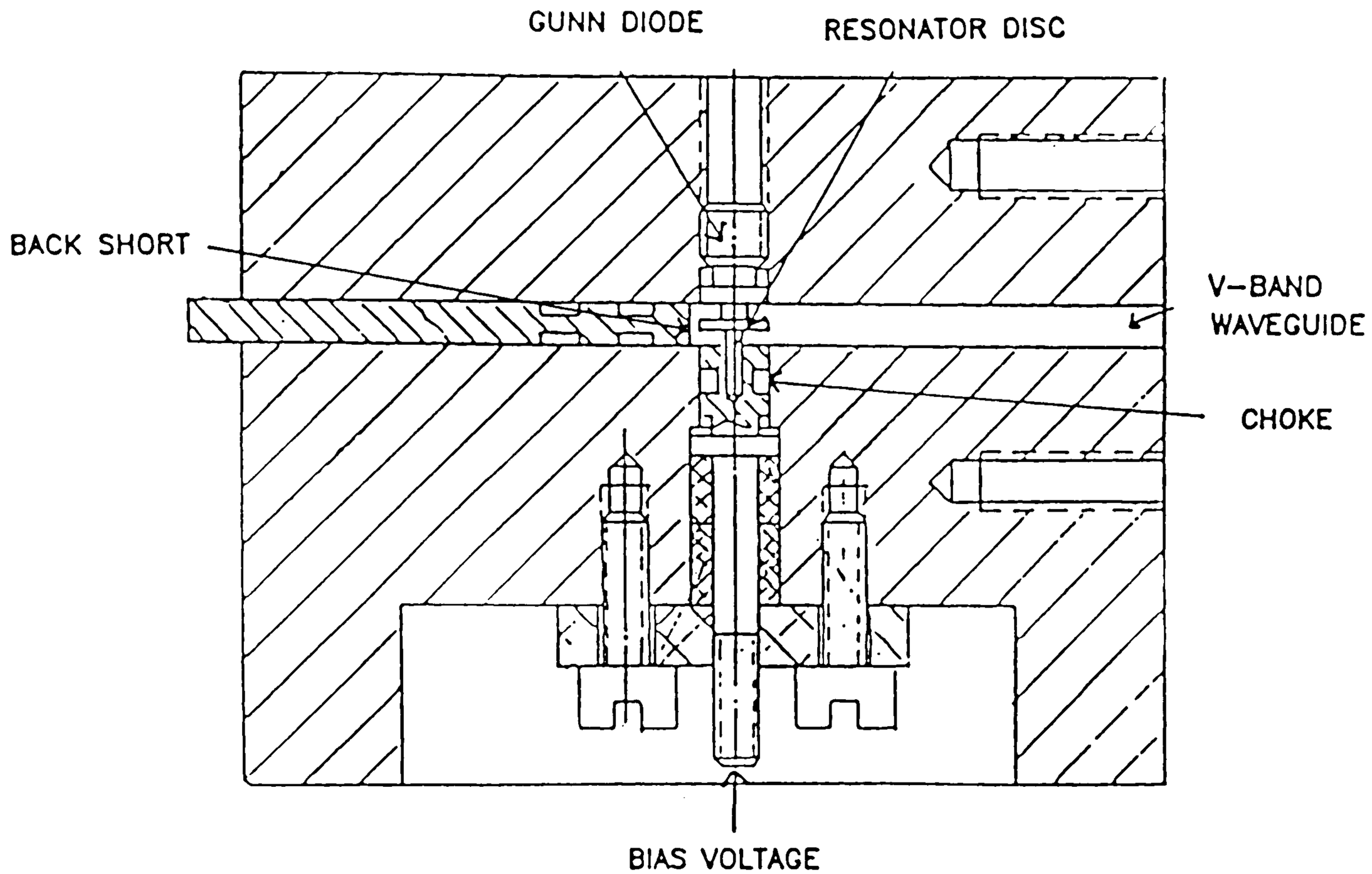

FIG. 4.2 60GHz RECEIVER GUNN OSCILLATOR.

power can pass through the small gap between the choke and its cylindrical hole. The choke was also insulated by anodising to stop the power supply from shorting.

An Alpha V9660A 60GHz single balanced mixer with a 6dB conversion loss was used to downconvert to a 60MHz IF. The exact frequencies of the 60GHz transmitter and receiver oscillators were not known, because no accurate frequency measurement equipment was available. However, this did not matter since it was only the 60MHz difference between the two oscillators that was important, because this had to be maintained within the passband of a bandpass filter. A 60GHz bandpass filter should have been used in front of the mixer to reject the image frequency twice the IF frequency (120MHz) away from the transmitted signal near 60GHz, but was not used because it would have been too difficult to make. This meant that the noise present at the image frequency was also downconverted to IF, increasing the noise level by 3dB. The 60GHz mixer was followed by a 30dB gain, 1.2dB noise figure integral IF amplifier. The output of this IF amplifier was passed through a 2nd order Butterworth bandpass filter with an insertion loss of 2.6dB and a 3dB bandwidth of 2MHz. This bandwidth was large enough to accommodate the frequency drifting of the transmitter and receiver oscillators, but was small enough to significantly reduce the wideband noise at the IF and therefore improve the sensitivity of the receiver. The output of the bandpass filter was passed through an RHG ICLT 6010 logarithmic amplifier. A log amplifier produces an output voltage proportional to the log of the signal power at its input. The output voltage is therefore proportional to the received field strength or signal power in dB. As well as having this useful feature, a log amplifier also compresses the dynamic range of its input, making it easier to record the signal on a tape recorder which has a limited dynamic range. The transfer characteristic of the log amplifier used is shown in figure 4.3, which shows an input dynamic range of 80dB, and a transfer slope

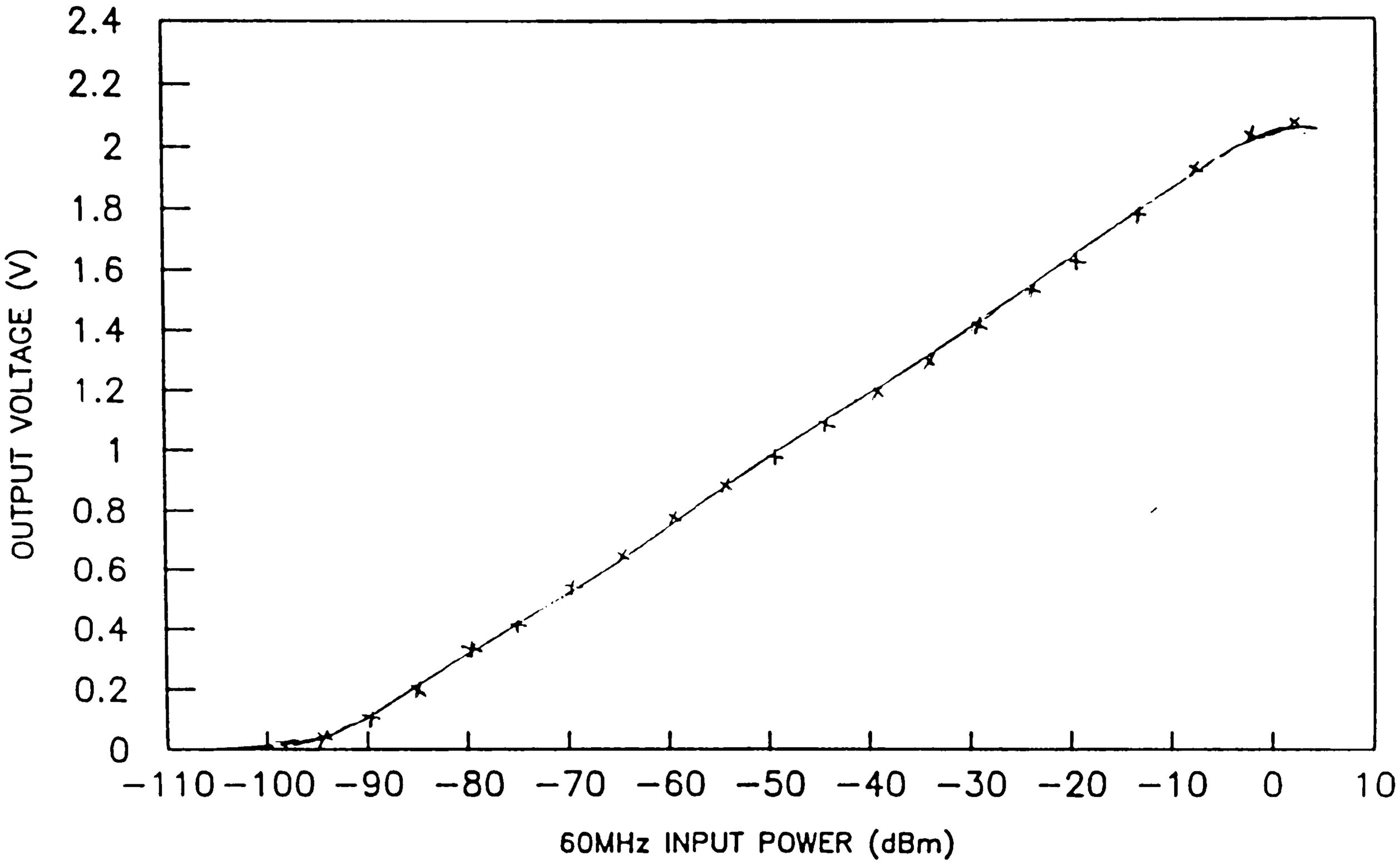

FIG. 4.3 TRANSFER CHARACTERISTIC OF LOG AMPLIFIER.

(the change in output voltage divided by the change in input signal power) of 23mV/dB. The accuracy was +/-0.5dB.

Fig 4.4 shows the overall input/output characteristic of the receiver system. The useful linear range at the input to the 60GHz mixer was from -35dBm to -105dBm, resulting in a 70dB dynamic range. Since all the analyses had to be carried out in the laboratory, the signal level had to be recorded in a suitable form for transfer after each set of measurements. Therefore, the output from the log amplifier was recorded on an FM instrumentation tape recorder (a Racal Store 4DS). An FM recorder was used because, unlike a conventional tape recorder, it can record signals down to DC. The recorder had one direct or voice (non-FM) channel which was used for making a voice commentary during the measurements. The recorded signal was digitised and analysed in the laboratory as described in section 4.4.

The transmitter and receiver had to be put in diecast boxes in order to minimise the effects of ambient temperature changes which caused frequency drifting. Tests carried out in the laboratory have demonstrated that the stability of the transmitter/receiver system was sufficient to keep the I.F signal within the pass band of the bandpass filter on an hourly basis. However, outdoors, the frequency drift rate was much higher and was dependent on the wind speed. The IF signal typically only stayed within the pass band of the bandpass filter for 10 to 20 minutes. When fine tuning was necessary, this was accomplished by a small change of power supply voltage to the receiver Gunn Oscillator.

The measurements with the non-phase-locked sources were performed on the amplitude rather than the phase of the received signal. An analysis of the phase (eg..

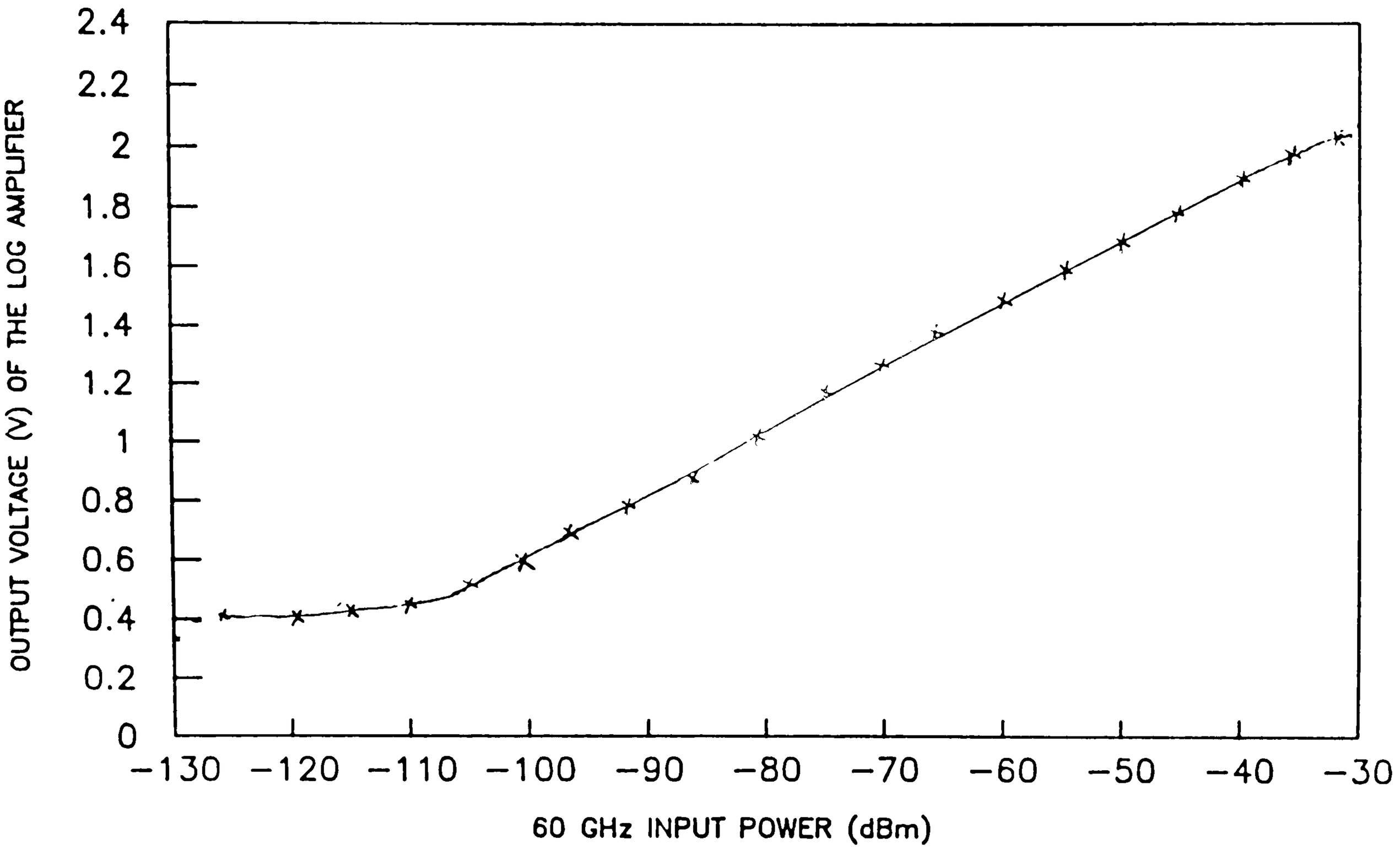

FIG. 4.4 INPUT/OUTPUT CHARACTERISTIC OF THE RECEIVING SYSTEM.

the measurement of doppler shifts) could not be made because of the high phase noise and frequency drifting of the 60GHz oscillators.

4.2 PHASE-LOCKED SYSTEM

Towards the end of the research project, two phase-locked 60GHz oscillators became available. They were used for most of the signal envelope measurements conducted within buildings, for all the FSK bit error rate measurements, and for the spectral spreading (doppler) measurements. A block diagram of the phase-locked system is shown in figure 4.5. The transmitter and receiver are shown in Photograph 1 and 2 respectively.

The transmitter and receiver used Alpha 956U1 phase-locked oscillators with frequency stabilities of +/-1 in 10^8 over the temperature range 0 to 50^0C when phase-locked to external Vectron 224-8658 100MHz crystal oscillators. A 50mW, 59.9GHz phase-locked oscillator was used for the transmitter and a 10mW, 58.9GHz phase-locked oscillator was used for the local oscillator of the receiver. For measurements which required a very low noise level and therefore a very narrow IF filter bandwidth, or which required a very stable IF frequency, a single external 100MHz crystal oscillator could be used as the reference frequency for both phase-locked oscillators.

The down converter of the receiver used the same 60GHz mixer as the non-phased-locked receiver, although the IF frequency this time was 1GHz. This IF was amplified by a separate Miteq AM-3A-0515 32dB gain, 1.5dB noise figure 1GHz amplifier. Its output was passed through a 1GHz bandpass filter for image rejection and then was further down converted to an IF of 60MHz. The 60MHz IF used a bandpass filter having a 3dB bandwidth of 1.5MHz. The output of the bandpass

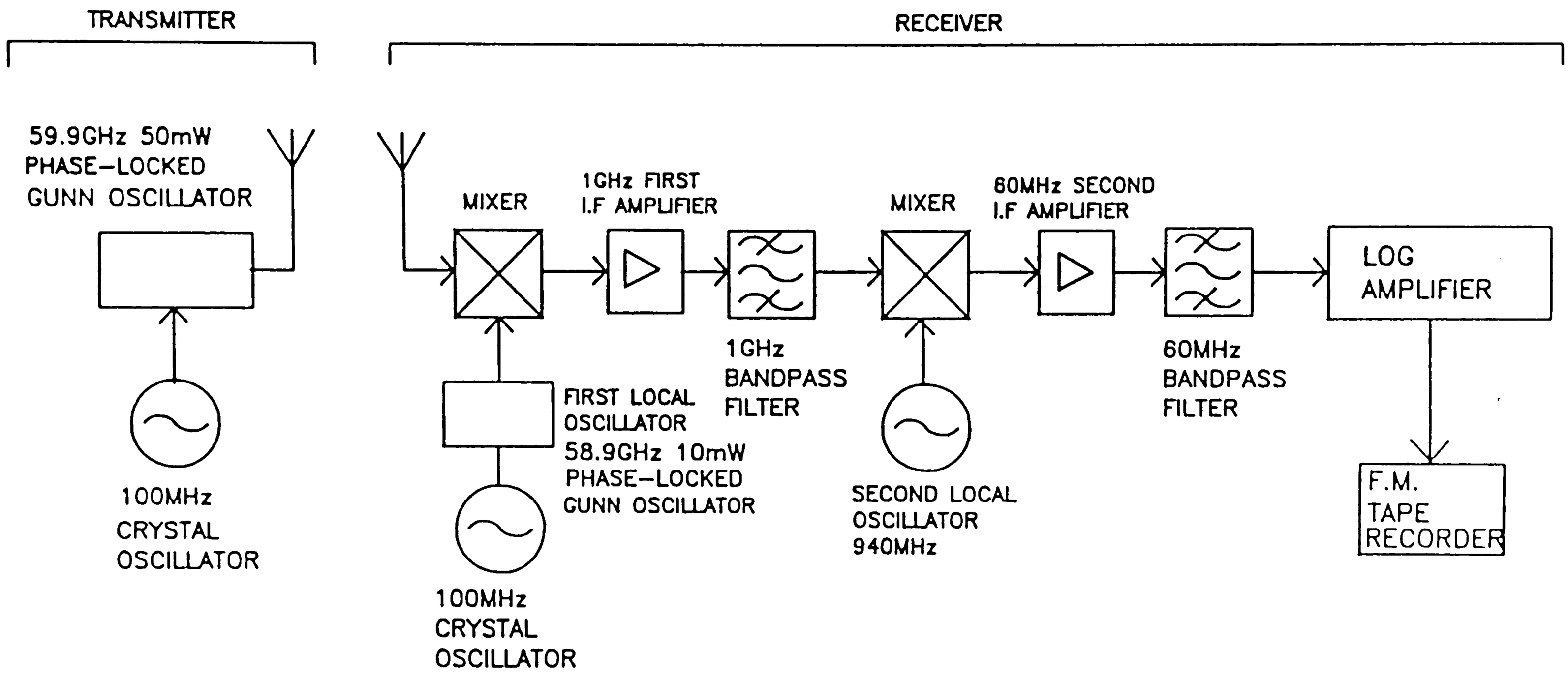

FIG. 4.5 PHASE–LOCKED SYSTEM FOR PROPAGATION MEASUREMENTS.

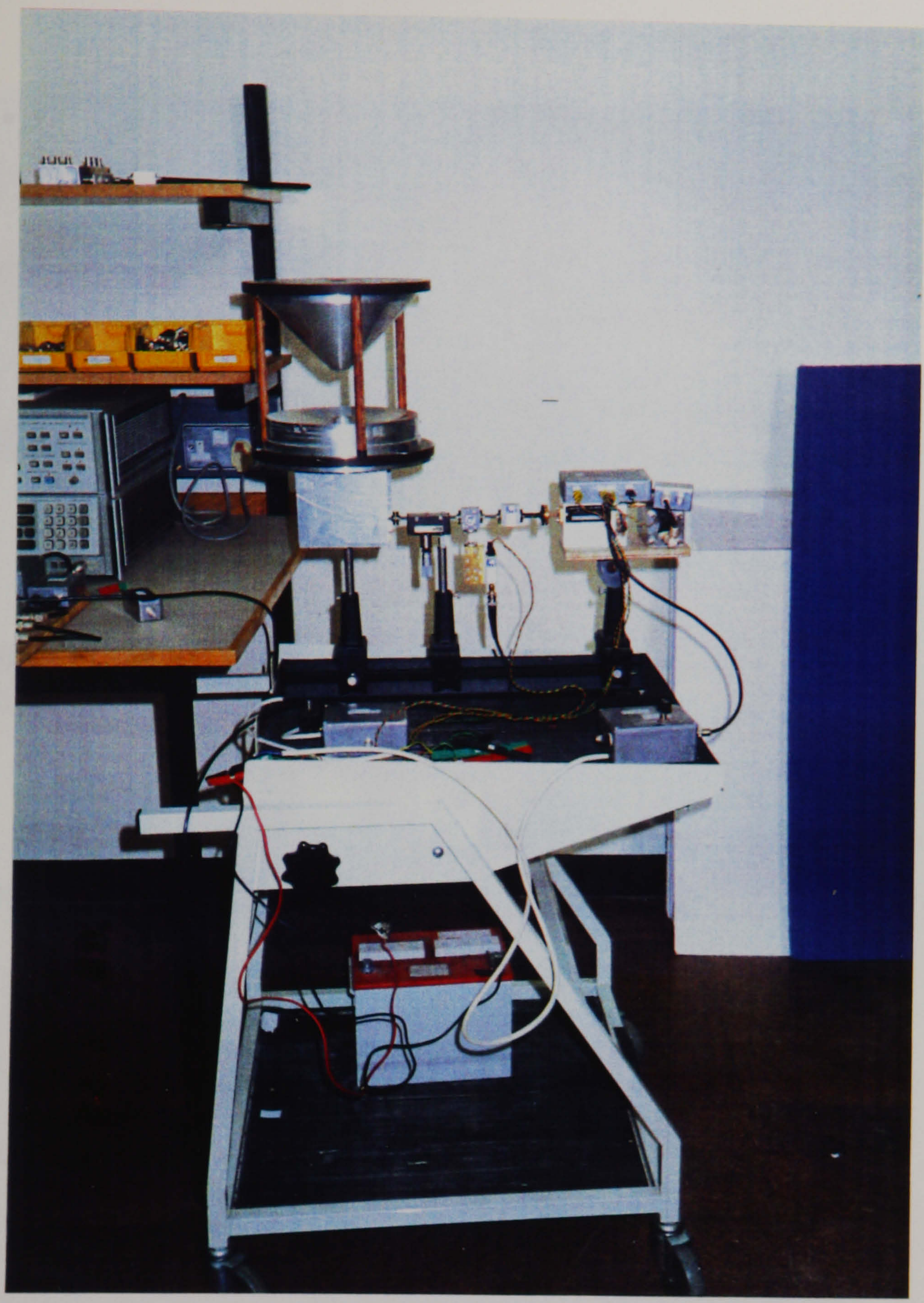

PHOTOGRAPH 1: TRANSMITTER

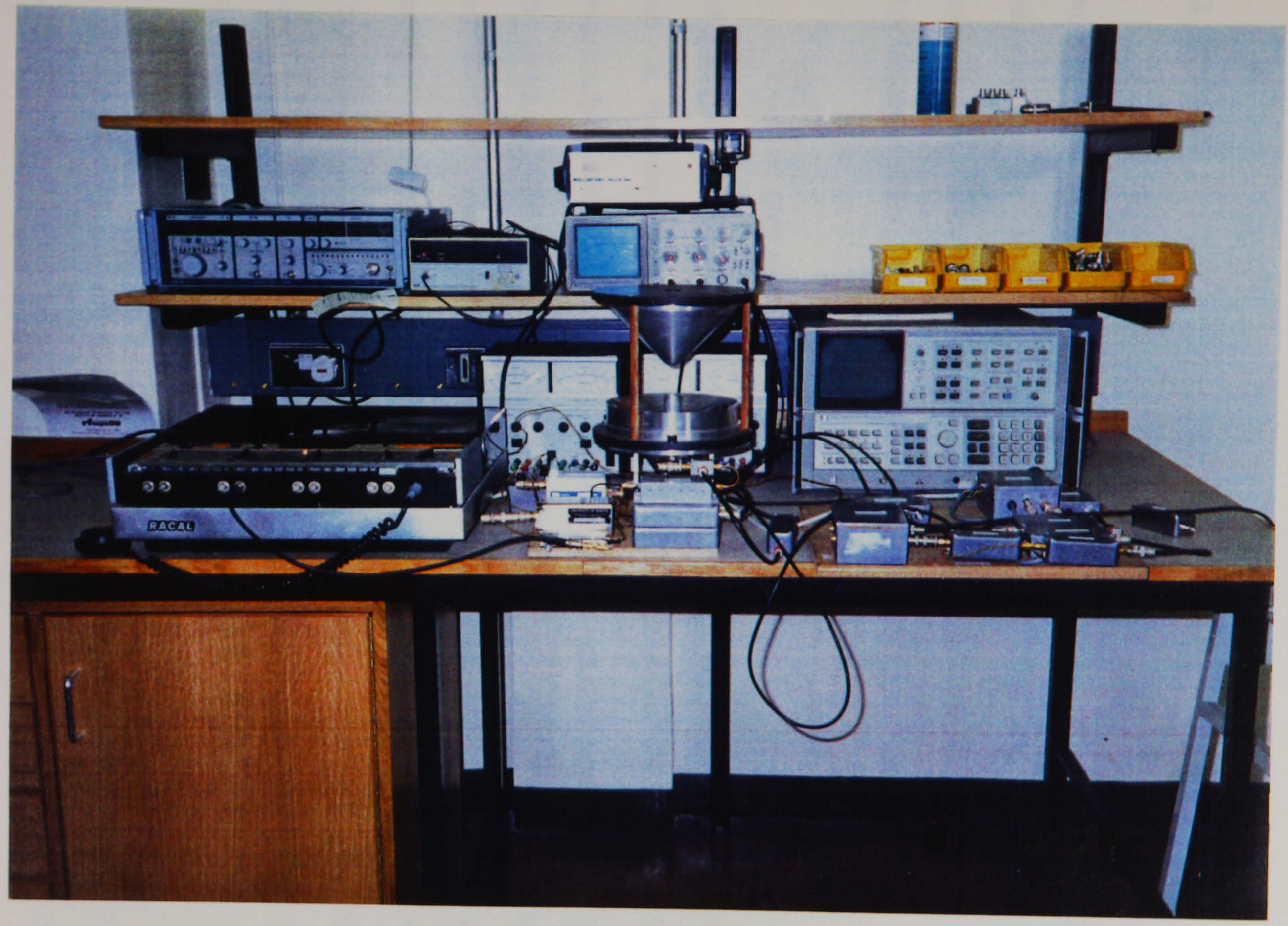

PHOTOGRAPH 2: RECEIVER

filter was passed through the log amplifier and then recorded on the FM tape recorder as described in section 4.1. The input/output characteristic of the receiver is shown in fig. 4.6.

4.3 AERIALS

The aerials used for the measurements were (i) two different types of omnidirectional aerial; (ii) two Flann 2524 20dB standard gain horn aerials with beamwidths of 18^0, and (iii) two Alpha 858 006 V-1/385 high directivity horn-lens aerials having beamwidths of 2.4^0 in both E- and H- planes, and gains of 37dB with sidelobes which were greater than 27dB below the main lobe.

The first type of omnidirectional aerial (type 1) is shown in figure 4.7. Only one was made and it was only available for a short periqd of time, so could only be used for the early measurements which were those conducted outdoors. It had an elevation beamwidth of about 20^0, a gain of about 6dB and was vertically polarised. An anechoic chamber was not available, so accurate beamwidth and gain measurements could not be made due to reflections interfering with the measurements. The mode in the rectangular waveguide is the normal TE_{10} mode and is converted to a TM_{01} mode in the circular waveguide by the mode transducer. The energy is radiated from the circular horn to the parabola which reflects it to the cone reflector which then reflects it horizontally outwards.

The second type of omnidirectional aerial is shown in figure 4.8. Two were made, which had gains of about 7dB, beamwidths of about 20^0 and were circularly polarised. The normal TE_{10} mode in the rectangular waveguide is converted into a TE_{11} mode in the circular waveguide by a tapered transition mode transducer. This linearly polarised mode is converted to circular polarisation by a quarter wavelength

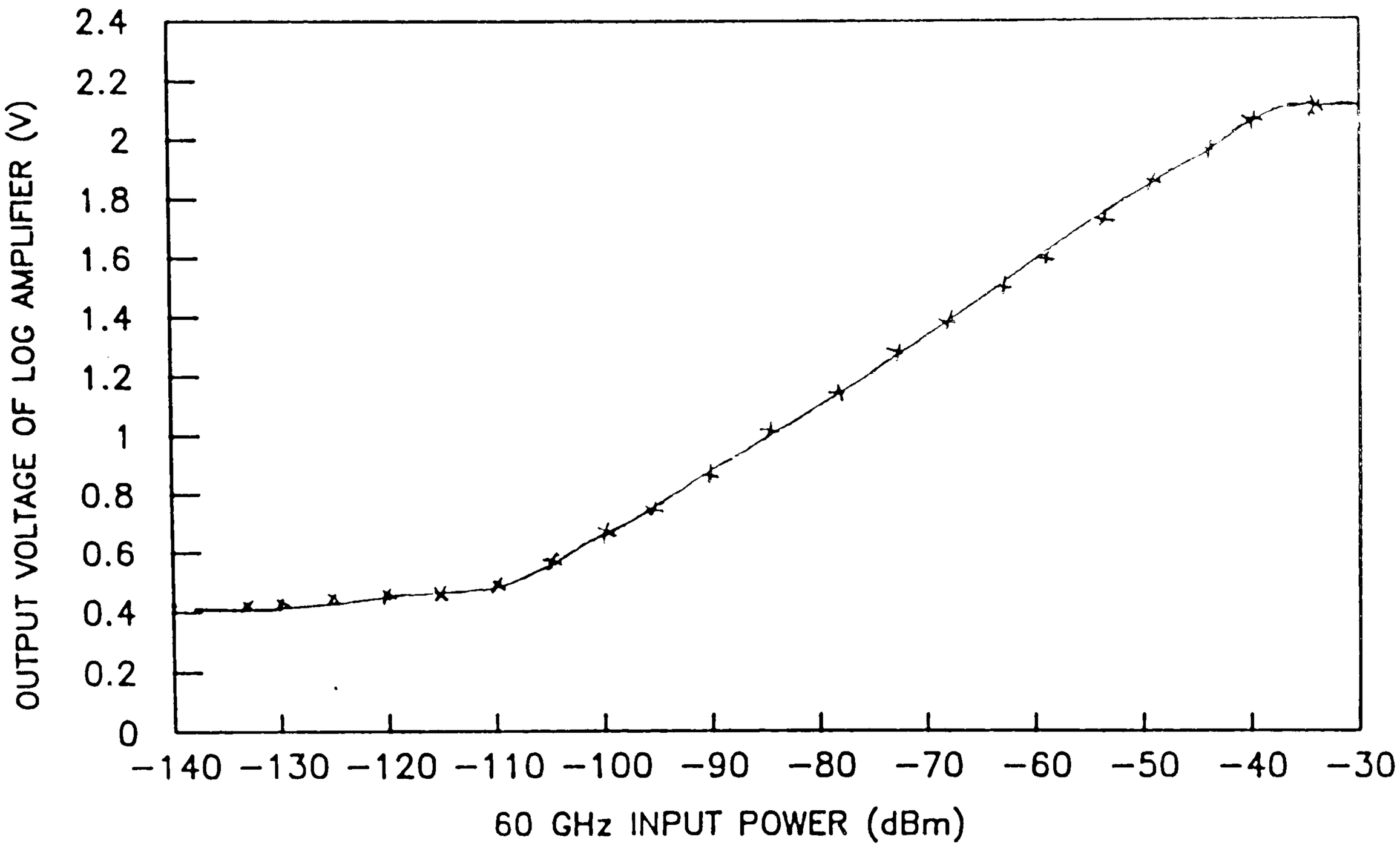

FIG. 4.6 INPUT/OUTPUT CHARACTERISTIC OF PHASE LOCKED SYSTEM.

dielectric plate. The circular horn radiates the electromagnetic waves from the waveguide, which are reflected from reflectors a, b and c, and then are radiated horizontally outwards as shown in figure 4.8.

The high directivity horn lens aerials were used in the measurements for the determination of the penetration loss of building materials and walls, and for the edge diffraction measurements. This type of aerial was used when measurements had to be free of any significant reflected components.

4.4 DIGITISING OF THE RECEIVED SIGNAL ENVELOPE

The received signal recorded on the FM tape recorder was in analogue form, and required a considerable amount of processing to enable suitable analyses to be performed. A large amount of data is necessary in order to find the influence of the different factors on the propagation process. An efficient method of handling this data involves periodic sampling, digitising, formatting, and storing such that computational aids may be used. Therefore, the received signal stored in analogue form on the FM tape recorder was digitized by connecting to an analogue to digital converter before the analysis program was initialised.

Initially, a Nicolet 2090-111A digital storage oscilloscope was used as an analogue to digital converter and the digitised data was transferred to a Hewlett Packard model 9826 desk top computer and stored directly on a floppy disk. The floppy disk was formatted into 32 tracks where each track was capable of storing 4096 samples. The digitised data was calibrated to indicate the received signal power at the input of the receiver in dBm and was stored in an array before processing. The digital storage scope could only continuously sample and store up to 4096 samples, so that if a 1KHz sampling frequency was used, only 4 seconds of the

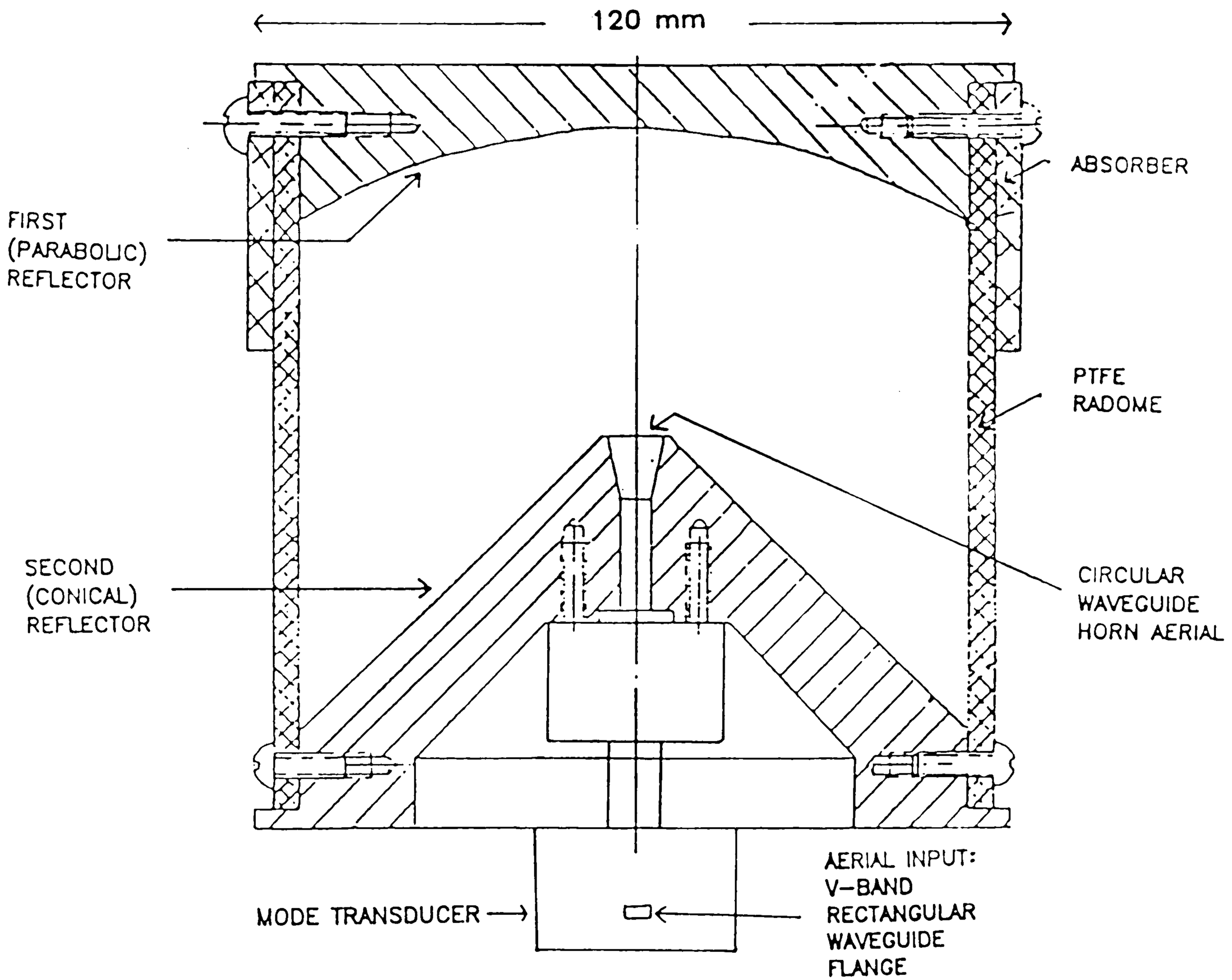

FIG. 4.7 OMNIDIRECTIONAL AERIAL (TYPE 1)

recorded signal could be digitised without interruption. This was partially solved by writing a computer program which could combine two or more separate recordings, stored as separate files, for the analysis of the recorded data. However, there were still gaps between the separate recordings.

To overcome the above problems, an IBM model AT personal computer incorporating a 20 megabyte hard disk was later used for digitising and analysing the recorded data. The analogue to digital converter was a Data Translation DT2821 board, designed to fit in one of the expansion slots of the IBM computer. It had a resolution of 12 bits, and a maximum sampling frequency of 30KHz when the data was stored directly on the hard disk. The sampling frequency, the number of channels used and the gain were controlled by a computer program supplied with the A/D board. The board also had a digital to analogue converter, which was sometimes used to check the data stored on the hard disk by monitoring its output on a digital storage oscilloscope. The data samples created by the analogue to digital conversion process were written in an unformatted binary file on the hard disk of the computer. This enabled the converter to operate at maximum speed by using the most compact data format available. Before the analysis could proceed, the data had to be converted to a formatted ASCII text file. This was then read, and the data was calibrated to indicate the received signal power at the receiver input in dBm. The recorded signal envelope was digitised in small separate sections when analysing fast fading, whereas the whole recorded signal was digitised when determining the median received signal power.

4.4.1 Analysing the Received Signal Envelope.

Having obtained the received signal envelope in a usable form, it was necessary to devise the statistical analysis programs to interpret the results. The

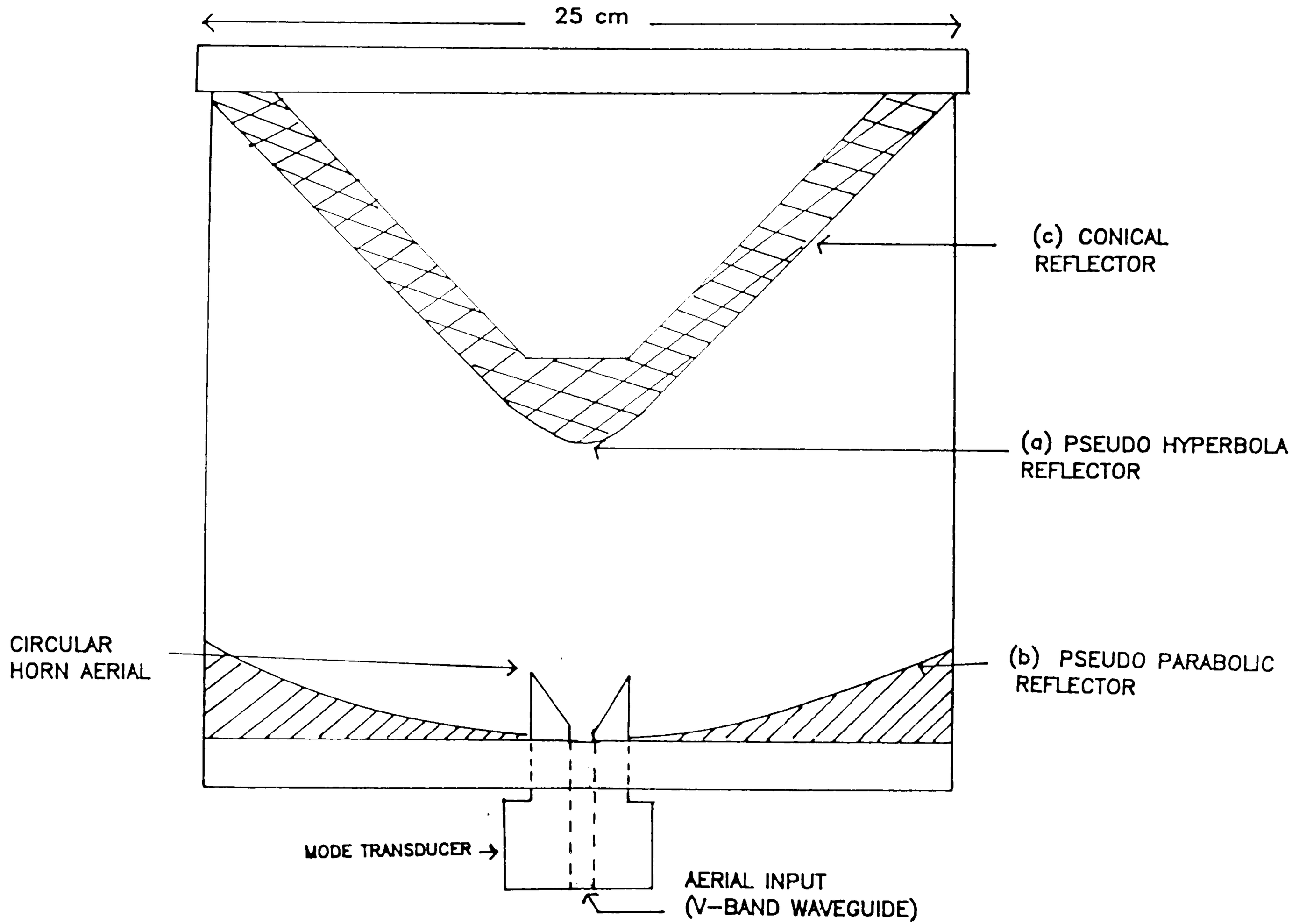

FIG. 4.8 OMNIDIRECTIONAL AERIAL (TYPE 2)

N.B. Designed by Dr. D. Edward, Department of Electrical and Electronic Engineering, University of Bristol.

analysis program was written in Basic for the Hewlett Packard desk top computer and later was written in Pascal for the IBM PC, as documented in Appendix A. The programs were written for reading and retrieving the data files, and for data analysis. The data analysis included calculating the mean or median and the probability distribution of the received signal power, performing a regression analysis, and plotting the results. The majority of the statistical analyses was performed on the IBM computer. The data was also transferred to a Honeywell level 68 mainframe computer running the Multics operating system, for analysis with the Minitab statistical analysis package.

The interconnection of the equipment for the data acquisition process is shown in figure 4.9. The signal envelope was monitored continously at conversion time using a digital storge oscilloscope operating at a slow scan rate. By this means the presence of interference could be instantly recognised and appropriate allowances could be made in the subsequent analysis.

4.5 EXPERIMENTAL PROCEDURE.

The propagation measurements were conducted both within buildings and outdoors in and around Bristol University. Some of these locations are shown in fig 4.10. Within buildings, most of the measurements were made at night when there were no people in the rooms and corridors who would otherwise interfere with the measurements.

The received signal power recorded was a function of time, but often had to be plotted as a function of distance. In order to convert from time to distance, the start and stop positions of the measurements (corresponding to the start and stop times) were spoken and recorded on the voice channel of the FM recorder.

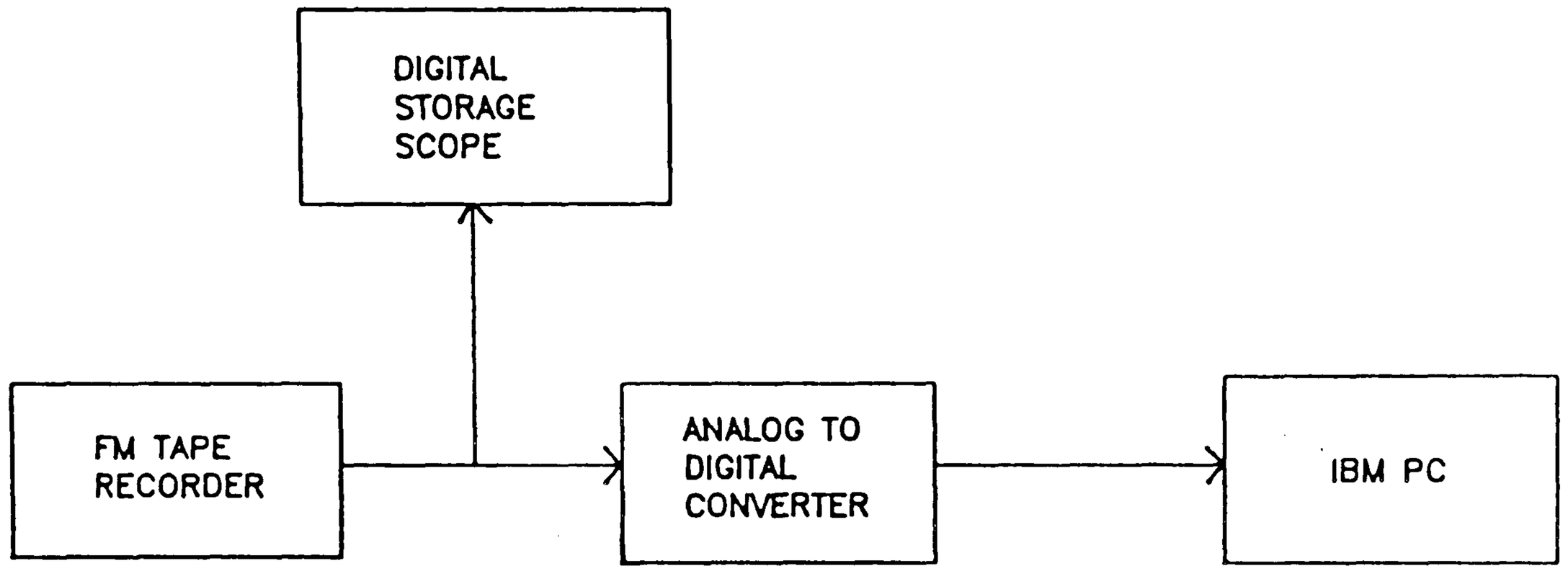

FIG. 4.9 DATA ACQUISATION PROCESS

Measurements were conducted by walking while carrying the transmitter or by pushing it on a trolley, at a speed as near to constant as possible so that the time to distance conversion was linear. The positions of objects between the start and stop positions were spoken and recorded on the voice channel, and were later used to check that the speed was sufficiently constant. For the majority of the field test conditions, the transmitter and the receiver were positioned 1.5m above the floor.

Initially, only the non-phase-locked system was available for the propagation measurements. The measurements conducted outdoors used the non-phase-locked system while most of the measurements conducted indoors (received signal envelope and data transmission) used the phase-locked system.

In order to ensure that the analysis program was working correctly, the output from a Rayleigh fading simulator was recorded on the FM tape recorder. The recorded signal was digitized and analysed for its amplitude distribution characteristics, and as expected, the measured distribution closely followed the theoretical Rayleigh distribution.

In order to reveal the fast fading statistics of the received signal envelope, the recorded data was sampled at intervals of less than one tenth of a wavelength. With this sampling interval, there should be practically no aliasing, and preliminary measurements have shown that the statistics derived from the measurements made were accurate. By not using an excessively high sampling rate, the amount of data stored was kept to a minimum - a very important consideration when using a small computer.

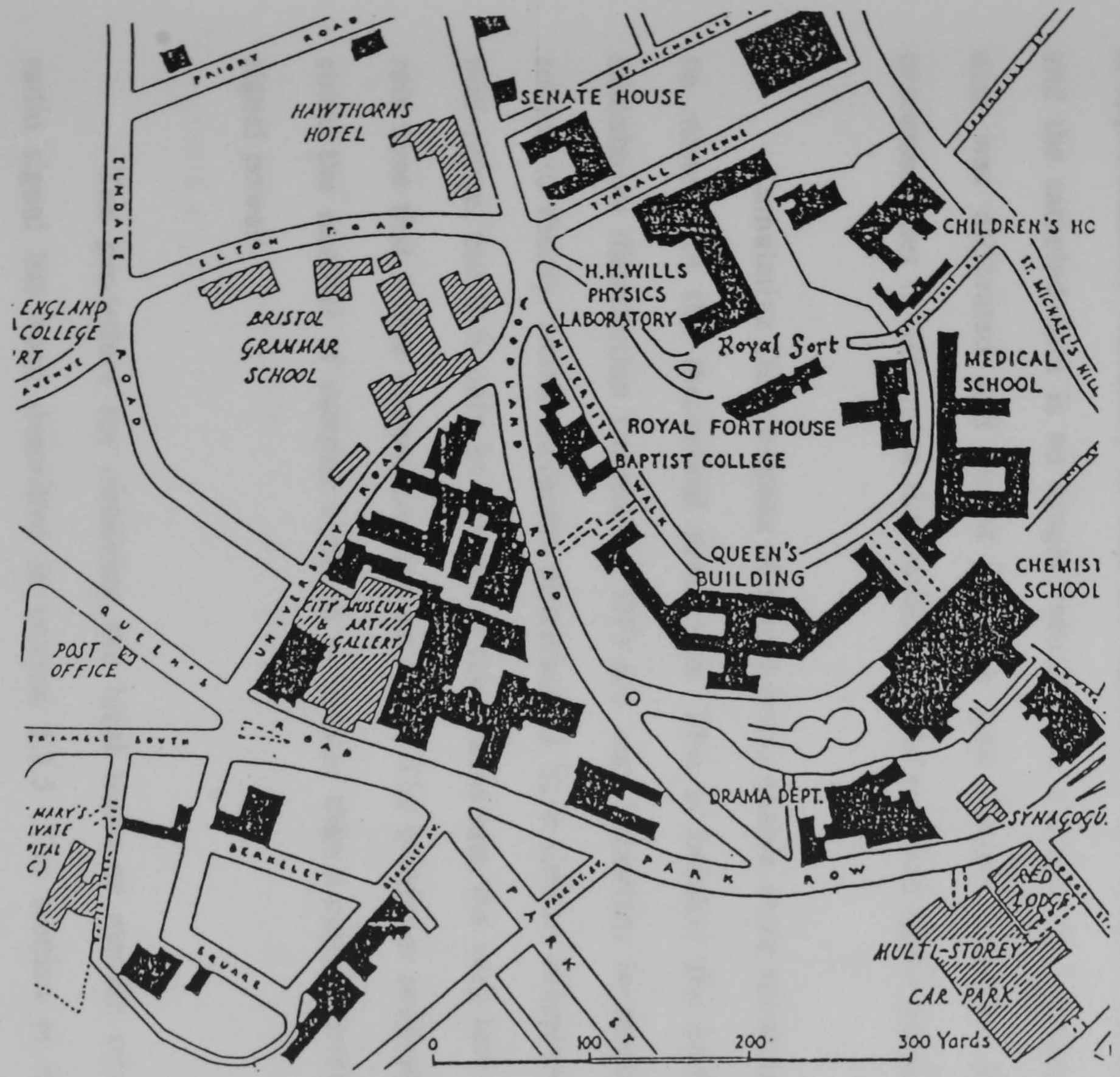

FIG. 4.10 LOCATIONS OF THE TEST AREAS AROUND BRISTOL UNIVERSITY

For the analysis of fast fading the sampled data was computed within 40 wavelengths (see section 3.3.5) so that there would be minimal variations due to slow fading. This method was used when analysing the multipath fading outdoors. However, for the measurements conducted within buildings for the determination of the envelope distribution of the received signal power, a scanning technique was used in collecting the data [2]. Within the scanned locations, the mean signal power is approximately stationary so that the analysis of the fast fading can be conducted and the sampled data is no longer restricted to a single 40 wavelength sweep. The data was calibrated and stored on 5.25 inch floppy disks so that it could be processed later to determine the statistics of the received signal envelope.

Cumulative Distributions of signal levels enable more accurate comparisons to be made with the theoretical prediction. This is because the end regions of the cumulative distribution function (CDF) are very important in relating experimental results to theory. Many different distributions have similar characteristics over their mid-range, but it is only by extending the graphs into the very low and high outage rate zone that a true comparison can be made. The computer program was written to count the number of samples equal to or greater than a certain level of the received signal power.

The procedure for obtaining the local mean or median power of a mobile radio signal has been described in section 3.3.5. The median or mean power was obtained over 50 samples which corresponded to a travelled distance of about 40 wavelengths. In most measurements, the median was chosen instead of the mean because the median can be accurately determined if more than half of the samples are above the noise level, while the mean will depend on the receiver noise level [3]. In order to determine the propagation exponent, the median signal power in dBm

was plotted against the logarithm of the distance and a straight line curve fit was performed by using a linear regression technique.

The median signal power was computed directly from the calibrated data in dBm. However, when the average signal power was computed, the calibrated received signal data was first converted from dBm to linear power values. The average was performed and the result was converted back to dBm. To produce the histogram of the spatial distribution of the received signal envelope (used for some of the measurements within buildings), the computer sorted the samples into 20 blocks, each one corresponding to a 4dB increment of the dynamic range of the system.

In most of the measurements conducted, the receiver was stationary and the transmitter was moved away from it. The recorded signal represents a measure of the signal amplitude as a function of distance and multipath effects. However, in the measurements to determine the penetration loss through walls and building materials, the transmitter and receiver were set at a fixed separation distance and the object under test was placed half way between the transmitter and receiver . The received signal was compared with that obtained without the obstacle in order to obtain the penetration loss.

REFERENCES

[1] Haydl, W.H., "Fundumental and Harmonic operation of Millimeter-wave Gunn Diodes," IEEE Trans. on Microwave Theory and Tech., vol. 31, No. 11, Nov. 1983, pp.879 -889.

[2] Hoffman, H.H, and Cox, D.C., "Attenuation of 900MHz Radio Waves Propagating into a Metal Building," IEEE Trans. on Antennas and Propagation, Vol. Ap-30, pp 808-811.

[3] Cox, D.C., Murray, R.R., and Norris, A.W., "Measurements of 800MHz Radio Transmission into Buildings with metallic Walls," B.S.T.J., Vol. 62 pp 2695-2717, Nov. 1983.

CHAPTER 5

PROPAGATION MEASUREMENTS OUTDOORS

5.1 INTRODUCTION

Since integrated portable communication systems are required to operate outdoors, propagation measurements conducted outside buildings will be described in this chapter. The propagation characteristics will be quite different for a system operating in an outdoor, mobile environment than for one operating in an indoor environment because the outdoor environment consists of fast moving vehicles as well as slow moving people. It is necessary to describe both the multipath and shadowing effects in characterising the propagation channel. The received signal power, averaged in order to remove the multipath fading, varies as a negative power of the distance between the transmitter and receiver. A simple two path propagation model derived in chapter three predicted a dependence of $1/d^2$ at 60GHz.

The behaviour of the mobile propagation channel is strongly dependent on the type of environment in which the mobile is located. The direct signal may be obstructed by buildings and trees. Therefore, different types of environments will need to be considered. The environment can be classified as open areas, areas with partial obstructions and areas with almost complete obstructions. In open areas with no nearby obstructions, the multipath will be mainly determined by the properties of the surrounding ground, and it will usually be very low. The partial obstructions case may be represented by a road lined with trees, by open residential areas with houses, or by rural areas with buildings or trees. Finally, almost complete obstructions can be represented by cities with tall buildings where a direct signal is available for only a small percentage of the time.

The measurements have been conducted outdoors in order to determine the effect of multipath on the envelope distribution and the median signal power variations with distance. Also, measurements were made to determine the effect of an obstacle obstructing the LOS path, and the diffraction of the signal into the shadow region. Finally, measurements were conducted by radiating the 60GHz signal into a building in order to determine the resulting penetration loss.

No specific investigation has been carried out on the influence of adverse weather conditions, due to the fact that all measurements were carried out in dry weather and no weather monitoring equipment was available.

5.2 TEST EQUIPMENT

The propagation measurements conducted outdoors used the non-phase-locked system described in chapter 4 because the phase-locked system was not available when the measurements were made. The stability of the non-phase-locked sources was only sufficient to keep the I.F. signal within the bandpass filter for 10 to 20 minutes. To check that the frequency stability was acceptable, the received signal power along a single road was recorded. The receiver was stationary while the transmitter was moved away from the receiver at a constant speed until the end of the road, and then was moved back towards the receiver. The recorded signal power was almost identical for the outward and return movements. This demonstrates that stable measurements could be made. After each measurement, the receiver Gunn local oscillator frequency was varied to see if the IF signal was still within the passband of the 60MHz IF bandpass filter. In nearly every case it was, but if it was not, the measurement was repeated. Before a measurement was made, the IF was always centred in the passband of the 60GHz IF filter.

5.3 LINE-OF SIGHT PROPAGATION MEASUREMENTS WITH REFLECTIONS MINIMISED

Line-of-sight (LOS) measurements were conducted with the transmitter and receiver placed on the flat roof of the Queen's building, a reinforced concrete building at the University of Bristol. For these measurements, the standard 20dB gain horn aerials were used for the transmitter which was 2.5m above the level of the roof and the receiver which was 1.5m above the level of the roof. The transmitter-receiver separation was varied from 4m to 50m by moving the transmitter along the roof. The received signal power was recorded every one metre whilst making sure that there was minimal reflection from the roof of the building by moving the transmitter so that the received signal power was not affected by reflection. The received signal should therefore have been only due to the free space law plus oxygen absorption law.

A measurement beyond 50m separation was carried out by placing the transmitter at one corner on the roof at a height of 30m above ground level, while the receiver was placed at a distance of 100m from the transmitter. The receiver was placed in an open area with a grass surface at a height of about 1.5m above ground level. The received signal power was recorded at this location, again making sure that there were minimal reflections from the environment. The received signal power is plotted against distance together with the theoretical free-space curve as shown in fig. 5.1. The figure shows that the measured curve closely follows the free-space curve. At 100m separation, a difference of about 1.5dB between the measured and free-space path loss can be observed, and this can be attributed to oxygen absorption. If the separation between the transmitter and receiver was increased to a longer distance, the decrease in the received signal power would be significantly steeper due to high atmospheric attenuation compared to the theoretical

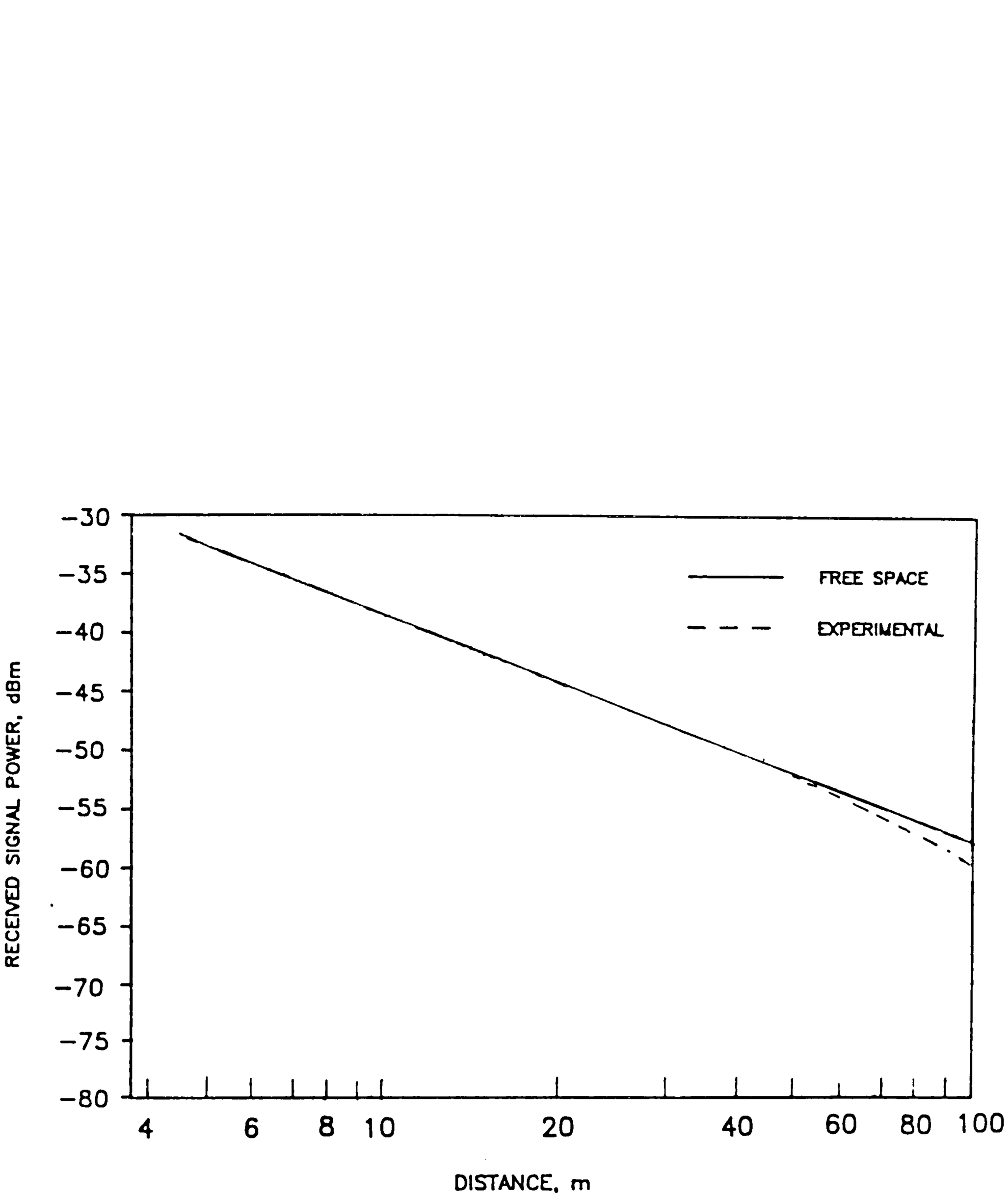

FIG. 5.1 GRAPH OF RECEIVED SIGNAL POWER AGAINST DISTANCE FOR LOS CONDITIONS WITH MINIMAL REFLECTIONS.

free space law. These measurements were not made however, because suitable test sites at large separation distances were not available.

5.4 MEASUREMENTS IN DIFFERENT ENVIRONMENTS

The behaviour of the mobile propagation channel is strongly dependent on the type of environment in which the mobile is located. Therefore, the measurements were conducted in three different environments in order to determine their influences on the received signal characteristics. From the measurements, the received signal power can be determined as a function of transmitter-receiver separation. The measurements were made in dry weather so that the variation with time of the received signal power was negligible. The transmitter used a 20dB gain standard horn aerial and the receiver used the type 1 omnidirectional aerial described in chapter 4. The handheld transmitter was moved away from the receiver at a constant speed and the received signal power was recorded on the FM tape recorder.

For most of the time, there was a LOS path between the transmitter and receiver along both sides of the road and the measurements were conducted with the transmitter and receiver positioned at a height of about 1.5m above the ground.

5.4.1 Description of the environments and the received signal.

The first measurements were conducted along University Walk, an asphalt road which had University Buildings along one side and parked cars and a 3m high brick wall along the other side (environment A). Fig 5.2 shows a photograph of this environment. It was a private University road approximately 10m wide, and part of it was bordered with mature trees. The measurements were conducted when there was no moving vehicles or pedestrians along the road, and were made up to a

distance of 130m. Fig 5.3 shows part of the recorded signal power at a distance of about 100m from the receiver where large signal fluctuations occurred due to multiple reflections from trees, cars, buildings and walls. As at lower frequencies. up to 25dB fades can be experienced.

Since the radio link in an urban environment consists of boundaries of asphalt roads and pavements in the horizontal plane and building walls in the vertical plane, it would be helpful to isolate the contribution of these surfaces in a propagation study. Therefore the second measurements were conducted in an open area of a park with a short grass surface and with no nearby vertical structures so that reflections could only have been from the grass surface (environment B). Fig. 5.4 shows a photograph of this environment. The measurements were made up to a distance of about 200m from the receiver. Part of the recorded signal power at a distance of 100m from the receiver is shown in figure 5.5. Fluctuations can be observed due to the reflected wave from the grass surface interfering with the direct signal. However, the fades are much lower than they were for environment A, and fades of only up to 5dB below the mean level can be observed. This can be attributed to the roughness of the grass surface which prevents a strong specular reflection and instead produces weak diffuse reflections. As a result the reflected signals are much weaker than the direct signal, so they only produce small fluctuations in the received signal power.

The third set of measurements were conducted along a busy road with buildings along both sides. Fig 5.6 shows a photograph of this environment. During the measurements there were many vehicles moving along the road and pedestrians walking on the pavements. Measurements were made with a transmitter - receiver separation of up to 200m along this road (environment C). Figure 5.7 shows part of

FIG. 5.2 PHOTOGRAPH OF ENVIRONMENT A.

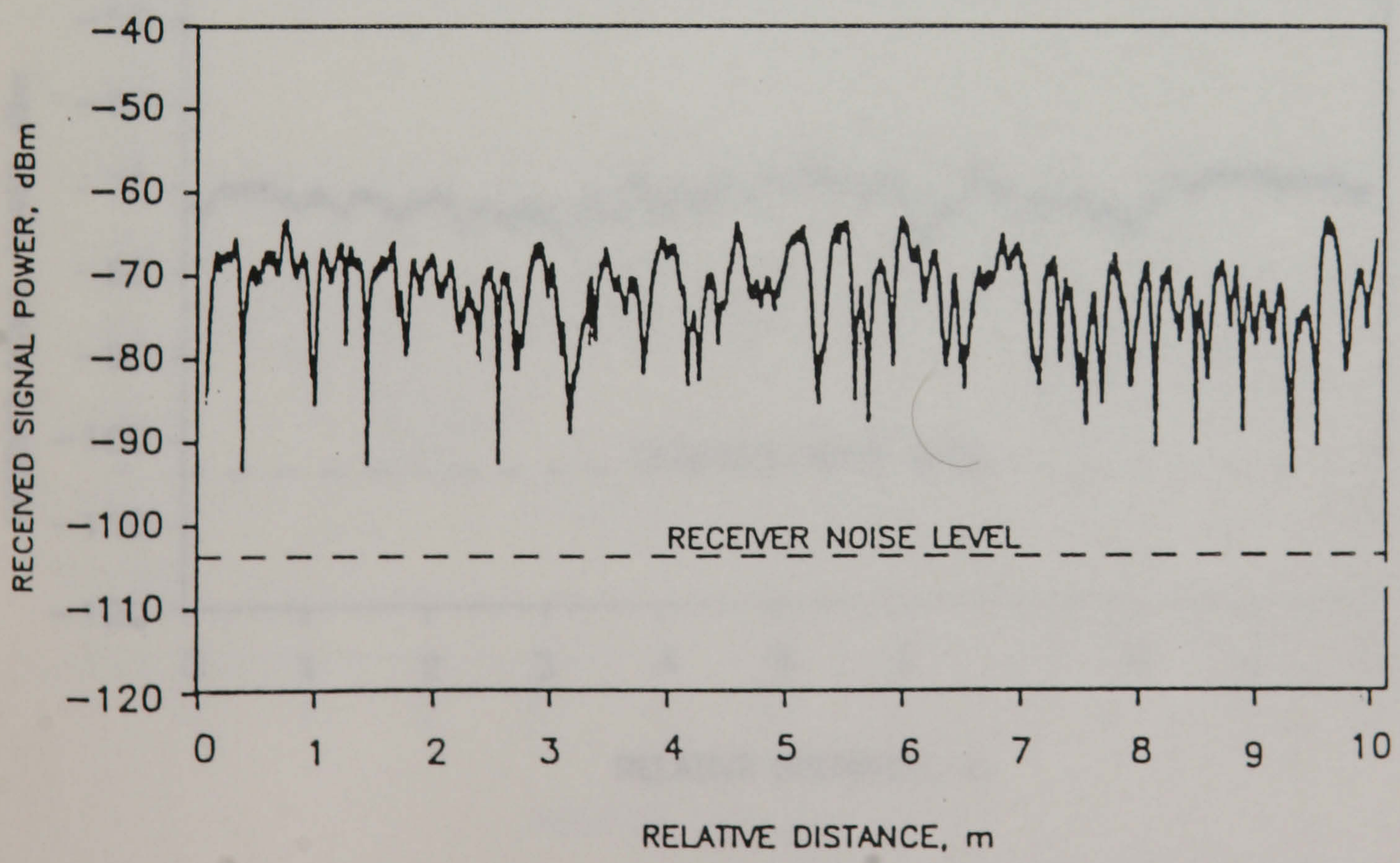

FIG. 5.3 PORTION OF THE MEASURED SIGNAL POWER AT ABOUT 100M SEPARATION ALONG A ROAD WITH PARKED CARS, BUILDINGS AND TREES ALONG THE SIDES (ENVIRONMENT A) WHEN THERE WAS A LOS PATH.

FIG. 5.4 PHOTOGRAPH OF ENVIRONMENT B.

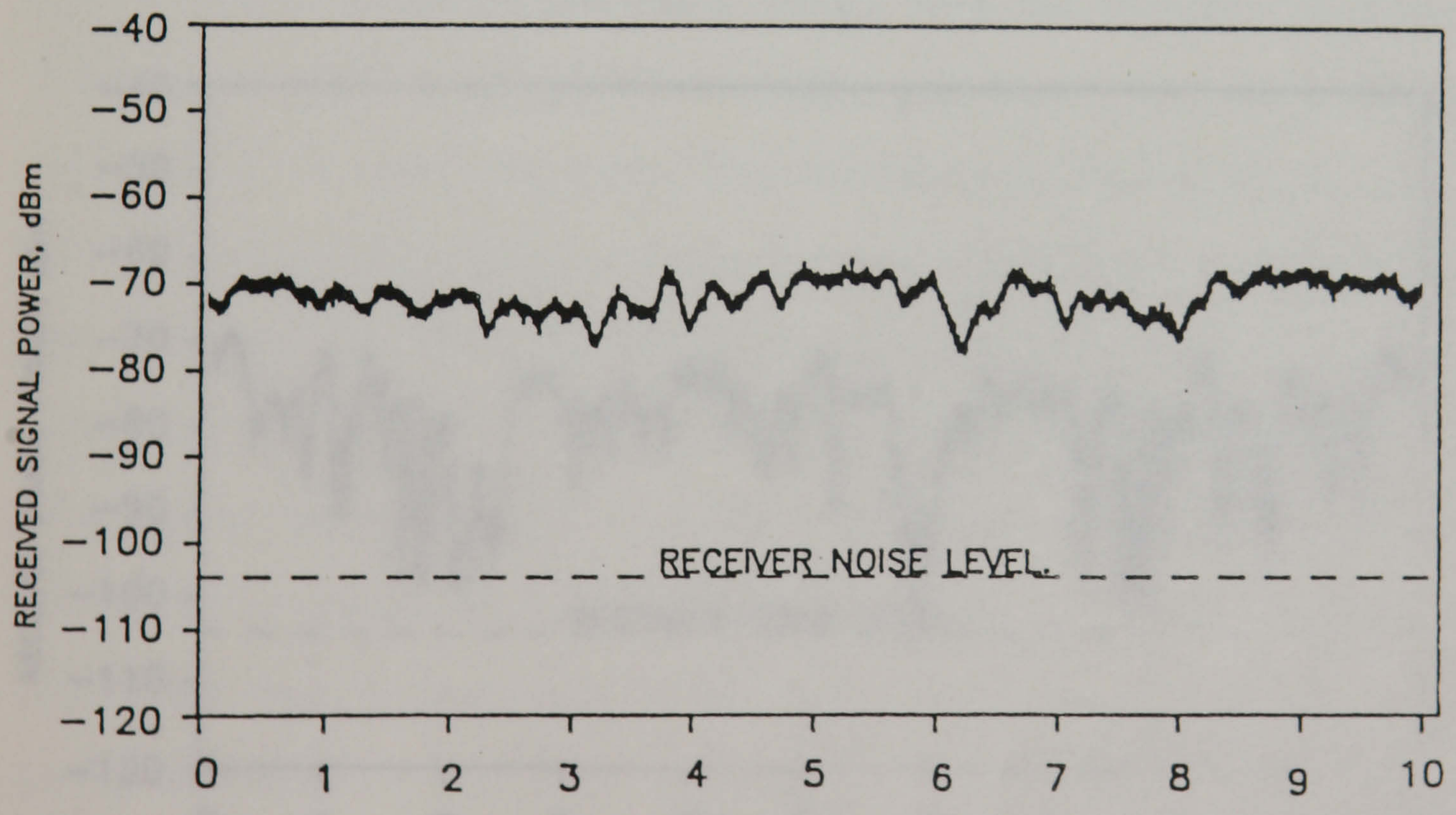

FIG. 5.5 PORTION OF THE MEASURED SIGNAL POWER AT ABOUT 100M SEPARATION FOR AN OPEN AREA WITH GRASS SURFACE. (ENVIRONMENT B). WHEN THERE WAS A LOS PATH

FIG. 5.6 PHOTOGRAPH OF ENVIRONMENT C.

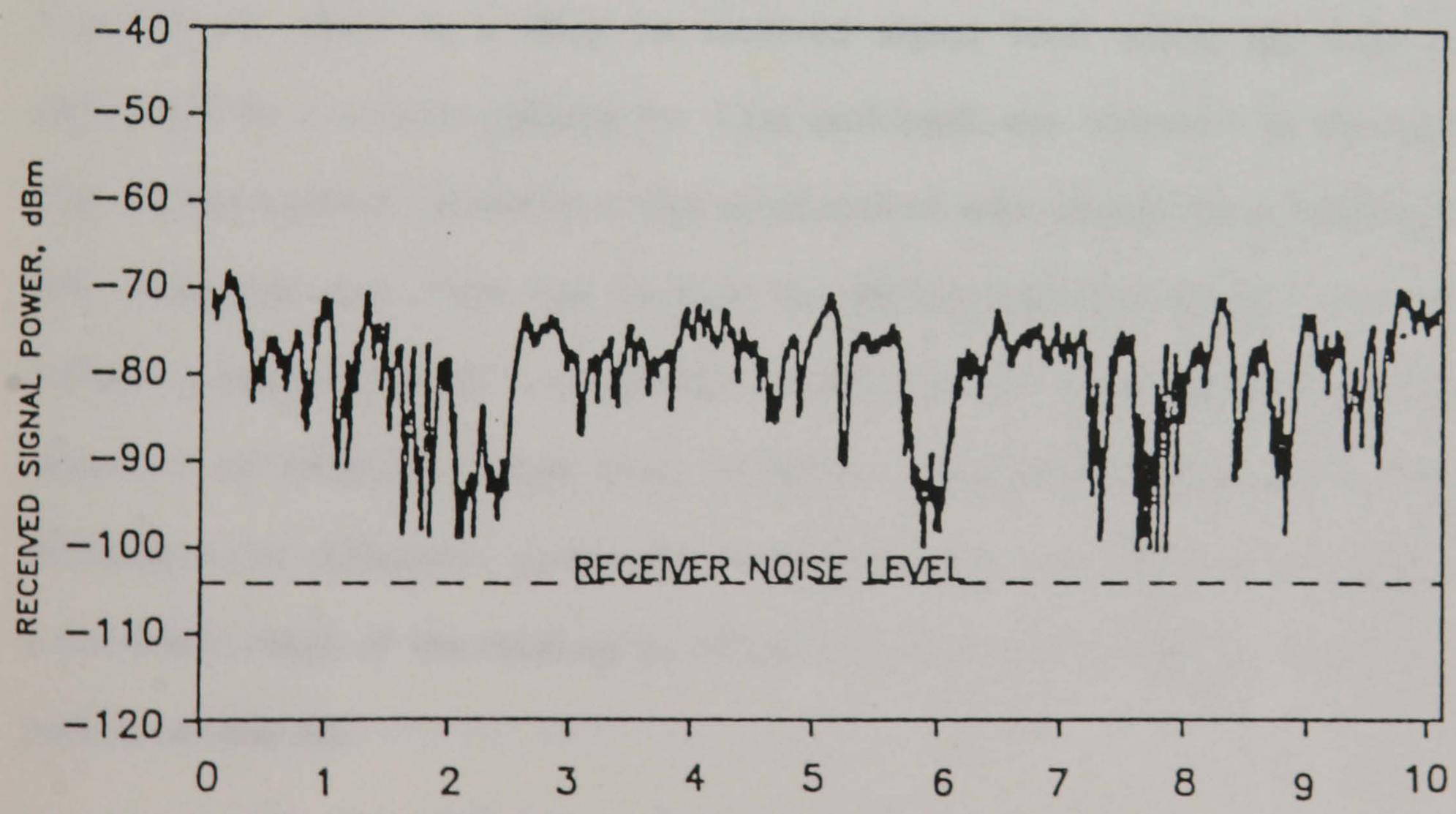

FIG. 5.7 PORTION OF THE MEASURED SIGNAL POWER AT ABOUT 100M SEPARATION ALONG A BUSY ROAD (ENVIRONMENT C) WHERE THE LOS PATH WAS INTERMITTENTLY BLOCKED.

the received signal power at a distance of about 100m when the transmitter was being moved away at a constant speed from the receiver. The signal variations due to the traffic have characteristically short durations and if a vehicle drove through the direct path, a drop in signal power of 15dB to 20dB occurred. Also observed on the recorded signal are many short term variations due to multipath fading, with some fades approaching 20dB. These variations occur all along the path in a near random manner. If the main beam was obstructed, this caused a decrease in the received signal power. As expected, the duration of fades was dependent on the time the obstruction was present, while the length and depth of fade was dependent on the type and number of vehicles passing by.

The results have demonstrated the influence of the surrounding objects and the type of ground on the received signal power. Fluctuations of the received signal power are due to reflections from and diffraction around the surrounding obstacles and the ground whose relative phases change when the transmitter is in motion. Furthermore, there is a drop in received signal level when the LOS path is obstructed by a vehicle passing by. Less multipath was observed in the open area with a grass surface compared to the environment with parked cars, buildings and a wall along the road. This was because the diffuse reflected signal from the grass surface is relatively weak, and the lack of any nearby vertical structures means that there are no reflections from these. However, open area environments can create difficulties for millimetre wave radio because there are insufficient scatterers within a sufficient range of the receiver to reflect the signal to the receiver when the direct path is obstructed.

5.4.2 Envelope Fading Distributions

The received signal power varies as the transmitter moves away from the receiver. There are two kinds of variation. One is the rapid variation caused by multipath propagation and the other is a much slower variation due to the changes in parameters like street width or building height. The first is fast fading which is caused by multipath reflections from buildings and other obstacles in close proximity to the transmitter. The second is called slow fading which occurs over distances large compared to the carrier wavelength. Furthermore the total range over which a radio link operates will be an important factor in determining the total propagation path loss. Therefore, it is necessary to establish the relationship between the median received signal power and the separation of the transmitter and receiver.

When analysing the fast fading, the received signal envelope was quantized in 1dB increments within a short distance over which there was virtually no change in the long term fading. Figure 5.8 shows the CDF of the computed data together with the theoretical Rayleigh distribution for environments A and B described earlier. The 0dB point of the signal power has been normalised to the median signal power. The results show that the distribution for both environments depart from the theoretical Rayleigh distribution due to the presence of the LOS path between the transmitter and the receiver. However, the distribution for environment A was quite close to the Rayleigh distribution, and only departed significantly from it at about 10dB below the median signal power. On the other hand, the distribution for environment B departed very significantly from the Rayleigh distribution, which was as expected, since the only significant reflected signal possible was from the ground, and this was weak due to the grass surface.

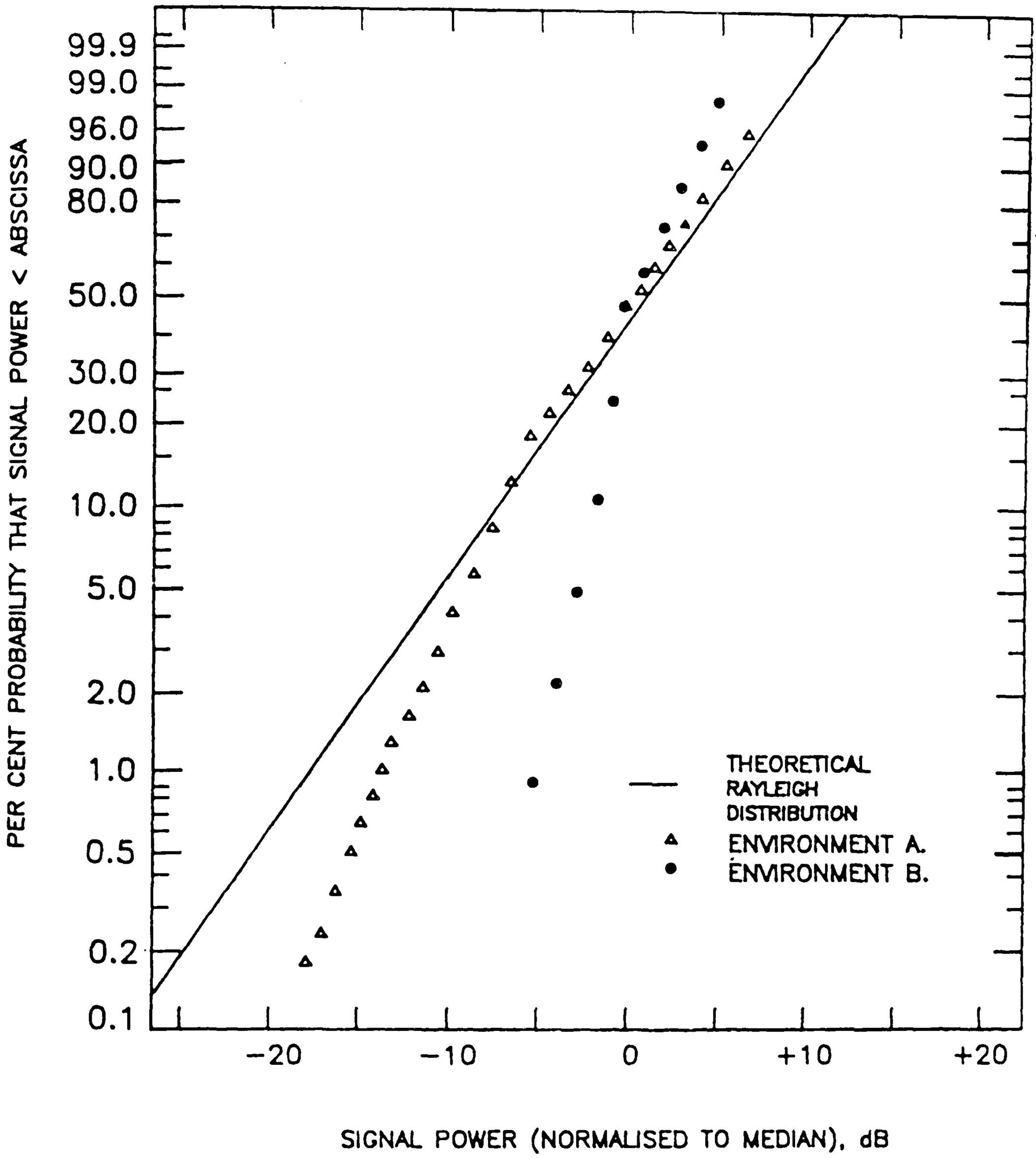

FIG. 5.8 CDF OF THE RECEIVED SIGNAL POWER RELATIVE TO THE MEDIAN FOR ENVIRONMENT A AND B.

5.4.3 Median Signal Power Laws

The median signal power was computed from the recorded data over forty wavelengths of travelled distance as was described in section 3.3.5.[1] These points are plotted as a function of the logarithm of distance as shown in figure 5.9 for environment A, and fig. 5.10 for environment B. The propagation exponents for each environment were computed from the median signal power by the least squares error method. The straight lines are least squares regression lines through the data points indicating the dependence of the median signal power on distance. It was found that the power exponent of the best fit straight line for environments A and B were 1.4, and 2.3 respectively. These propagation exponents are quite similar to those measured in reference [2], where they varied from 1.4 to 2.2 along a straight road with buildings on both sides up to a distance of 120m.

The propagation exponent of 1.4 for environment A indicates that the signal fell considerably less slowly than the value of 2.0 for the theoretical free-space equation. This may have been because the asphalt road and the brick wall produced strong reflections which prevented the energy from spreading out, and therefore concentrated it more along the path.

The propagation exponent of 2.3 for environment B was quite close to 2.0 which occurs in free-space. One reason why this exponent was greater than the free-space value was because of the oxygen absorption, which theoretically rises to 3dB at 200m. There were no nearby reflectors except for the ground, and this had a grass surface which can be considered as 'rough' at 60GHz, so the ground reflection was probably quite low. The propagation was therefore similar to free-space propagation, and this is confirmed by fig. 5.10 and the propagation exponent.

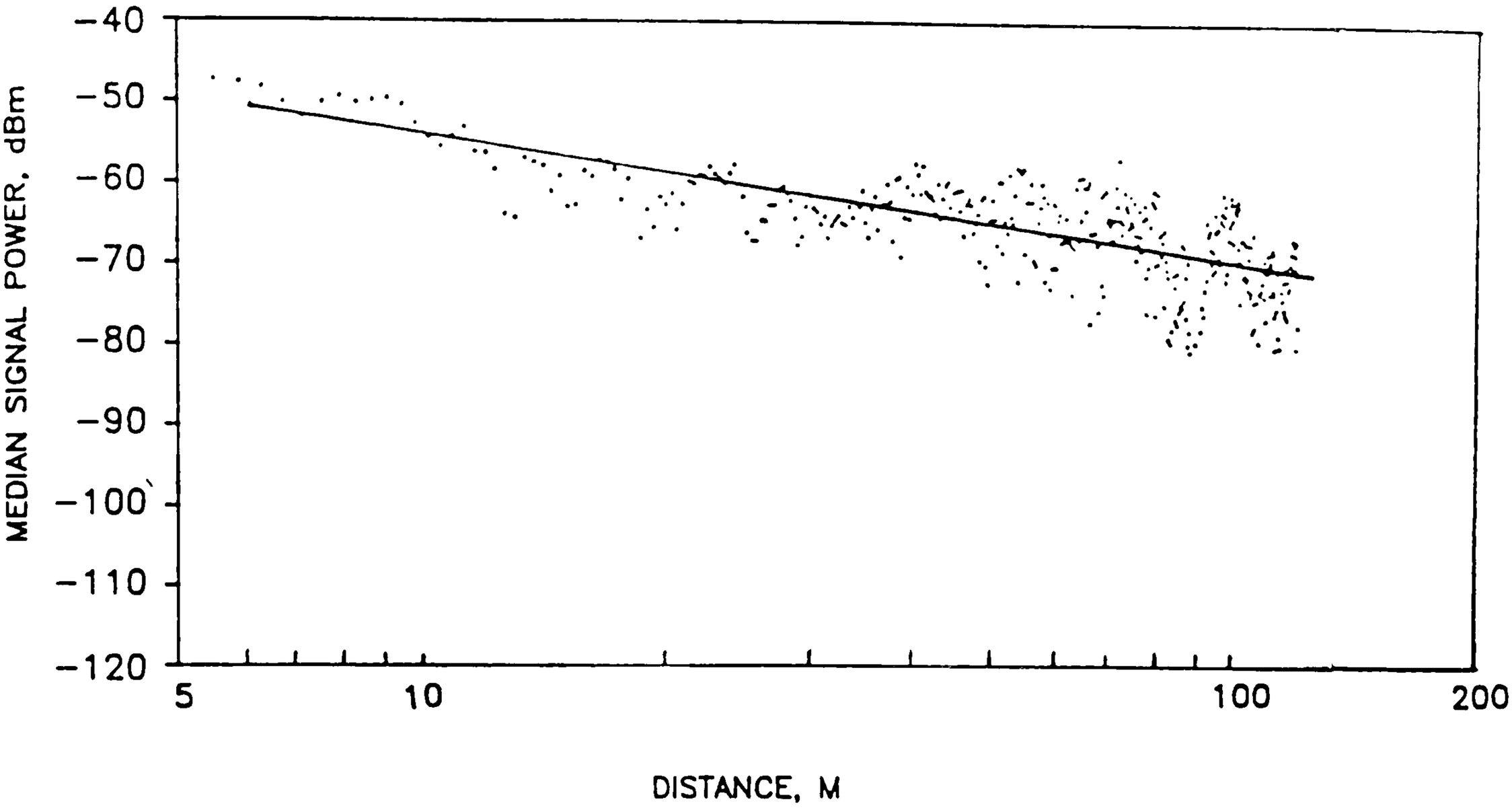

FIG. 5.9 SCATTER PLOT OF THE MEDIAN SIGNAL POWER AGAINST DISTANCE (LOG SCALE) FOR ENVIRONMENT A.

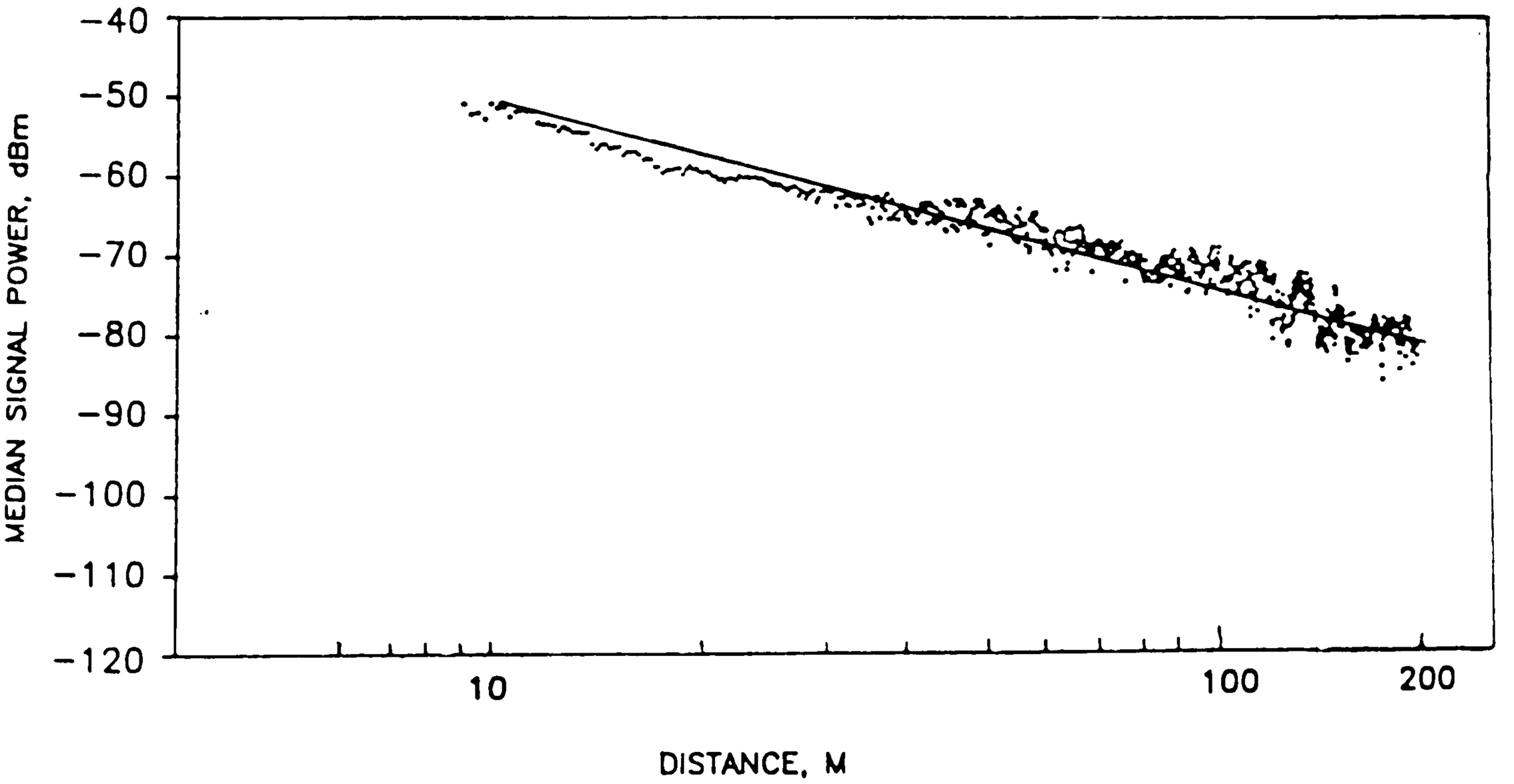

FIG. 5.10 SCATTER PLOT OF THE MEDIAN SIGNAL POWER AGAINST DISTANCE (LOG SCALE) FOR ENVIRONMENT B.

5.5 OBSTRUCTION MEASUREMENTS

Measurements demonstrating the effect of direct LOS dependence were also conducted. During the measurements the transmitter used a standard 20dB gain horn aerial and the receiver used the type 1 omnidirectional aerial.

The first measurement was conducted along University Walk with the transmitter moving towards the receiver at about 0.8m/s. The measurements were recorded when there was initially a LOS path, which was later blocked by a van. The transmitter - receiver separation was 150m, and the van was moving at a distance of 120m from the receiver at an estimated speed of 4m/s. Fig. 5.11 shows the recorded signal power. When the LOS path was obstructed by the van, the received signal power dropped below noise level for a duration of 1.5 sec, representing an attenuation of greater than 25dB. The result shows that propagation in an open road is difficult at 60GHz because there is an insufficient number of nearby scatterers to reflect the signal to the receiver when the direct path is obstructed.

The second measurements was conducted to determine the propagation effects contributed by an isolated tree in an area with a grass surface. The receiver was placed at 20m from the tree which had a trunk diameter of 100cm. The transmitter was moved at about 0.5m/s along a line perpendicular to that formed by the receiver and the tree. The transmitter was moved from a clear view of the receiver to a position where the main trunk obstructed the LOS path at 1m from the tree and then back to a clear view of the receiver. At all times, the transmitter aerial was pointing towards the receiver. Fig. 5.12 shows the recorded signal power. The deep fade was due to the tree trunk obstructing the direct path. The signal power

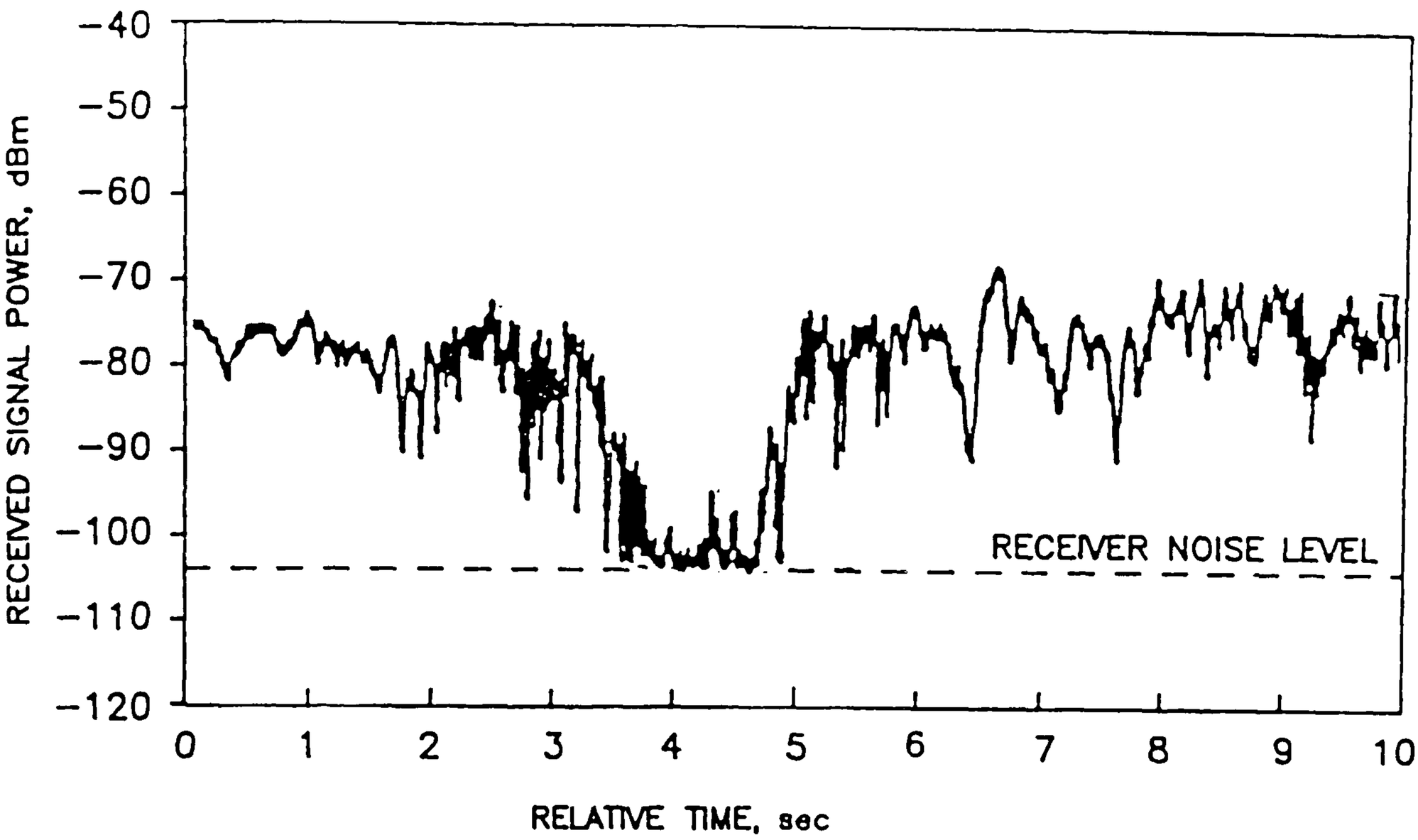

FIG. 5.11 RECEIVED SIGNAL POWER WHEN LOS PATH BETWEEN TRANSMITTER AND RECEIVER WAS OBSTRUCTED BY A VAN.

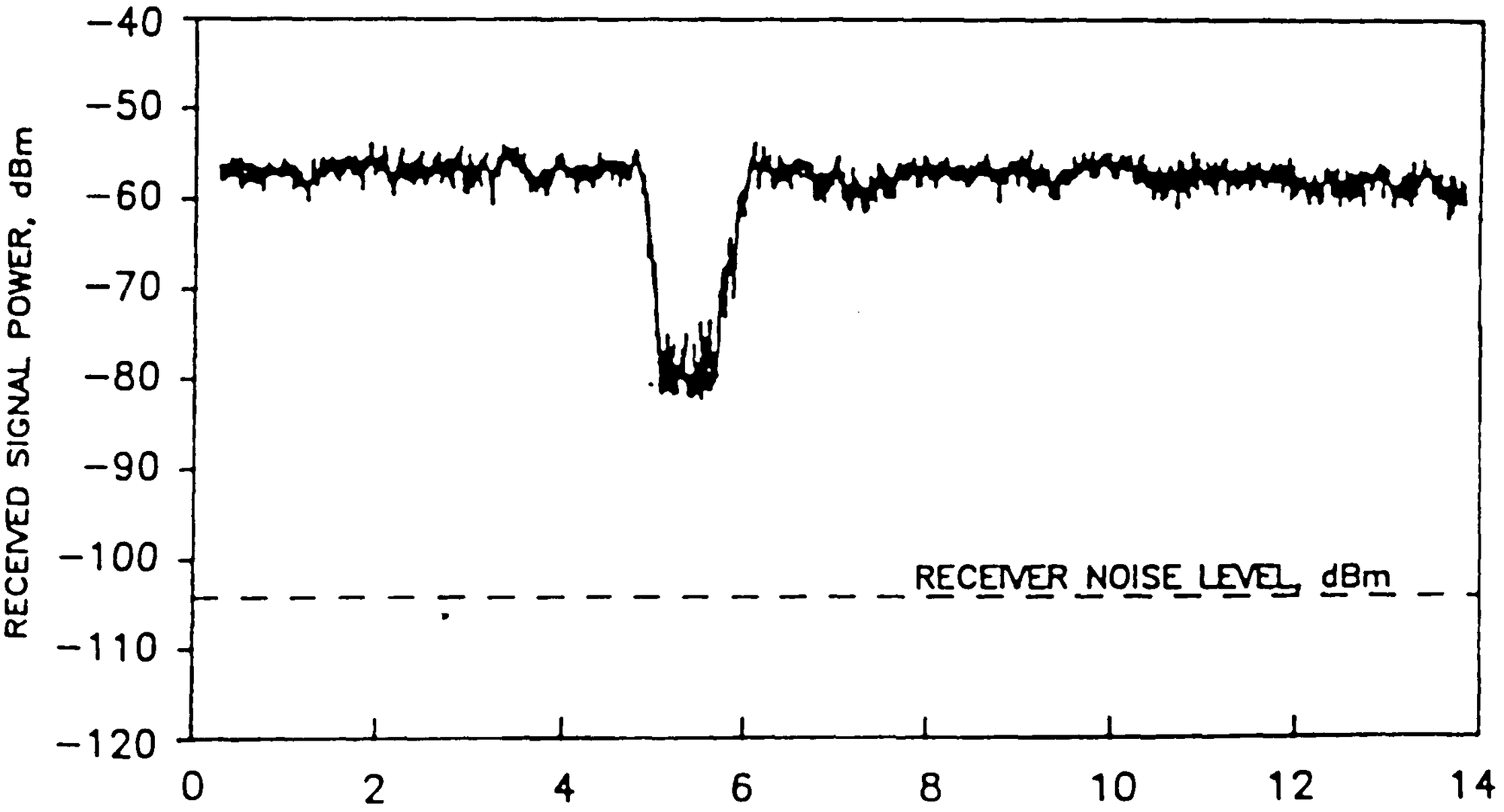

FIG. 5.12 RECEIVED SIGNAL POWER WHEN LOS PATH BETWEEN TRANSMITTER AND RECEIVER WAS OBSTRUCTED BY A TREE TRUNK.

dropped by about 25dB for a distance of about 80cm when the direct path was obstructed.

5.6 EDGE DIFFRACTION MEASUREMENTS CONDUCTED OUTDOORS

When radiation reaches an obstruction, diffraction occurs around its edges, so that some signal can be received in the shadow region. Edge diffraction measurements were conducted outdoors to see if the signal power was still usable.

5.6.1 Diffraction around the corner of a Building.

The transmission loss over a diffraction path depends on the shape and electrical characteristics of the diffracting edge. A vertical corner of a building may approach a "knife edge" which provides the minimum transmission loss if it is perfectly conducting. Both the transmitter and receiver used standard 20dB gain horn aerials.

The measurement was conducted at the edge of a building. The geometry of the site and the position of the transmitter and receiver are shown in figure 5.13a. The corner of the building was formed from poured and finished concrete. The transmitter and receiver were at 1.5m above ground level and the transmitter distance from the edge (d1) was 25m. The transmitter was moved along the shadow region parallel to the building while pointing the transmitter aerial at the edge. The received signal power was recorded for different distances between the receiving aerial and the wall (d2) with the receiver aerial always pointing towards the corner of the building.

The results are shown in figure 5.13b. When the transmitter, the edge and the receiver were aligned, the received signal power dropped by about 4dB

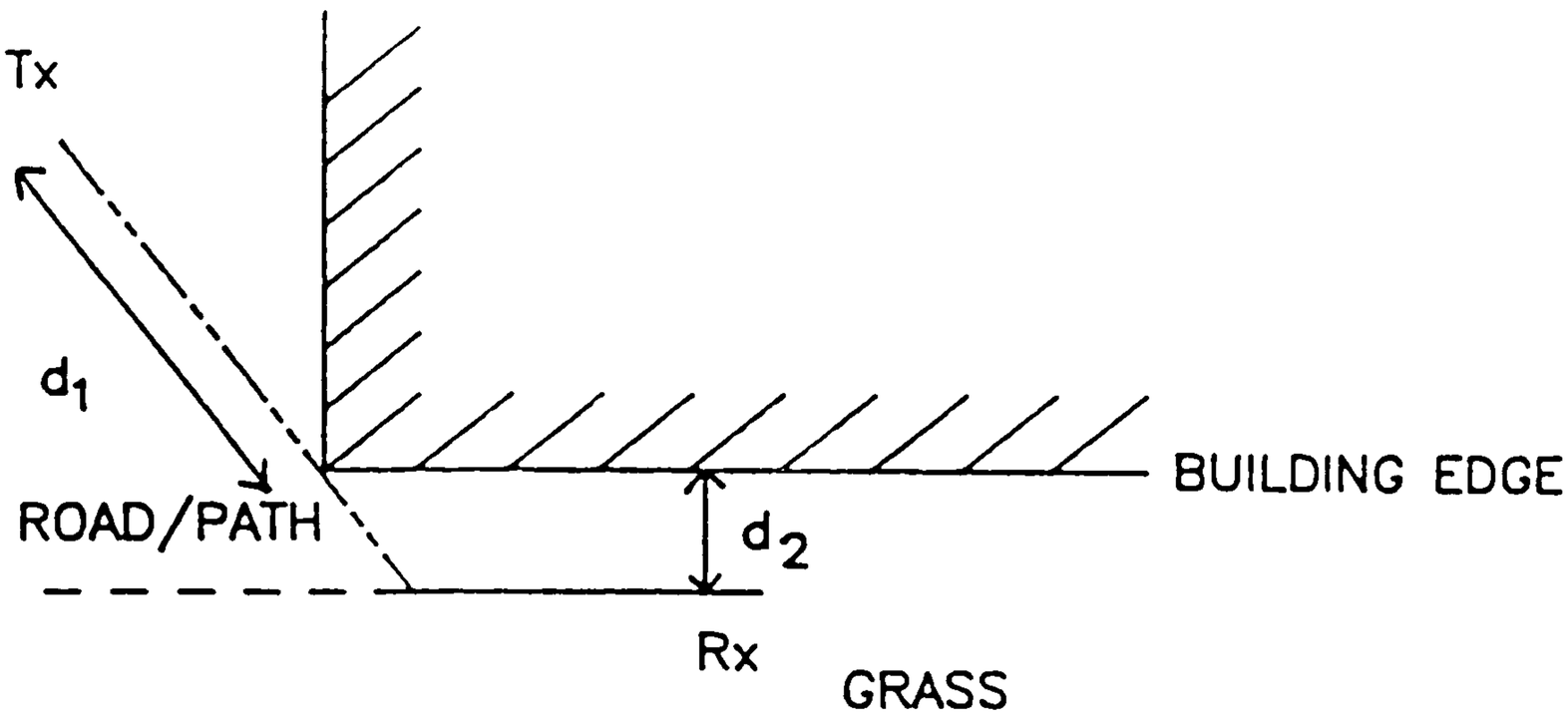

(a)

(b)

FIG. 5.13 EDGE DIFFRACTION MEASUREMENTS AT THE CORNER OF A BUILDING

compared with that measured under LOS conditions. As the receiver was moved into the shadow zone, the received signal dropped rapidly. Moving just a few metres into the shadow region causes an attenuation of about 40dB in the received signal power. Fig. 5.13b also shows that the degree of attenuation is very dependent upon the distance, d, separating the obstruction and the receiver.

5.6.2 Diffraction around a Curved Road.

Further measurements were conducted to determine the propagation behaviour along Elton Road, a curved road with bushes and trees along one side and buildings on the other. A plan view of the road is shown in fig. 5.14. The transmitter used a 20dB gain horn aerial and was initially placed 20m away from the receiver, which used the type 1 omnidirectional aerial. During the measurements the transmitter was moved from a LOS position into the shadow region around the corner of the road and the transmitter aerial was always pointing towards the receiver at the corner of the road when the LOS path was blocked by trees and bushes. The average power was nearly constant at the beginning of the road with some fades, and decreased slowly with the curvature of the road. There was a steep decrease after the end of the road where the LOS path was not present. This demonstrates that the receiver output power is directly dependent on a LOS path. As shown in figure 5.15, the received signal power around the corner of the road dropped by about 25 to 30dB in a travelled distance of a few metres.

5.7 PROPAGATION OF 60GHz SIGNALS INTO BUILDINGS

There is a requirement for portable communications indoors as well as outdoors. Although this will probably require 60GHz radio distribution points within buildings, it is interesting to see how well 60GHz signals can penetrate into buildings, since propagation by this route may reduce the number of radio ports

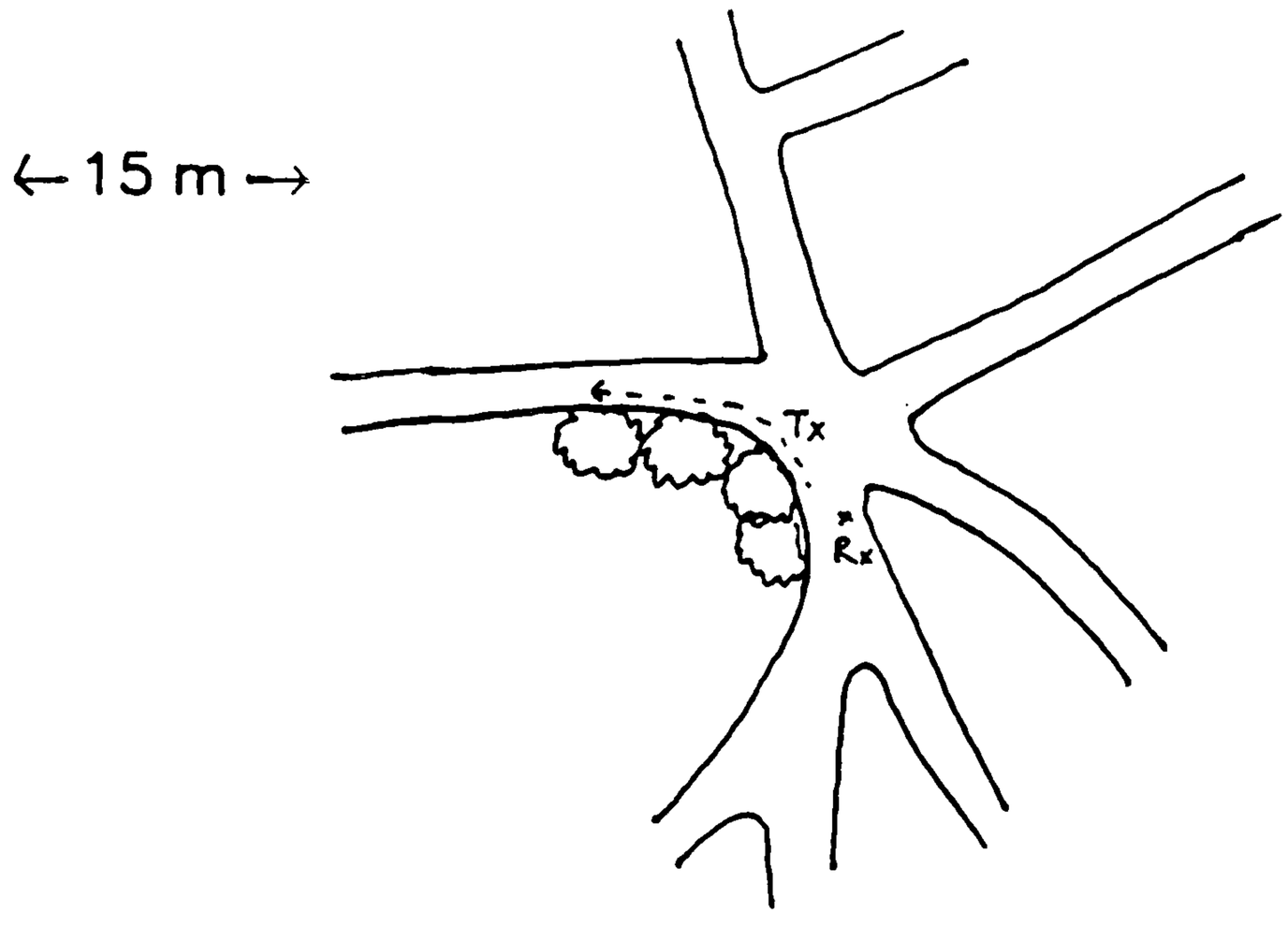

FIG. 5.14 PLAN VIEW OF MEASUREMENT AREA OF A CURVED ROAD BORDERED WITH TREES AND BUSHES.

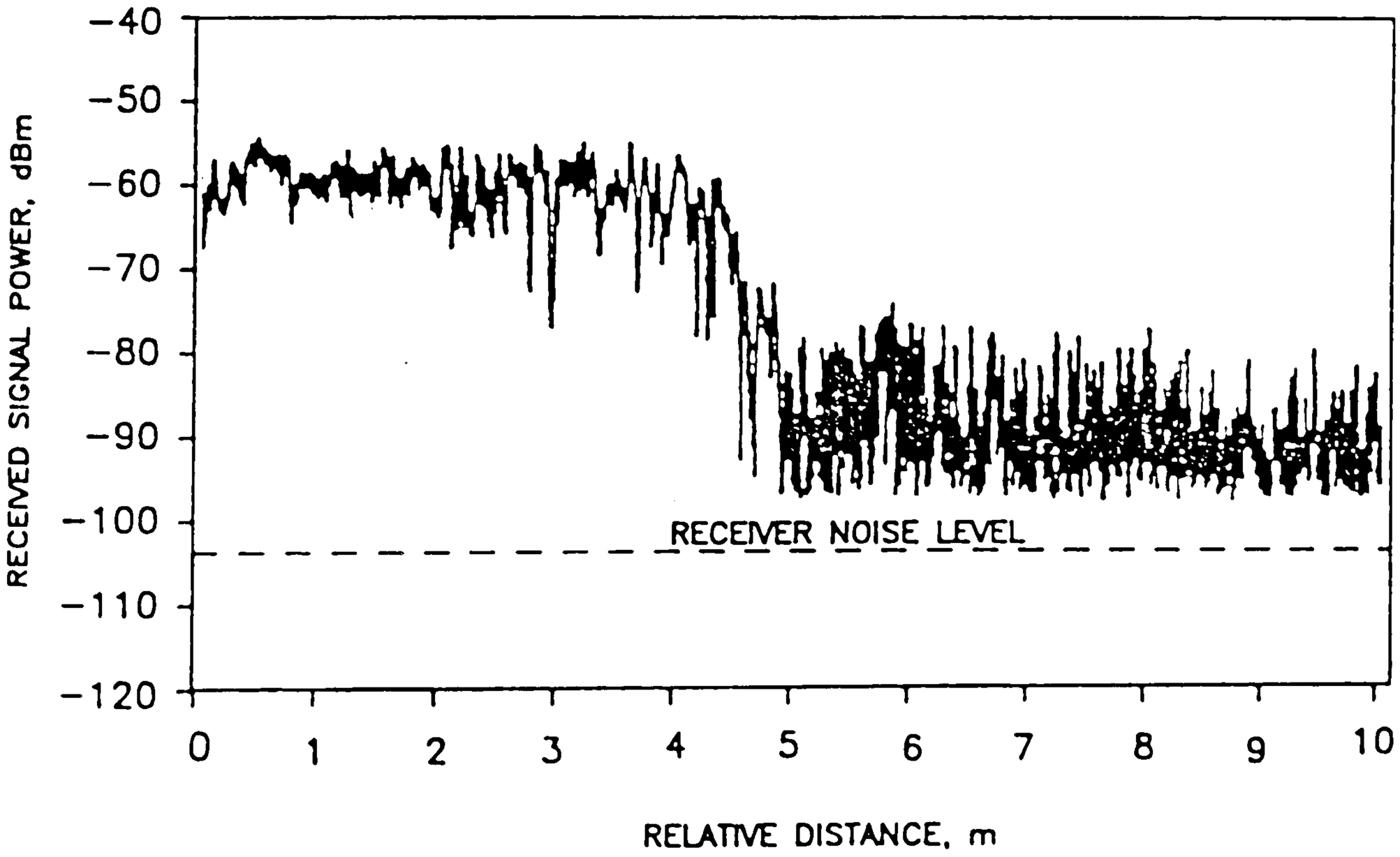

FIG. 5.15 RECEIVED SIGNAL POWER AS THE RECEIVER IS MOVED AROUND THE CORNER OF A CURVED ROAD BORDERED WITH TREES AND BUSHES.

required indoors. The measurements were made in the Queen's building, a reinforced concrete building having glass windows and concrete walls. These types of concrete walls were expected to exhibit high values of attenuation. There were five windows with aluminium frames which were 5m wide and 2m high. The thickness of the concrete walls was 40cm. The plan view of the building is shown in figure 5.16, which shows the corridor and the room where the receiver was placed during the measurements. The transmitter was placed 30m from the building at a height of 5m above ground level, and the receiver was placed in the first floor of the building at the same height as the transmitter. The receiver used a standard 20dB gain horn aerial and the transmitter used the type 1 omnidirectional aerial.

At each location, the handheld receiver was scanned at a height of about 1.5m above the floor. The receiver was subjected to a raster scan consisting of 10 parallel linear scans with 5cm increments in a 50cm by 50cm square. The motion of the receiver results in small scale signal variations which are caused by multipath propagation. Within this area, the mean signal power is approximately statistically stationary so that the median signal power and envelope fading statistics can be computed.[3,4] After making these measurements, the transmitter was moved to another location and the procedure was repeated. The median signal power was obtained at several receiver locations. The median was used instead of the mean because it is affected less by the receiver noise floor, for reasons described in section 4-5. In order to determine the penetration loss into the building, a reference level was measured just outside the window of the building. The reference power outside the building was approximated by taking the average of several median powers measured at different locations just outside the windows.[5]

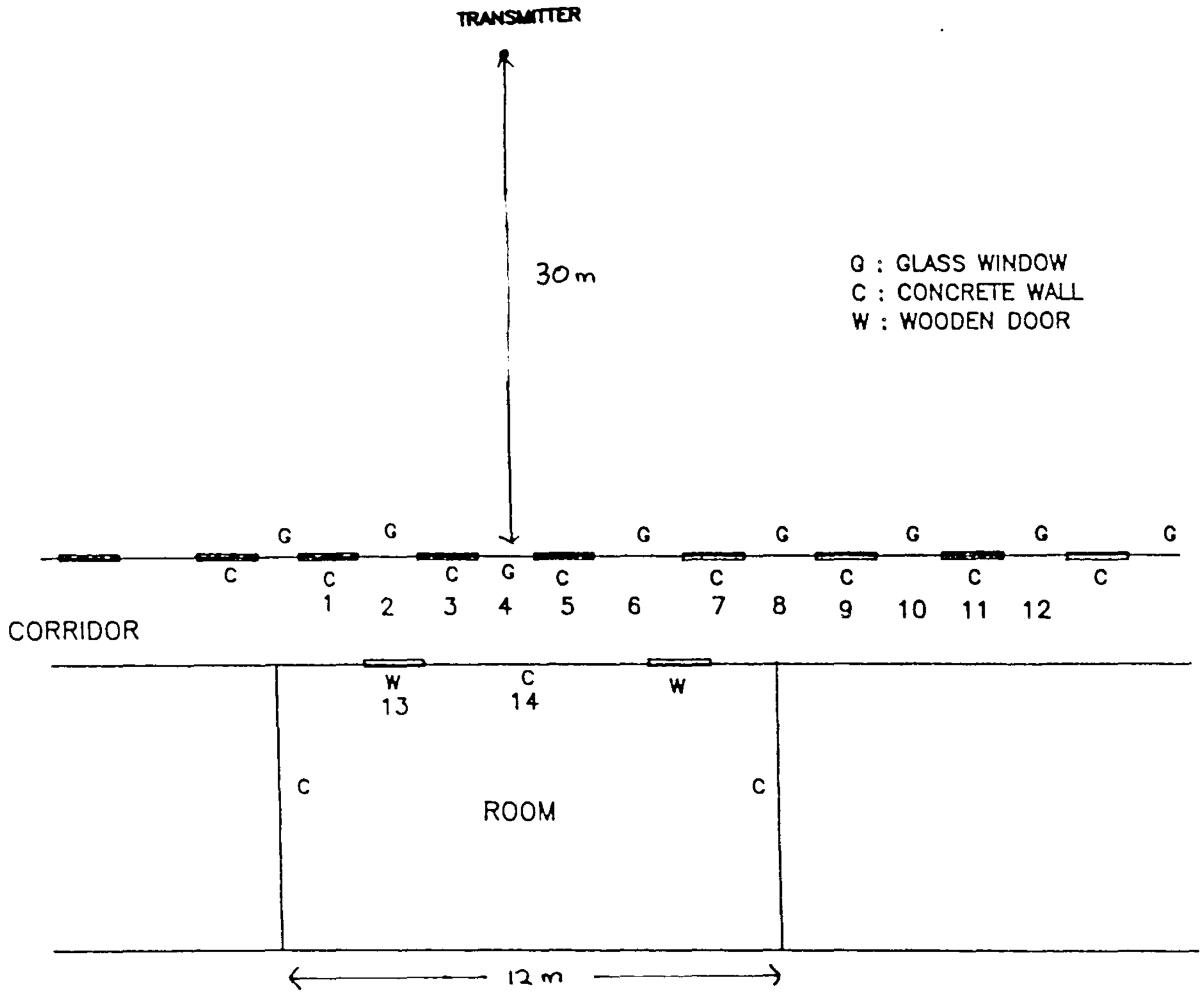

LOCATIONS	PENETRATION LOSS (dB)
1	25
2	5
3	33
4	4
5	> 45 (NOISE LEVEL)
6	5
7	> 45 (NOISE LEVEL)
8	14
9	> 45 (NOISE LEVEL)
10	27
11	> 45 (NOISE LEVEL)
12	37
13	24
14	> 45 (NOISE LEVEL)

FIG. 5.16 PLAN VIEW OF THE MEASUREMENT LOCATIONS FOR RADIATION OF 60GHz INTO A BUILDING AND THE MEDIAN SIGNAL POWER AT VARIOUS POINTS.

The median received signal power was computed for every location shown in figure 5.16. The penetration loss was later computed relative to the reference level outside the windows of the building. For a given distance, the penetration loss for each location within the building is the difference between the median signal power at that location and the reference signal power outside the building. Signal powers were measured at twelve locations along the corridor and two locations within the room adjacent to the corridor as shown in figure 5.16. The penetration losses for these locations are also shown in this figure. It can be seen that at the positions along the corridor behind the wall where there was no LOS path between the transmitter and receiver, the penetration loss was greater than when there was a LOS path. Within the room, the penetration loss was lower at the locations in front of the wooden doors compared to the locations in front of the wall. It was found that for this particular building, the penetration loss varied from 4dB to greater than 45dB.

When there was no LOS path between the transmitter and receiver the received signal power was found to be very low and often below noise level. The median signal was found to be higher behind windows and the door compared to behind the wall due to the higher penetration loss of the walls.

Generally, the 60GHz signal may enter the building directly from the transmitting aerial or may be reflected from many reflecting surfaces presented by the surrounding environment. Once inside, the signal experiences different kinds of objects such as walls, ceiling, floors etc. As a result the signal arrives through many different paths, each experiencing different attenuations.

REFERENCES

[1] Lee, W.Y.C., "Estimate of local average of a mobile radio signal," IEEE Trans. on Vehicular Tech., Vol VT-34, No. 1, February, 1985.

[2] Hawkins, N.D., Steele, R., Rickard, D.C., and Shepherd, C.R., "Path loss characteristic of 60GHz transmissions," Electronics Letters, Vol. 21, No. 22, Oct. 1985, pp.1054 - 1055.

[3] Cox, D.C. Murray, R.R., and Norris, A.W., "Measurements of 800 MHz radio transmission into buildings with metallic walls," B.S.T.J. Vol. 62, pp. 2695-2717 Nov. 1983.

[4] Cox, D.C., Murray,R.R., and Norris, A.W., "800 MHz measurements in and around suburban houses," B.S.T.J, pp.921-954, July-Aug, 1984

[5] Reduink, D.O., "Properties of mobile radio propagation above 400 MHz," IEEE Trans. 1971, VT-23, pp.143-159.

CHAPTER 6

PROPAGATION MEASUREMENTS WITHIN BUILDINGS.

6.1 INTRODUCTION

At certain times, there may be more people indoors than outdoors, especially in multistorey buildings. Therefore, there is a need for personal mobile communications in buildings. Experiments have been conducted (Chapter 5) to measure the penetration loss when radiating the 60GHz signal into a reinforced concrete building. It was found that the penetration loss was high when there was no LOS path through a glass window between the transmitter and receiver. Thus, for a usable signal level, the 60GHz signal must be radiated within buildings themselves.

Within buildings, the radiation of the 60GHz signal in general travels a shorter distance than outdoors because of the high penetration loss of walls and thereby experiences less oxygen absorption compared to the outdoors environment. The propagation characteristics will be determined by the environment and its contents of fixed and moving objects. Futhermore, the environment within buildings will introduce multipath fading and shadowing. Measurements, therefore, have been conducted within a reinforced concrete building at the University of Bristol to determine the propagation characteristics under LOS and non-LOS conditions.

The aim of the measurements was to study the reception of radio signals at 60GHz in different environments within buildings for both fixed and mobile conditions. The analysis includes the determination of the fading statistics of the received signal envelope under LOS and non-LOS conditions, the variation of the median signal power with distance for different types of rooms and corridors, the

attenuation of various building materials, the signal coverage, the power spectrum of the received signal and edge diffraction measurements.

For most of the measurements conducted, the transmitter and receiver were placed on a trolley at a height of about 1.5m above the floor. Unless stated otherwise, both the transmitter and receiver used phase-locked 60GHz oscillators and the type 2 omnidirectional aerials as described in chapter 4. Most of the measurements were conducted at night or during weekends in order to ensure that there would be no people around, whose movements would otherwise interfere with the measurements.

6.2 ENVELOPE MEASUREMENTS

Measurements were conducted to determine the envelope fading statistics for both mobile and stationary conditions with and without a LOS path. The received signal envelope was sampled at an interval of less than a tenth of a wavelength. Preliminary measurements have indicated that as long as the data sampling interval is less than a tenth of a wavelength, the statistics deduced from the measurements are accurate.

6.2.1 Envelope Distribution when the Transmitter was moving.

The first measurements were conducted at the entrance of the building, the plan view of which is shown in figure 6.1. As indicated, there was no furniture or equipment in the area. The walls and ceiling consisted of plaster covered concrete, and the floor was covered with varnished cork tiles. The height of the ceiling was about 5m. LOS measurements were conducted by placing the transmitter at 8m from the receiver, whereas for non-LOS measurements, the receiver was placed at the same distance but with the direct signal obstructed by the corner of a wall as shown

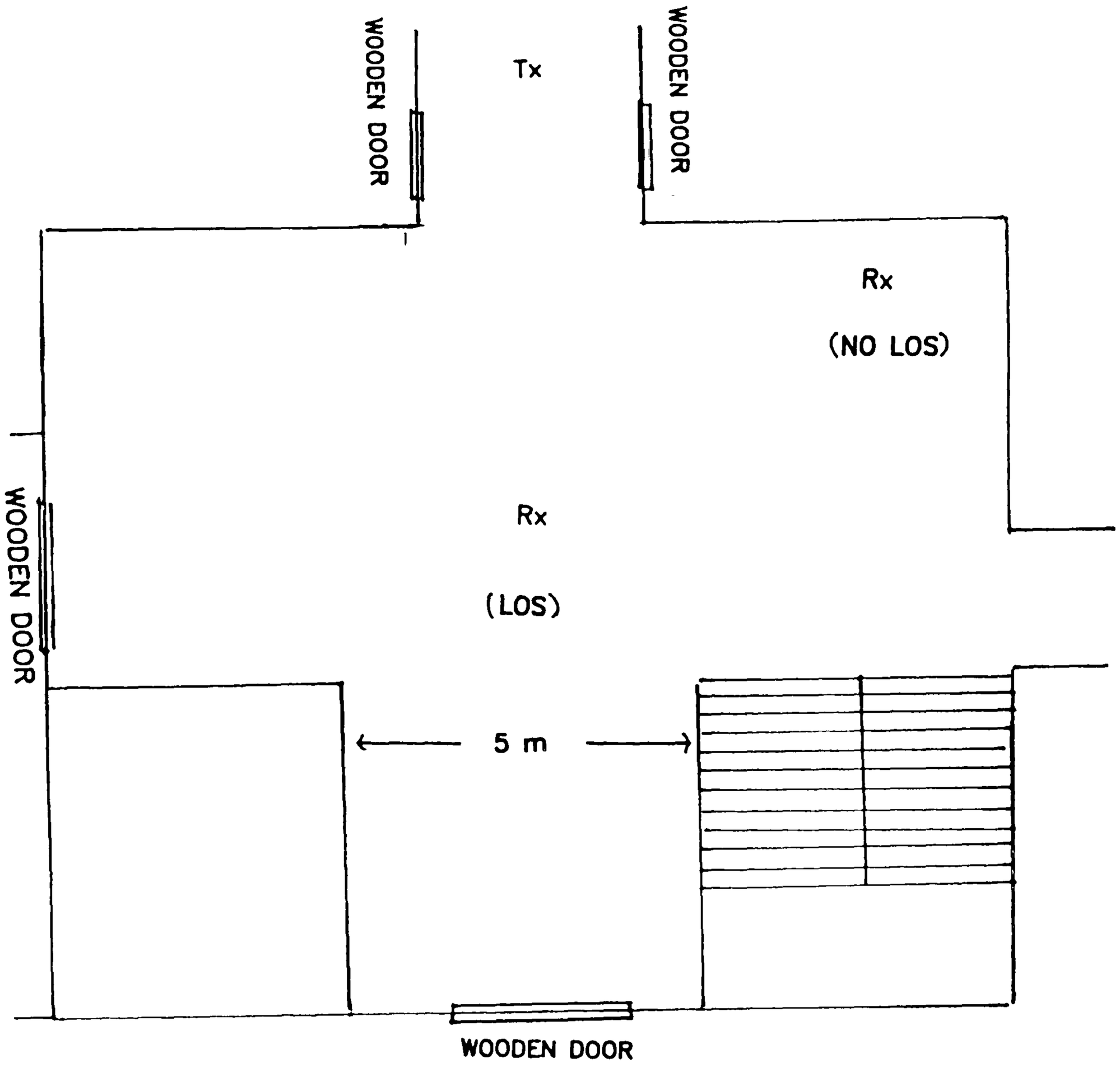

FIG. 6.1 PLAN VIEW OF THE MAIN ENTRANCE OF THE BUILDING.

in figure 6.1. During the measurements the transmitter was randomly moved horizontally in a 50cm by 50cm (100λ by 100λ) square.

A typical recording of the received signal power in dB when a LOS path was present between the transmitter and receiver is shown in figure 6.2. When there was no LOS path between the transmitter and receiver, a typical recording is shown in figure 6.3. The figures show that movements of the transmitter result in signal variations which are caused by multipath propagation. Multipath fading occurred due to reflections off the walls, the ceiling, and the floor. Received signal minima were up to 25dB below the mean signal power when there was no LOS path between the transmitter and receiver. However, when there was a LOS path between the transmitter and receiver, the median signal power was found on average to be about 10dB higher than when no LOS path was present, and there was less multipath fading.

The cumulative distribution function (CDF) of the received signal envelope was computed in 1dB increments for both LOS and non-LOS conditions. The computed data was plotted on Rayleigh paper as shown in figure 6.4, where a Rayleigh distribution produces a straight line. The medians of the distributions have been normalised to 0dB so that different types of distribution could be more easily compared.

When a LOS path existed between the transmitter and receiver, the envelope distribution departed from the Rayleigh distribution due to the presence of a strong direct signal. The signal received via this path is likely to be much stronger than the signal received via the reflected paths, so the distribution should depart from the Rayleigh distribution and become a Rician distribution.[1] However, when there was

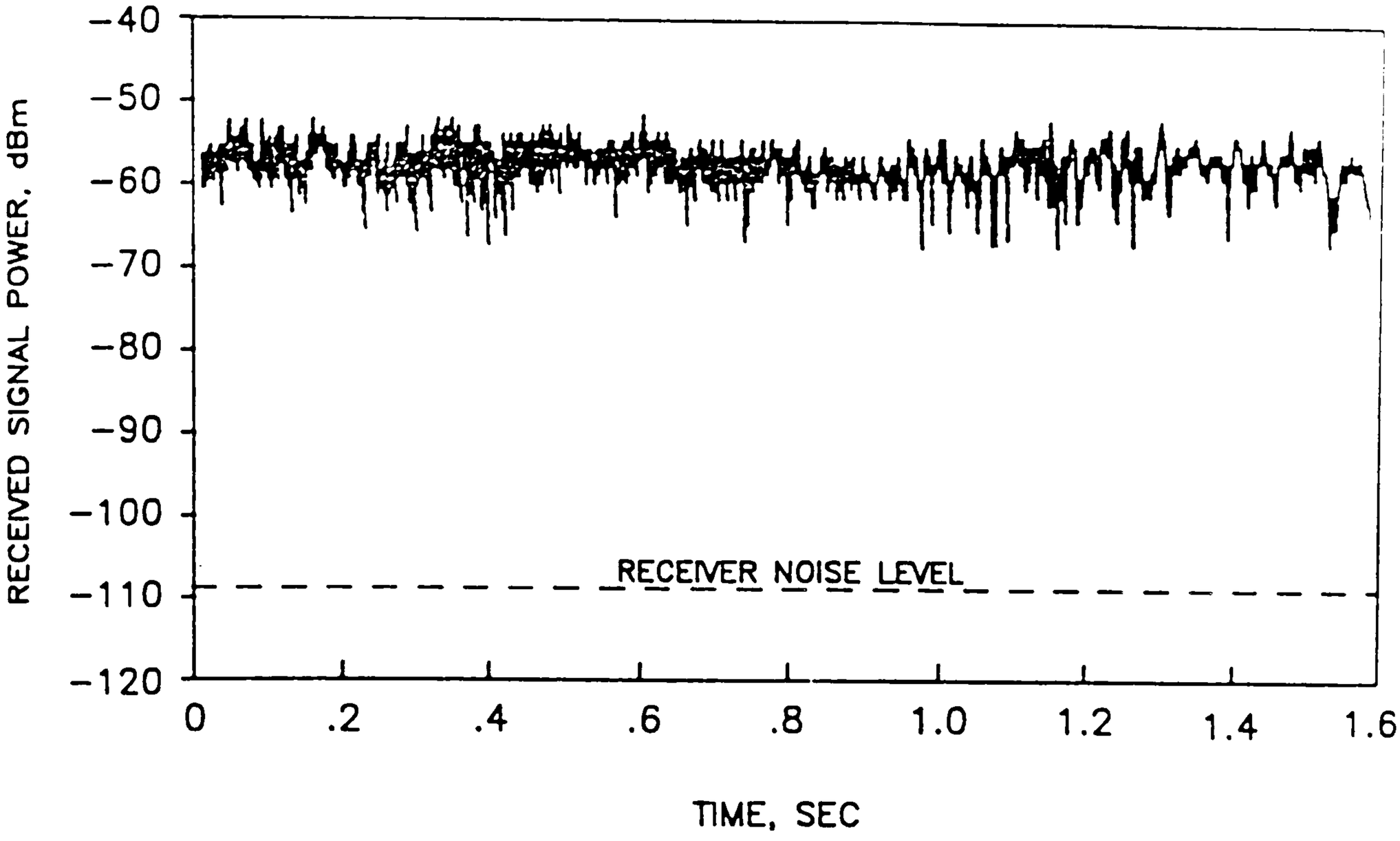

FIG. 6.2 RECEIVED SIGNAL POWER WHEN THERE WAS A LOS PATH BETWEEN TRANSMITTER AND RECEIVER FOR RANDOM SCANNING OF THE TRANSMITTER AT ABOUT 0.8m/sec

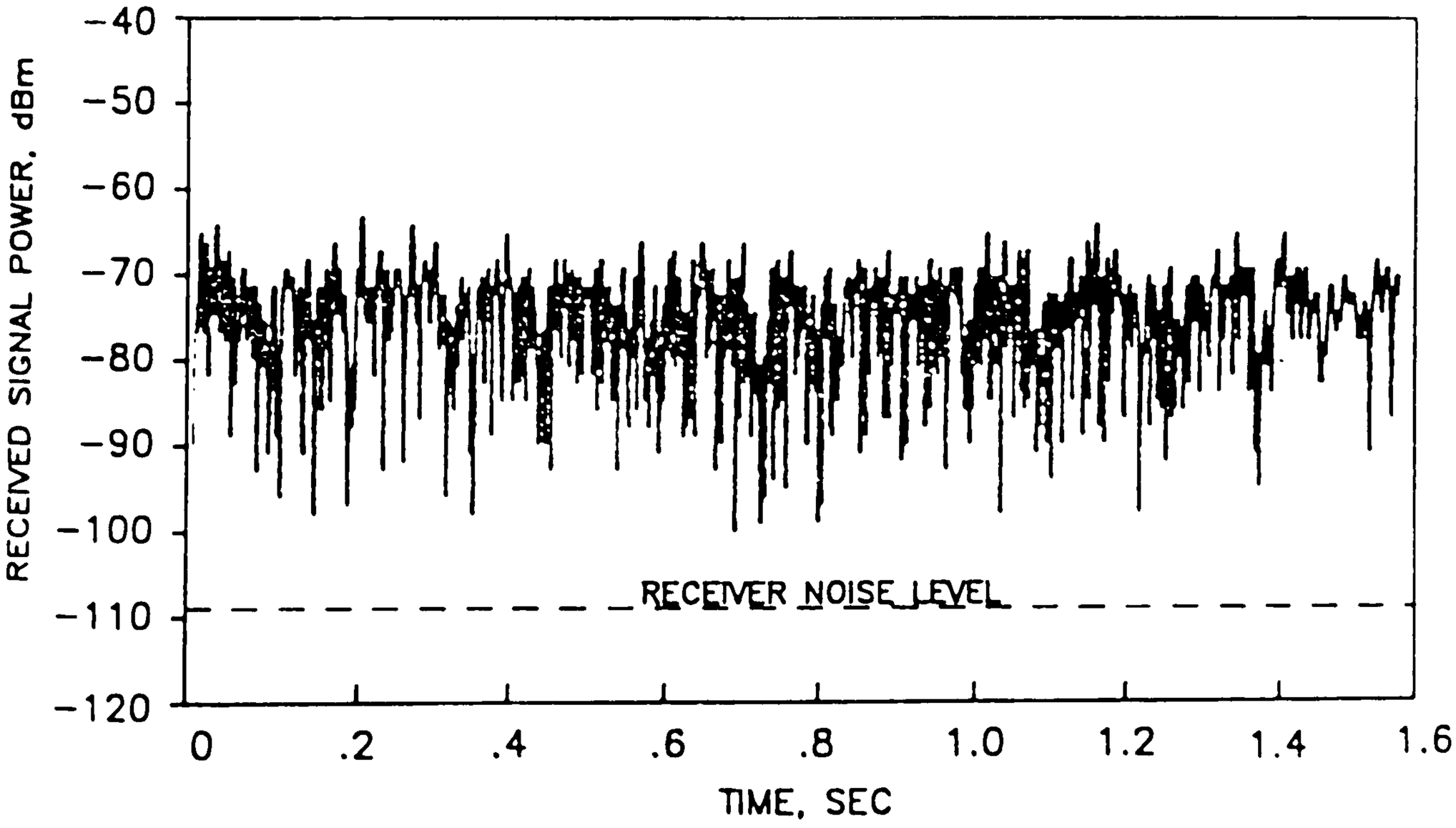

FIG. 6.3 RECEIVED SIGNAL POWER WHEN THERE WAS NO LOS PATH BETWEEN TRANSMITTER AND RECEIVER FOR RANDOM SCANNING OF THE TRANSMITTER AT ABOUT 0.8m/sec.

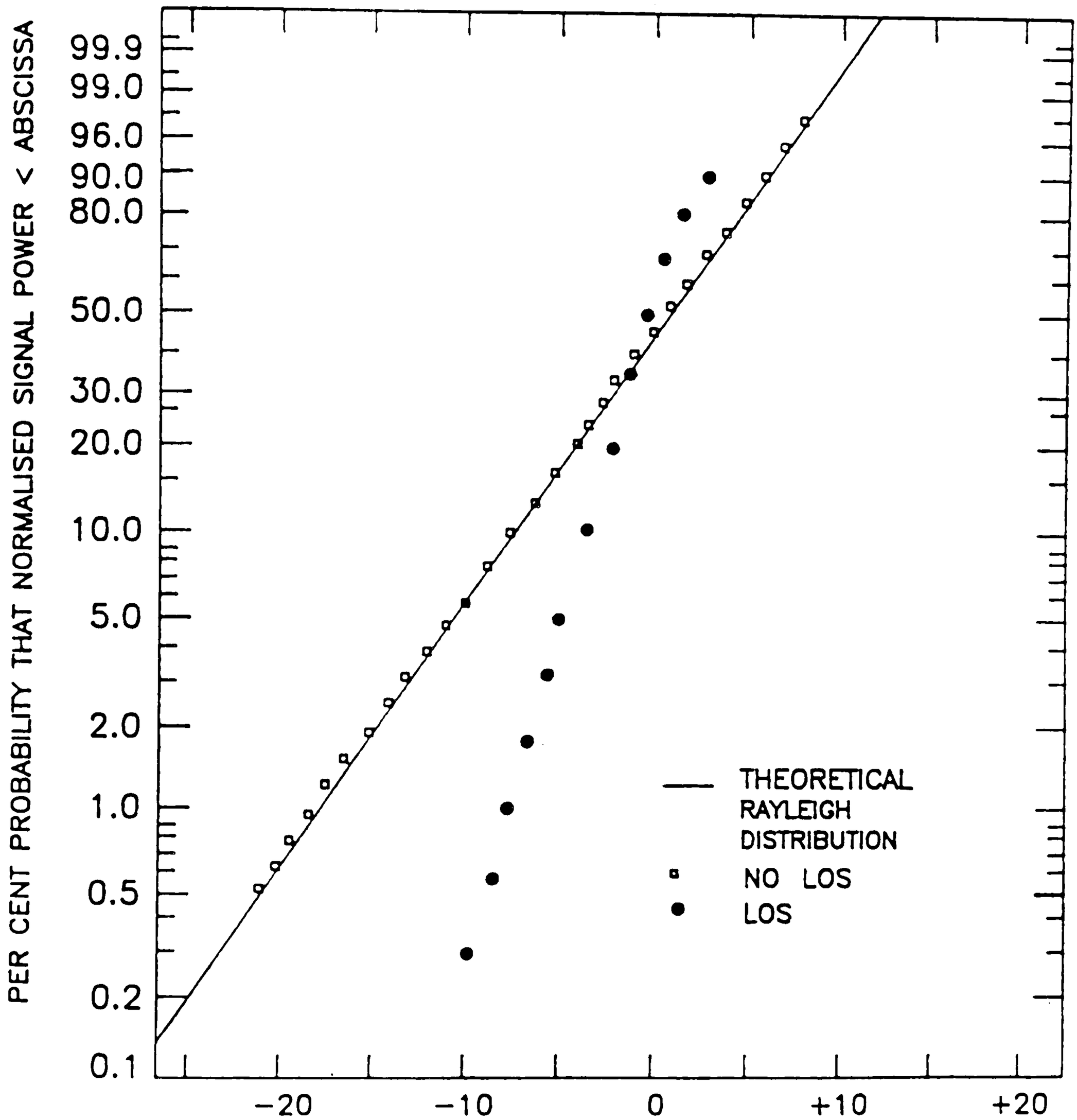

FIG. 6.4 CDF OF THE RECEIVED SIGNAL POWER FOR LOS AND NON−LOS CONDITIONS

no LOS path between the transmitter and receiver, the envelope closely followed the theoretical Rayleigh distribution. This was expected because when the received signal is dominated by reflection and diffraction with no strong and dominant direct component, the theoretical result should be a Rayleigh distribution.[2]

6.2.2 Envelope Distribution when a person was moving

The second measurements were conducted with the transmitter and receiver stationary for both LOS and non-LOS conditions. Since the signal reaching the receiver is randomly modified by people moving in the area as well as by the floor, the ceiling, the walls, and the furniture, it is interesting to find out what effect these have. The floor, ceiling, walls and furniture produce a static reflection pattern, whereas the movement of people cause randomly varying reflections off themselves, and randomly varying blockage of the direct and reflected paths between the transmitter and receiver, which must be considered. The measurements were made to simulate communications using a portable hand set where the LOS path is sometimes obstructed by the user when carrying the hand set.

The measurements were conducted within the Communications Research Laboratory, a plan view of which is shown in figure 6.5. One third of the room was filled with various types of electronic equipment and furniture. The room was made up of a concrete ceiling, four plastered concrete walls which had an average thickness of 30cm, and a floor covered with varnished cork tiles. The height of the ceiling was 3.5m. The wall of the room adjacent to the corridor had three wooden doors at 3m intervals. Each door was 1m wide and 2m high. The opposite wall had five aluminium window frame units which were 1.5m above the floor and were 2m wide and 2.5m high, separated by posts which were 0.35m wide and 0.25m deep. The other two sides of the room had neither doors nor windows.

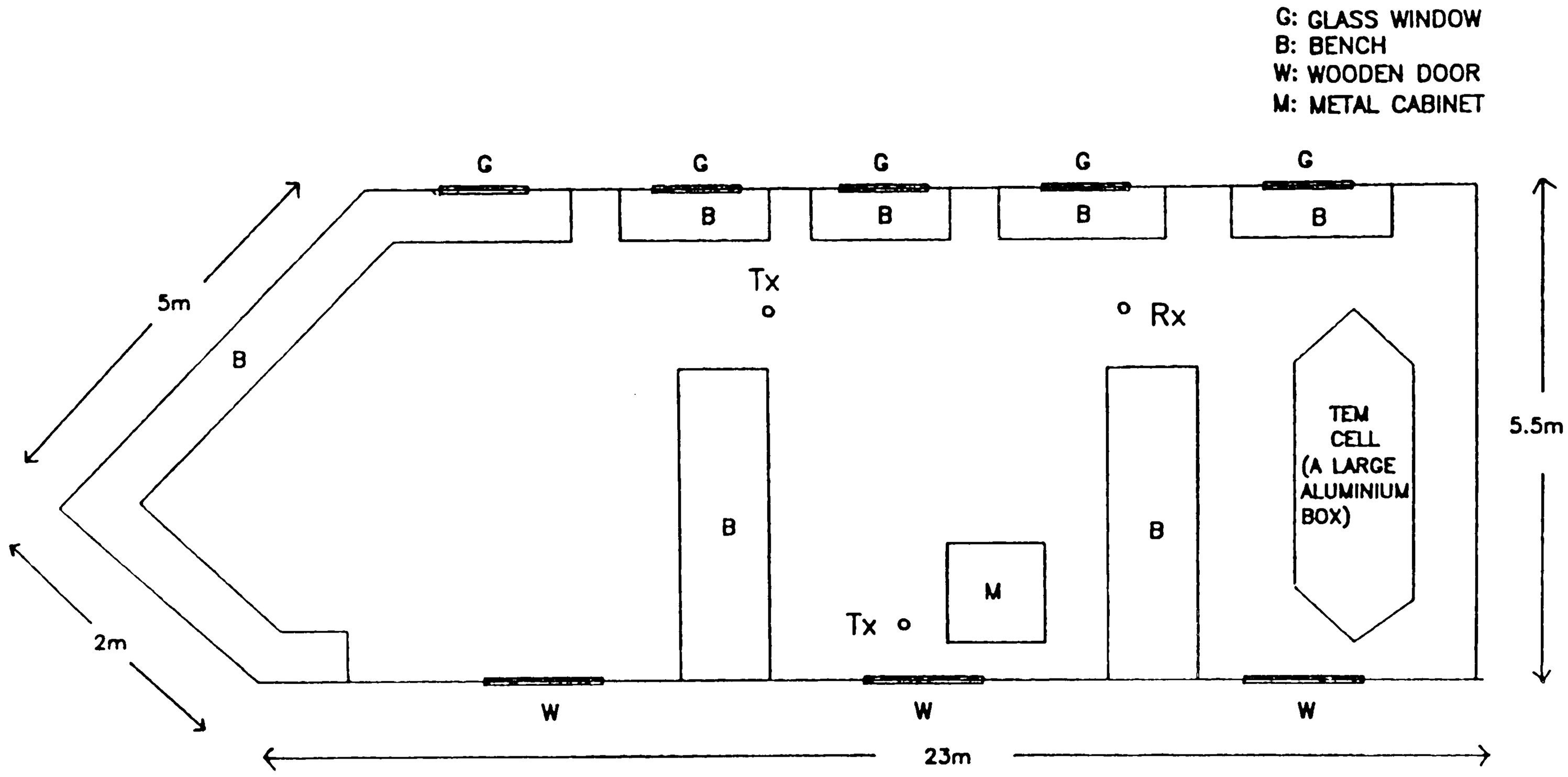

FIG. 6.5 PLAN VIEW OF THE COMMUNICATIONS RESEARCH LABORATORY

During the measurements, a person moved in front of and behind the receiver at a distance of about 0.25m and at a speed of about 1m/s. The received signal envelope statistics and the median signal power were found during the fading intervals. The measurements were conducted when the receiver was placed at 6m from the transmitter under LOS and non-LOS conditions as indicated in figure 6.5. For the non-LOS measurements, the transmitter was placed behind a metal cabinet so that the signal could only be received through reflection and diffraction.

The received signal power in dB was recorded and plotted against time as shown in figures 6.6a and 6.6b. It can be seen from these figures that when a person moved in front of the receiver and behind the receiver, fades occurred in bursts of 15 to 20sec duration separated by periods during which the received signal remained constant due to no movement. The burst characteristics were due to the signal reaching the receiver being randomly modified by the person moving in front of and behind the receiver. The transmitted signal will have transversed a variety of paths to reach the receiver and will therefore be subject to multipath fading. It shows deep fades of over 20 to 25dB in amplitude.

For the LOS measurements, when a person was moving in front of the receiver the fading of the received signal was more severe. The fading was not only due to changes in multipath reflections, but also due to the change of penetration loss of the person and therefore the change in level of the LOS signal as he moved. The results have shown that the typical dynamic range for fading was about 20dB. When a person was moving behind the receiver when a LOS path existed, the characteristics of the received signal were statistically more stationary, and the fading was less bursty, with a smaller dynamic range of 2 to 4dB. When there was

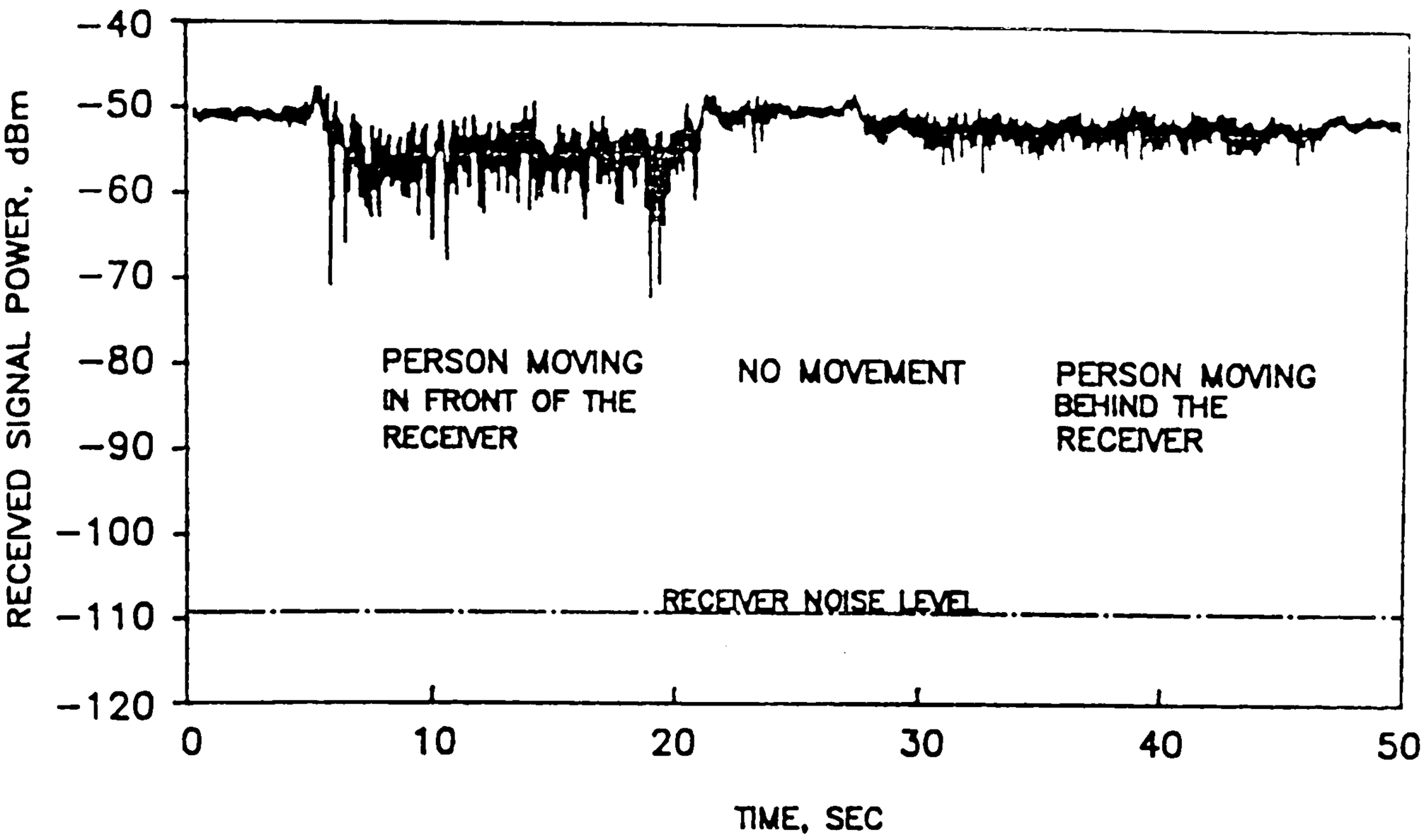

FIG. 6.6a RECEIVED SIGNAL POWER WITH THE TRANSMITTER AND RECEIVER FIXED AND A PERSON MOVING IN FRONT OF AND BEHIND THE RECEIVER (LOS)

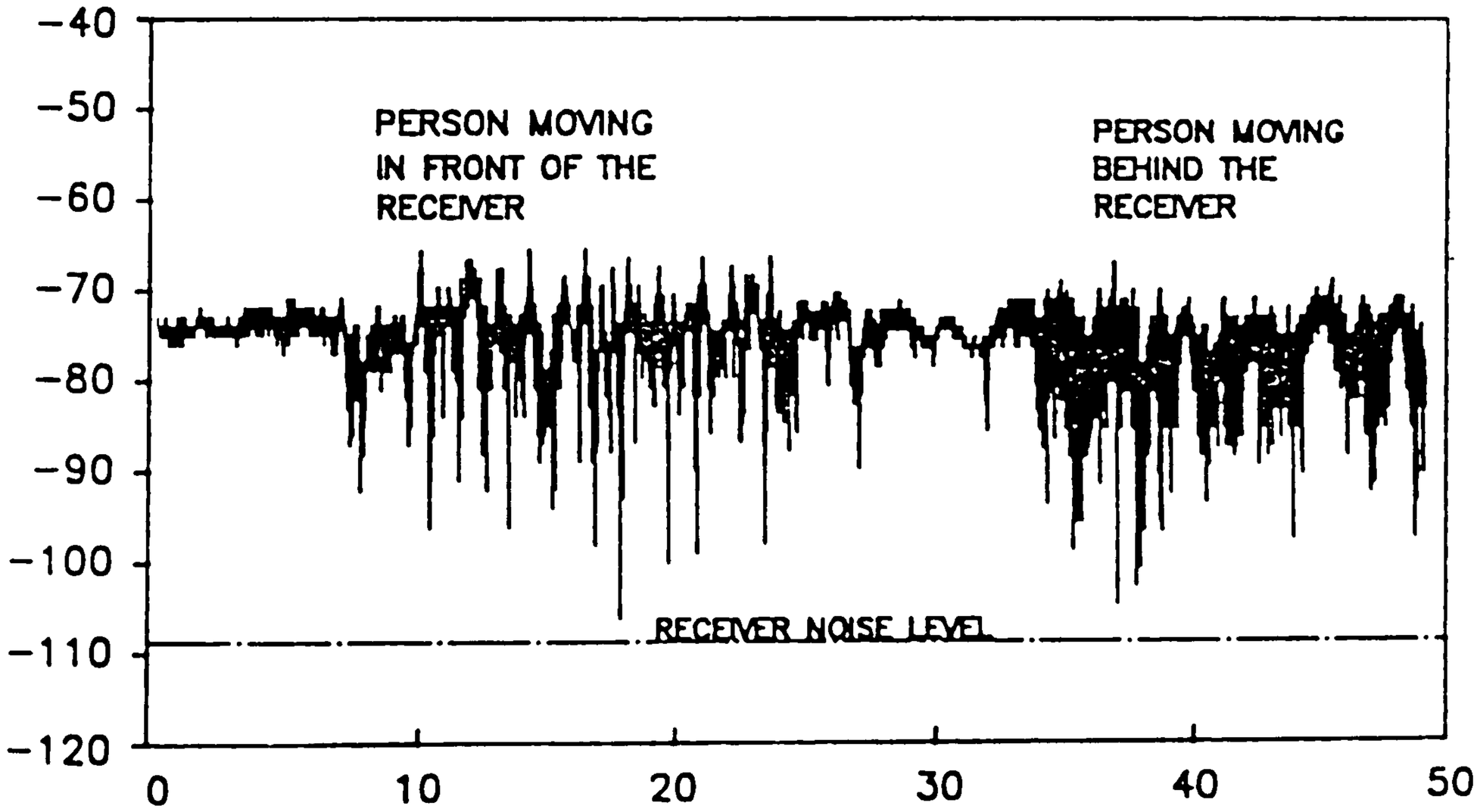

FIG. 6.6b RECEIVED SIGNAL POWER WITH TRANSMITTER AND RECEIVER FIXED AND A PERSON MOVING IN FRONT OF AND BEHIND THE RECEIVER. (NO LOS)

no LOS path between the transmitter and receiver, the median received power remained low, and the received signal envelope had deeper fades compared to the LOS measurements. It made little difference if the person moved in front of or behind the receiver.

The CDFs of the received signal envelopes during the bursty periods were computed. They were plotted on Rayleigh paper in 1dB increments of the received signal power which was normalised to the median signal power as shown in figure 6.7. It is interesting to note that when a person moves in front of and behind the transmitter with LOS conditions, the distribution departs from the Rayleigh distribution. However, when a person was moving in front of the transmitter, the distribution is closer to the Rayleigh distribution compared to when a person was moving behind the transmitter.

The results are as expected, because when a person was moving behind the receiver, the level of direct signal is likely to be high and therefore more dominant than the level of the reflected signals. When a person moves in front of the receiver, the level of the LOS signal will be less dominant relative to the level of the reflected signals, so that the distribution will be closer to the Rayleigh distribution.

When there was no LOS path between the transmitter and receiver, the distribution was found to follow the Rayleigh distribution when a person moved in front of or behind the receiver, as shown in figure 6.7.

6.2.3 Envelope Distribution with two people moving along a corridor.

Measurements were also conducted by placing the fixed transmitter and receiver 14m apart in a corridor which was 1.5m wide and 4m height. The side walls

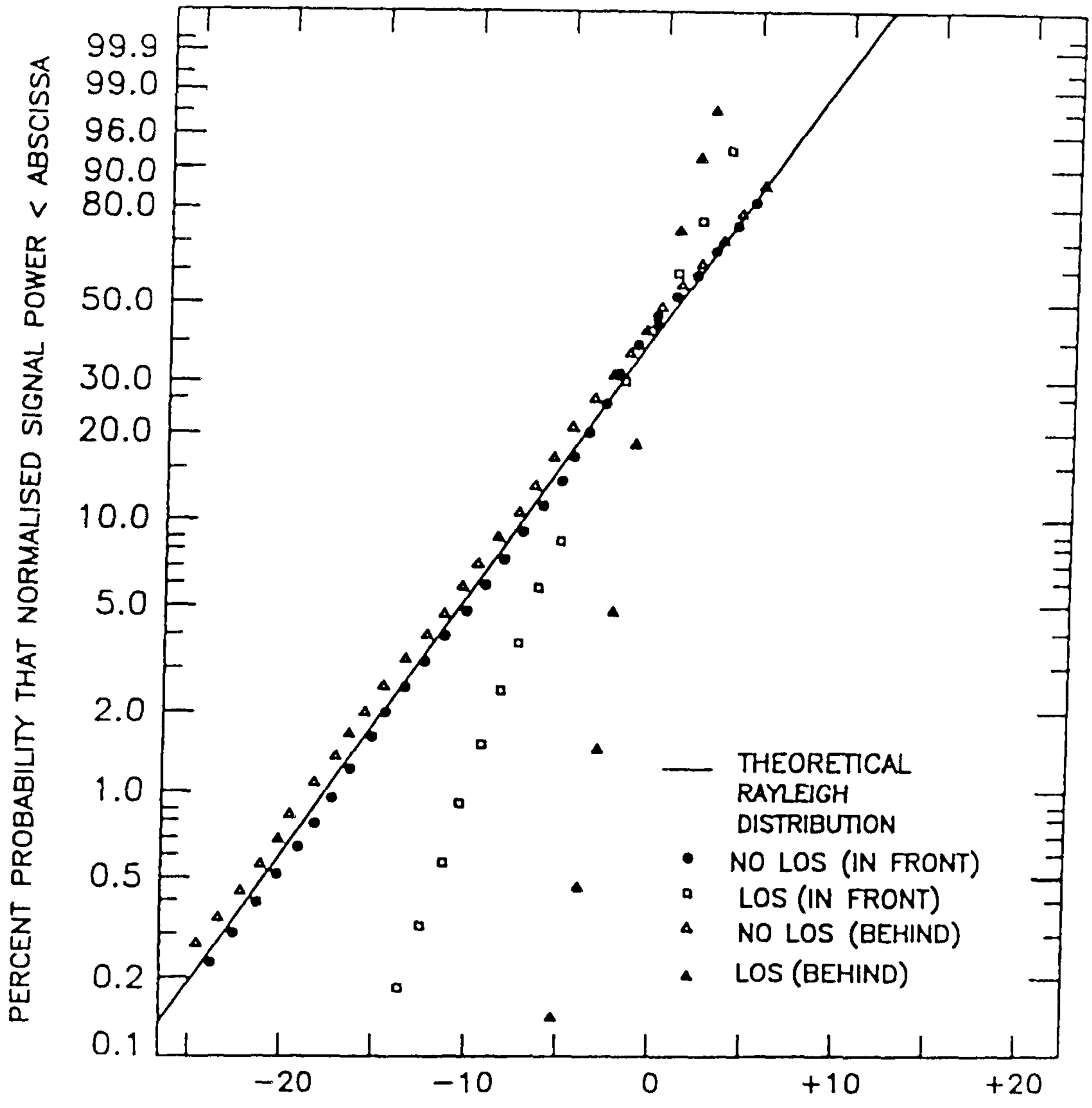

FIG. 6.7 CDF OF THE RECEIVED SIGNAL POWER FOR LOS AND NON-LOS CONDITIONS WITH A PERSON MOVING IN FRONT OF AND BEHIND THE RECEIVER

and the ceiling of this corridor were of plaster covered concrete and the floor was covered with varnished cork tiles. The thickness of the side walls was about 40cm. There were wooden doors at 6m intervals on one side and 2.5m intervals on the other. During the recording period, two people walked to and fro between the transmitter and receiver at a speed of about 1m/s. The recorded signal power in dB is shown in figure 6.8.

The CDF of the received signal envelope was computed in 1dB increments of the recorded signal power as shown in figure 6.9. The results have shown that the envelope distribution was found to follow the Rayleigh distribution. This may be due to several strong reflections from the smooth walls, floor and ceiling of the narrow corridor and also the LOS path which were randomly obstructed by the two people walking to and fro between the transmitter and receiver. The result is that no path reaching the receiver was dominant so a Rayleigh distribution occurred.

6.2.4 Envelope Measurements along a corridor.

A further set of measurements were conducted along a long corridor. The side walls and the ceiling of the corridor were mainly plaster covered and the floor had varnished cork tiles. The thickness of the side walls was about 40cm. The corridor had wooden doors along side of it at intervals of 2.5m which were 2m high by 1m wide. There was a staircase in the middle of the corridor, and at the end of the corridor, there was a 45^0 corner.

During the measurements, the receiver was placed at the beginning of the corridor. The transmitter was initially positioned 1m from the receiver and was moved away at a constant speed up to a distance of 63m and into the shadow region created by the 45^0 corner. Fig. 6.10 shows the recorded signal power along the

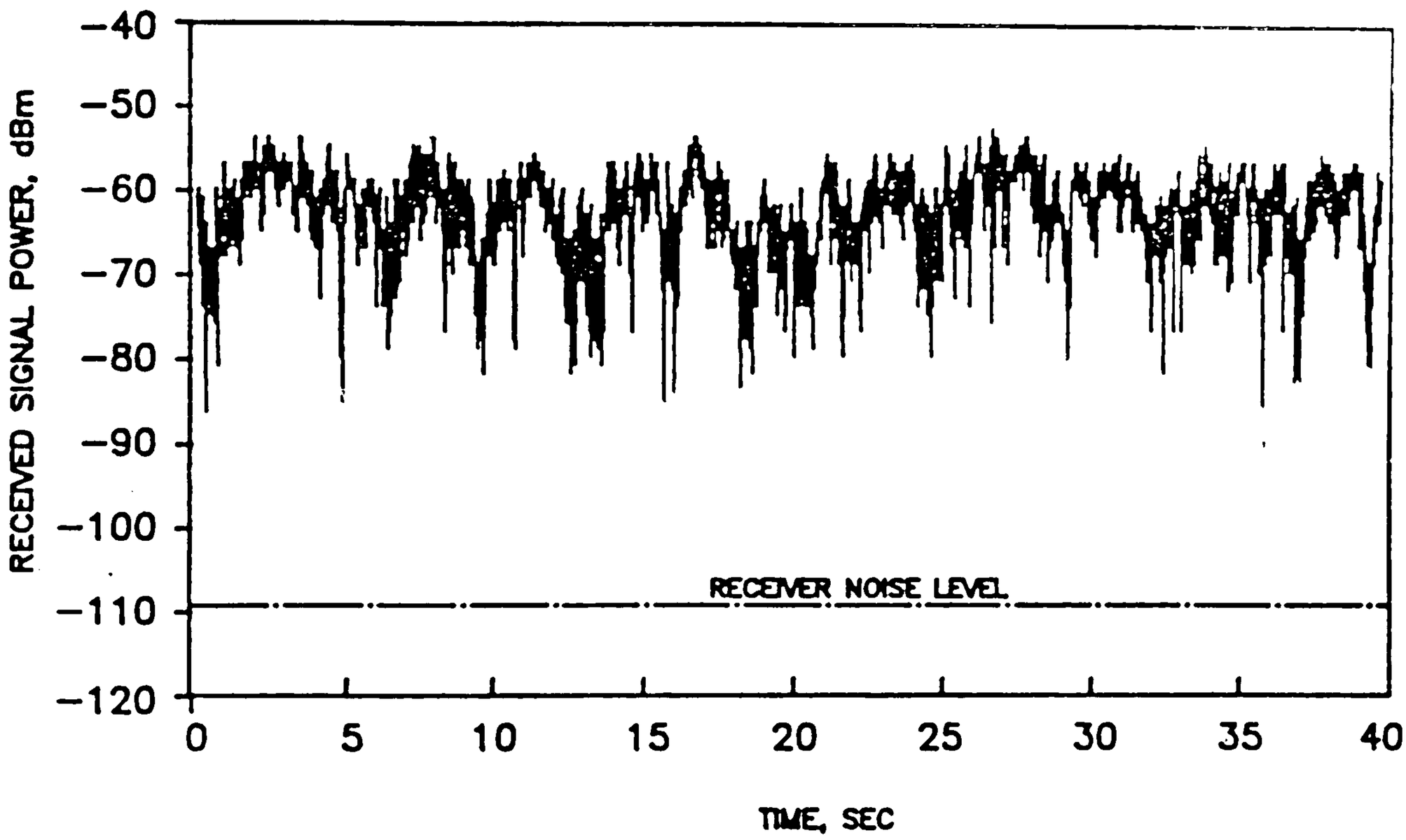

FIG. 6.8 RECEIVED SIGNAL POWER WITH TWO PEOPLE WALKING BETWEEN FIXED TRANSMITTER AND RECEIVER ALONG A CORRIDOR.

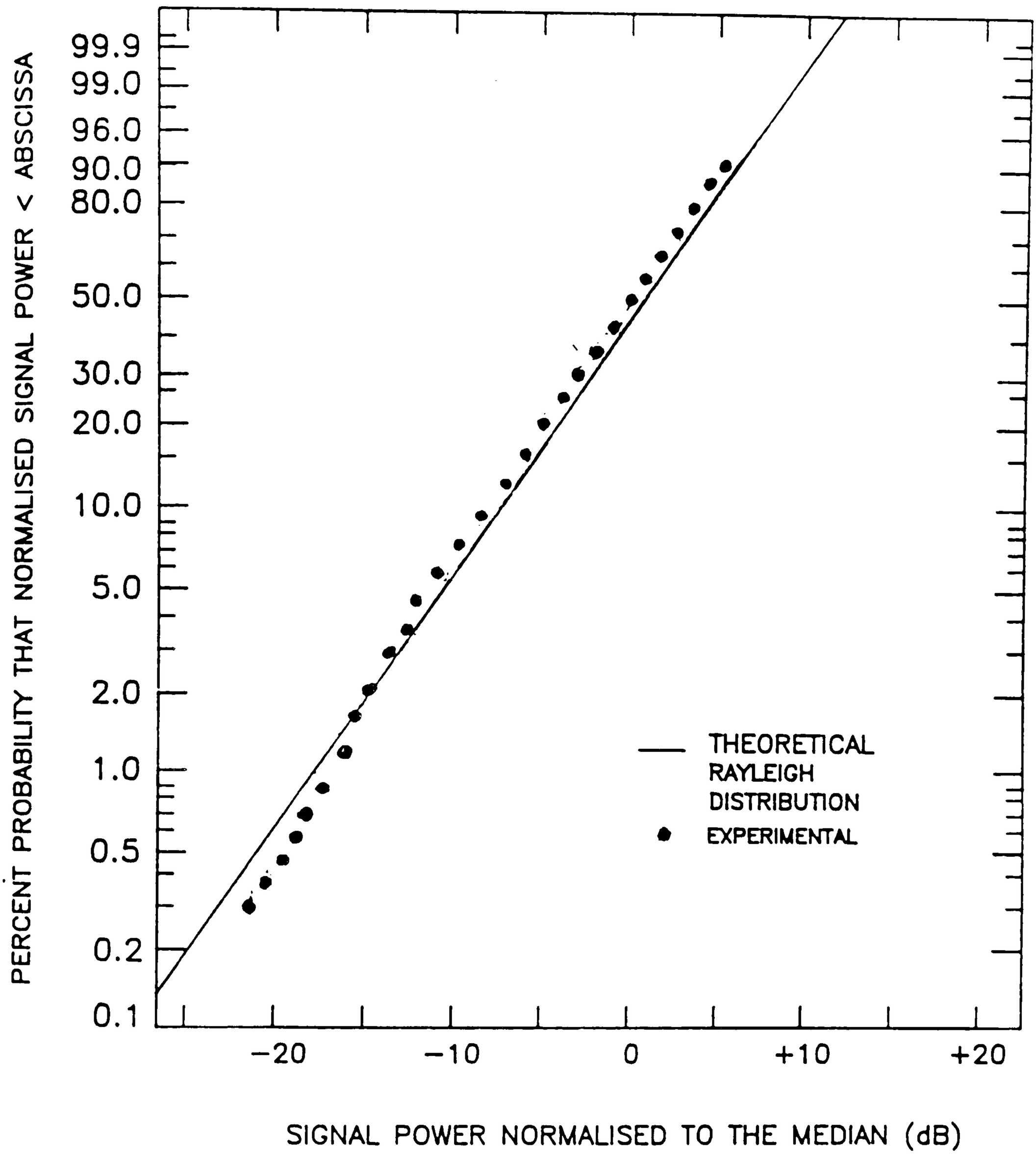

FIG. 6.9 CDF OF THE RECEIVED SIGNAL POWER WITH TWO PEOPLE WALKING BETWEEN THE FIXED TRANSMITTER AND RECEIVER.

corridor. Multipath fading as a result of the movement of the transmitter is observed with some fades approaching 35dB in depth which is due to the reflections from the walls, the ceiling and the floor. The figure also illustrates the effect of the 45^0 corner on the received signal power. After turning the corner, the received signal power fell rapidly to an extremely low level. It fell by 40 to 50dB in a travelled distance of 6m.

6.2.5 Envelope Fading at different speeds.

Finally, measurements were also conducted by moving the transmitter at two different speeds (2m/s and 0.83m/s) along a narrow corridor with dimensions 14m x 1.5m x 3.75m (length x width x height). The received signal power with speeds of 2m/s and 0.83m/s are shown in fig. 6.11a and 6.11b respectively. The reflection of the signal from walls, floor and ceiling cause the received signal power at the receiver to experience deep fades. From the figure it is clear that the received signal power at the higher speed fluctuates faster than the received signal power at lower speed. At the higher speed, more fades occurred per second.

6.3 MEDIAN RECEIVED SIGNAL POWER AGAINST DISTANCE MEASUREMENTS.

Propagation measurements were conducted in different rooms and corridors within the same building to determine the influence of room or corridor size, shape, construction and content on the variation of the median received signal power with distance for LOS conditions. During the measurements, the transmitter was moved at a constant speed from 1m away up to a distance of 14m away from the receiver. Four rooms and corridors were examined: a Laboratory, an office, a narrow corridor and a wide corridor.

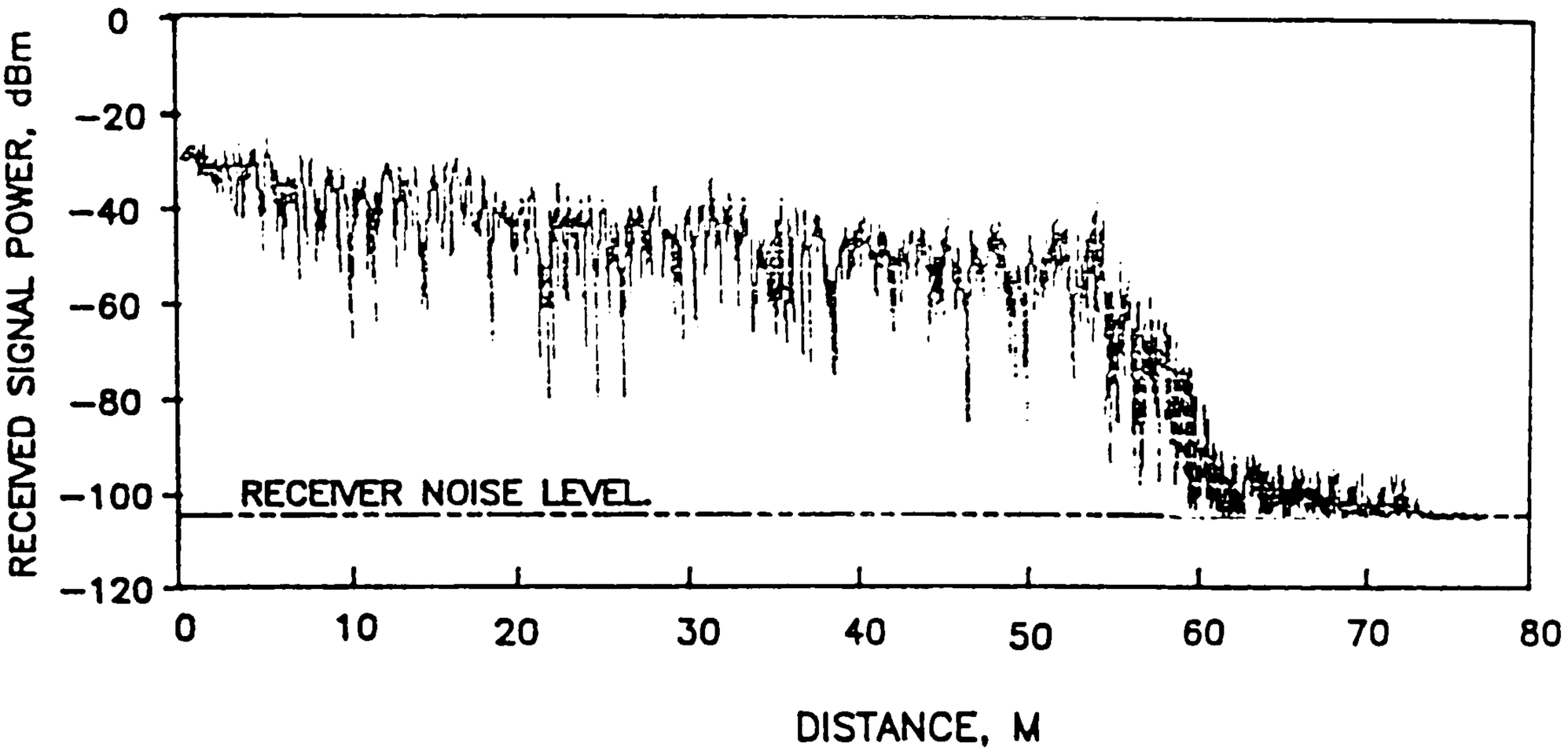

FIG. 6.10 RECEIVED SIGNAL POWER ALONG THE CORRIDOR INTO THE SHADOW REGION.

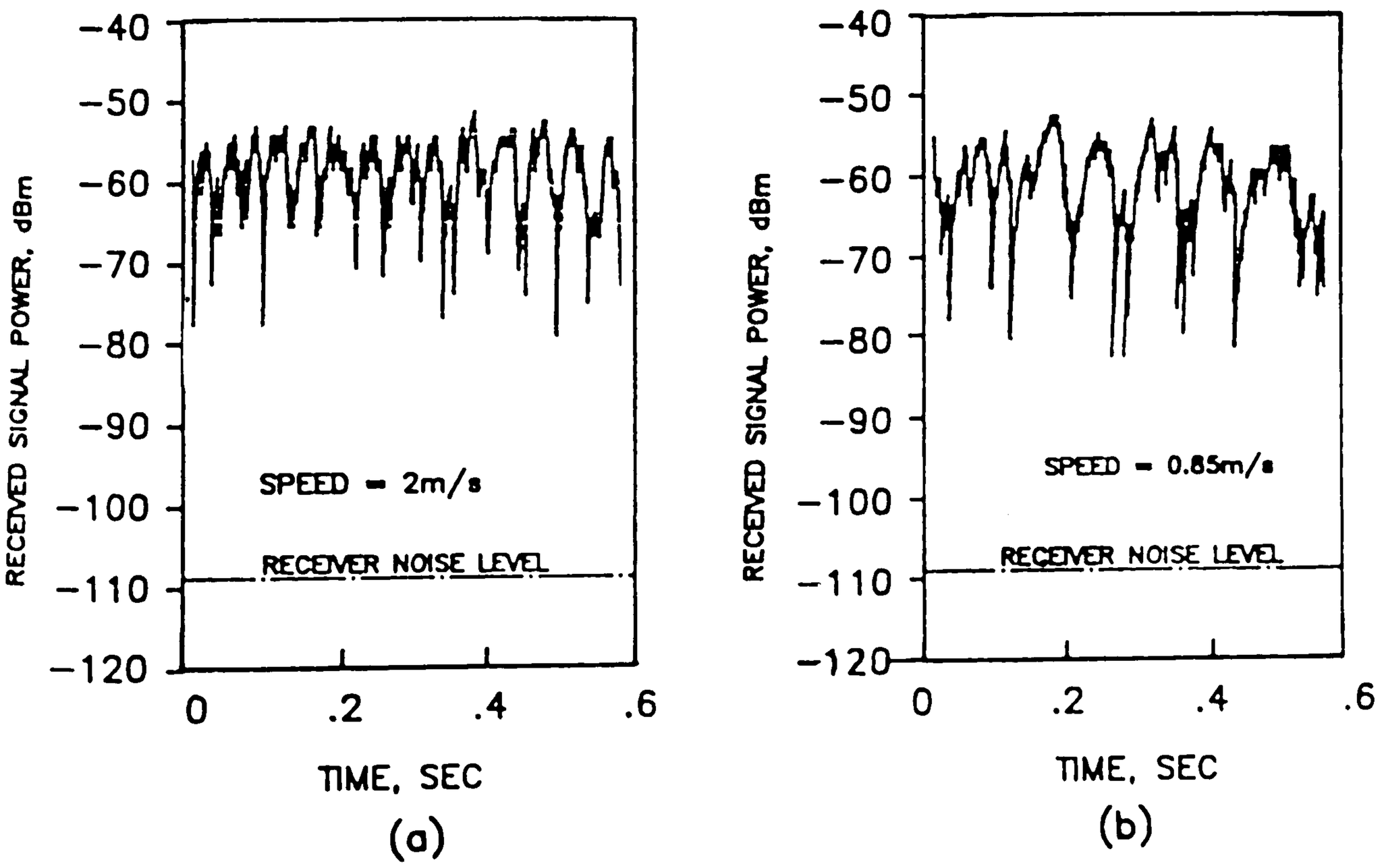

FIG. 6.11 RECEIVED SIGNAL POWER WHEN THE TRANSMITTER WAS MOVING AT SPEEDS OF 2m/s AND 0.85m/s

The first measurement was conducted within the Communications Research Laboratory at the second level of the Queen's Building as described in section 6.2.2.

The second measurement was conducted in an office which was 15.5m x 3.5m x 5m (length x width x height). It was being used as a postgraduate work room, and contained a lot of furniture such as wooden tables, chairs and cupboards, but there was no electrical equipment. The construction and content of the room are shown in figure 6.12. It consisted of plaster covered concrete walls which were about 30cm thick. One of the walls had three wooden doors which were 2m high and 1m wide. The wall opposite this had four aluminium window frames and two concrete posts which separated the windows. The aluminium window frames were 2m wide and 2.5m height and the posts were 0.35m wide and 0.25m deep. The floor was made of concrete and was carpeted.

The third measurement was conducted along a narrow corridor (corridor 1) which was 18m x 1.8m x 2.7m (length x width x height). The plan view is shown in figure 6.13. One side of the corridor had metal lockers protruding about 30cm from the side wall. The walls and ceiling were made of plaster covered concrete and the floor was covered with varnished cork tiles.

The final measurement was conducted along a wide corridor (corridor 2) which was 18m x 3m x 2.5m (length x width x height). The side walls were made of 40cm thick plastered covered concrete which had wooden display boxes with glass panelling on both sides. The ceiling was mainly plaster covered concrete and the floor was covered with varnished cork tiles. A plan view of the corridor is shown in figure 6.14.

P: PLASTERBOARD PARTITION
W: WOODEN DOOR (1m x 2.5m)
T: TABLE
C: CHAIR
G: GLASS WINDOW (2m x 2.5m)

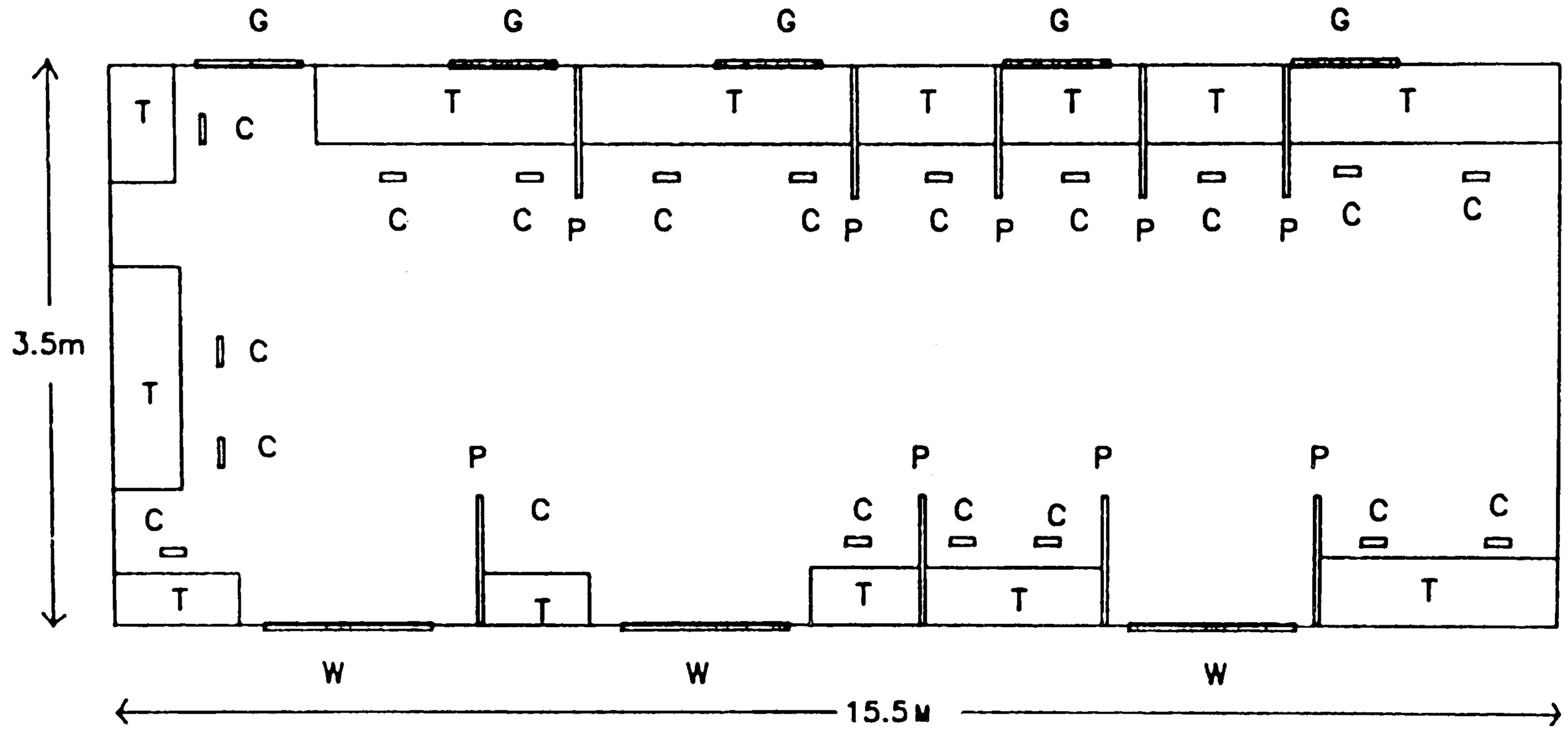

FIG. 6.12 PLAN VIEW OF THE POSTGRADUATE WORK ROOM.

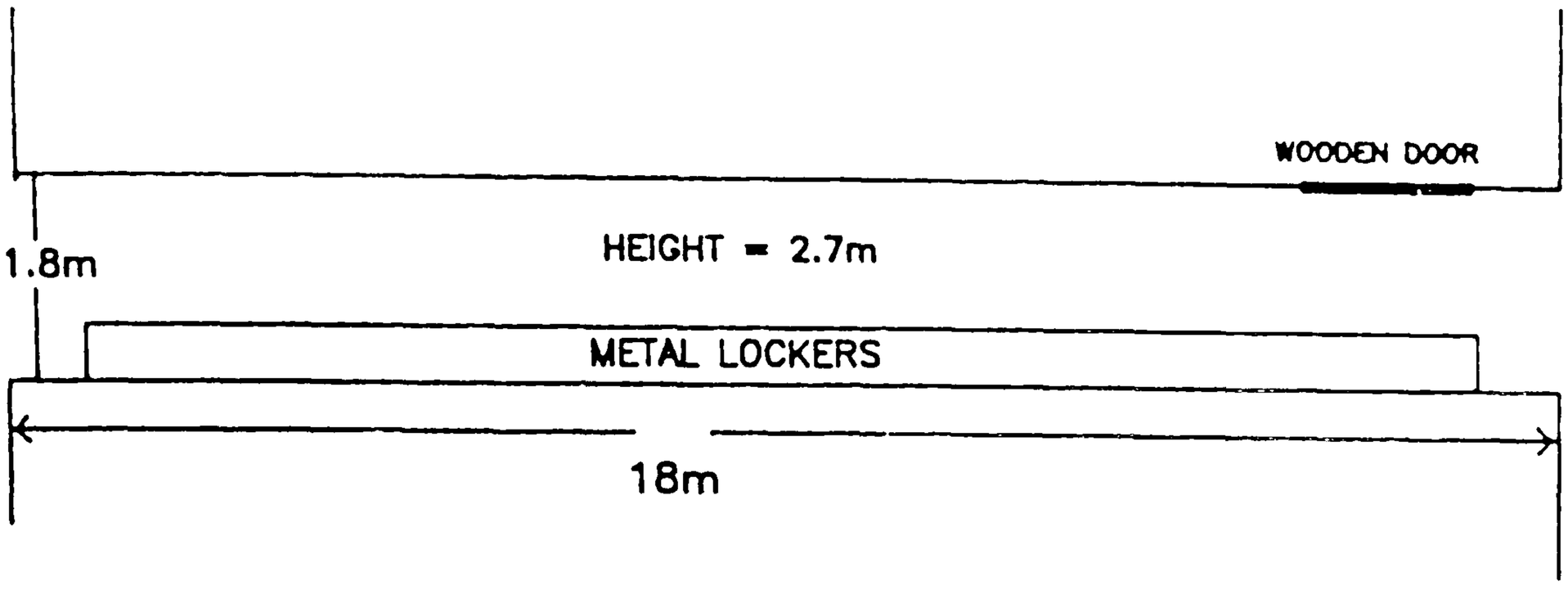

FIG. 6.13 PLAN VIEW OF A CORRIDOR WITH METAL LOCKERS ON ONE SIDE.(CORRIDOR 1)

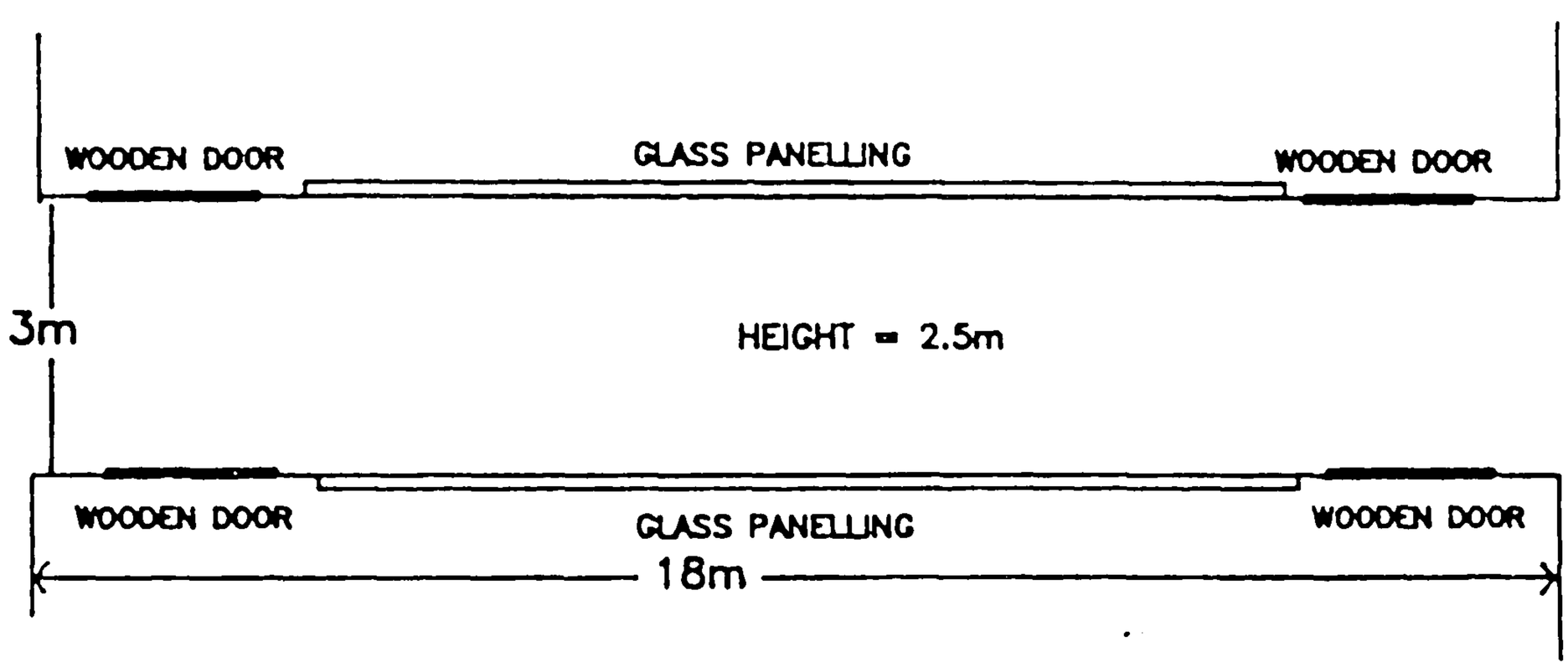

FIG. 6.14 PLAN VIEW OF A CORRIDOR WITH GLASS PANELLING ON BOTH SIDES.(CORRIDOR 2)

During the measurements, the transmitter was moved at a constant speed from 1m away up to a distance of 14m away from the receiver.

The received signal powers for the four measurements are plotted against distance as shown in figures 6.15 to 6.18. In general the median level of the received signal power decreased with distance. Superimposed are fluctuations due to reflections interfering with the direct path. Multipath fading of the received signal power is observed in all regions as the transmitter moves. Fluctuations, in general, seem to be similar in all rooms and corridors, although they are less severe in the office. This is possibly because it had a carpet on the floor and a lot of furniture against the walls which may have significantly reduced strong reflections from the floor and the walls.

The median received signal power was calculated over forty wavelengths of travelled distance in order to remove the short-term variations [5] as described in section 4.5. This was plotted against distance (log scale) as shown in figure 6.19 to 6.22. The solid line is the least squares regression fit to the median points. The propagation power law within the laboratory containing a lot of electrical equipment was $1/d^{1.71}$ and within the office with furniture it was $1/d^{2.17}$. Within the narrow corridor (corridor 1) with metal lockers on one side and the corridor with glass panelling (corridor 2) on both sides, the power laws were $1/d^{1.37}$ and $1/d^{1.2}$ respectively.

The results have indicated that the power law varies with different environments. The power laws for the two corridors were similar, and the received signal power fell more slowly than it would in free space ($1/d^2$). This was probably due to the smooth parallel walls, floor and ceiling which produced strong specular

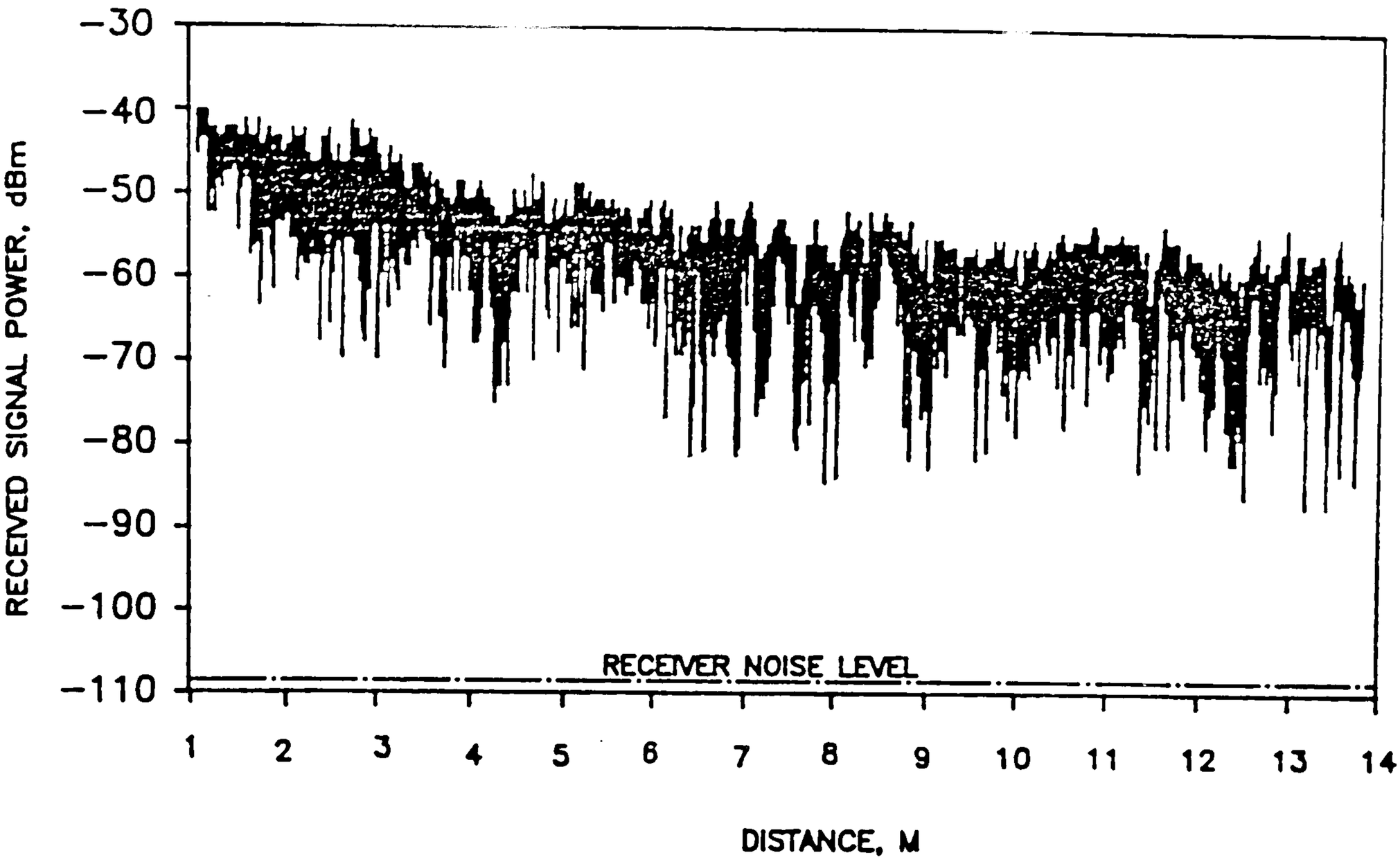

FIG. 6.15 RECEIVED SIGNAL POWER WITHIN COMMUNICATIONS RESEARCH LABORATORY.

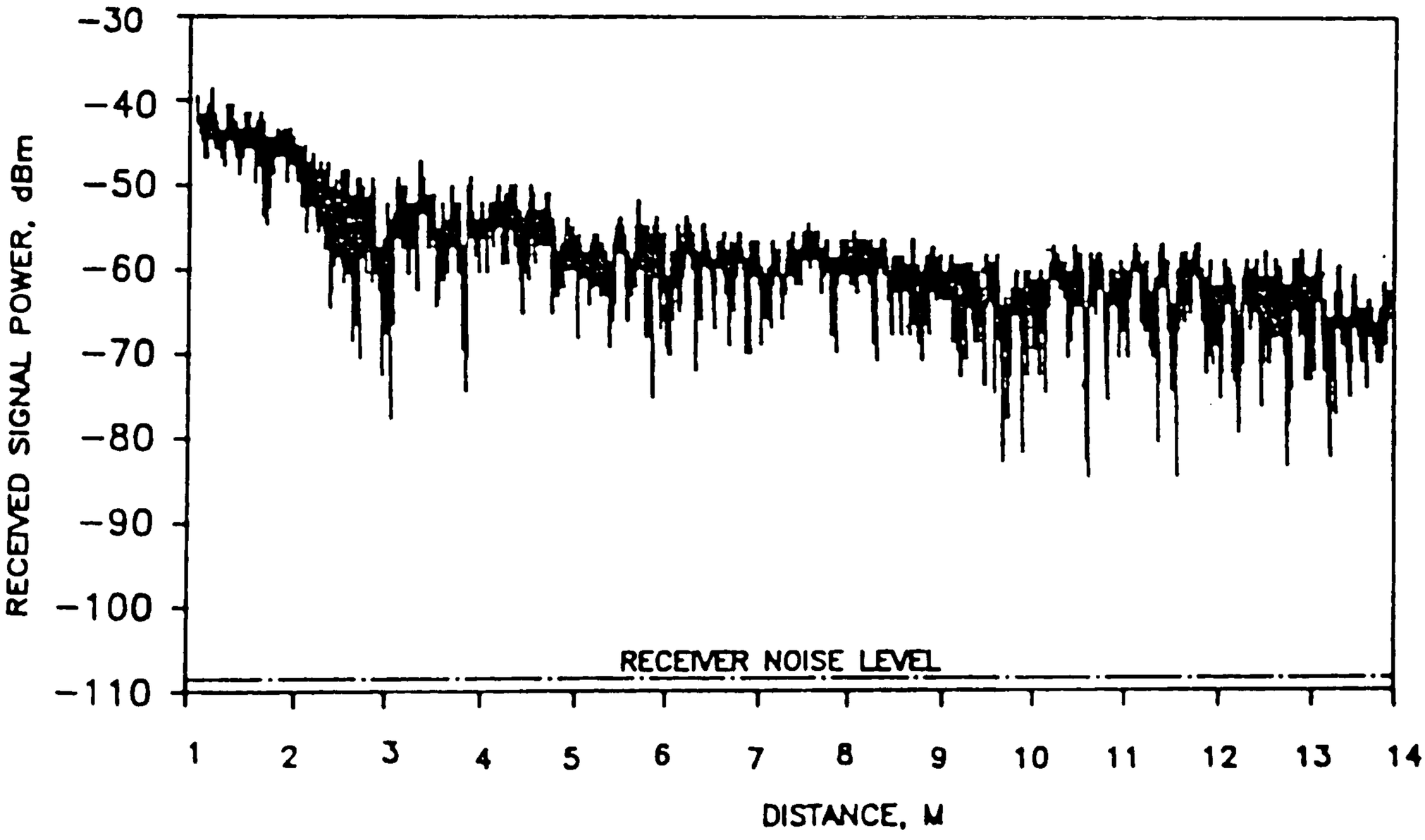

FIG. 6.16 RECEIVED SIGNAL POWER WITHIN A POSTGRADUATE WORK ROOM.

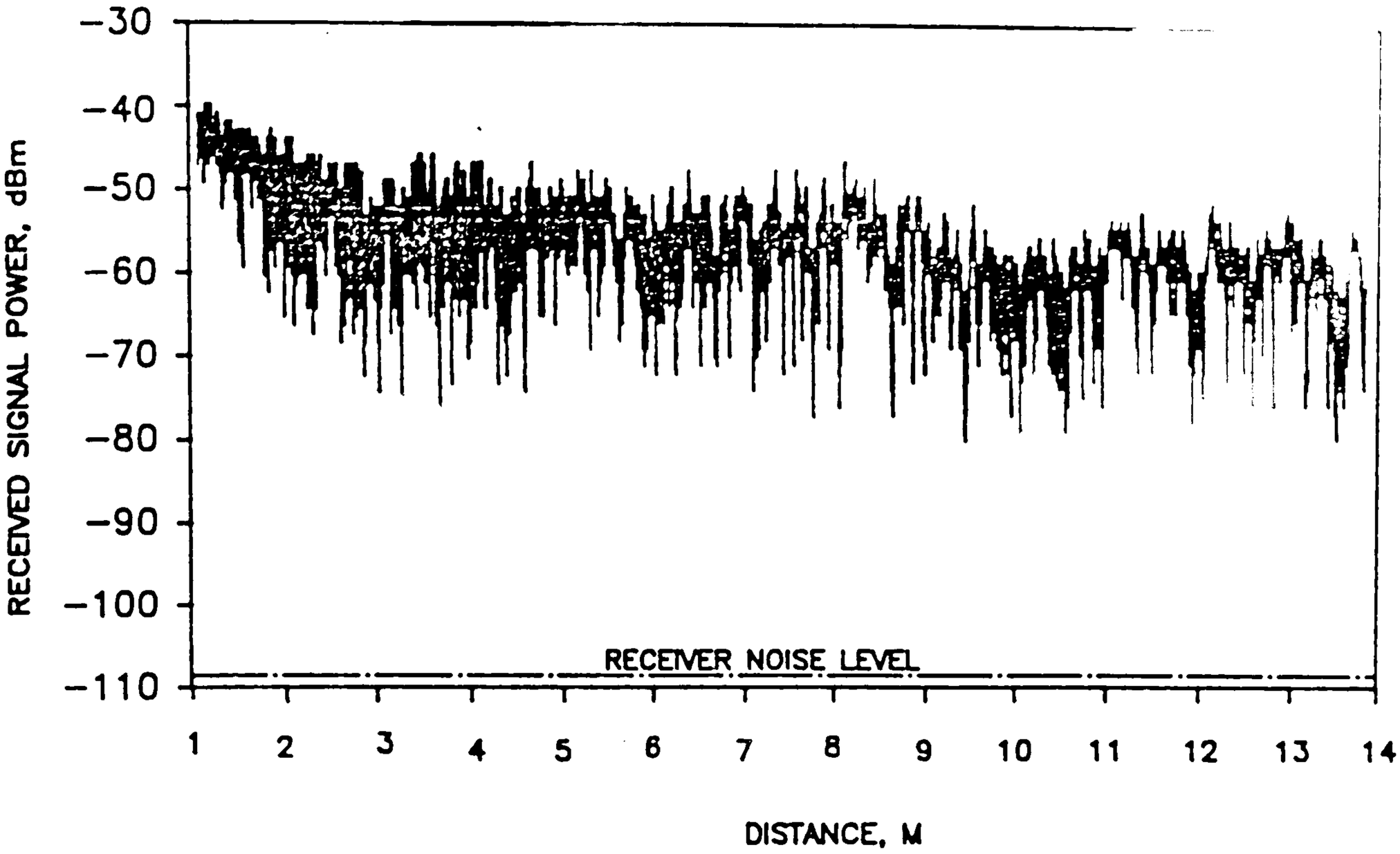

FIG. 6.17 RECEIVED SIGNAL POWER ALONG CORRIDOR 1.

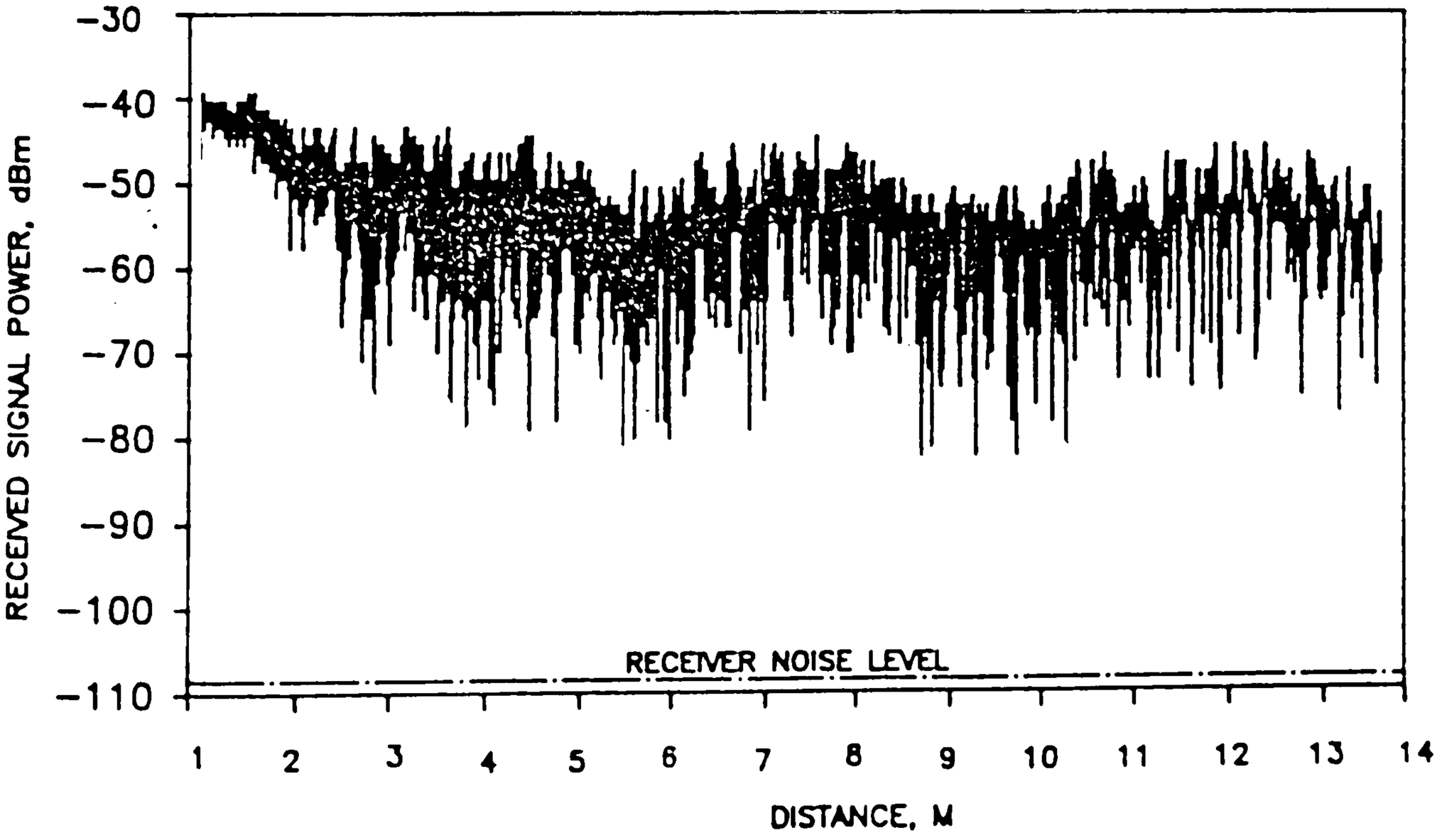

FIG. 6.18 RECEIVED SIGNAL POWER ALONG CORRIDOR 2.

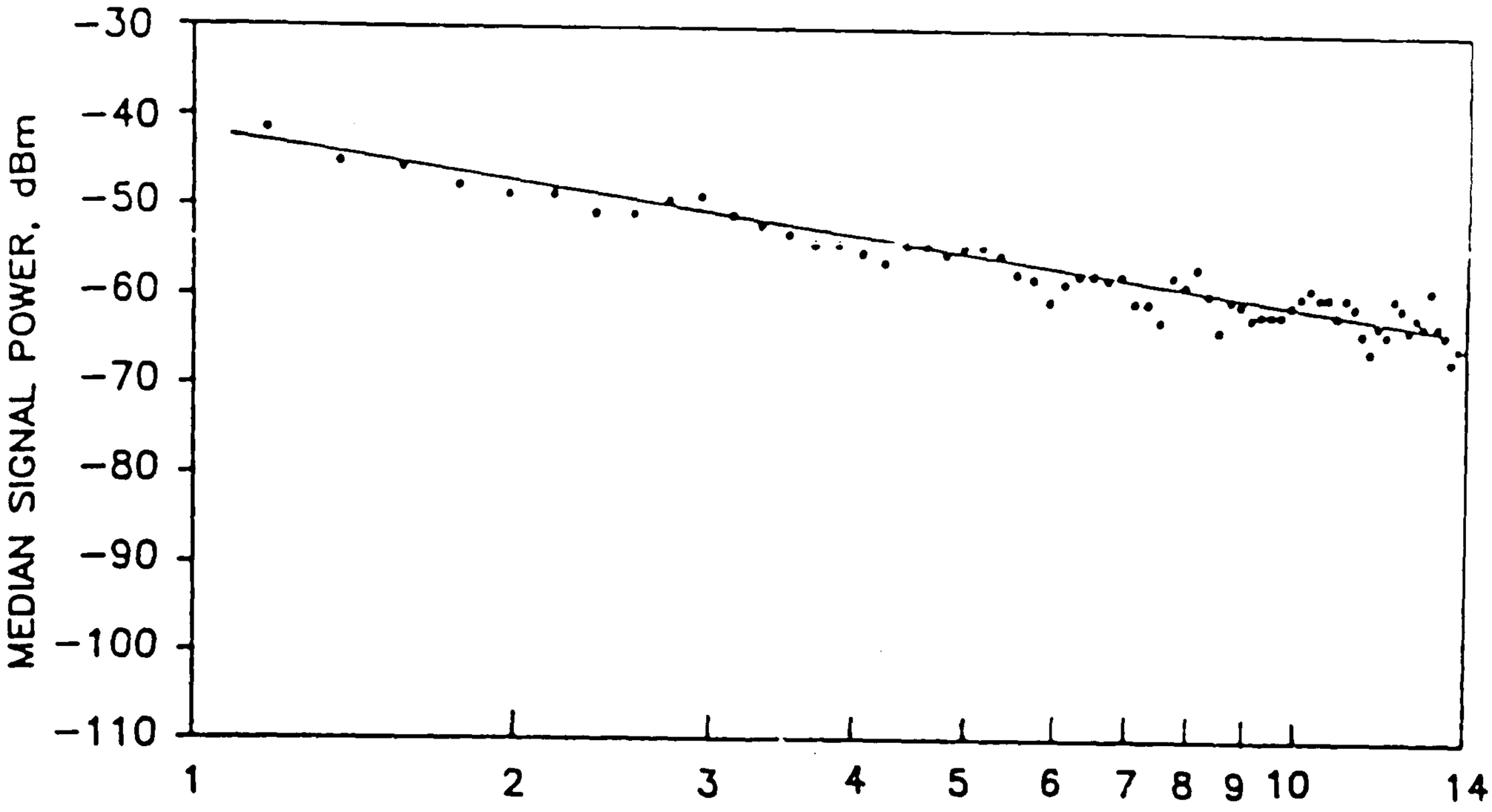

FIG. 6.19 SCATTER PLOT OF THE MEDIAN SIGNAL POWER AGAINST DISTANCE (LOG SCALING) IN COMMUNICATION RESEARCH LABORATORY

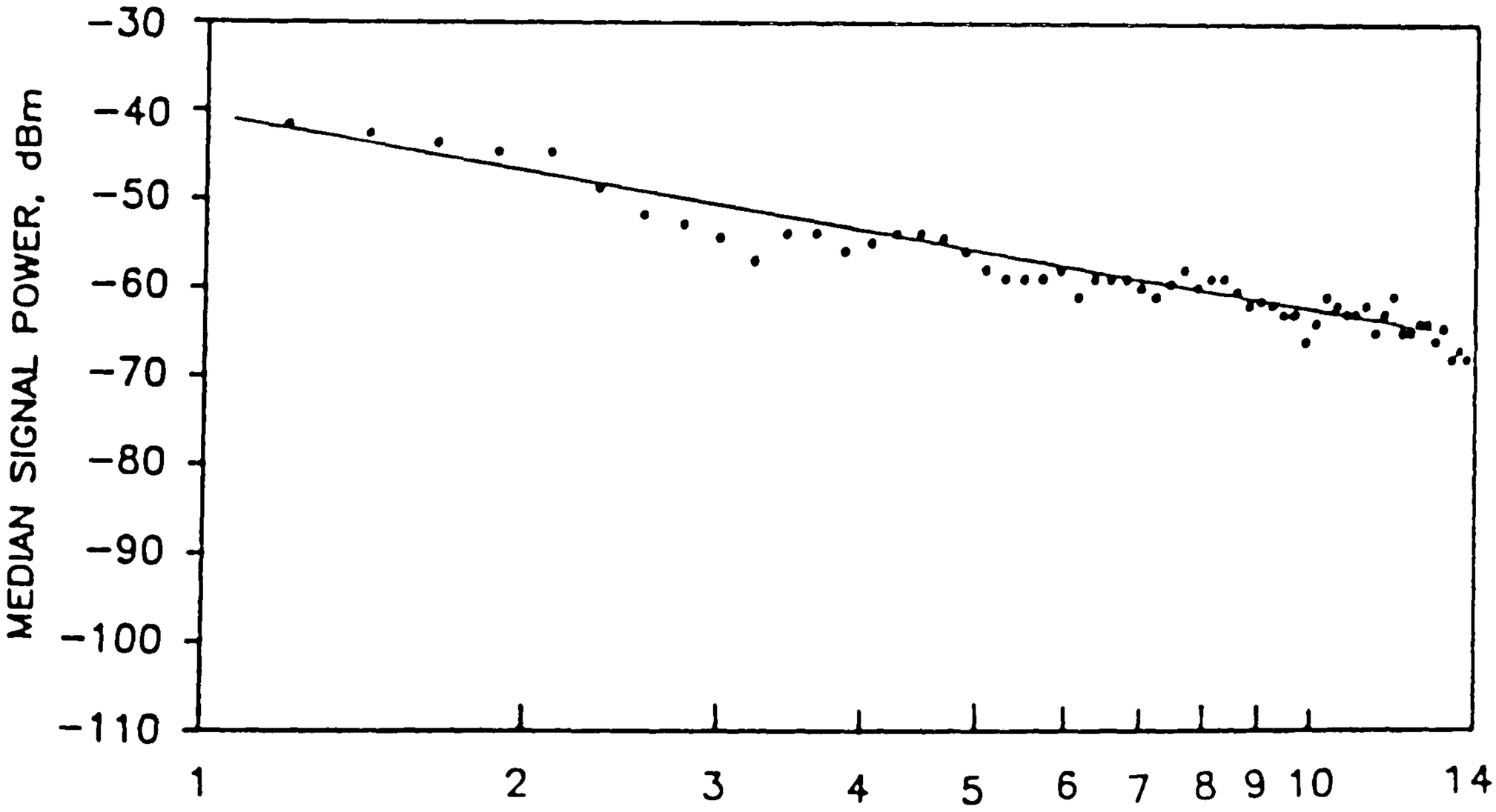

FIG. 6.20 SCATTER PLOT OF THE MEDIAN SIGNAL POWER AGAINST DISTANCE (LOG SCALING) IN A POSTGRADUATE WORK ROOM

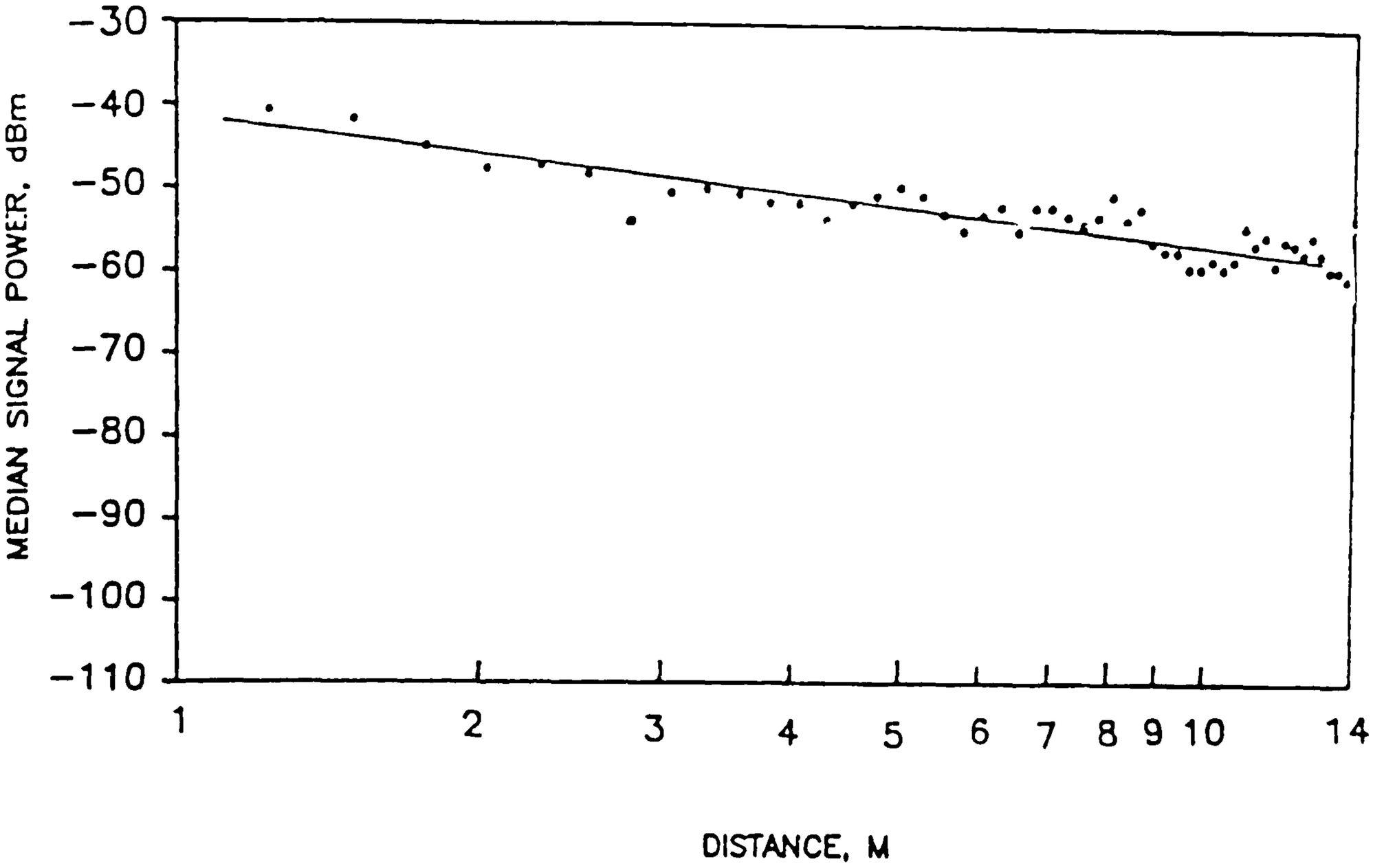

FIG. 6.21 SCATTER PLOT OF THE MEDIAN SIGNAL POWER AGAINST DISTANCE (LOG SCALING) ALONG CORRIDOR 1

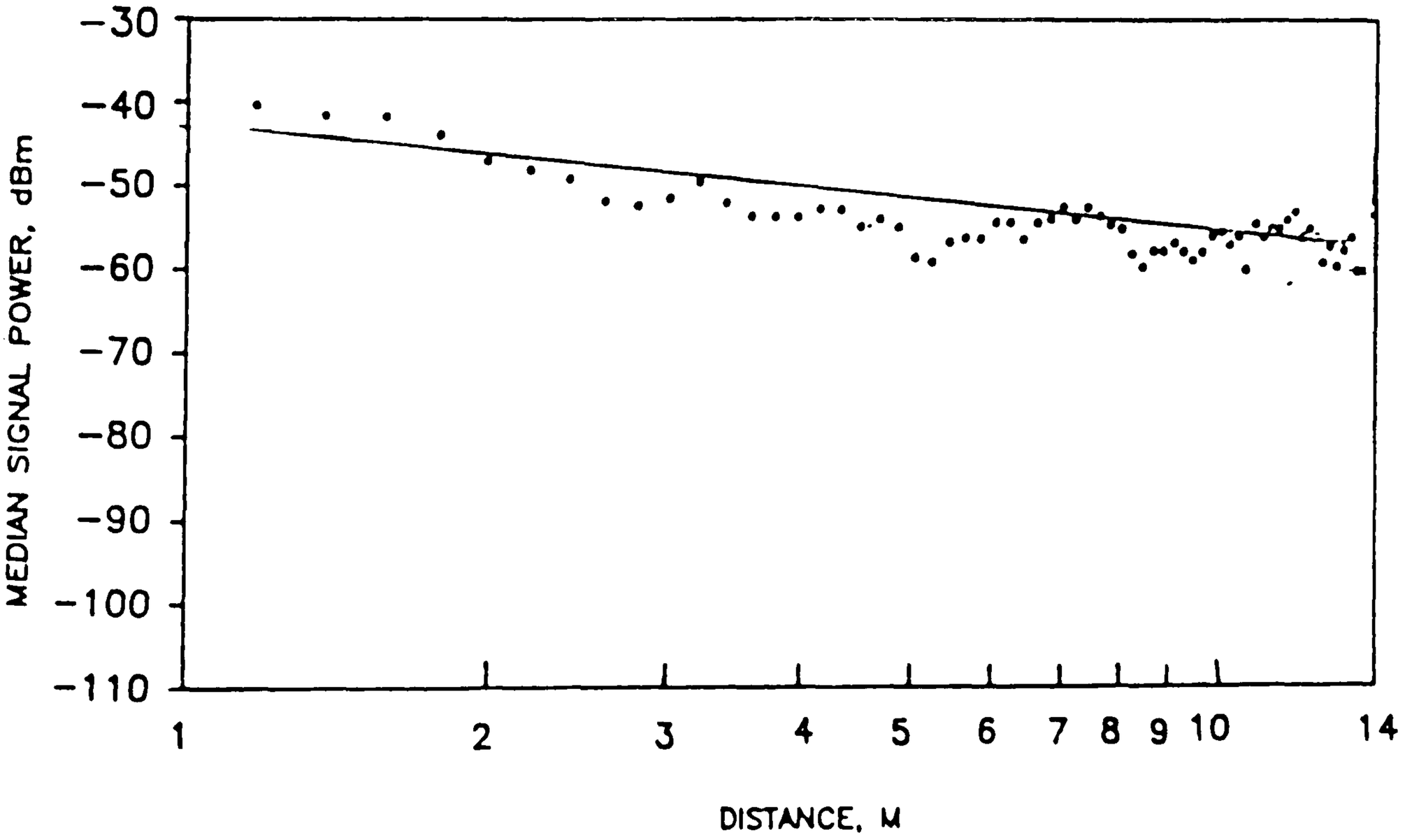

FIG. 6.22 SCATTER PLOT OF THE MEDIAN SIGNAL POWER AGAINST DISTANCE (LOG SCALING) ALONG CORRIDOR 2

reflections which channelled the power to the receiver. Instead of spreading out in all directions, the 60GHz signal was concentrated in two directions along the corridor. Within the Laboratory, the power law was found to be higher compared to the corridors but still lower than it would be in free-space. Presumably, the channelling effect was still present, but to a smaller degree because the benches and equipment prevented strong specular reflections off the walls. Strong reflections could still have occurred off the floor and ceiling. The power law within the office ($1/d^{2.17}$) was slightly higher but quite close to the free-space power law of $1/d^2$. This was probably because the furniture and carpet prevented strong reflections off the walls and the floor so that propagation was closer to free space. This was confirmed by the fact that the envelope fading was less severe than it was in the two corridors and the Laboratory.

6.4 RECEIVED POWER SPECTRUM.

Measurements were conducted to determine the spectrum of the received signal under mobile and stationary conditions. The two 60GHz phase-locked oscillators were locked to a single crystal to reduce frequency drifting. The received signal was down-converted from 59.9GHz to a 1GHz IF using the test receiver shown in fig. 6.23 and was further down-converted to about 3KHz by a mixer and local oscillator derived from a synthesised signal generator at 3KHz above 1GHz. This 3KHz output was connected to an FFT digital spectrum analyser so that the spectrum could be observed.

The first measurement was conducted with both the transmitter and receiver stationary, separated by 8m. The output spectrum is shown dotted in fig 6.24a and fig. 6.24b. This indicates the received signal frequency without doppler shift, and

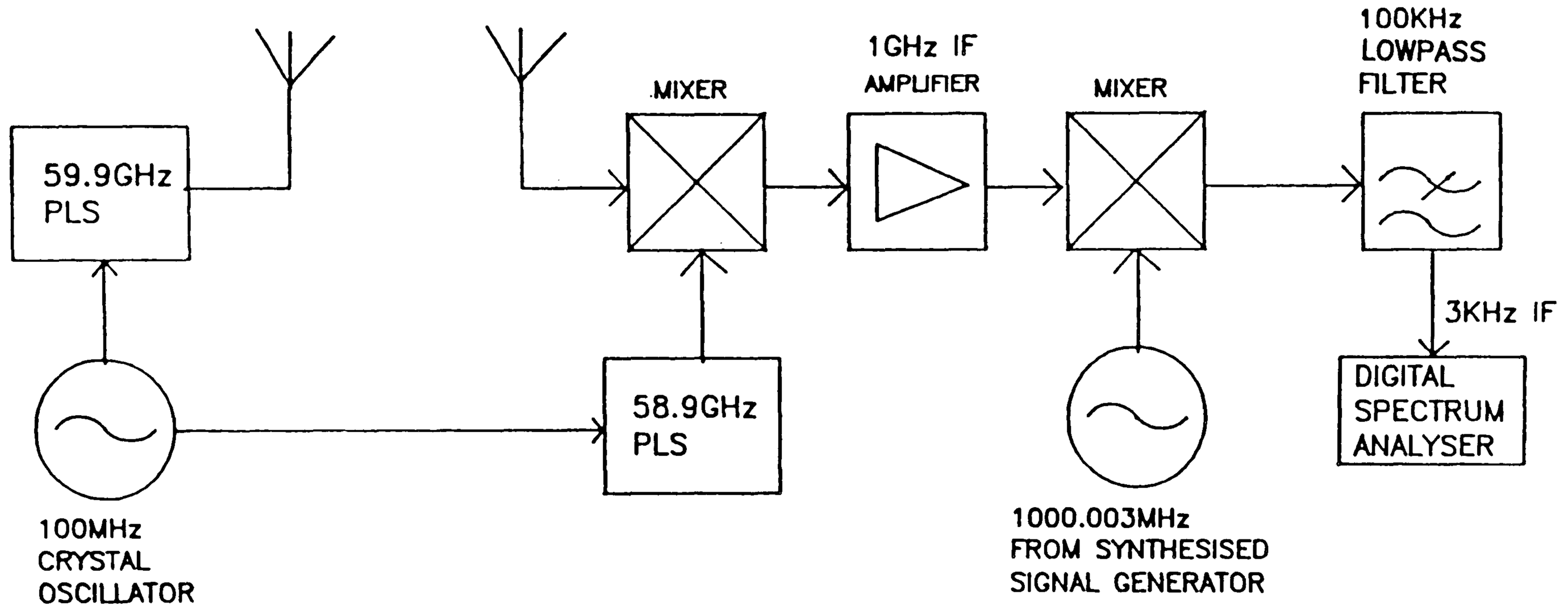

FIG. 6.23 EQUIPMENT FOR POWER SPECTRUM MEASUREMENTS.

the noise level. The centre frequency of the spectrum analyser was adjusted so that this signal was at the centre of the display.

The second measurement was conducted with the transmitter and receiver fixed and a person walking between the transmitter and receiver when the LOS path was not blocked. The results are shown in figure 6.24a. The broad spectrum was due to changes in path lengths of the signals reflected off the moving person which therefore are doppler shifted as a result of the person walking between the transmitter and receiver.

The third measurement was conducted by moving the transmitter away from the receiver at a constant speed of about 1m/s with a LOS path. The output spectrum of figure 6.24b shows that a frequency shift (fd) of about 200Hz occurred due to the Doppler effect on the LOS path. This was in agreement with theoretical doppler shift which is 200Hz for 60GHz at a speed of 1m/s. As shown in the figure, a broad peak shifted by +3fd occurred which could have been due to the signal reflecting back to the transmitter, which then reflected it to the receiver. The effective velocity of this path is 3 times the velocity of the transmitter, which explains the shift of +3fd. The broad spectrum between -fd and +fd can be attributed to many reflections arriving from different angles. The effective velocity of the paths vary between +/- velocity of the transmitter so that the paths have doppler shifts between -fd and +fd.

6.5 ATTENUATION OF BUILDING MATERIALS

A knowledge of the attenuation of building materials is necessary for the determination of the feasibility of integrated portable communication systems operating within buildings. The measurements were conducted by placing the

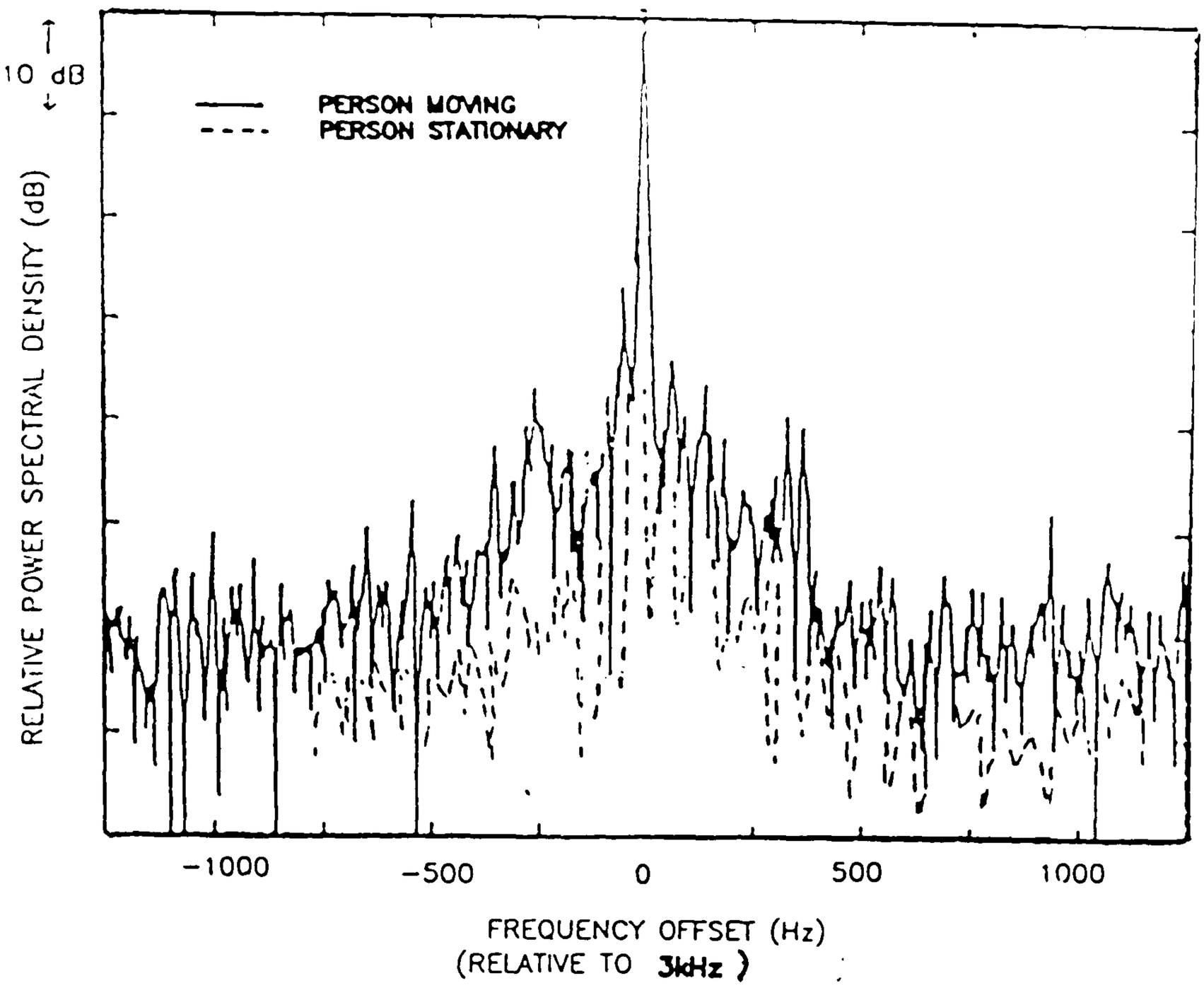

(a) A PERSON MOVING BETWEEN THE FIXED TRANSMITTER AND RECEIVER

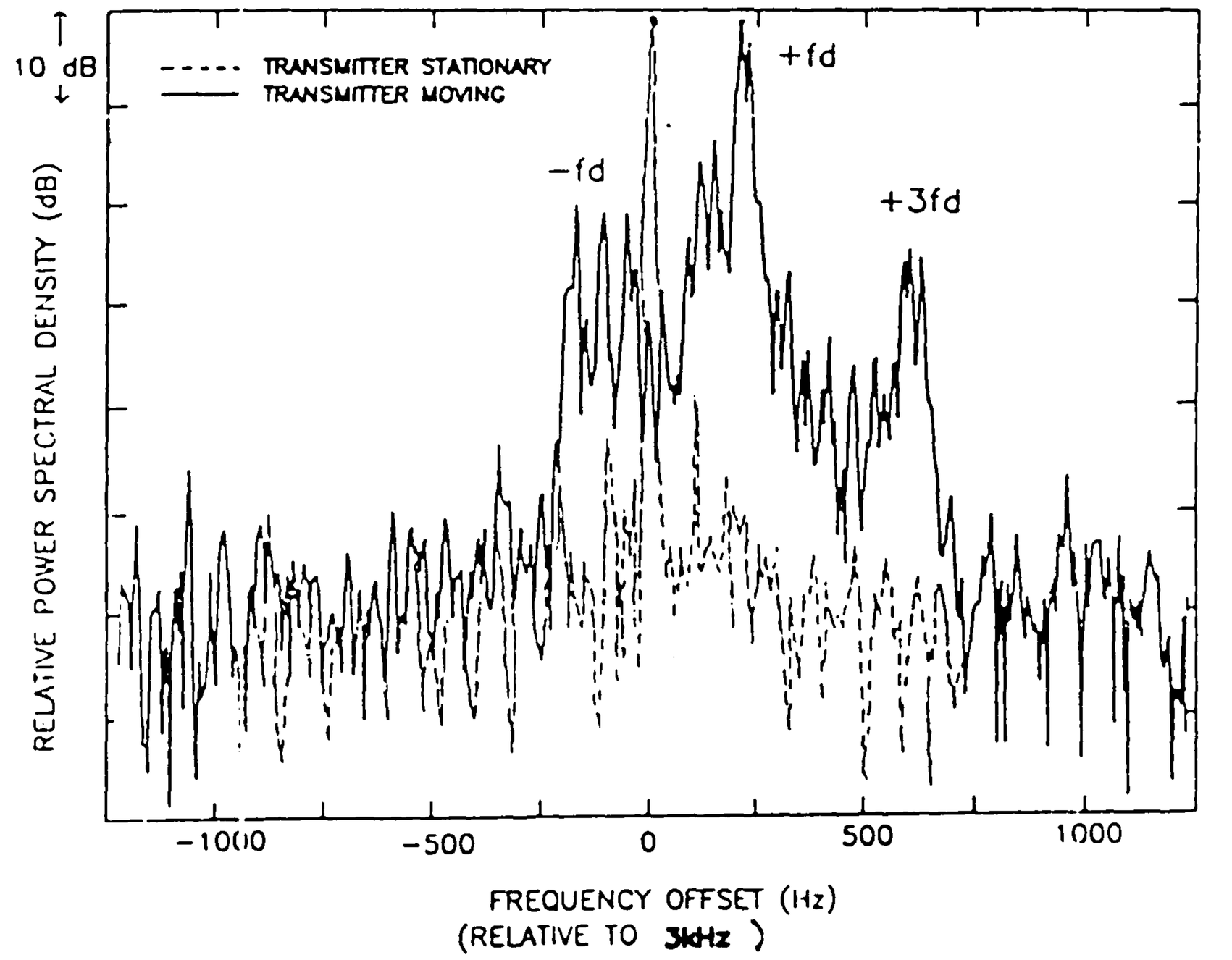

(b) TRANSMITTER MOVING AWAY FROM THE RECEIVER.

FIG. 6.24 FREQUENCY SPECTRUM OF THE RECEIVED 60GHz SIGNAL.

transmitter and receiver pointing at each other with the object in between and the received signal power was noted. The transmitter and receiver were also placed in the same position pointing at each other in the absence of an object. The penetration loss is the difference in the received signal power in dB with and without the object.

In the measurements, the transmitter used one of the horn lens aerials which had a beamwidth of 2.4^0 and a gain of 37dB. This type of aerial was used to minimise the reflections from other obstacles surrounding the object under test. The receiver used a standard 20dB gain horn aerial. The results of the penetration loss measurements are shown in the table in figure 6.25. The results show that the attenuation of different materials varies widely. The most common material used for external walls is plaster covered concrete, which is very effective in screening the signal. However, softwood has a moderate attenuation of about 4dB for a thickness of about 20mm. These results give a general outline for the attenuation of different types of materials used within buildings. The test with the aluminium sheet resulted in the received signal power falling to the noise level of the receiver. Theoretically, it should have an attenuation loss of 100's of dB, so this measurement shows that the level of the reflected signals reaching the receiver aerial was greater than 52dB below the direct signal. Generally, if the partitions within buildings are made from concrete or metal, they will contain the 60GHz signal whereas if the partitions are made from the chipboard or wood the signal can be expected to cover several rooms.

6.6 SIGNAL COVERAGE WITHIN BUILDINGS

The determination of coverage area and frequency reuse intervals is necessary for various indoor radio communications. For example, the integrated portable communication systems described in chapter 2 require a well defined and

OBJECTS	THICKNESS	ATTENUATION	ATTENUATION
CHIPBOARD	25 mm	14.07 dB	0.56 dB/mm
SOFTBOARD	20 mm	4 dB	0.2 dB/mm
PLYWOOD	17 mm	4.33 dB	0.25 dB/mm
CARDBOARD	2 mm	2 dB	1 dB/mm
HARDBOARD	3 mm	1.8 dB	0.6 dB/mm
ALUMINIUM	1 mm	> 52 dB	> 52 dB/mm
PLASTER COVERED CONCRETE WALL	40mm	>52 dB	>1.3 dB/mm

FIG. 6.25 ATTENUATION OF BUILDING MATERIALS

limited operational range and the ability to re-use the same frequency many times within the same building. The parameters which determine the coverage within buildings are the signal distribution, the mean or median signal power on a per room basis and the coupling between each room. Measurements were conducted within the Queen's building to determine the above parameters.

The first set of measurements were conducted in an office area with metal partitions and doors which had 2m high glass windows which reached the ceiling. A plan view of the area is shown in fig. 6.26. Only one room within the area had a wooden door. The height of the ceiling was about 5m. This environment represents the worst case for the propagation at 60GHz because of the severely attenuating metal partitions. These measurements were made before the phase-locked system was available so the non-phase-locked system was used, together with a standard 20dB gain horn aerial for the transmitter and the type 1 omnidirectional aerial for the receiver.

In order to determine the coverage area within a particular location, the measurements must relate to the whole area being surveyed and indicate the probability of a signal of suitable power being received. This was done by recording the received signal power while the transmitter was carried around the area to be surveyed, ensuring that it spent a similar amount of time in each place. This method has also been used by others [3].

The measurements were conducted by placing the stationary receiver as shown in Fig. 6.26. To sample each room, the transmitter was evenly moved around at a slow walking pace to cover as much area as practicable. The mean signal power within each room was determined by converting the received signal power in dB to

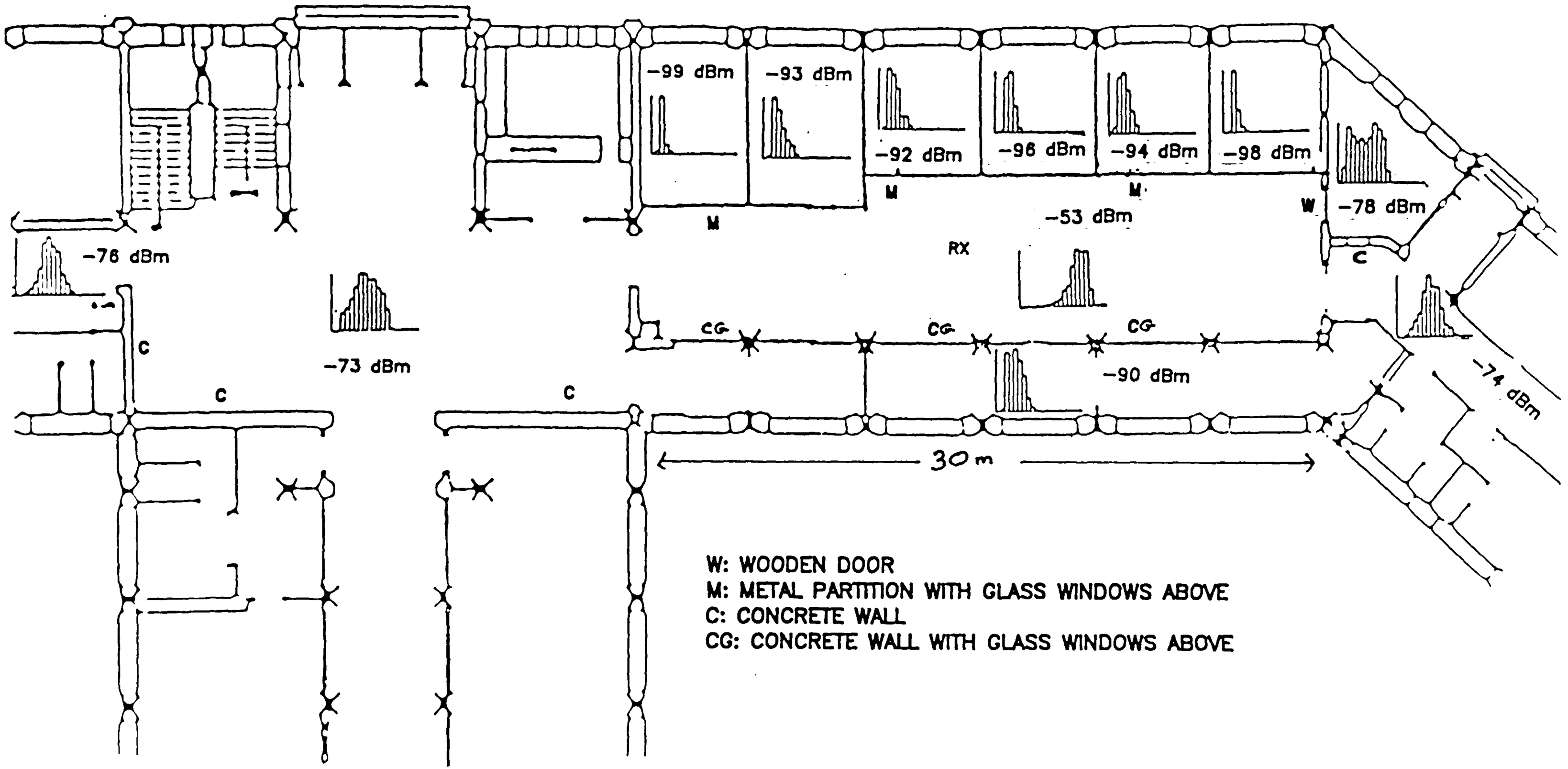

FIG. 6.26 PLAN VIEW OF AN OFFICE AREA IN THE ELECTRICAL ENGINEERING DEPARTMENT AND THE HISTOGRAM OF THE RECEIVED SIGNAL POWER AT VARIOUS POINTS.

linear power data before averaging. The computed mean value was then converted back to dB.

The digitized data was also sorted into 10 blocks from -44dBm to -104dBm in 6dB increments. These blocks were used to produce the histogram of the received signal power which directly indicates the probability of successful communication within the observed area.

Fig 6.26 shows the mean received signal power and the histogram distribution of the received signal power of each location. The results show that the mean received signal power was high when both the transmitter and receiver were in the same room. However, when the transmitter and receiver were in separate rooms the mean received signal power was very low except for the rooms which had a wooden door between them. The mean received signal power was high for the locations where there was a LOS path between the transmitter and receiver.

The results have shown that reflections from the metal partitions improve the signal power within a room although with severe multipath effects. The metal partitions are very effective in screening the 60GHz signals although some leakage does occur through the wooden door.

The second set of measurements was conducted with the phase-locked system and the type 2 omnidirectional aerials for both the transmitter and the receiver on the ground floor of the building. A plan view of the area is shown in figure 6.27. The partitions of this area were plaster covered concrete walls having a thickness of about 40cm. The doors of the rooms were made from 5cm thick wood which was found to a have a low attenuation for 60GHz signals. The measurements were

conducted at every location indicated in figure 6.27. The transmitter was placed in the foyer at the entrance to the building. During the measurements, for each measurement point, the transmitter was scanned horizontally over a 100 wavelength by 100 wavelength (50cm by 50cm) square so that the median signal power could be found at that point.[4] The scanning consisted of 11 parallel sweeps, the sweeps being 5cm apart. The median signal power should be approximately stationary within this scanned area.

The median received signal power at the locations measured are shown in fig. 6.27. The results have shown that when there was a LOS path or a wooden door between the transmitter and receiver, the median received signal power was higher than when the LOS path was blocked by a 40cm thick plaster covered concrete wall. When there was no LOS path, leakage through wooden doors was possible but it was too small to give adequate coupling between rooms or corridors. This is illustrated by three median signal power measurements which were made at transmitter-receiver separation distances of about 11m. The first was a LOS measurement (location 8), the second was blocked by a wooden door (location 11) and the third was blocked by a 40cm thick plaster covered concrete wall (location 12). The losses relative to the LOS path were 7dB for the path through the wooden door and 27dB for the path through the concrete wall.

Measurements were also conducted to determine the received signal power when the transmitter and receiver were not in the same room. The receiver was placed at the centre of the room and the receiver in the corridor adjacent to the room. Between the room and the corridor was a 40cm thick plaster covered concrete wall which had three wooden doors.

TRANSMITTED POWER = 50mW
TYPE 2 OMNIDIRECTIONAL AERIALS USED FOR TRANSMITTER AND RECEIVER

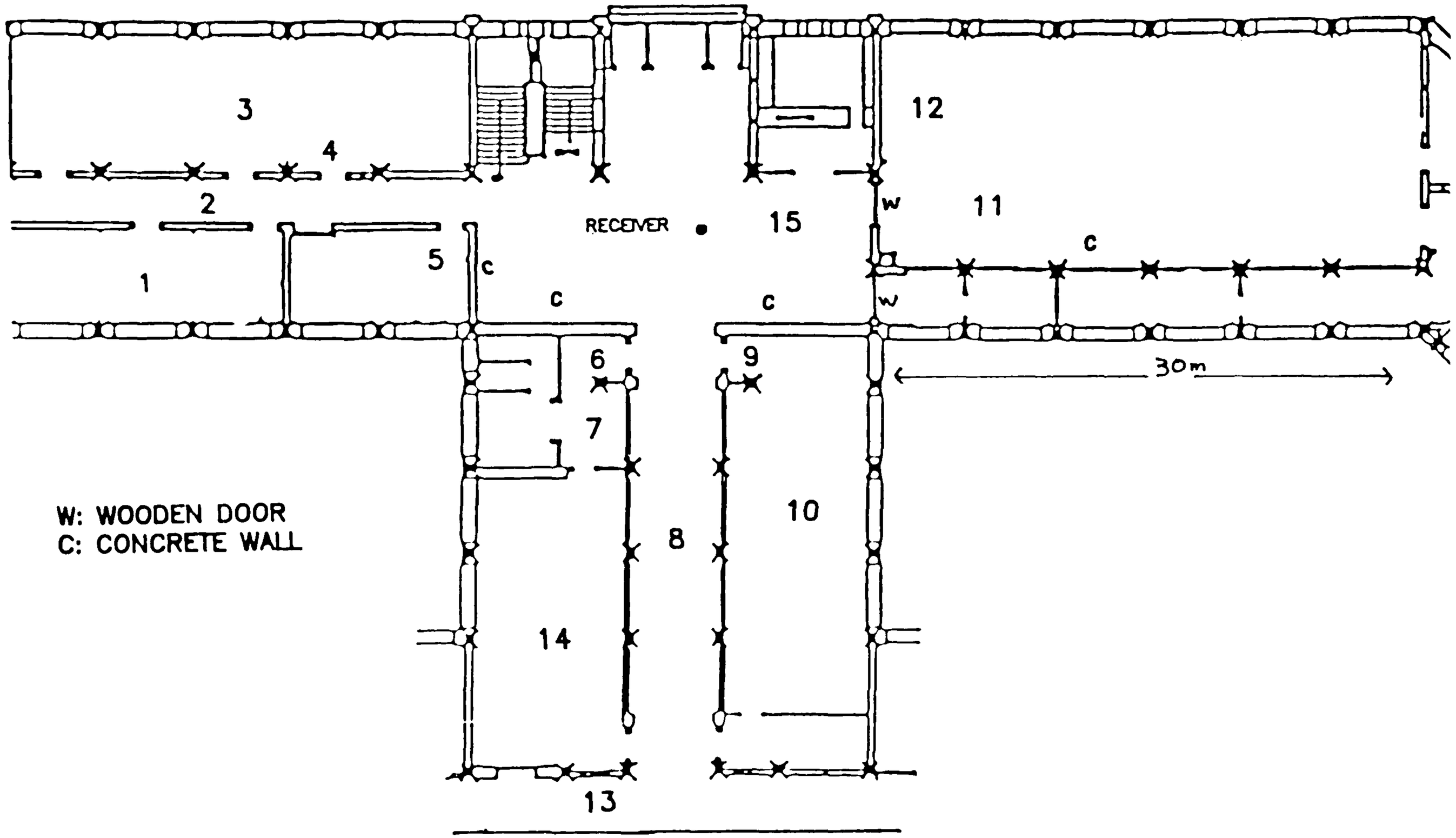

W: WOODEN DOOR
C: CONCRETE WALL

LOCATIONS	MEDIAN SIGNAL POWER, dBm
1	<−109
2	−68
3	<−109
4	−103
5	−91
6	−95
7	<−109
8	−62
9	−94
10	−98
11	−85
12	−85
13	−101
14	<−109
15	−50

FIG. 6.27 PLAN VIEW OF AN AREA WITH CORRIDORS AND ROOMS AT THE GROUND FLOOR OF THE BUILDING AND THE MEDIAN POWER AT VARIOUS LOCATIONS.

This was one of the earlier measurements, so used the non-phase-locked system, a standard 20dB gain horn aerial at the transmitter and the type 1 omnidirectional aerial at the receiver. The transmitter was moved at a constant speed along the corridor and the received signal power was recorded. As shown in figure 6.28, it was found that a usable signal was obtained only when the transmitter was close to the wooden doors, and between the doors, the signal fell to the noise floor of the receiver. The poor transmission between the room and the corridor was due to the high attenuation of the concrete wall, although leakage through the wooden doors was possible, which resulted in an increase of greater than 70dB for the middle door. The signal power received behind the other two doors was about 40dB lower, presumably because the signal had to pass through, reflect or diffract around the benches in order to reach the receiver as can be seen in fig. 6.29. Because of the severe attenuation of 60GHz signal through these types of partitions, coverage would be reduced to within a single room. However, the results show that useful propagation through wooden doors is possible at 60GHz although it was unable to provide complete coverage of the adjacent corridor in this particular case.

Further measurements were conducted by placing the receiver at a height of 3.5m above the floor in the Communications Research Laboratory described in section 6.2.2. These measurements were conducted in order to determine the coverage within a room when the radio port is at ceiling height, which is the most likely position that it would be placed. The receiver was placed at the centre of the room as shown in figure 6.30. The transmitter was placed on the trolley at a height of 1.5m and was randomly moved within a 50cm by 50cm square at the locations indicated in fig. 6.30. The median received power was then computed at these locations.

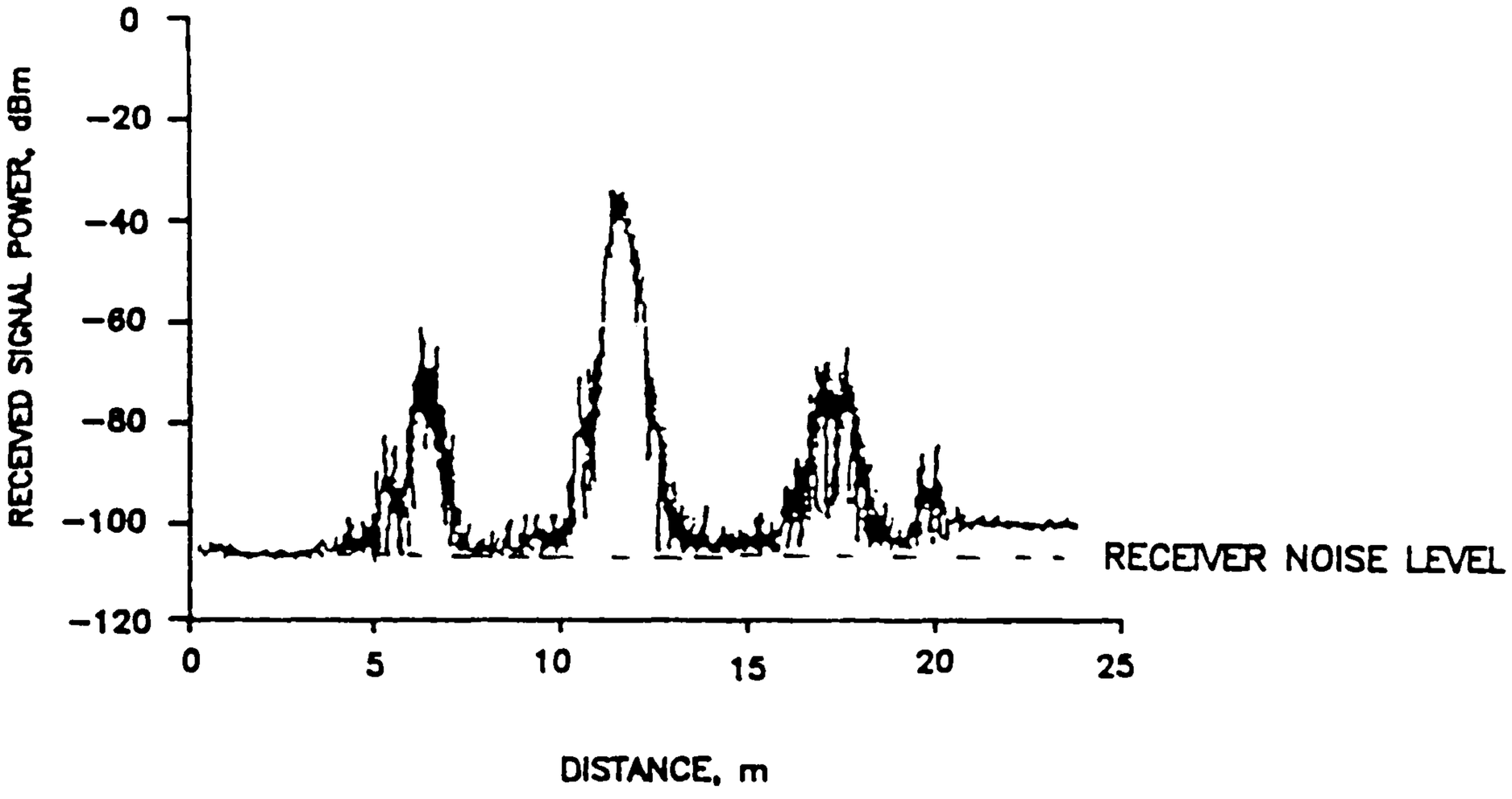

FIG. 6.28 RECEIVED SIGNAL POWER WHEN THE RECEIVER WAS IN THE COMMUNICATIONS RESEARCH LABORATORY AND THE TRANSMITTER WAS MOVED ALONG THE ADJACENT CORRIDOR.

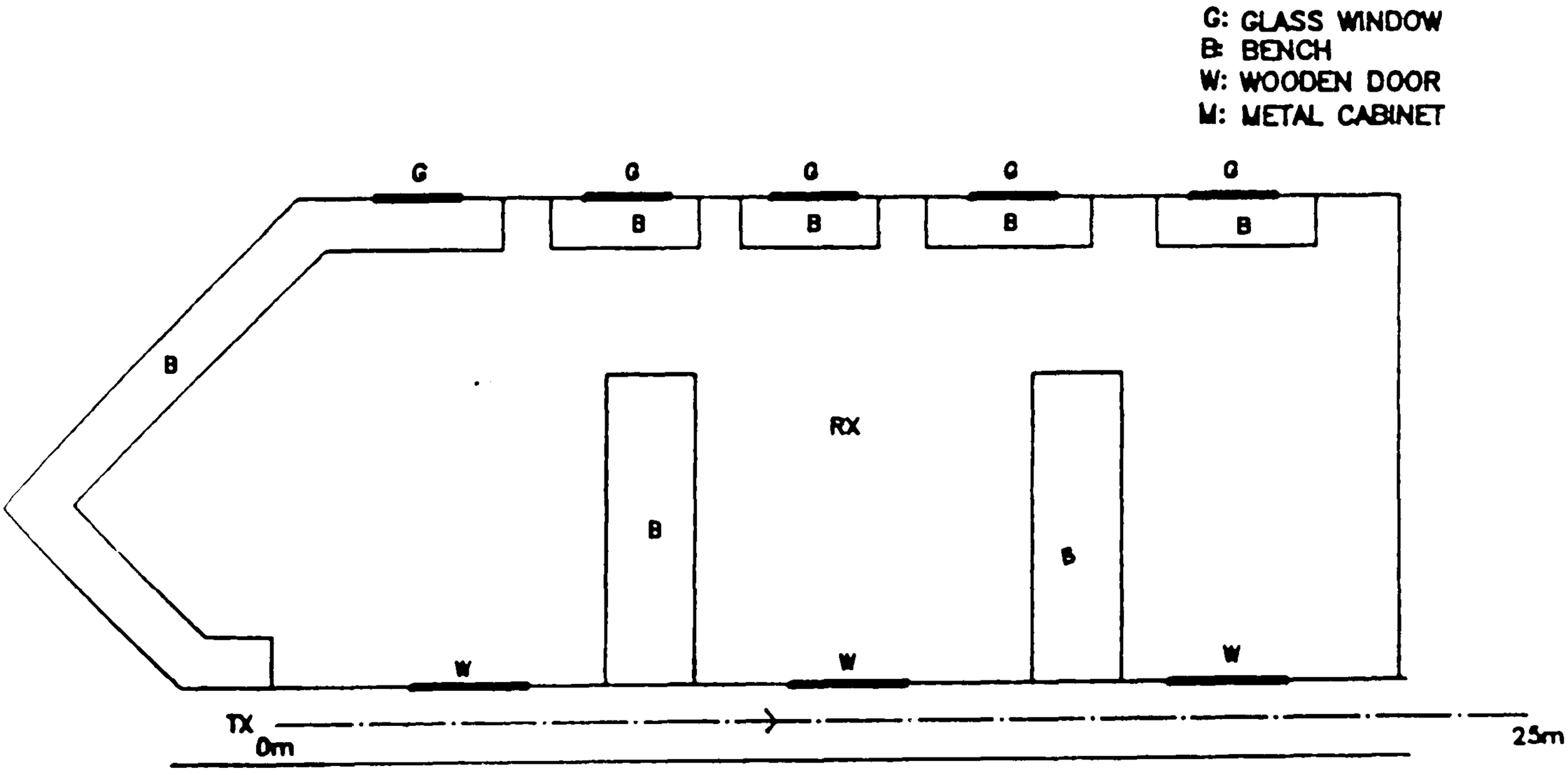

FIG. 6.29 PLAN VIEW OF THE LABORATORY.

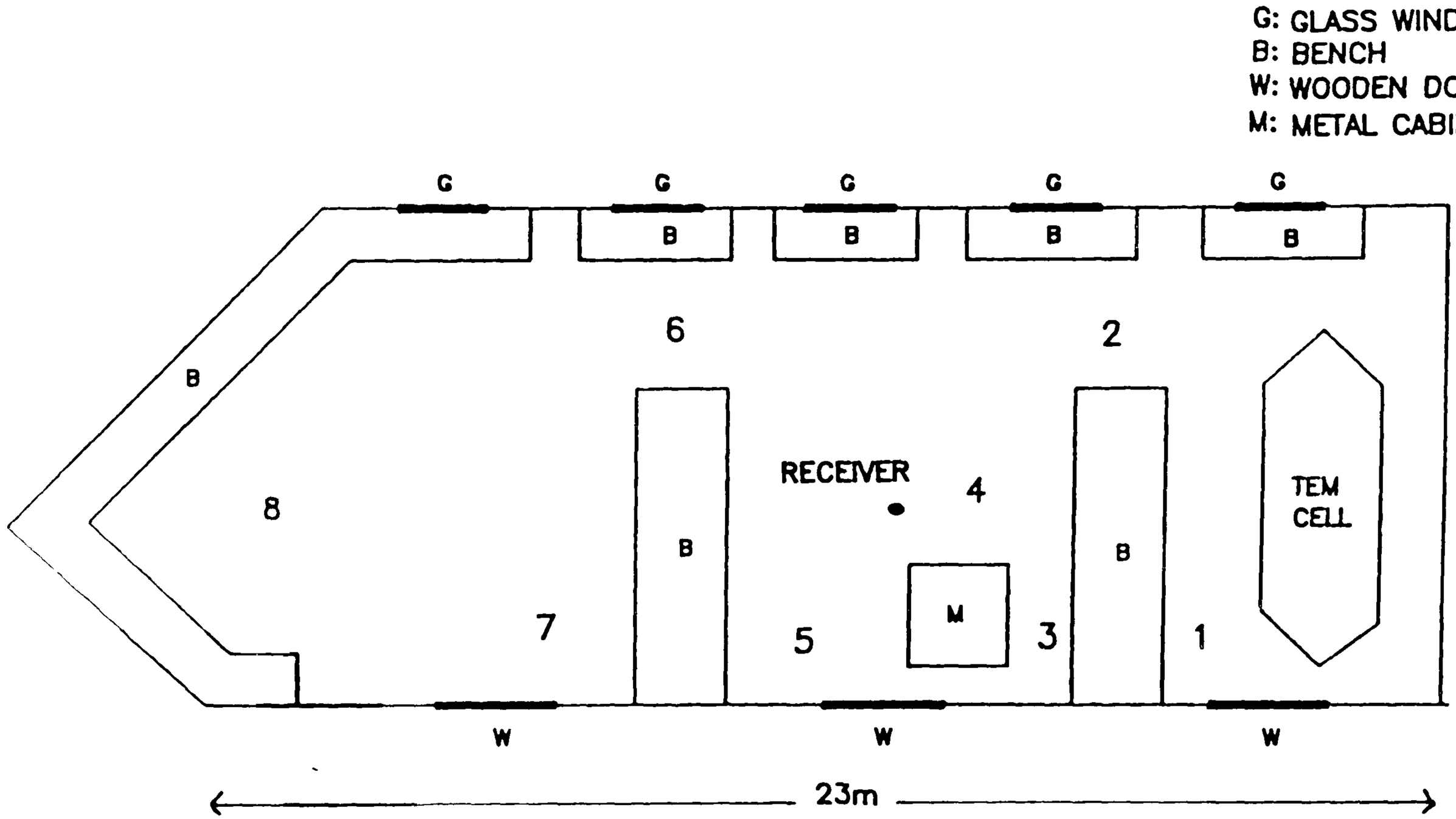

LOCATIONS	MEDIAN SIGNAL STRENGTH dBm
1	−63.78
2	−51.74
3	−62.83
4	−64.35
5	−63.04
6	−55.50
7	−65.50
8	−64.50

FIG. 6.30 MEDIAN RECEIVED SIGNAL POWER AT VARIOUS POINTS IN THE COMMUNICATIONS RESEARCH LABORATORY.

The results have indicated that the signal power was at its lowest behind obstructions but was generally higher compared to when the receiver was 1.5m above the floor. The signal could cover the whole room even though there was no LOS path between the transmitter and receiver at certain locations. It therefore seems that a good position for the radio ports is at the height of the ceiling in the middle of the room. The received signal was also fairly low when the transmitter was directly below the receiver, because the omnidirectional aerials transmit little perpendicular to their main lobe. One method of improving the signal power here would be to use an aerial which radiates more power downwards, by using for example an aerial with a cardiod shaped polar pattern instead of the torus shaped pattern of the omnidirectional aerial used.

Generally, within buildings, the coverage area at 60GHz, unlike at UHF [3] is limited by the structure of the buildings. The building could be partitioned into several coverage areas which may be as small as a room by radiating from a radio distribution port using an aerial attached to the ceiling. The screening effect depends on the type of material used for the partitions.

6.7 EDGE DIFFRACTION MEASUREMENTS

Propagation of electromagnetic waves into shadow regions can exist as a consequence of edge diffraction. Measurements have been conducted qualitatively outdoors to determine the effects of edge diffraction at the corner of a building as was described in chapter 5. Indoor measurements have also been conducted to determine the order of magnitude of edge diffraction effects at 60GHz experimentally so that they can be compared with theory. The propagation measurements were conducted by using an aluminium sheet which is considered to be opaque to 60GHz signals. This aluminium sheet was 1.2m by 2.5m and the

thickness was about 1mm, so it can considered to be knife edge at 60GHz. The measurements were conducted within a large empty room on the first floor of the building. The plan view of this room is shown in figure 6.31.

The transmitter used one of the high directivity horn lens aerials described in chapter 4 pointing towards the vertical edge of the knife edge at a distance of 10m. This distance was used to ensure that the knife edge was in the far-field region of the aerial. The receiver used a 20dB gain horn aerial and was placed at 0.5m from the edge. The transmitter and receiver were at heights of 1.5m above the floor.

LOS measurements were taken at 1cm intervals from the edge into an unobstructed region along a line perpendicular to the signal path as shown in figure 6.31. The non-LOS measurements were taken by moving the receiver at 10cm intervals into the shadow region. For the non-LOS measurements, the receiving aerial was pointed towards the knife edge. The normalised distance, u, measured from the geometrical shadow boundary were computed by using equation 3.26

$$u = Y\sqrt{\frac{2d_1}{\lambda(d_1 + z)z}} \qquad (6.1)$$

where λ is the wavelength, d1 is the distance between the transmitter and the edge and z is the distance between the receiver and the edge as shown in fig. 6.31. The normalised distance u is positive in the illuminated region and negative in the shadow region. Fig. 6.32 shows the experimental and theoretical curve obtained from fig. 3.18 of chapter 3. It can be seen that the experimental curve is nearly identical to the theoretical curve for values of u less than 3. When the receiving aerial is located in the illuminated region, LOS conditions are maintained. It is interesting to note that at a certain distance edge diffraction may actually increase the received

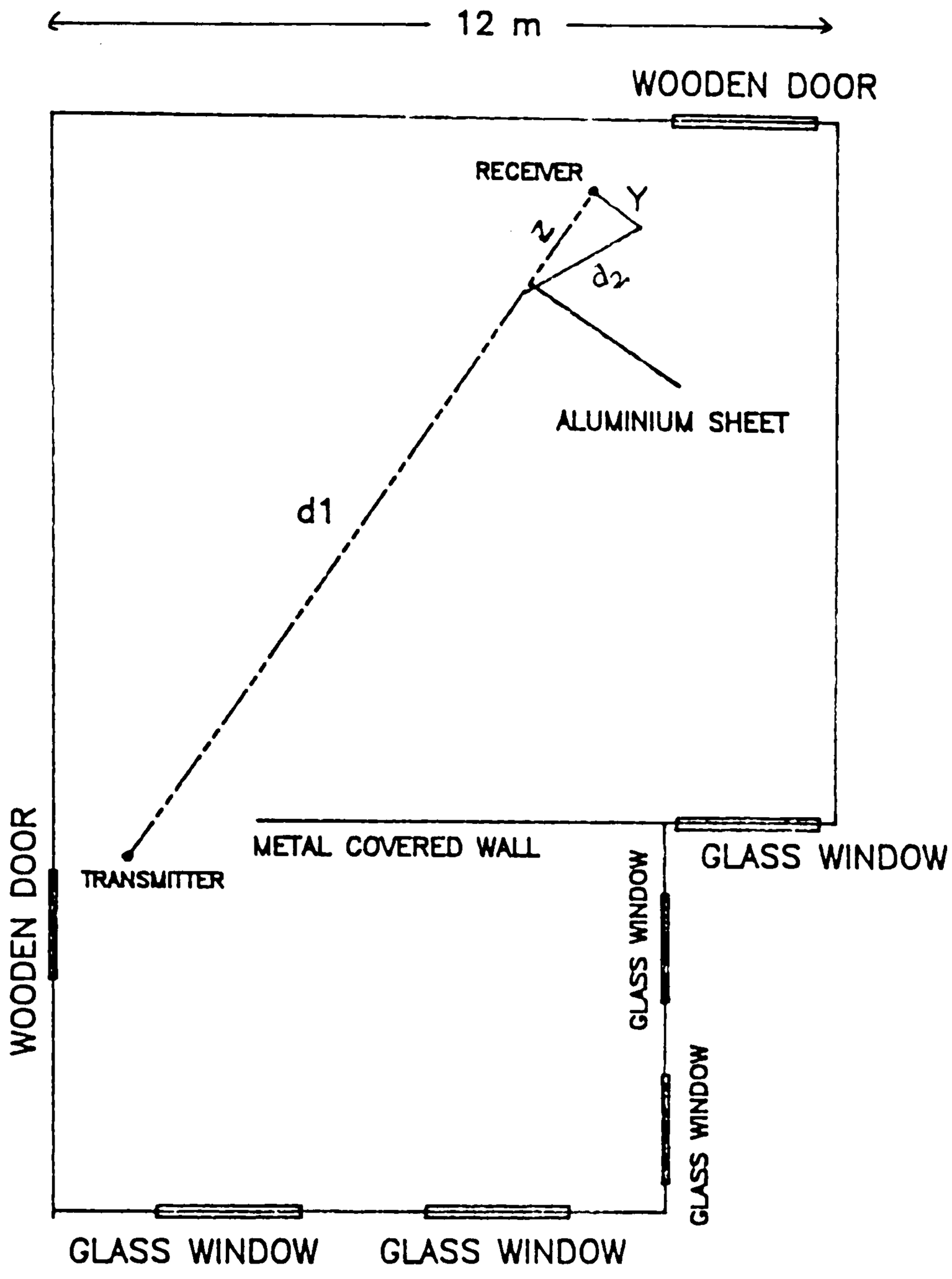

FIG. 6.31 PLAN VIEW OF THE SET–UP FOR EDGE DIFFRACTION MEASUREMENTS WITHIN BUILDINGS.

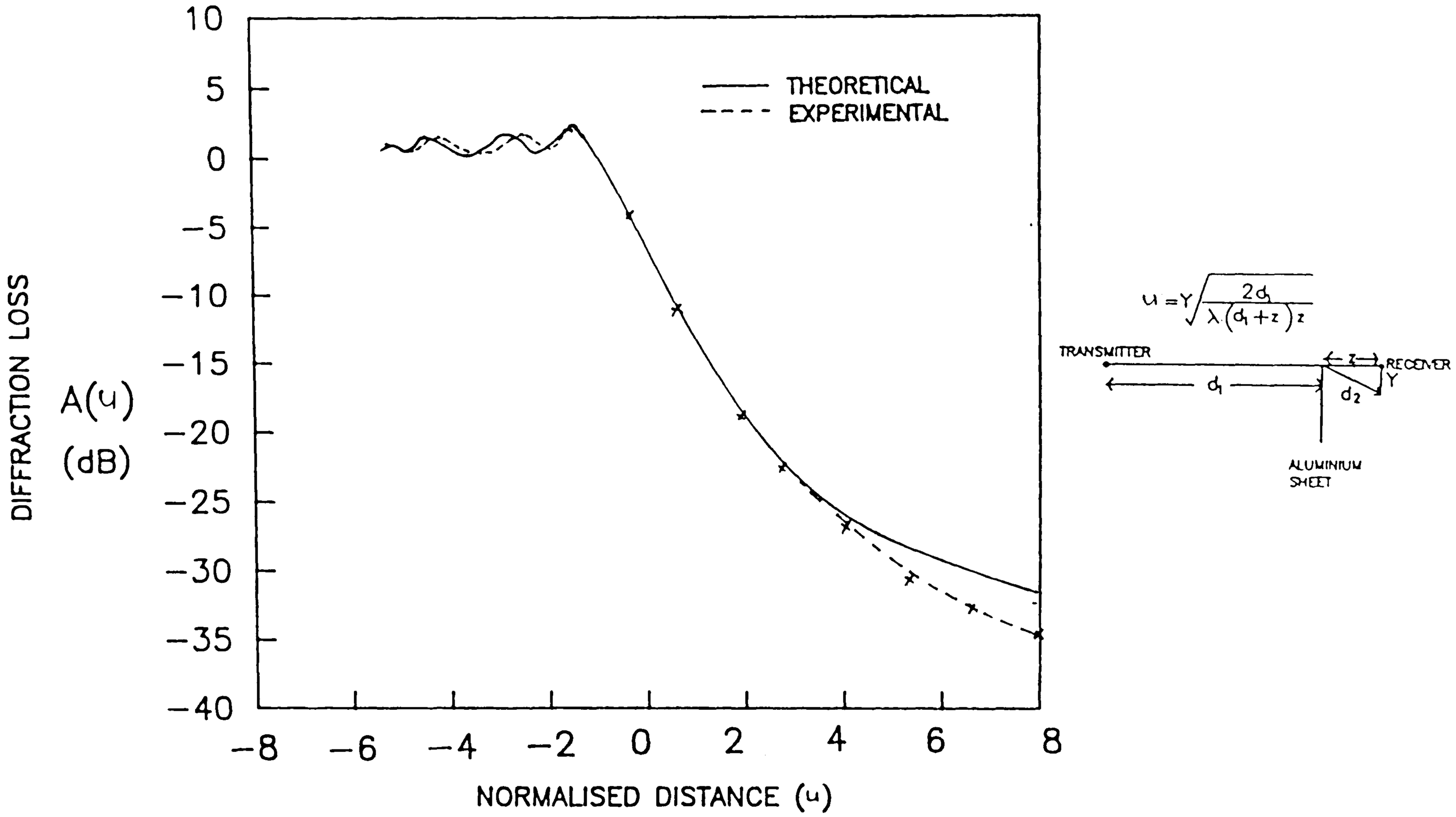

FIG. 6.32 KNIFE EDGE DIFFRACTION RESULTS AT 60GHz

signal power, though the increase is small. When the LOS path just skims over the edge, and the lower half of the incident beam is cut off the received signal power is reduced by 6dB. As the receiving aerial is moved into the shadow region, the received signal power decreases rapidly. However for u greater than 3, the experimental curve departed from the theoretical curve. The difference between the two curves is probably due to the fact that the theoretical curve is only correct for z >> y, which was no longer true for u greater than 3. When u=8, the different between the theoretical and measured value was about 4dB. The results have indicated that the loss at a diffracted angle of 11^0 (u=3) was 22dB above the free-space loss, which is not excessively large. Thus, the knife edge diffraction loss at 60GHz is not particularly high for such a large angle of diffraction.

In practice, obstructions cannot be considered to be knife edges, so diffraction measurements were attempted around the metal covered wall shown in fig 6.31 which protruded into the room. It was found, however, that even for a small diffraction angle of 3^0, the received signal was dominated by reflected signals. It is therefore likely that the diffraction around most obstructions will be small, and that the reflections must be relied upon.

REFERENCES

[1] Rice, S.O., "Statistical properties of a sinewave plus random noise," Bell Sys. Tech. J., Vol. 27 pp 109-157, Jan. 1948.

[2] Clarke, R.H. "A statistical theory of mobile radio reception" Bell Sys. Tech. J. Vol. 47, pp 957-1000, July 1968.

[3] Pugliese, G. and Alexander, S.E., "Cordless communication within buildings: results of measurements at 900MHz and 60GHz," British Telecom Technol. Journal, No.1, July 1983, pp.99 - 105.

[4] Cox, D.C., Murray, R.R., and Norris, A.W., "800MHz measurements in and around suburban houses," B.S.T.J., pp 921-950, July-Aug, 1980.

[5] Lee, W.C., "Estimate of local average power of mobile radio signal," IEEE Trans. on Vehicular Technology, Vol. VT-34, No. 1, February 1985.

[6] Rokkos, N., Johnson, R.A., "Diffraction of millimeter wave communication signals into shadow regions," CORADCOM-81-1, U.S. Army Communication Research and Developement Command. Fort Mormouth, NJ 07703 (1981)

CHAPTER 7

BIT ERROR RATE (BER) MEASUREMENTS.

The modulation system used at 60GHz must be capable of transmitting high bit rate digital signals, so it can be assumed that a digital modulation method will be used. An analogue signal such as speech can be digitised to convert it to a digital signal. One practical way of estimating the ability of transmitting data through a 60GHz radio link is by performing bit error rate (BER) measurements under fading conditions.

7.1 DIGITAL MODULATION METHODS.

A simple radio frequency digital communication system is shown in figure 7.1. The input data may be used to modulate a high frequency carrier in one of several possible ways [1]. If amplitude shift keying (ASK) is used then the digital signal is used to vary the amplitude of the carrier. Another method is frequency shift keying (FSK), where the digital signal varies the frequency of the carrier. Yet another method is phase shift keying (PSK) where a phase of 0^0 and 180^0 is used for the marks and spaces. Other digital modulation techniques are available, eg. Quadrature Phase Shift Keying (QPSK), Offset Quadrature Phase Shift Keying (OQPSK) and Minimum Shift Keying (MSK) which are mainly modified and improved forms of the basic types [3,4], but are more difficult to implement, so are not considered here.

The modulated carrier is often up-converted to a suitable radio frequency for transmission. At the receiver, the radio frequency is converted to a lower frequency. This is then demodulated and followed by decision circuitry which decides if a 0 or a 1 was transmitted. The decisions will not always be correct due to

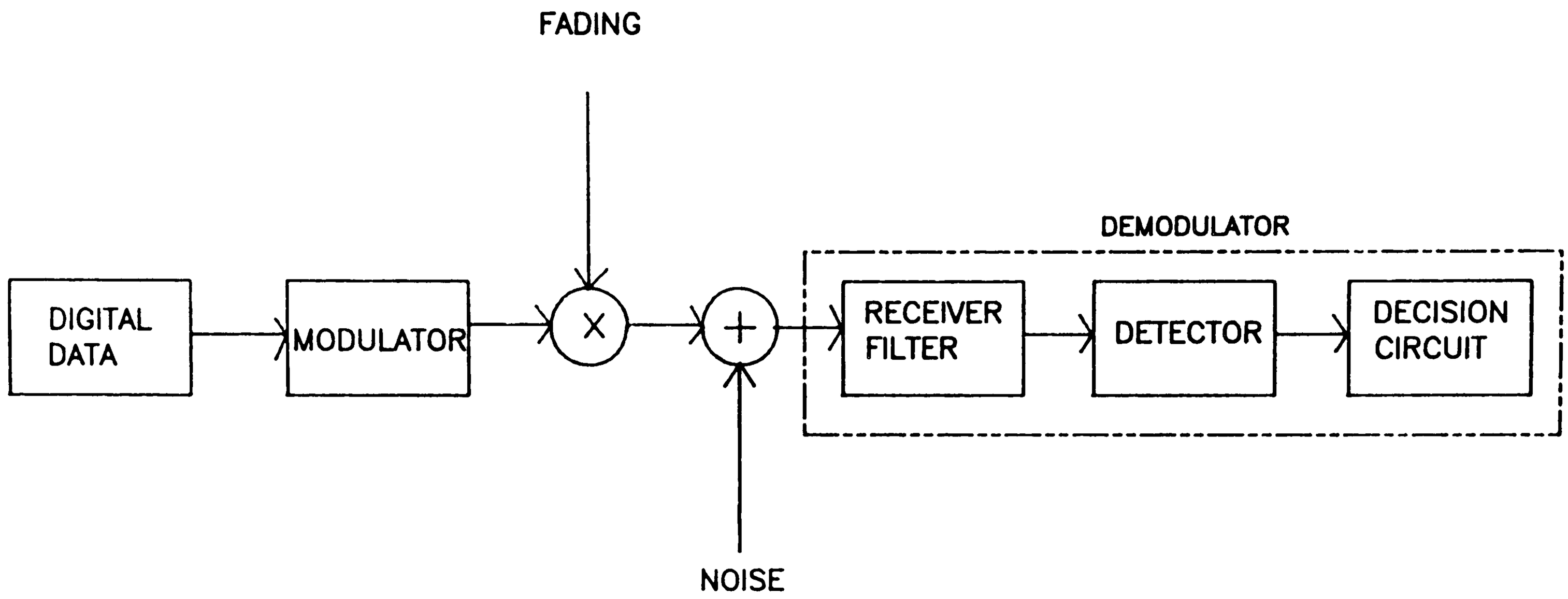

FIG. 7.1 BLOCK DIAGRAM OF DIGITAL COMMUNICATION SYSTEM.

the distorting effects of the channel. A measure of performance of a digital system is the bit error rate (BER). In all modulation systems the BER performance is degraded by the fading characteristics of the channel because many errors occur during deep fades.

In mobile radio communications, the characteristics of the radio channel vary constantly due to motion of the transmitter and receiver and due to multipath propagation. For mobile data communications, these variations can cause bit error bursts of various length. However, it is possible to reduce the probability of deep fades by using diversity reception [5,6,7] which reduces the BER. Error correction coding techniques [8] can also be used to reduce the BER. At 60GHz, the interference from impulsive noise sources such as thermostats or car ignition can be considered to be negligible compared to the UHF band.

ASK is not used for digital data transmission at higher frequencies (above HF), despite its simplicity, for three reasons. Firstly, the BER performance in noise is worse than for FSK and PSK. Secondly, the transmitted signal does not have a constant amplitude, so the amount of power which may be radiated is limited by the peak power handling capability of the transmitter, so it is not used efficiently. Thirdly, for optimum detection of an ASK signal, i.e., for a minimum BER, the detection threshold is a function of the received SNR [1]. This will change as the signal fades, and the threshold should also be changed. As a result, ASK modulation is not used in the mobile environment. In practice, better performance can be obtained by using other modulation methods which do not require a detection threshold dependent on the received SNR. Therefore only PSK and FSK are considered and evaluated in the following sections.

7.2 BIT ERROR RATE PERFORMANCE

The BER is defined as the ratio of the total number of bits detected in error to the total number of bits received over a defined time period. This is also the definition of the probability of error, Pe. The BER depends on many factors: the signal to noise ratio (SNR), the modulation method used, the channel characteristics, the signal shaping, the bit rate, and also the type of demodulator used.

The BER is very dependent on the SNR. The normalised SNR is usually used to assess the performance of different digital modulation methods. It is defined as E/N_o, where E is the received signal energy per bit and N_o is the noise power density in one hertz of the available bandwidth. It can also be shown to be equal to signal power/noise power in a bandwidth equal to the bit rate, or SNR x receiver filter noise bandwidth/bit rate. The normalised SNR is used because it allows the performance of different digital modulation systems operating at different bandwidths to be compared directly.

Multipath propagation and shadowing causes fading which degrades the SNR. This causes a high BER when the signal falls to near the noise level of the receiver. Random FM due to doppler shifts causes errors in digital angle modulation systems, and time delay spread due to multipath propagation produces intersymbol interference which causes errors. The BER caused by envelope fading can be reduced by increasing the transmitted power. However, increasing the transmitted power does not reduce the effects of random FM and time delay spread. Both of these result in an irreducible error rate. This means that as the SNR increases, the BER reduces until it reaches the irreducible error rate, after which point, no improvement in BER occurs.

7.3 BER PERFORMANCE IN SLOW NON-SELECTIVE RAYLEIGH FADING.

7.3.1 Definition of Slow Non-Selective Rayleigh Fading.

Theoretical analyses of the error performance of data communication systems are usually based on the assumption of slow, non-selective Rayleigh fading. [2]

The slow fading assumption means that the fade rate is slow, so that doppler spreading is small and has negligible effect on the BER. The non-selective fading assumption means that the fading is flat over the channel bandwidth, that is, the time delay spreading is small and has negligible effect on the BER.

With digital modulation systems, carrier waves are modulated for known durations to represent marks and spaces. The effect of multipath on such systems is fading of the carrier wave and time dispersion of the envelope carrying the information about marks and spaces. Time dispersion will result in intersymbol inteference if the time delay spreads are appreciable compared to the bit period. For a bit period of T sec, fading is essentially non-selective if the multipath time delay spread, T_m, satisfies the relationship [2]

$$T >> T_m \tag{7.1}$$

For example, if $T = 30T_m$, then the irreducible error rate is approximately equal to $4x10^{-4}$ with raised cosine pulses [9].

When the transmitter or receiver is in motion, the carrier wave also experiences frequency dispersion due to doppler shifting. The maximum doppler shift, f_m, can be obtained from equation 3.5 as

$$f_m = \frac{vf_c}{c} \tag{7.2}$$

where v is the speed of motion, c is the speed of light and f_t is the transmission frequency.

Fading occurs at various rates up to the value of the maximum doppler shift. The slow-fading model cannot be used when the period of fades is comparable to the bit period. Thus, slow fading for mobile transmission only applies when [2]

$$T << \frac{1}{f_m} \tag{7.3}$$

where T is the bit period and f_m is the maximum doppler shift.

The maximum data rate that was used in the experiment was 480kbit/sec, so T=2.08μs for this data rate.

Assume that the longest difference in path lengths indoors is 20m, so the time delay spread, T_m, is (path difference)/c = 0.067μs, thus $T >> T_m$. If the transmitter is moved at a speed of 0.5m/s, then the maximum doppler shift, f_m, is 100Hz, so $1/f_m$ = 10000μs, thus $T << 1/f_m$. The data rate chosen for the measurements therefore satisfied the assumption of slow non-selective Rayleigh fading.

If a data rate of 2Mbit/sec is used, so that T= 0.5μs, $T >> T_m$ still applies. Therefore, the assumption of slow non-selective Rayleigh fading is still approximately valid.

With the above assumptions, the irreducible error rate can be neglected, so the BER in a Rayleigh fading channel can be calculated by adopting the results from the probability of error for a steady signal in white Gaussian noise (WGN).

7.3.2 Mathematical Calculation of the BER with Slow Non-Selective Rayleigh Fading.

Mathematically, the probability of error for different modulated systems working in white Gaussian noise (WGN) is given by [2]

$$P_e = \frac{1}{2}\exp\left(-\frac{\gamma}{2}\right) \qquad \text{(NON-COHERENT FSK)} \qquad (7.4)$$

$$P_e = \frac{1}{2}\exp\left(-\gamma\right) \qquad \text{(DPSK)} \qquad (7.5)$$

$$P_e = \frac{1}{2}\operatorname{erfc}\left(\sqrt{\frac{\gamma}{2}}\right) \qquad \text{(PSK)} \qquad (7.6)$$

$$P_e = \frac{1}{2}\operatorname{erfc}\left(\sqrt{\gamma}\right) \qquad \text{(COHERENT FSK)} \qquad (7.7)$$

where γ is the instantanous SNR, and erfc(x) is the complementary error function, given by [2]

$$\operatorname{erfc}(x) = \frac{2}{\sqrt{\pi}}\int_x^{\infty} e^{-t^2}\,dt \qquad (7.8)$$

where x and t are general variables.

Equations (7.4) to (7.7) are derived theoretically using statistical decision theory, and are plotted in fig. 7.2. [2]

In a Rayleigh fading environment, the received SNR varies due to multipath fading, so the BER cannot be based on one constant SNR. The average BER or Pe for the Rayleigh fading case is given by

$$\overline{P}_e = \int_0^\infty P_e(\gamma).p(\gamma)d\gamma \qquad (7.9)$$

where $p(\gamma)$ is the pdf of the SNR for Rayleigh fading.

In a Rayleigh environment, the pdf of the received signal envelope is given by equation 3.7 as [9]

$$p(r) = \frac{r}{b_o} \exp\left(-\frac{r^2}{2b_o}\right) \qquad \text{for } r > 0 \qquad (7.10)$$

where r is the envelope of the fading signal and b_o is the average power of the short-term fading. Since the received thermal noise is not affected by the fading, the average noise power, P_n can be assumed to be constant. The instantaneous SNR is therefore given by

$$\gamma = \frac{r^2}{2P_n} \qquad (7.11)$$

and if Γ is the mean SNR, then

$$\Gamma = \frac{b_0}{P_n} \qquad (7.12)$$

Also,

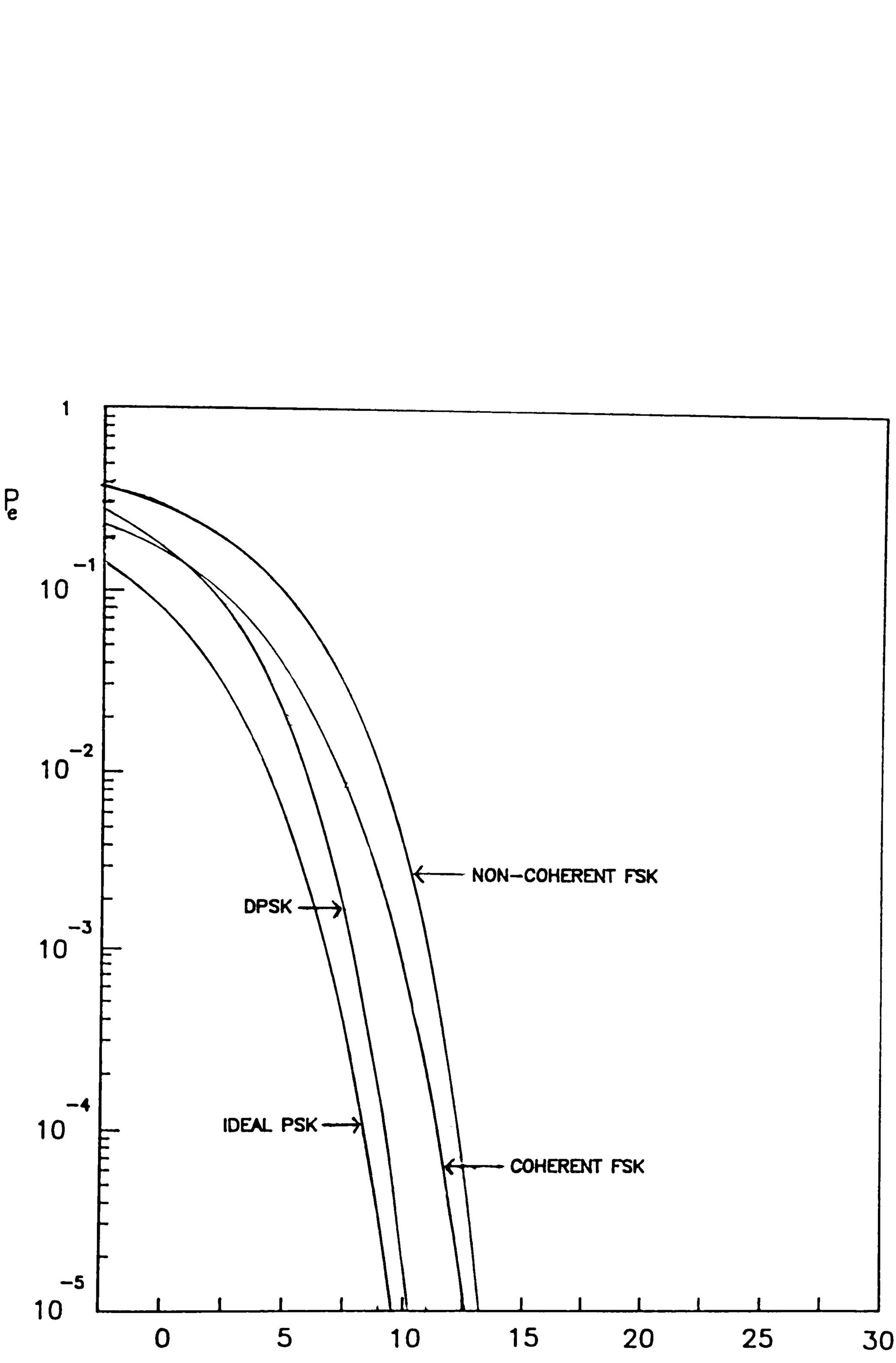

FIG. 7.2 BER FOR SEVERAL SYSTEMS IN WGN

$$p(\gamma) = \frac{p(r)}{(d\gamma/dr)} \tag{7.13}$$

so

$$p(\gamma) = \frac{p(r)}{\left[\frac{2r}{2P_n}\right]} \tag{7.14}$$

Thus, from equations (7.10), (7.11), (7.12) and (7.14), the pdf of the output SNR is

$$p(\gamma) = \frac{1}{\Gamma} \exp(-\frac{\gamma}{\Gamma}) \tag{7.15}$$

Substituting equation (7.15) and equation (7.4) to equation (7.7) into equation (7.9) gives [2]

$$\bar{P}_e = \frac{1}{2 + \Gamma} \qquad \text{(NON-COHERENT FSK)} \tag{7.16}$$

$$\bar{P}_e = \frac{1}{2 + 2\Gamma} \qquad \text{(DPSK)} \tag{7.17}$$

$$\bar{P}_e = \frac{1}{2}\left[1 - \frac{1}{\sqrt{1 + \frac{1}{\Gamma}}} \right] \qquad \text{(PSK)} \tag{7.18}$$

$$\bar{P}_e = \frac{1}{2}\left[1 - \frac{1}{\sqrt{1 + \frac{2}{\Gamma}}} \right] \qquad \text{(COHERENT FSK)} \tag{7.19}$$

The above equations are plotted in fig. 7.3. It can be seen that the BER increases greatly due to the Rayleigh fading.

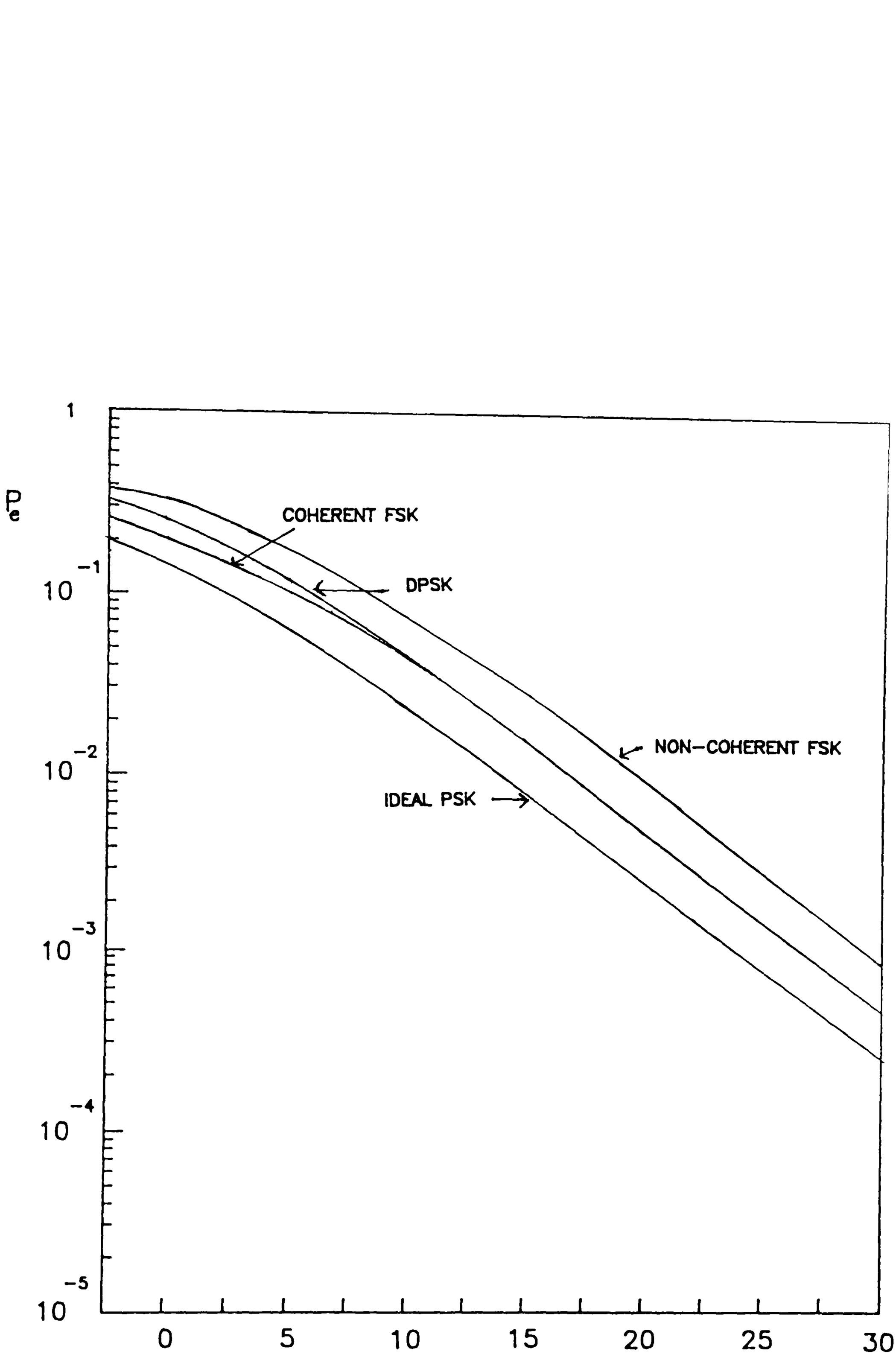

FIG. 7.3 BER FOR SEVERAL SYSTEMS IN WGN WITH RAYLEIGH FADING.

At large SNR's, for all these systems in the Rayleigh fading environment

$$\bar{P}_e \propto \frac{1}{\Gamma} \qquad (7.20)$$

So if both the BER and Γ have log scales, the graphs are straight lines with negative slopes for $\Gamma >> 1$.

7.4 CHOICE OF DIGITAL MODULATION METHOD FOR 60GHz.

The theoretical derivations in the previous section have indicated that coherent detection methods result in lower BER's at a given SNR both with and without Rayleigh fading. In practice, however, coherent detection methods are not commonly used because of the problem of establishing the reference in a channel characterised by deep fades. Instead, non-coherent system such as NCFSK and DPSK are employed for the majority of applications because they do not require additional reference circuitry for demodulation. The choice at 60GHz was therefore made between these two systems.

The theoretical analysis of the previous section has indicated that DPSK gives a better performance than NCFSK both in WGN and in slow non-selective Rayleigh fading. The irreducible error rate caused by frequency selective fading (time delay spread) for both non-coherent FSK and DPSK is roughly the same. It does, however, depends on the pulse shaping, and raised cosine pulses are found to be more tolerent to delay spread than square pulses[9].

When the fading is not slow, i.e, when the mobile is moving at a high speed so that the doppler spreading is high, NCFSK has a lower irreducible error rate than DPSK. For DPSK, the irreducible error rate is given by [9]

$$P_{e(DPSK)} \simeq \frac{1}{2}\left[\frac{\pi f_m}{f_s}\right]^2 \qquad (7.21)$$

for $2\pi f_m T$ small, where f_m is the maximum doppler shift and f_s is the bit rate. For FSK, the irreducible error rate is given by [9]

$$P_{e(FSK)} \simeq \frac{1}{8}\left[\frac{f_m}{f_p}\right]^2 \qquad (7.22)$$

where f_p is the peak frequency deviation and for $f_p >> f_m$. From equations(7.21) and (7.22) and if $f_p = f_s/2$ is used, then

$$\frac{P_{e(DPSK)}}{P_{e(FSK)}} \simeq 10 \qquad (7.23)$$

Therefore the irreducible error rate for FSK is about 10 times lower than that for DPSK. The minimum data rate that was used in the experiment was 240kbit/sec so f_p = 120kHz. At 60GHz, if the transmitter is moved at a speed of 0.5m/s, then fm = 100Hz. From equation (7.22) the irreducible error rate for the NCFSK is about 8.7×10^{-8} and is about 8.6×10^{-7} for DPSK from equation 7.21, which are both negligible. Theoretically, the results obtained from the experiment should experience a negligible irreducible error rate due to doppler shift at this speed.

However, for the outdoor environment, if a vehicle is moving at 30m/s (67mph) then f_m = 6kHz and the irreducible error rates for the DPSK and NCFSK would be about 3.1×10^{-3} and 3.1×10^{-4} respectively. The random FM and therefore

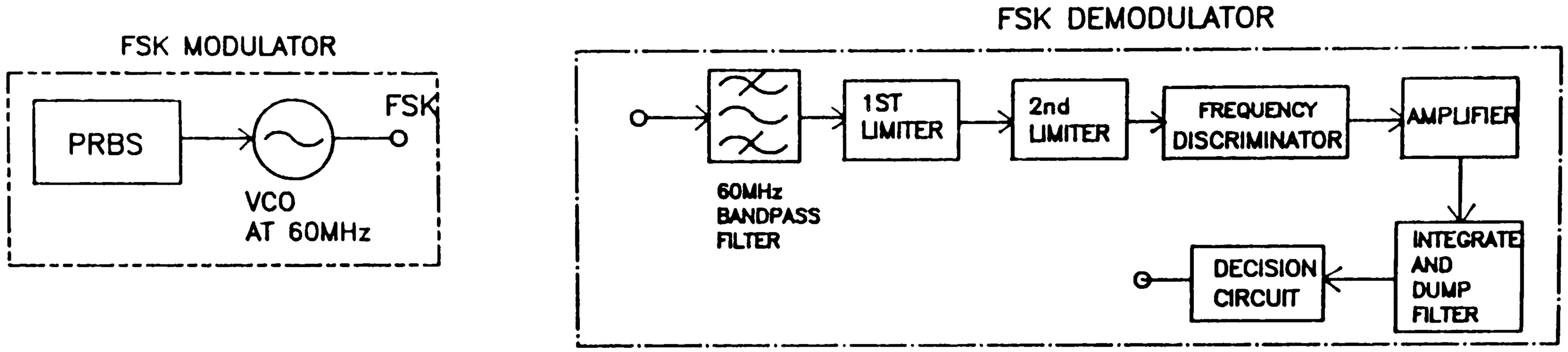

FIG. 7.4 BLOCK DIAGRAM OF FSK MODEM USED FOR THE BER MEASUREMENTS.

the irreducible error rate will increase if the triple doppler shifts measured in section 6.4 occur. Because the signal power received is likely to be weak, a lower bit rate may be necessary which would increase the irreducible error rate. The BER performance of DPSK is unacceptably high. Therefore if the system is to be used outdoors with fast moving vehicles, FSK is more suitable. However, the measurements were not conducted outdoors because the transmitter and receiver modem had to be linked with a cable. This is because the error detector used needed to be provided with both the transmitted and received bit sequences.

Another advantage of NCFSK is that it is easier to implement than DPSK. Therefore, NCFSK was chosen because it was thought that it would result in a simple future 60GHz transceiver, and because it has the best BER at high vehicle speeds.

7.5 DESCRIPTION OF THE FSK MODEM.

The design and construction of the modulator and demodulator of the non-coherent FSK test system are described in this section.

Fig. 7.4 shows the block diagram of the FSK modem. One method of producing FSK is by feeding the digital baseband data to an FM modulator. This is known as direct binary FSK. It can be generated by using circuits which switch the frequency of an oscillator [10]. One of these methods makes use of a free running oscillator whose frequency is controlled by a voltage. This is called a voltage controlled oscillator (VCO).

The data was generated by using a 7 bit shift register and an exclusive-or gate to produce a 127 bit length pseudo random binary sequence (PRBS).

Transmission rates of 240 and 480kbit/sec were used. The FSK encoder had a centre frequency of 60MHz, and was realised by feeding the PRBS to a 60MHz VCO. The ratio of peak frequency deviation to bit rate used was 0.5. Fig. 7.5 shows the output spectrum of the FSK modulator at 240 and 480kbits/sec.

The demodulator consists of a 60MHz bandpass filter, a limiter, a frequency discriminator, an integrate and dump filter, and a decision circuit. The bandpass filter removes components of noise outside the signal band in addition to shaping the received signal. It was a second order Bessel filter, whose noise bandwidth was 373kHz for the 240kbits/sec and 752kHz for the 480kbits/sec measurements. The limiter and frequency discriminator produce an output voltage level proportional to the input frequency, and when receiving an FSK signal, the output alternates between the two logic voltage levels. The characteristics of the discriminator must be linear so that the output voltage response is proportional to the input frequency. Because the amplitude of the received FSK signal varies due to fading, a pre-detection amplitude limiter is used. Integrate and dump circuitry and decision circuitry were used to convert the two noisy logic levels into a reconstituted data signal.

7.6 CHARACTERISING THE FSK MODEM

The FSK modem needs to be characterised by measuring the BER performance in WGN before it can be used with the 60GHz system. This is to ensure that the performance of the system is optimum. In order to do this, WGN was added to the modulated signal at 60MHz as shown in fig. 7.6.

In order to determine the SNR, the band limited signal and noise power were measured separately at the bandpass filter output by using a power meter. If the

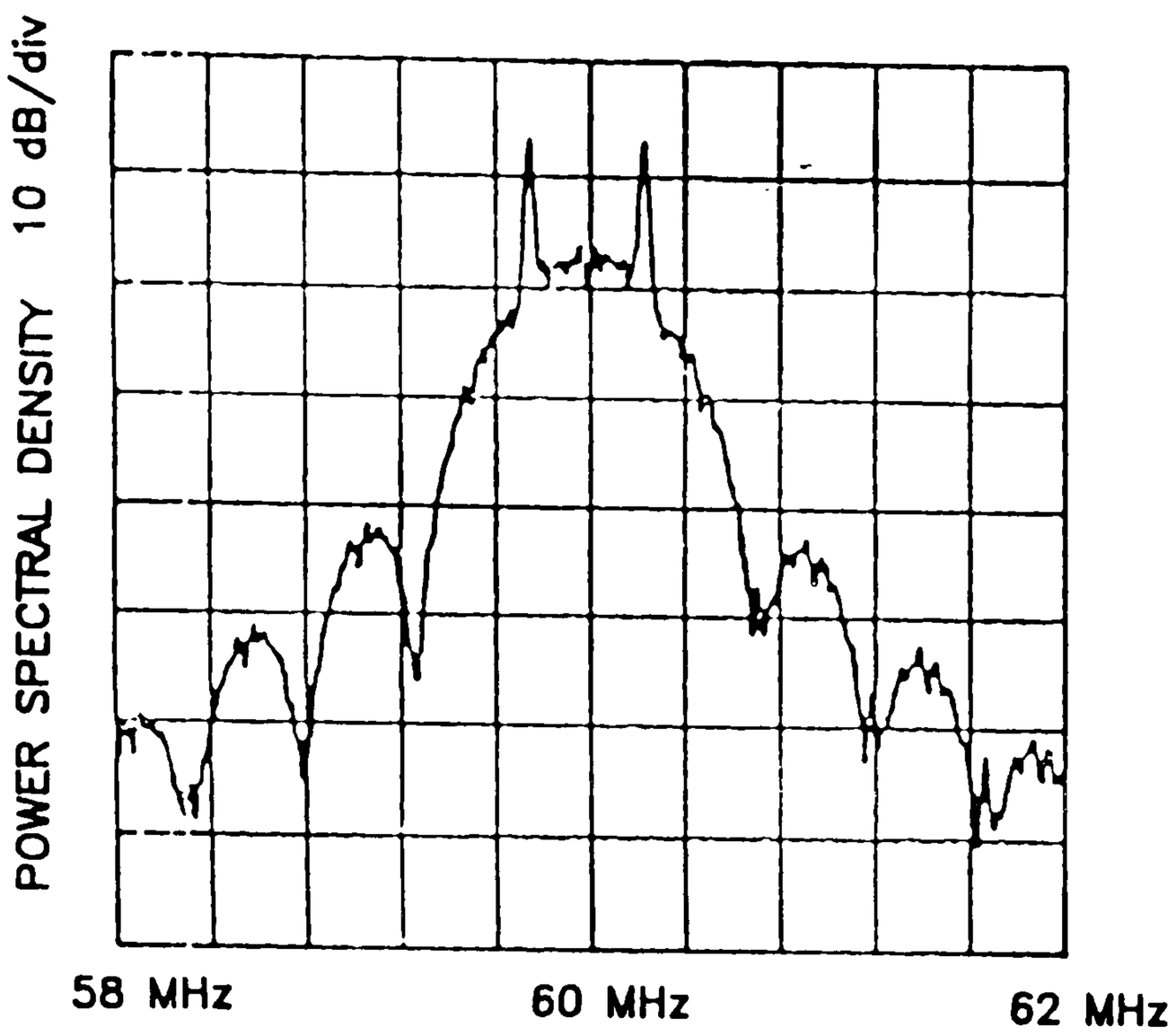

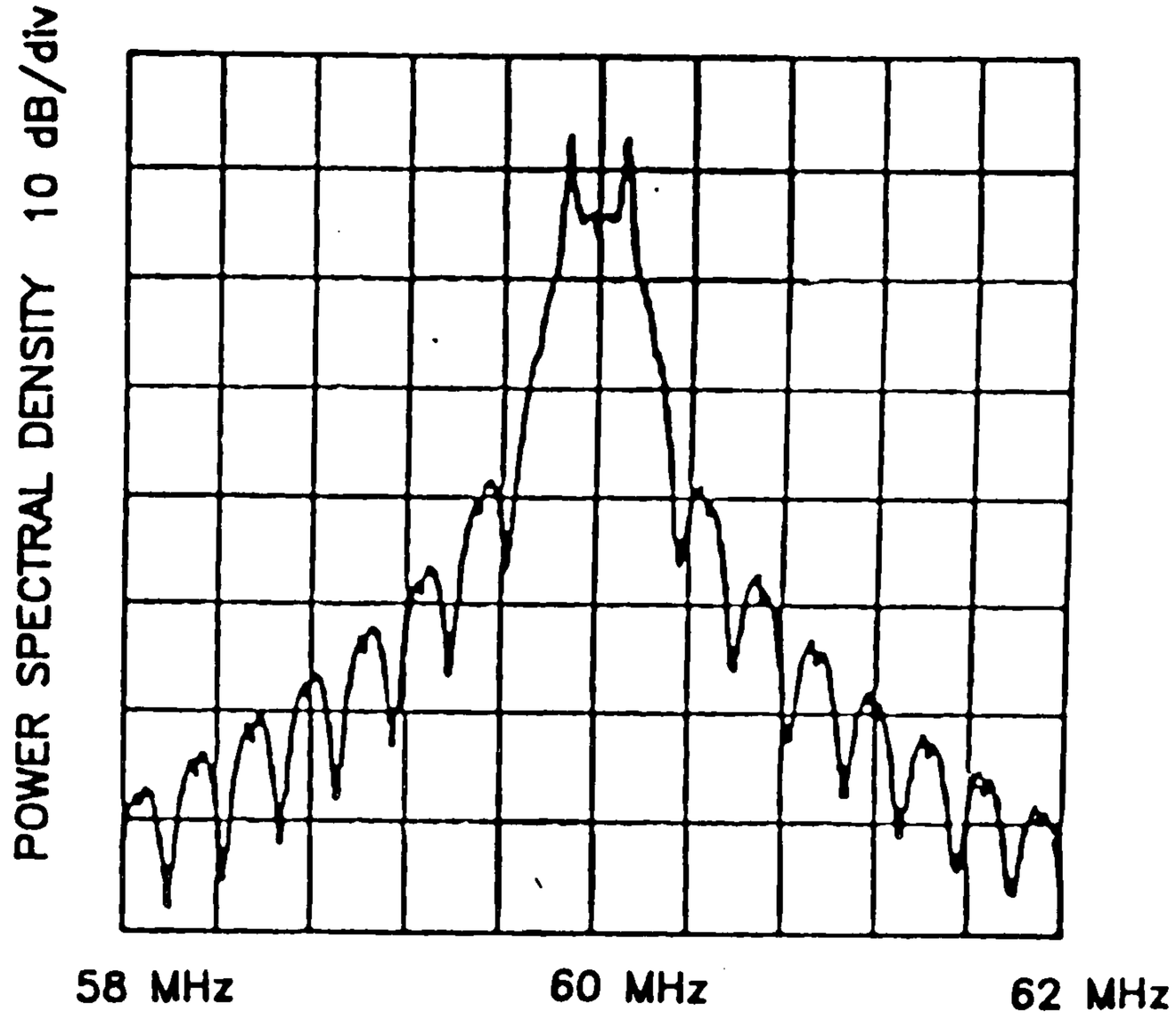

FIG. 7.5 OUTPUT SPECTRUM OF THE 60MHz FSK MODULATOR

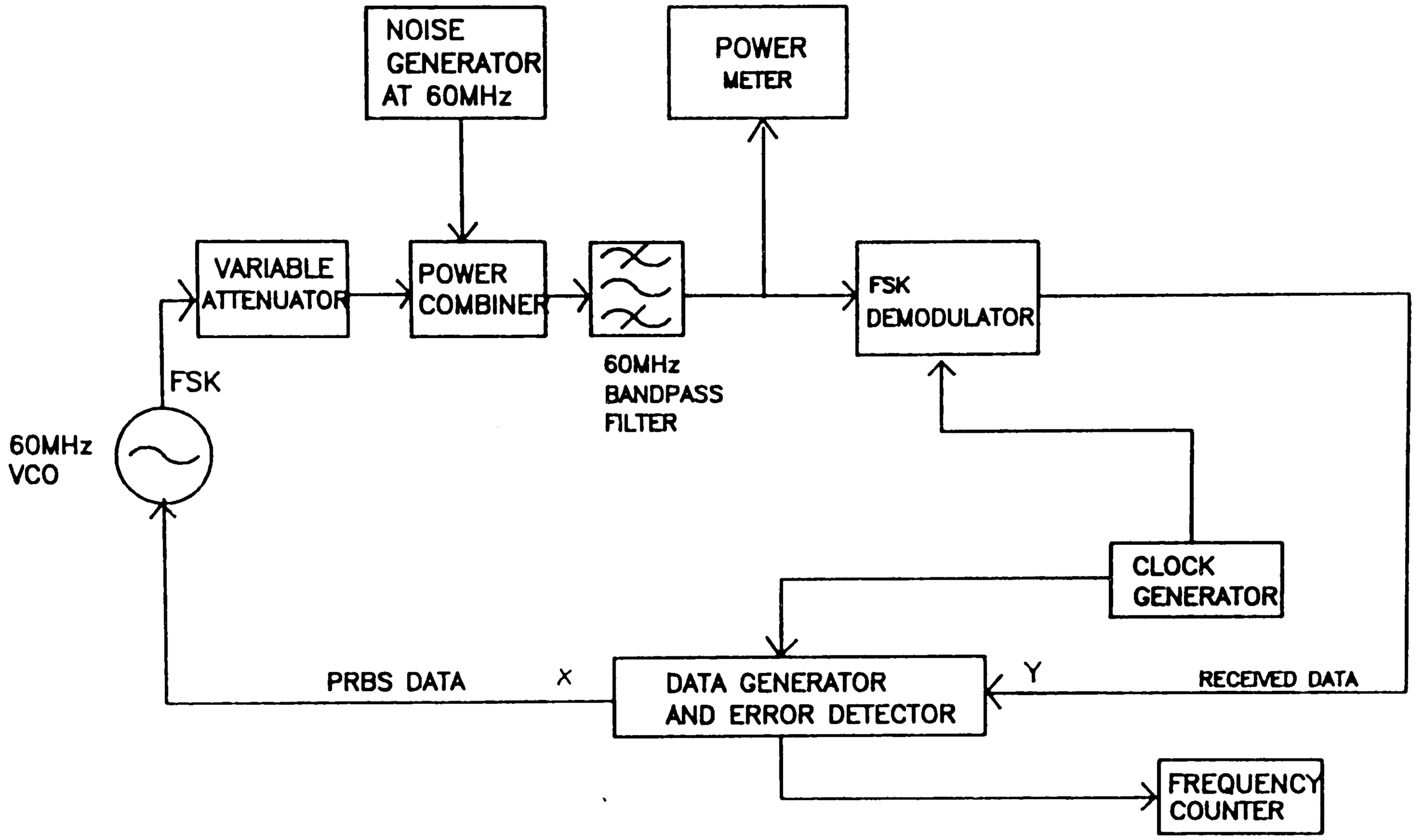

FIG. 7.6 EQUIPMENT FOR BER MEASUREMENTS IN WGN FOR FSK MODEM.

noise power is P_n and the signal power is P_s, then the normalised SNR is found from

$$SNR_{norm} = \frac{P_s}{P_n} \cdot \frac{B_n}{f_s} \qquad (7.24)$$

where B_n is the noise bandwidth of the bandpass filter and f_s is the data rate in bits/sec.

The demodulated data at point Y in fig. 7.6 was then compared with the transmitted data at point X on a bit-by-bit basis. The error detector circuit used an exclusive-or gate and the output of this was sampled with the sampling pulse stream derived from the clock generator. An error pulse is obtained at the output of the error detector at the sampling pulses whenever the transmitted and demodulated data differ.

The error pulses were counted on a frequency meter over a 10sec period for a certain value of SNR. The error counting measurements were repeated for different SNR's. The ratio of the number of errors counted per second to the number of bits transmitted per second in the 10 second period gives the BER for the modem. Hence, if the reading of the frequency meter is f_e for a transmitted data rate f_s, then the BER is given by

$$BER = \frac{f_e}{f_s} \qquad (7.25)$$

The curve for the measured BER versus SNR in WGN was plotted as shown in figure 7.7 together with the theoretical curve. The results show that the FSK

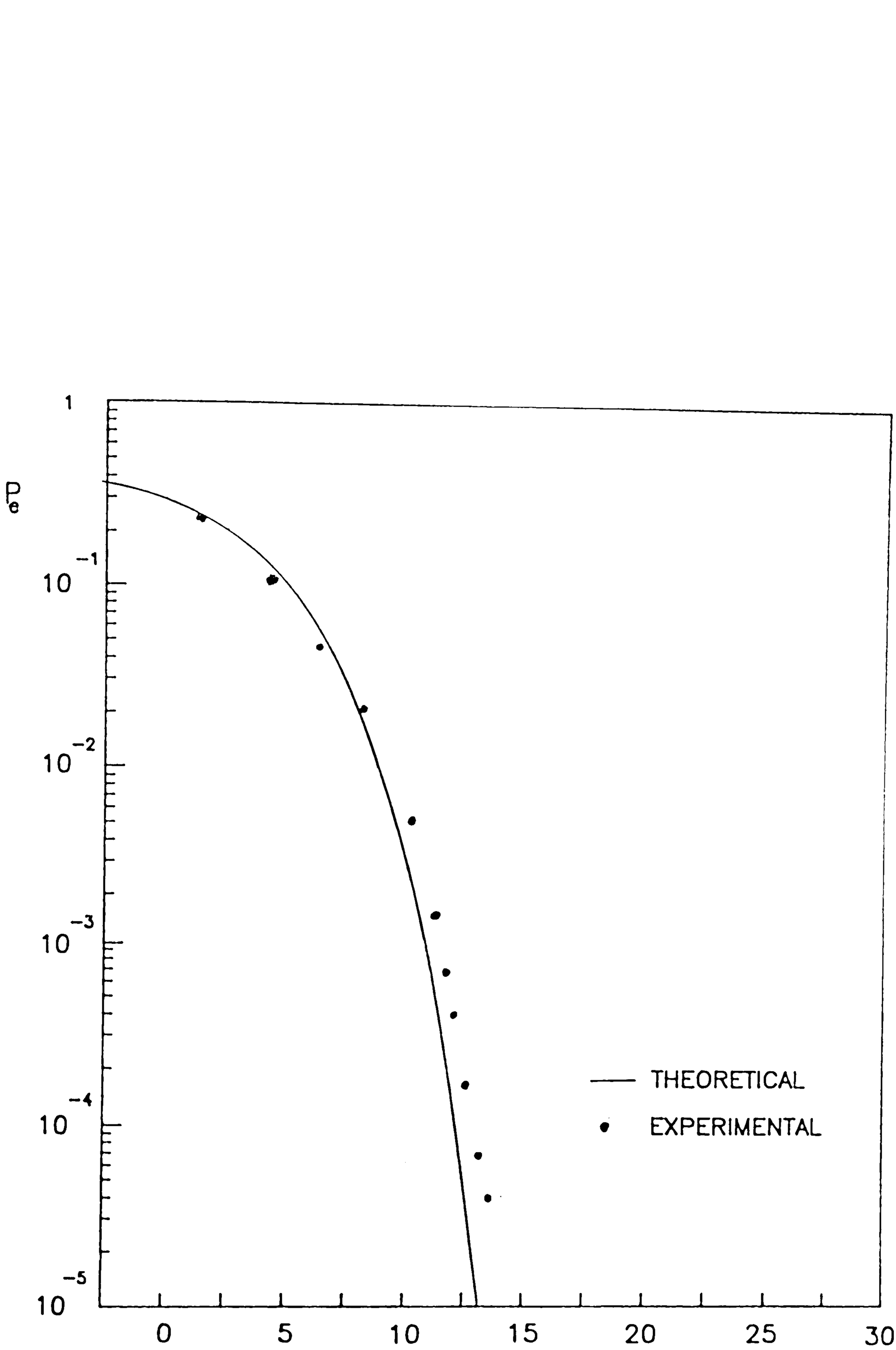

FIG. 7.7 BER FOR NON-COHERENT FSK IN WGN

modem falls within 1dB of the theoretical performance expected for FSK with discriminator detection.

7.7 TRANSMISSION OF FSK THROUGH THE 60GHz LINK

The BER measurements were made with the experimental system shown in figure 7.8. The output of the FSK generator was up-converted to 60GHz by an Alpha 964V01E modulator. The output of the modulator consisted principally of 2 sidebands at 59.96GHz and 59.84GHz (60MHz above and below the 59.9GHz output from the phase-locked oscillator). Because it was too difficult to design a filter at 60GHz, both sidebands were transmitted. The loss of the modulator was 10dB which is the modulator input power at 59.9GHz in dBm minus the output power of the wanted 59.96GHz sideband in dBm. The transmitted power was therefore 10dB below the 50mW output power of the transmitter, which is 5mW. At the receiver, the 58.9GHz phase-locked local oscillator down-converted the transmitted sidebands to 1.06GHz and 0.94GHz. The bandpass filter passed only the 1.06GHz sideband, which was further down-converted to 60MHz by using a mixer and a 1GHz local oscillator.

The phase-locked system described in chapter 4 was used, because the narrow-band received signal would have quickly drifted out of the pass-band of the 60MHz IF bandpass filter with the non-phase-locked system. It is assumed that temperature compensation and/or AFC could be applied to commercial transmitters and receivers in the future, so that the complexity and expense of phase-locking is avoided. The aerials used for the BER measurements were the omnidirectional aerials (type 2) described in chapter 4.

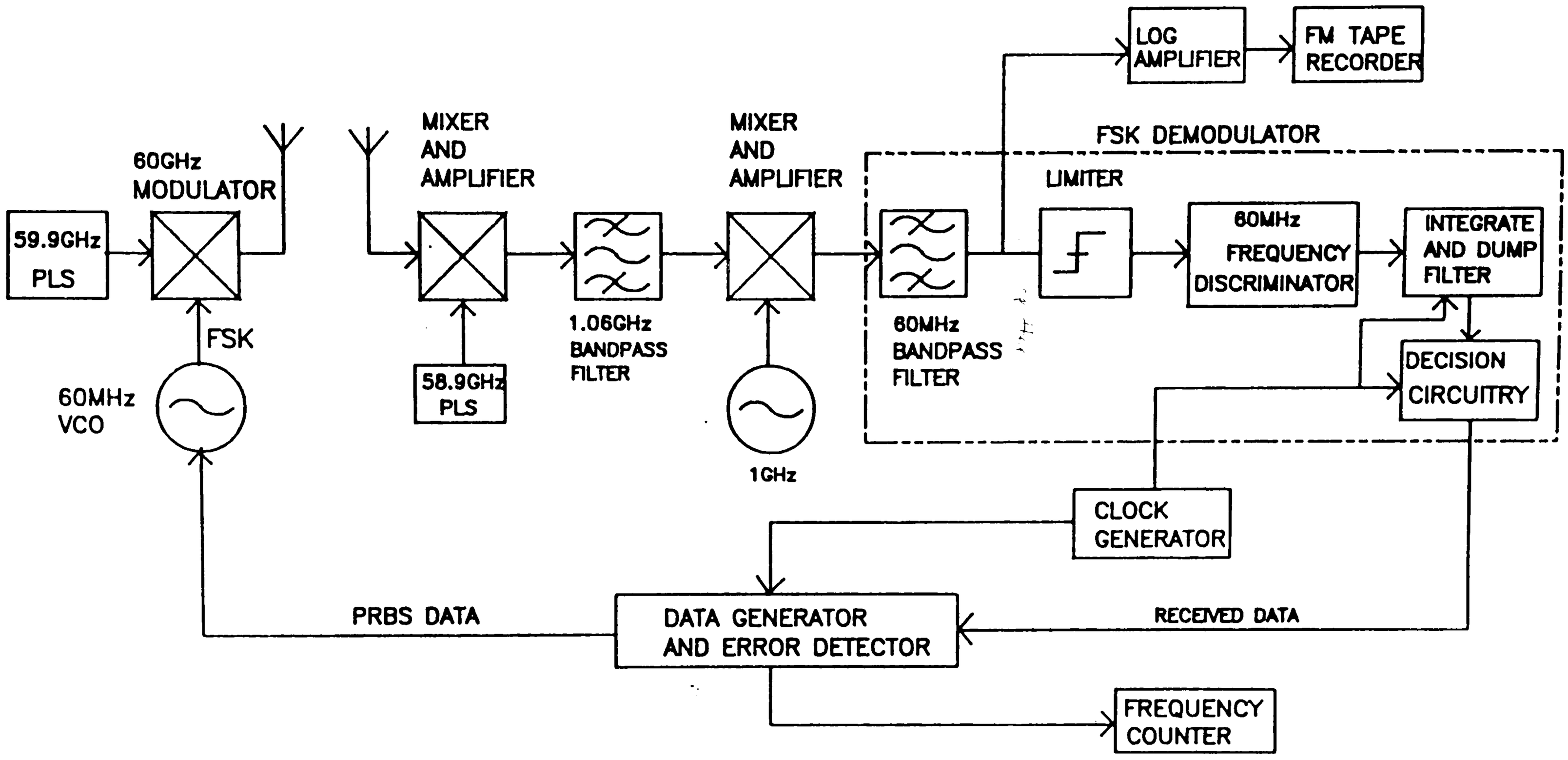

FIG. 7.8 BIT ERROR RATE MEASUREMENT EQUIPMENT

7.8 EXPERIMENTAL PROCEDURE AND RESULTS.

The procedure of the BER measurements described in section 7-6 was used to obtain the BER for different SNR's. For these measurements, instead of adding the WGN, the signal was transmitted through the 60GHz radio link.

The first measurements were conducted when there was a LOS path between the stationary transmitter and receiver. The results obtained are plotted in fig. 7.9.

The second measurements were conducted by randomly moving the transmitter in a horizontal plane in order to produce fading, and the received signal envelope was recorded on the FM tape recorder. The received signal envelope during the fading period was computed in order to obtain the mean received signal power and the envelope distribution. It was later calibrated to give the mean normalised SNR for that particular level. The procedure was repeated for different power levels and therefore SNR's.

The third measurements were conducted when there was no LOS path between the transmitter and receiver. The transmitter was placed behind a metal cabinet, so that the signal was received through reflections from surrounding objects and diffraction around the metal cabinet. The received signal envelope was recorded on the FM tape recorder and was later analysed in order to determine the mean signal power and the envelope fading statistics.

When there was a LOS path between the transmitter and receiver, the envelope distribution departed from the Rayleigh distribution. However, for non-LOS conditions, where the signal was received through reflections from and diffractions around the surroundings, a near Rayleigh distribution was obtained.

The BER was plotted against the mean normalised SNR for both LOS and non-LOS conditions together with the theoretical curve derived earlier for non-coherent FSK in Rayleigh fading as the dotted line shown in fig. 7.9. For comparison, the theoretical non-coherent FSK curve of the BER with no fading was plotted as the full line on the same graph.

It is interesting to note from the figure that, for non-LOS conditions, where the envelope was found to obey the Rayleigh distribution, the experimental curves for the BER are a close fit to the theoretical curves for Rayleigh fading. The BER performance was worse for Rayleigh fading when there was no LOS path compared to the non-Rayleigh fading when there was a LOS path. For Rayleigh fading, in order to maintain a BER of 1 in 10^3, an increase of about 18dB in mean SNR was required compared to when there is no fading. However, when there was a LOS path between the transmitter and receiver, a BER of 1 in 10^3 required an increase of about 13dB in average SNR compared to that in the absence of fading.

The results also indicate that for the conditions of the experiments conducted, no irreducible error rate under LOS or non-LOS conditions occurred. This implies that the time delay spread was much less than the bit duration of the transmitted data so it experienced negligible intersymbol interference. This is because the path lengths in the room were short and there were presumably not many strong multiple reflections. The lack of an irreducible error rate also implies that the random FM due to doppler shifts was much smaller than the FM of the FSK signal. This is because the mobile transmitter was moved at a slow speed. In other areas, particularly outdoors, much higher doppler shifts and much higher time

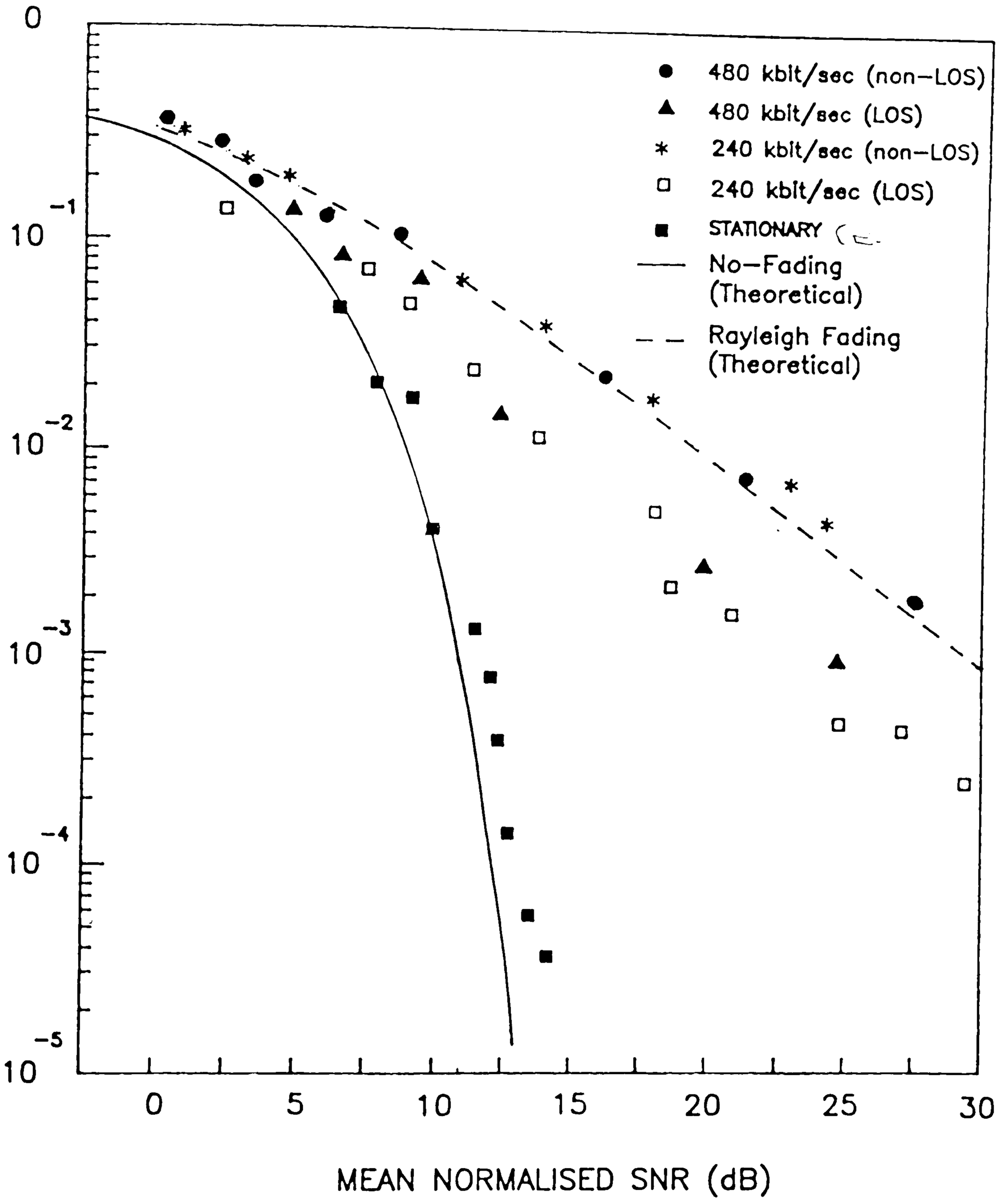

FIG. 7.9 BER IN FADING AND NON-FADING CONDITIONS FOR NON-COHERENT FSK.

delay spreads could be experienced, so under these conditions, an irreducible error rate would perhaps have occurred.

7.9 METHODS OF IMPROVING THE BER PERFORMANCE

The results show that a high SNR is required to obtain a reasonable BER when Rayleigh fading is present. Since Rayleigh fading occurs under non-LOS conditions when the SNR is at its lowest, the BER may be too high for a working system that has to cover an entire room with only one radio distribution port. The bit rates used were 240kbit/sec and 480kbit/sec which are relatively low. If, however, a higher bit rate is used, the BER would be higher because of the wider bandwidth which results in a higher noise power and therefore a worse SNR. In addition, in some locations, particularly outdoors where path lengths are usually longer, the time delay spread may be much greater, so higher bit rates may result in a very high irreducible error rate due to intersymbol interference. It is therefore desirable to find methods to significantly improve it. The BER could be improved by increasing the transmitted power. For example, by using a non-phase-locked transmitter, the loss in the modulator could be eliminated because the 60GHz oscillator could be frequency modulated directly, so that no modulator is needed. This would increase the transmitted power by 10dB in this case, and would also make transceivers less costly and complex. Diversity reception is another possibility which would greatly reduce the BER. It also can be used in conjunction with coding techniques which may provide a good solution to the problem.

Another possibility is to use DPSK instead of FSK, because it gives better performance in slow non-selective Rayleigh fading.[1] However, a modulator is needed for the transmitter which has a typical loss of about 4 dB. If it is also used

outdoors, they may be problems due to high vehicle speeds. These would produce a worse irreducible error rate than they would in FSK.

REFERENCES

[1]. Schwartz, M., Bennet, W.R. and Stein, S.,"Communication Systems and Techniques," McGraw-Hill, 1965.

[2] Stein, S., and Jones, J.S., "Modern communication principles," McGraw-Hill, 1967.

[3] Stremler, F.G., "Introduction to communication systems," Addison Wesley, 1982.

[4] Gronemeyer, S.A. and McBride, A.L., "MSK and offset QPSK modulation," IEEE Trans. on Comm., August, 1976.

[5] Jakes, W.C., "A comparison of specific space diversity techniques for reduction of fast fading in UHF mobile radio systems," IEEE Trans. Vech. Tech., Vol. VT-20, pp81-92, Nov., 1971.

[6] Parson, J.D., and Pongsupaht, A., "Error-rate Reduction in VHF mobile radio data systems using specific diversity reception techniques," Proc. IEE, Pt. F, Vol. 127, December, 1980, pp 475-484.

[7] Parson, J.D. Henze, M., Ratliff, P.A., and Withers, M.J.,"Diversity techniques for mobile radio reception," The Radio and Electronic Engineer, Vol. 45, no. 7, pp 357-367, 1975.

[8] Mabey, P.J., "Mobile radio data transmission - Coding for error control," IEEE Trans. on Vehicular Tech vol. VT-27, No. 3, August 1978.

[9] Jakes, W.," Mobile Microwave Communication," McGraw-Hill, 1974.

[10]. Bowyer, L.R., and Highleyman, W.H., "An analysis of Inherent Distortion in Asynchronous Frequency Shift Modulator," B.S.T.J. Vol. 41. pp 1695 - 1736, Nov. 1962.

CHAPTER 8

CONCLUSIONS AND SUGGESTIONS FOR FUTURE WORK

The aim of the research presented in this thesis was to investigate the narrow band propagation characteristics at 60GHz both within buildings and outdoors. The BER performance of FSK modulation at 240 and 480kbit/sec within buildings was also investigated.

Outdoor and indoor communications to mobile terminals is subject to envelope variations. Small scale variations occur due to multipath propagation, and large scale variations occur due to shadowing. Also, the signal power decreases with increasing distance due to the spreading out of the radiated power. Furthermore, multipath propagation results in delay spread and therefore displays frequency selective fading. In a digital system, it causes intersymbol interference which causes an irreducible error rate. Also, mobile terminals experience random FM due to doppler shifts which causes errors in digital systems.

The outdoor results have shown that up to a distance of 100m where reflections were minimised, the received signal power followed the theoretical free space law plus the oxygen absorption law. Also, the results have indicated that the surrounding objects and the type of ground have an influence on the received signal power. More multipath fading has been observed for an environment with many surrounding objects compared to an open area. More open environments have less fading.

For the outdoors environment under LOS conditions the envelope distribution departed from the Rayleigh distribution. Also under LOS conditions, the median

signal power fell with distance, where the rate of fall depended on the type of environment. For a LOS path, the more open the environment, the faster the fall in received median power. The propagation power law was found to be $1/d^{2.3}$ for an open area with a grass surface and $1/d^{1.4}$ along a road with buildings, parked cars and walls along the sides.

The results have indicated that the received signal power after diffraction around obstacles such as the corner of a building is too small to be usable in the mobile environment. In one measurement, a movement of just a few metres into the shadow region caused an attenuation of about 40dB in the received signal power, although the attenuation was dependent on the distance from the obstruction.

Open areas can create difficulties for communications at 60GHz when the LOS path is obstructed, because there may be no nearby objects to reflect the signal to the receiver. Even along a road with buildings and cars parked along the sides, one of the measurements has shown that when a LOS path was obstructed by a van, the received signal power fell by more than 25dB. This means that the reflected signals were weak so they were unable to provide a usable signal power at the receiver.

Propagation of 60GHz into buildings, from lamp post height for example, is not feasible due to the high attenuation of 60GHz through walls and other partitions because the exterior and interior building walls act as shields. It was found that for the particular building measured, the penetration loss varied from 4dB to greater than 45dB. Therefore, in order to provide services within buildings, the radio distribution ports need to be installed indoors.

For the outdoor environment, if a 60GHz system is to be employed, careful consideration must be given when installing aerials so that the obstruction loss due to obstacles is minimised. This could be possible by using base station diversity. Several radio distribution ports may be necessary to fill in the signal behind obstructions. The system designer will always have to ensure that a LOS path or a strong reflection exists between the transmitter and receiver.

Indoors, the results have indicated that when no LOS path existed, there was a very good fit to the Rayleigh distribution because the signal received was by reflections and there was no dominant direct signal. However, when a LOS path was present, there was a relatively poor fit to the Rayleigh distribution because the direct wave was much stronger than the reflected waves. Instead, the received signal envelope tended to follow a Rician distribution.

Fading is not only caused by the transmitter or receiver moving, but also by people moving. When there was no LOS path and a person was moving in front of or behind the receiver, the distribution followed the Rayleigh distribution. However, when there was a LOS path the distribution tended to follow a Rician distribution. The fading was more severe when the LOS path was intermittently blocked by a person moving in front of the receiver.

Measurements of power laws within buildings have been made with a LOS path for different environments. The results have indicated that under LOS conditions within a Laboratory and particularly within corridors, the median signal power fell with distance more slowly than it would in free space. This may be due to the channelling effect of the received power caused by strong reflections from the walls, floor and ceiling. However, in a furnished and carpeted office, the median

signal power fell with distance slightly faster than it would in free-space. This was because strong reflections off the walls were prevented by many chairs, desks and bookshelves, and a strong reflection off the floor was prevented by a carpet. The power laws measured in different indoor environments do not however represent worst case conditions. This is because a LOS path results in a high received signal power and because it is usually rare indoors for there to be a LOS path over a long distance. The non-LOS case causes the biggest problem because generally, the received signal power is at its lowest because of the high obstruction losses, and the fast fading is at its most severe (Rayleigh) compared to the fading experienced under LOS conditions (Rician).

The results from the attenuation of building materials have shown that the attenuation varies widely for different materials. The most common materials used for external walls such as concrete blocks are very effective in screening the 60GHz signal. However, materials such as chipboard and hardboard have a fairly low attenuation.

The results also have indicated that room-to-room coverage depends on the type of partitions used. The high attenuation of concrete walls or partitions with metal linings prevent the signal from radiating to adjacent rooms. Although the signal attenuation through wooden doors was low, the signal power was usually only strong enough close to them. A rapid fall in the received signal power therefore occurs beyond the room. This results in the capability of greater frequency reuse and a higher reduction of co-channel interference due to the screening effects of the partitions. The screening effect of these partitions means that one radio distribution port would be required per room. Also, the low attenuation of wooden doors

suggests that if the walls are made of chipboard, the signal would perhaps cover several rooms.

The indoor results have indicated that a high signal power occurs with knife edge diffraction. However, practically occurring diffractors (obstacles) do not have knife edges, and the received signal power due to diffraction is generally small compared to that due to reflections. If the signal in the shadow region is too low, the reflections from the surrounding environment, for example from the wall, could be improved by applying a reflective coating.

The power spectrum of the received signal has indicated that it experienced frequency spreading between +/- the maximum doppler shift due to the doppler shifting of the direct and reflected paths. In the measurements, frequency shifts which were three times the maximum theoretical doppler shift have been observed. These were thought to be due to the signal being reflected back to the transmitter, which reflected it to the receiver. The doppler spreading is small at the speeds of motion usually experienced indoors compared to the expected transmission bandwidth, so its effects are likely to be small.

The type of modulation chosen for the transmission of binary data was non-coherent FSK. This was because theoretically, the irreducible error rate performance of FSK with random FM due to doppler shifts is about ten times lower than for DPSK, which could be important outdoors, and because of the simplicity of the design and construction of an FSK modem.

The results from the BER measurements in Rayleigh fading have indicated that no irreducible error rate occurred. This implies that the delay spread was much

less than the bit duration of the FSK signal so that the inter-symbol interference was small. This is because the indoor path length is short and probably because multiple reflections were not very strong. Furthermore, the transmitter was moved at a slow speed so the doppler shifts were small with negligible random FM. It has been proved theoretically that the irreducible error rate due to doppler shifts at this bit rate is very low. With the present system, a higher bit rate could not be achieved because of the limitations of the hardware used. Since no irreducible error rate occurred at 480kbit/sec, it is posssible that higher bit rates could be successfully used without problems of intersymbol interference. However, in other areas, particularly outdoors, the time delay spread may be higher, so a lower bit rate would have to be used. High bit rates also mean that the frequency stability of the 60GHz oscillators is less of a problem, so a non-phase-locked system would perhaps be acceptable. With this, generating FSK is easier because it can be done by applying data to the varactor of the 60GHz transmitter oscillator. Therefore, a modulator would not be required, which would simplify the transmitter and would eliminate the modulator power loss.

In conclusion, the following points can be made. The signal coverage at 60GHz could be improved by careful location of the radio distribution ports, and by choosing suitable types of aerials and radiated power levels. Suitable placement of the radio ports can provide reasonable signal coverage. For example, in the urban outdoor environment, many radio distribution points distributed throughout the area would reduce the obstruction losses. A possible position for these radio distribution ports is on lamp posts, traffic signals or building walls. The choice of the radiated power and aerial radiation pattern would depend on the environment. For example, in an open area, omnidirectional aerials could be used since there are less

obstructions. This could be applied for example in stadiums or in open public places. In urban environments, for example, along streets, directional aerials could be used.

Within buildings, a single room or corridor could be served by a single 60GHz distribution port attached to the ceiling. Optical fibre links could be connected to the 60GHz distribution ports for trunking purposes. A good position for a 60GHz radio distribution port in a room is in the middle of the room at ceiling height. With this placement, reflections off the side walls probably improve the received signal power behind obstructions. If the reflections are weak, the received signal power could perhaps be increased by applying some form of reflective coating to the walls.

By using a different polar pattern for the aerial, the coverage within a room could be improved. The polar diagram of the omnidirectional aerial used had a torus shape. However, the received signal power was low when the transmitter was directly below the receiver when it was located near the ceiling. This was because the omnidirectional aerials transmit or receive little perpendicular to their main lobes. An aerial with a cardioid shaped polar pattern would probably give an improvement in the received signal power and therefore an improved BER at this location.

The BER obtained may be too high for a working system and a substantial improvement will have to be made to the BER performance. Most of the errors are caused by the fading. If data transmission is going to be used in this kind of environment, i.e within a single room, Diversity reception in conjunction with coding techniques could improve the BER performance and therefore could provide a good solution to the problem.

SUGGESTIONS FOR FUTURE WORK.

Included in this section are suggestions for further research that could be conducted for a better understanding and implementation for future 60GHz communication systems.

The results presented in this thesis has been measured in a reinforced concrete building consisting mainly of plaster covered concrete partitions. It would be interesting to find the indoor propagation characteristics of different buildings having different types of partitions, since they may extend the coverage into adjacent rooms. A different polar pattern of the aerial to improve the signal coverage in a particular environment could also be investigated.

The results have shown that no irreducible error rate occurred at 480kbit/sec within buildings. It would be of interest to try other areas within buildings and outdoors and to try higher data rates to see if an acceptable BER can be obtained. Furthermore, different aspects of digital encoding, diversity, modulation and multiplexing techniques could be considered. It is also of interest to try to characterise the BER performance using more complicated modulation methods such as DPSK, OQPSK, MSK etc. Furthermore, the feasibility of a simple non-phase locked system using FSK modulation for the transmission of wideband data by using automatic frequency control (AFC) could be investigated.

Other possible applications at 60GHz are short range point-to-point links and local distribution networks. These areas of research could also be investigated, for example, the local distribution of wideband services such as 'cable' TV distribution into houses. The extremely wide bandwidth available could permit the transmission

of a high data rate with low delay spread for a stationary local distribution network. It also could help to reduce the co-channel interference between various local distribution networks.

APPENDIX A

COMPUTER PROGRAMMES

```
program load;
{This program reads data from a binary file produced by}
{A/D program and stores data in a formatted ASCII file }

var
  ipfile     :file of integer; {binary file from A/D prog}
  opfile     :text;            {formatted ASCII op   file}
  ipfname    :string[80];      {input filename           }
  opfname    :string[80];      {output filename          }
  firstsamp  :integer;         {first samp from ip file  }
  lastsamp   :integer;         {last samp from ip file   }
  samp       :integer;         {samp number              }
  data       :integer;         {data samp from ip file   }

begin
  write('Enter input filename: ');
  readln(ipfname);
  assign(ipfile,ipfname);
  write('Enter output filename: ');
  readln(opfname);
  assign(opfile,opfname);
  write('Enter first sample: ');
  readln(firstsamp);
  write('Enter last sample: ');
  readln(lastsamp);
  reset(ipfile);
  rewrite(opfile);
  for samp:=1 to lastsamp do begin
    read(ipfile,data);
    if samp>=firstsamp then write(opfile,data:10);
  end;
  close(ipfile);
  close(opfile);
end.
```

```
program plot;
{Program plots data stored in ASCII file produced by    }
{program load. Runs with turbo pascal & turbo graphix   }
{version 3. Change MaxPlotGlb in file typedef.sys to    }
{1500 to plot up to 1500 points                         }

{The following 6 lines include turbo graphix system
files}
{$I c:\turbogra\typedef.sys}
{$I c:\turbogra\graphix.sys}
{$I c:\turbogra\kernel.sys }
{$I c:\turbogra\windows.sys}
{$I c:\turbogra\axis.hgh   }
{$I c:\turbogra\polygon.hgh}

const
  maxnumsamp = 1500; {max num samps that can be read    }
type
  str80 = string[80];
  dataarray = array [1..maxnumsamp] of real;
var
  data      :dataarray;  { stores data read from file   }
  numsamp   :integer;    { num samps read from data file}
  ch        :char;       { menu option letter          }
  points    :plotarray;  { stores points to be plotted  }

function isin(ch:char; s:str80):boolean;
var
  charpos  :integer;
begin
  isin:=false;
  for charpos:=1 to length(s) do
    if s[charpos]=ch then isin:=true;
end;  {isin}


function menu:char;
var
  ch   :char;
begin
  writeln;
repeat
  writeln('Display data');
  writeln('Save');
  writeln('Load');
  writeln('Quit');
  writeln('Plot');
  writeln;
  write('Choose one (D, S, L, Q, P): ');
  readln(ch);
  writeln;
```

```
    ch:=upcase(ch);
  until isin(ch,'DSLQP');
  menu:=ch;
end; {menu}


procedure display;
var
  samp     :integer;
begin
  for samp:=1 to numsamp do
    writeln(samp,':',data[samp]:15:5);
  writeln;
end; {display}


procedure save;
var
  samp      :integer;
  fname     :string[80];
  temp      :real;
  datafile :text;
begin
  write('Enter filename: ');
  readln(fname);
  writeln;
  assign(datafile,fname);
  rewrite(datafile);
  temp:=numsamp; { change its type from integer to real }
  write(datafile,temp);
  for samp:=1 to numsamp
    do writeln(datafile,data[samp]);
  close(datafile);
end; {save}


procedure plotxy;
var
  samp       :integer;
  firstsamp :integer;
  lastsamp  :integer;
begin
  write('Enter firstsamp: ');
  readln(firstsamp);
  write('Enter lastsamp: ');
  readln(lastsamp);
  initgraphic;
  clearscreen;
  definewindow(1,0,0,xmaxglb,ymaxglb);
  defineworld(1,firstsamp,100,lastsamp,0);
  selectworld(1);
  selectwindow(1);
  setbackground(0);
  drawborder;
```

```
  drawaxis(8,-7,0,0,0,0,0,0,true);
  for samp:=firstsamp to lastsamp do begin
    points[samp-firstsamp+1,1]:=samp;
    points[samp-firstsamp+1,2]:=data[samp];
  end;
  drawpolygon(points,1,lastsamp-firstsamp+1,0,0,0);
  repeat until keypressed;
  leavegraphic;
end;

procedure load;
var
  samp      :integer;
  fname     :string[80];
  temp      :real;
  datafile :text;
begin
  write('Enter filename: ');
  readln(fname);
  writeln;
  assign(datafile,fname);
  reset(datafile);
  writeln('Enter number of samples: ');
  readln(numsamp);
  for samp:=1 to numsamp do begin
    read(datafile,data[samp]);
    data[samp]:=data[samp]-2060;
    data[samp]:=data[samp]*5;
    data[samp]:=120-(2680-data[samp])/23;
  end;
  close(datafile);
end; {load}


begin
  repeat
    ch:=upcase(menu);
    case ch of
      'D': display;
      'S': save;
      'L': load;
      'P': plotxy;
    end;
  until ch='Q';
end.
```

```
program calib;
{This program reads data stored in ASCII file produced  }
{by the program load, converts it to dB and stores it in}
{another file                                            }

const
  maxnumsamp = 5000; {max num samps that can be read     }
type
  str80 = string[80];
  dataarray = array [1..maxnumsamp] of integer;
var
  data      :dataarray;  {stores data read from a file   }
  numsamp   :integer;    {number of samples read fromfile}
  ch        :char;       {menu option letter             }


function isin(ch:char; s:str80):boolean;
var
  charpos   :integer;
begin
  isin:=false;
  for charpos:=1 to length(s) do
    if s[charpos]=ch then isin:=true;
end; {isin}


function menu:char;
var
  ch    :char;
begin
  writeln;
  repeat
    writeln('Display data');
    writeln('Save');
    writeln('Load');
    writeln('Quit');
    writeln;
    write('choose one (D, S, L, Q): ');
    readln(ch);
    writeln;
    ch:=upcase(ch);
  until isin(ch,'DSLQ');
  menu:=ch;
end; {menu}


procedure display;
var
  samp    :integer;              { sample number variable }
begin
  for samp:=1 to numsamp do
    writeln(samp,': ',data[samp]);
```

```
  writeln;
end; {display}


procedure save;
var
  samp       :integer;     {sample number variable          }
  fname      :string[80]; {calibrated data file name       }
  temp       :real;        {converts an integer to a real }
  datafile   :text;        {calibrated data file            }
begin
  write('Enter filename: ');
  readln(fname);
  writeln;
  assign(datafile,fname);
  rewrite(datafile);
  temp:=numsamp; { change its type from integer to real }
  for samp:=1 to numsamp do
    writeln(datafile,data[samp]);
  close(datafile);
end; {save}


procedure load;
var
  samp       :integer;        { sample number variable    }
  fname      :string[80];     { filename of ip file       }
  datafile   :text;           { ip file                   }
begin
  write('Enter filename: ');
  readln(fname);
  writeln;
  assign(datafile,fname);
  reset(datafile);
  write('Enter number of samples: ');
  readln(numsamp);
  for samp:=1 to numsamp do begin
    read(datafile,data[samp]);
    data[samp]:=data[samp]-2060;
    data[samp]:=data[samp]*5;
    data[samp]:=-trunc((2680-data[samp])/23);
    data[samp]:=trunc(data[samp]-2.5);
  end;
  close(datafile);
end; {load}


begin
  repeat
    ch:=upcase(menu);
    case ch of
      'D': display;
      'S': save;
      'L': load;
```

```
    end;
  until ch='Q';
end.
```

```
program dbmean;
{This program calculates mean, standard dev, max and min}
{from calibrated data in dB stored in a file              }

const
  maxnumsamp=5000; {max num samps that can be read       }
type
  str80=string[80];
  dataarray=array[1..maxnumsamp] of real;
var
  data        :dataarray;
  meanval     :real;
  std         :real;
  maxval      :real;
  minval      :real;
  numsamp     :integer;
  ch          :char;


function isin(ch:char; s:str80):boolean;
var
  charpos :integer;      { position in character string  }
begin
  isin:=false;
  for charpos:=1 to length(s) do
    if s[charpos]=ch then isin:=true;
end; {isin}


function menu:char;
var
  ch  :char;
begin
  writeln;
  repeat
    writeln('Enter data');
    writeln('Display data');
    writeln('Basic statistics');
    writeln('Save');
    writeln('Load');
    writeln('Quit');
    writeln;
    write('Choose one (E, D, B, S, L, Q): ');
    readln(ch);
    writeln;
    ch:=upcase(ch);
  until isin(ch,'EDBSLQ');
  menu:=ch;
end; {menu}


procedure display(numsamp:integer);
var
  samp     :integer;
```

```
  datsamp  :real;
begin
  for samp:=1 to numsamp do begin
    datsamp:=20*(ln(data[samp])/ln(10));
    writeln(samp,':',datsamp:15:5);
  end;
  writeln;
end; {display}


procedure enter;
var
  samp  :integer;
begin
  write('Enter number of items: ');
  readln(numsamp);
  writeln;
  for samp:=1 to numsamp do begin
    write('Enter item ',samp,': ');
    readln(data[samp]);
    writeln;
  end;
end; {enter}


function mean(numsamp:integer):real;
var
  samp :integer;
  avg  :real;
begin
  avg:=0;
  for samp:=1 to numsamp do
    avg:=avg+data[samp];
  mean:=20*(ln(avg/numsamp)/ln(10));
end; {mean}


function stddev(numsamp:integer):real;
var
  samp :integer;
  std  :real;
  avg  :real;
begin
  avg:=mean(numsamp);
  avg:=exp((avg/20)*ln(10));
  std:=0;
  for samp:=1 to numsamp do
    std:=std+((data[samp]-avg)*(data[samp]-avg));
  std:=std/numsamp;
  stddev:=-(ln(sqrt(std))/ln(10));
end; {stddev}


function getmax(numsamp:integer):integer;
```

```
var
  samp   :integer;
  max    :real;
  get    :real;
  dbdat  :real;
begin
  max:=20*(ln(data[1])/ln(10));
  for samp:=2 to numsamp do begin
    dbdat:=20*(ln(data[samp])/ln(10));
    if dbdat>max then max:=dbdat;
  end;
  getmax:=round(max);
end; {getmax}


function getmin(numsamp:integer):integer;
var
  samp   :integer;
  min    :real;
  dbdat  :real;
begin
  min:=20*(ln(data[1])/ln(10));
  for samp:=2 to numsamp do begin
    dbdat:=20*(ln(data[samp])/ln(10));
    if dbdat<min then min:=dbdat;
  end;
  getmin:=round(min);
end; {getmin}


procedure save(numsamp:integer);
var
  samp      :integer;
  fname     :string[80];
  temp      :real;
  datafile  :text;
begin
  write('Enter filename: ');
  readln(fname);
  writeln;
  assign(datafile,fname);
  rewrite(datafile);
  temp:=numsamp; {change its type}
  write(datafile,temp);
  for samp:=1 to numsamp do
    writeln(datafile,data[samp]);
  close(datafile);
end; {save}


procedure load;
var
  samp      :integer;
  scale     :integer;
```

```
  min       :real;
  fname     :string[80];
  temp      :real;
  datafile :text;
begin
  write('Enter filename: ');
  readln(fname);
  writeln;
  assign(datafile,fname);
  reset(datafile);
  write('Enter number of samples: ');
  readln(numsamp);
  for samp:=1 to numsamp do begin
    read(datafile,data[samp]);
    data[samp]:=data[samp];
    data[samp]:=exp((data[samp]/20)*ln(10));
  end;
  close(datafile);
end; {load}


begin
  repeat
    ch:=upcase(menu);
    case ch of
      'E':enter;
      'D': display(numsamp);
      'S': save(numsamp);
      'L': load;
      'B':begin
        meanval:=mean(numsamp);
        std:=stddev(numsamp);
        maxval:=getmax(numsamp);
        minval:=getmin(numsamp);
        writeln('mean: ',meanval:15:5);
        writeln('standard deviation: ',std:15:5);
        writeln('maximum sig. stren.: ',maxval:15:5);
        writeln('minimum sig. stren.: ',minval:15:5);
        writeln;
      end;
    end;
  until ch='Q';
end.
```

```
program dbmedian;
{This program reads data stored in file by program calib}
{and calculates the median in a small sector and stores }
{it into another array to be transferred to multics for }
{use with Minitab for plotting and for regression       }

const
  maxnumsamp=1000; {max num samps read from data file   }
type
  dataarray = array [1..maxnumsamp] of integer;
  medarray = array [1..400] of real;
var
  data      :dataarray;
  median    :medarray;
  nsect     :integer;
  nsamp     :integer;
  samp      :integer;
  sect      :integer;
  fname     :string[80];
  ipfile    :text;
  opfile    :text;


procedure bubble_sort (n:integer; var data:dataarray;
                       var median:real);
var
  temp  :integer;
  i     :integer;
  j     :integer;
  p     :integer;
begin
  for i:=2 to n do begin
    for j:=1 to i-1 do begin
      if(data[j] > data[i])then begin
        temp:=data[i];
        data[i]:=data[j];
        data[j]:=temp;
      end;
    end;
  end;
  p:=n div 2 + 1;
  if(n mod 2 = 0)then
    median:=(data[p]+data[p-1])/2
  else
    median:=data[p];
end;


begin
  write('Enter filename: ');
  readln(fname);
  writeln;
  assign(ipfile,fname);
  reset(ipfile);
```

```
write('Enter number of samples in each sector: ');
readln(nsamp);
writeln;
write('Enter number of sectors: ');
readln(nsect);
for sect:=1 to nsect do begin
  for samp:=1 to nsamp do
    read(ipfile,data[samp]);
  bubble_sort(nsamp,data,median[sect]);
  writeln;
  writeln('Here is the sorted list:');
  writeln;
  for samp:=1 to nsamp do
    write(data[samp]:10);
  writeln;
  writeln('The median is ',median[sect]:5:1);
 end;
 close(ipfile);
 write('Enter filename: ');
 readln(fname);
 writeln;
 assign(opfile,fname);
 rewrite(opfile);
 for sect:=1 to nsect do
   writeln(opfile,median[sect]:5:2);
 close(opfile);
end.
```

APPENDIX B

FSK MODEM

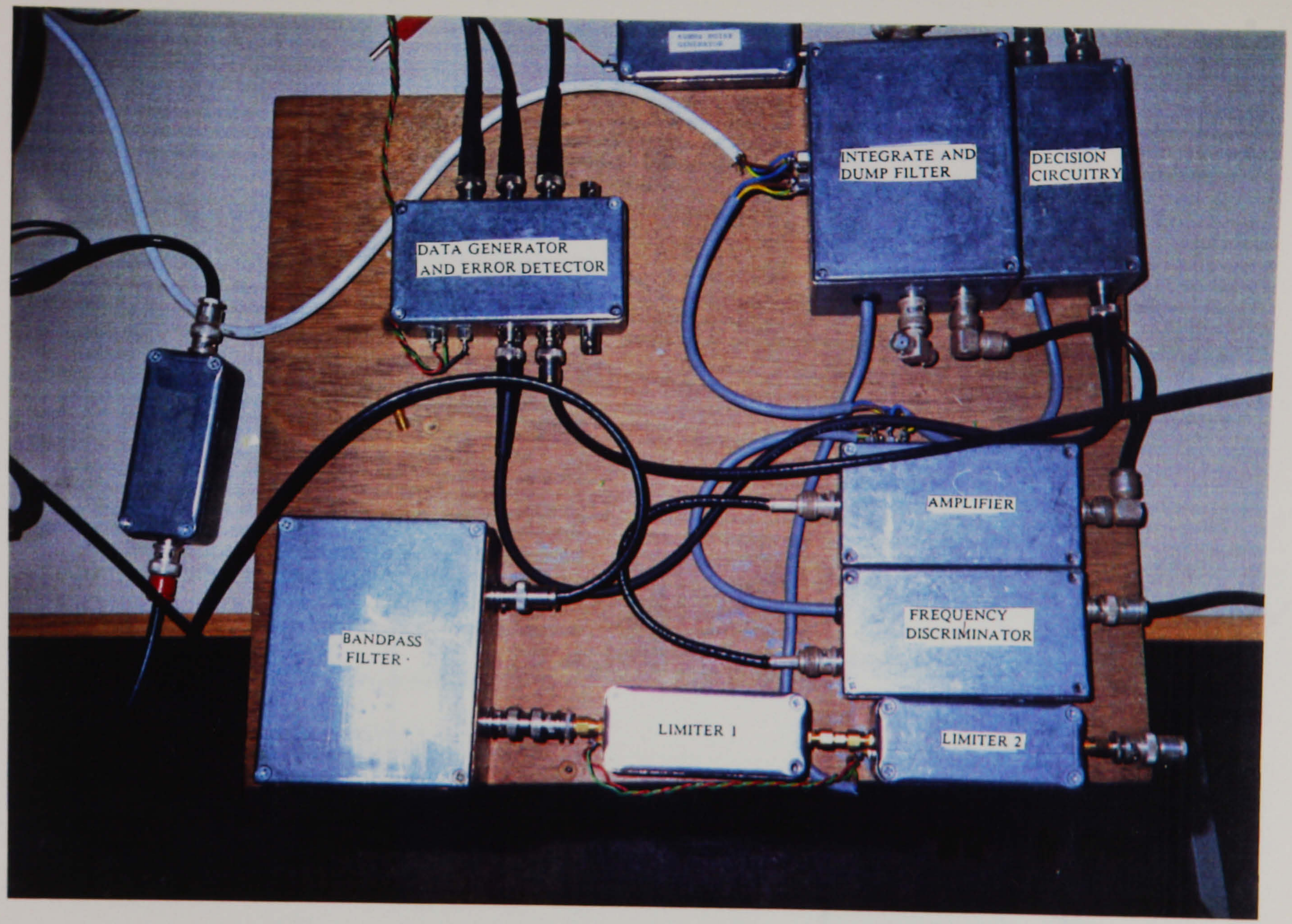

PHOTOGRAPH OF THE FSK MODEM

I

BANDPASS FILTER

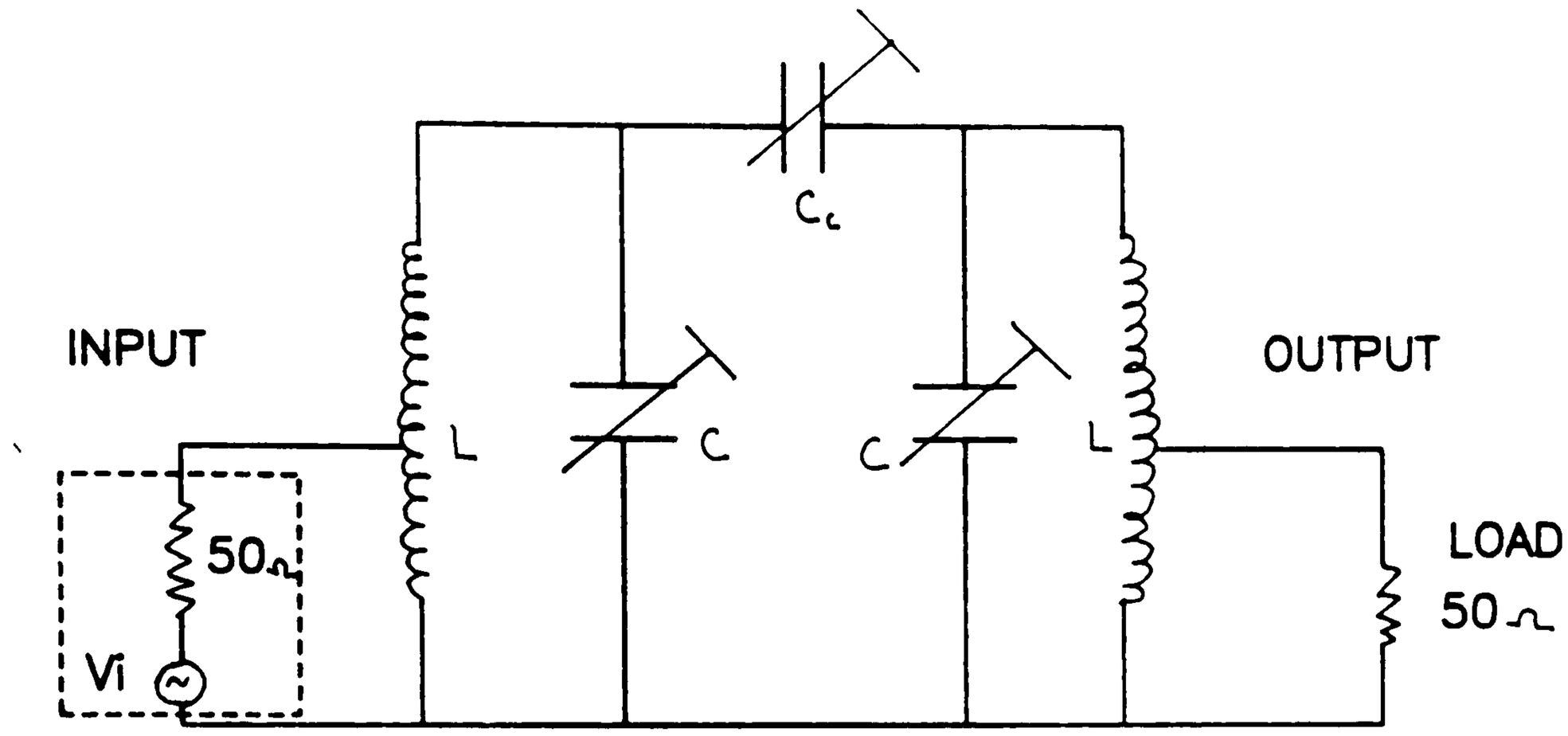

SIGNAL SOURCE

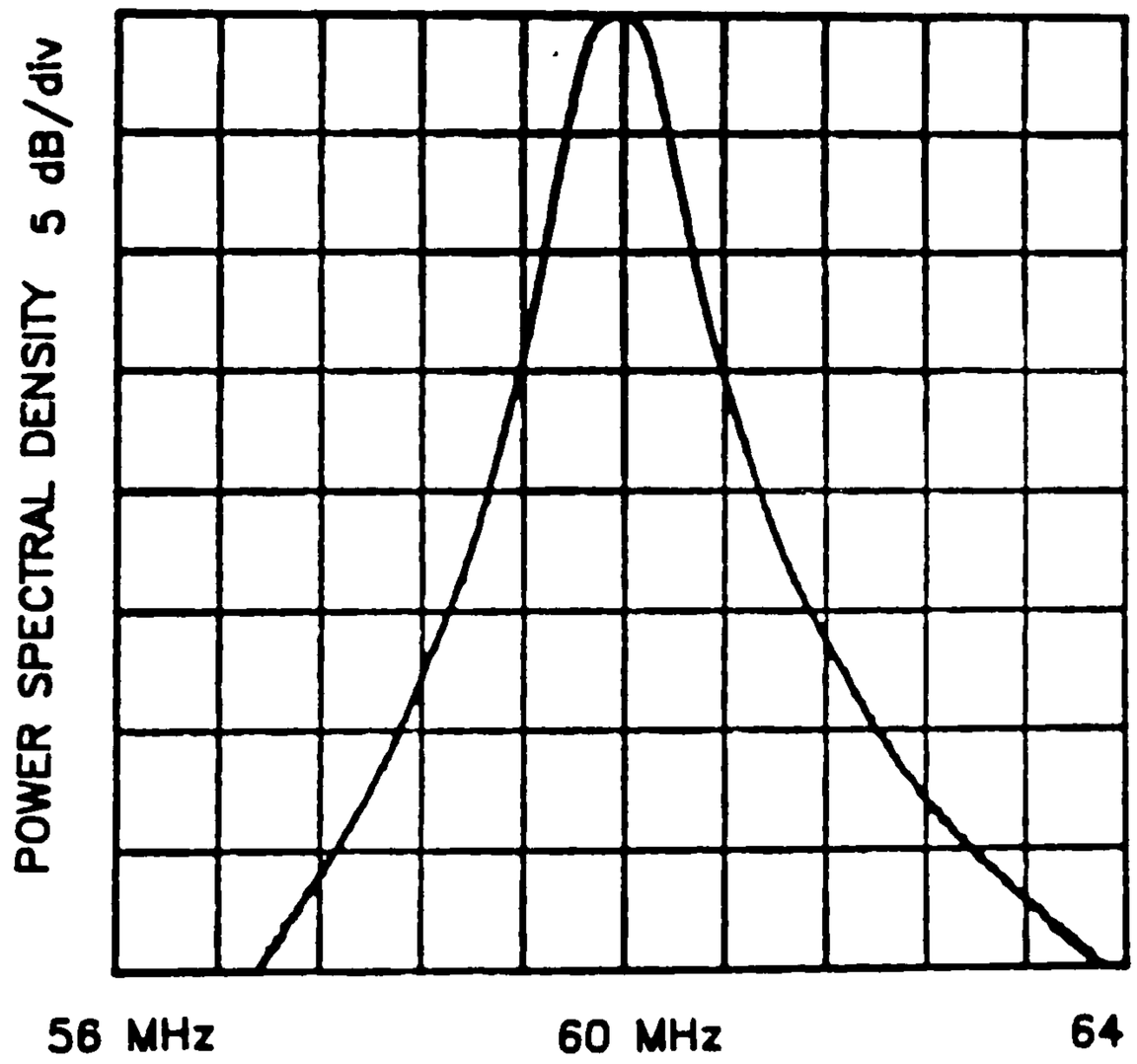

FREQUENCY

FREQUENCY RESPONSE OF THE BANDPASS FILTER CENTRE AT 60MHz
WITH NOISE BANDWIDTH OF 752KHz

II

LIMITER AND DISCRIMINATOR

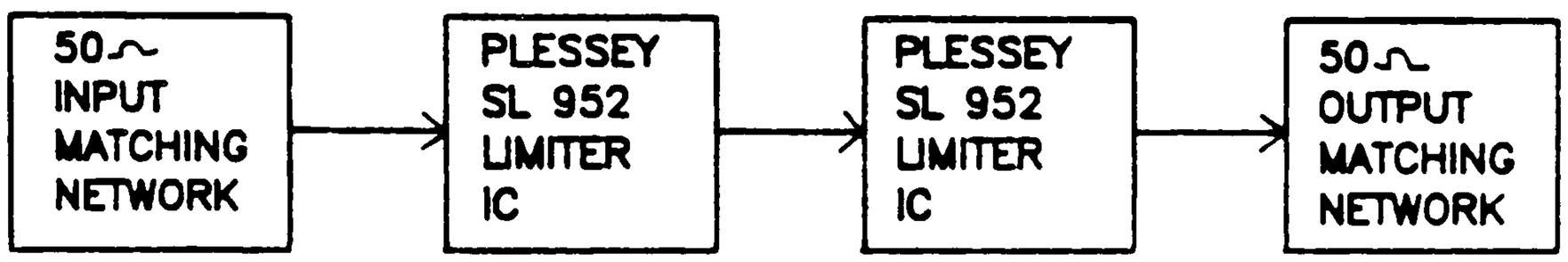

LIMITER

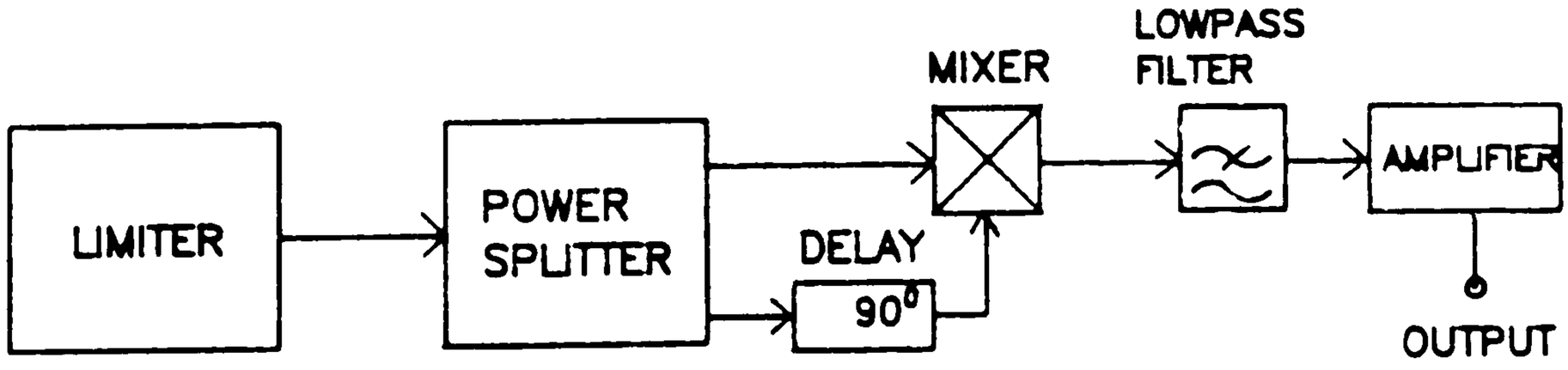

60MHz DELAY LINE DISCRIMINATOR

III

INTEGRATE AND DUMP AND DECISION CIRCUITRY

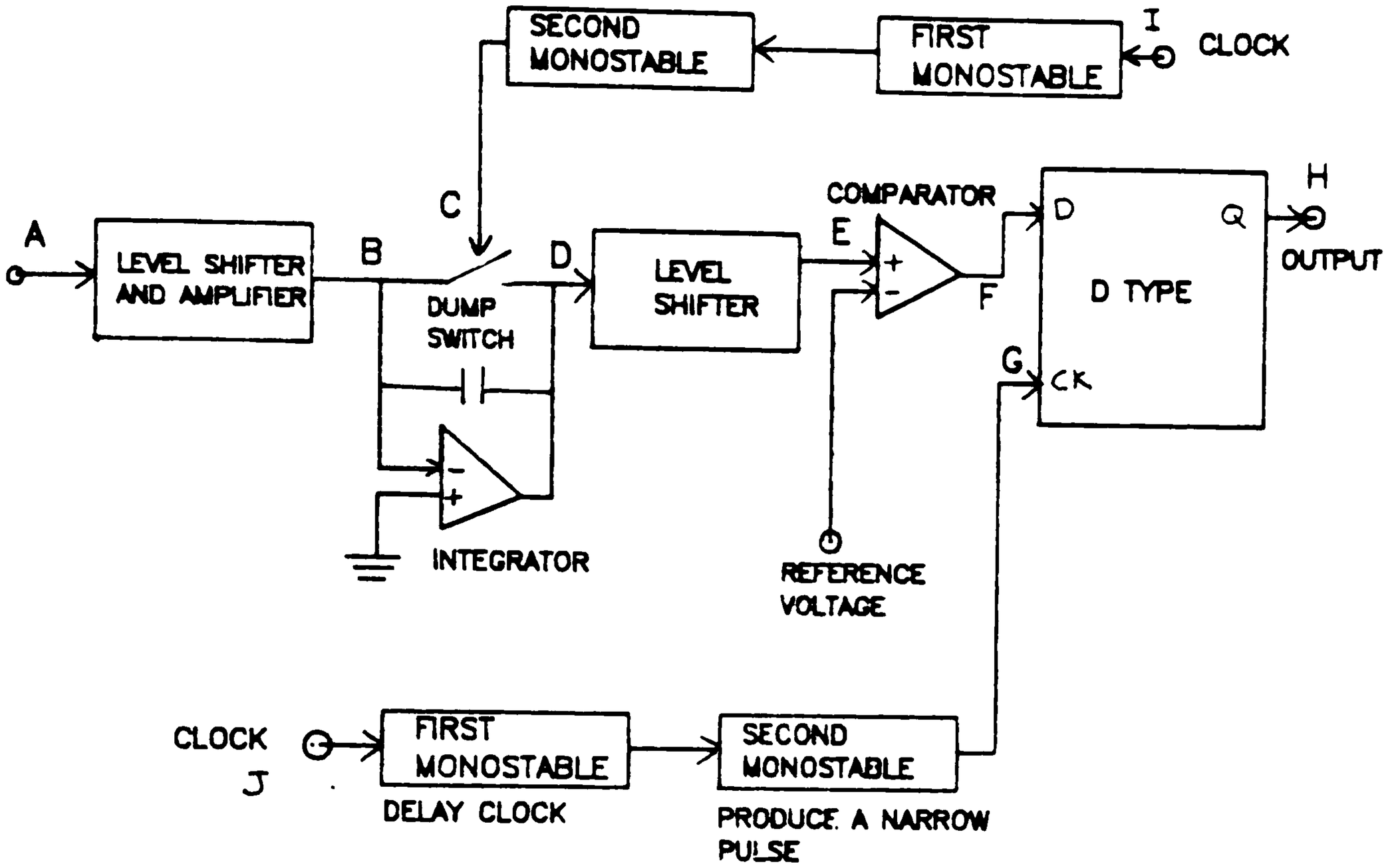

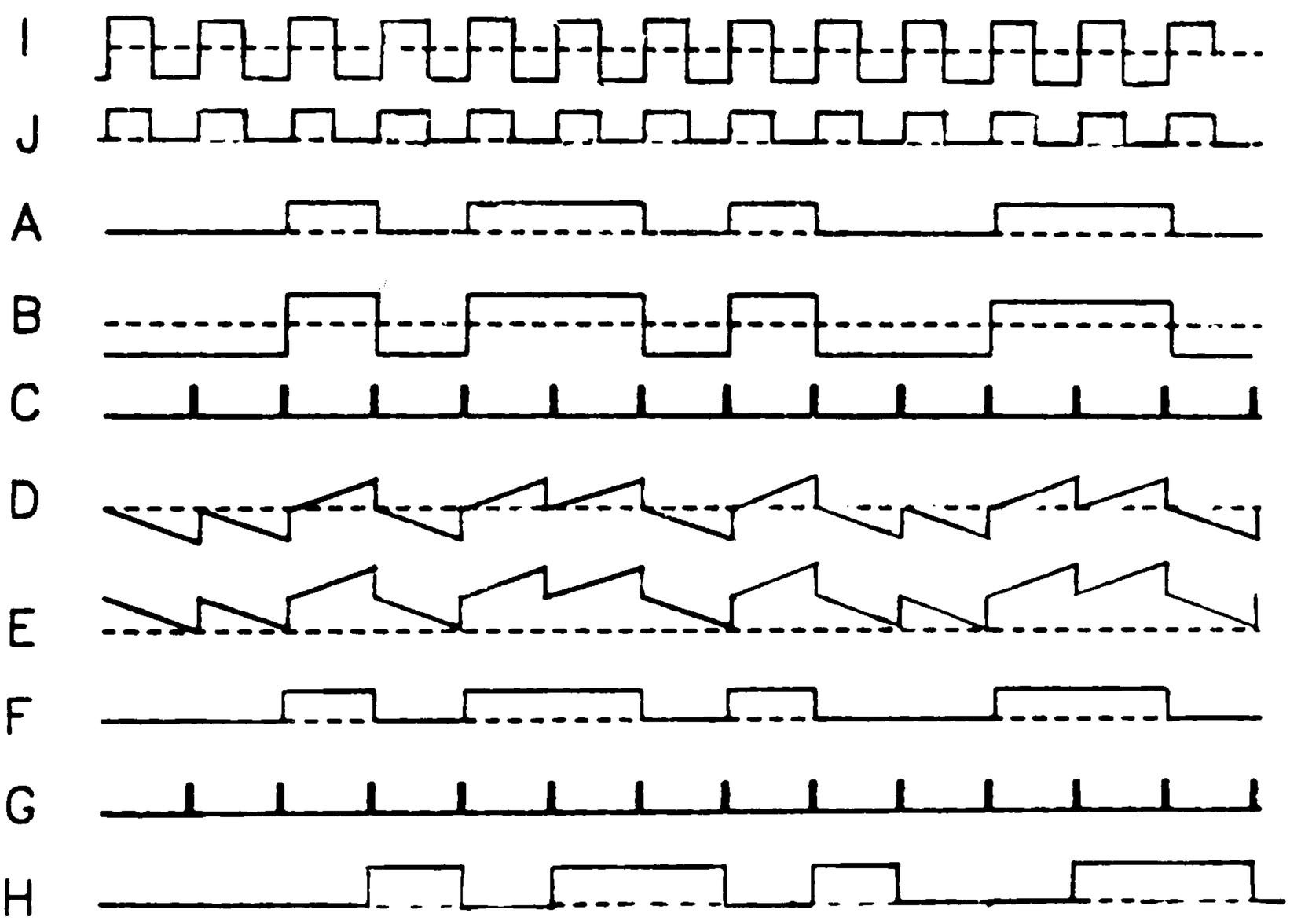

TIMING DIAGRAM OF INTEGRATE AND DUMP FILTER AND DECISION CIRCUITRY

IV

DATA GENERATOR AND ERROR DETECTOR

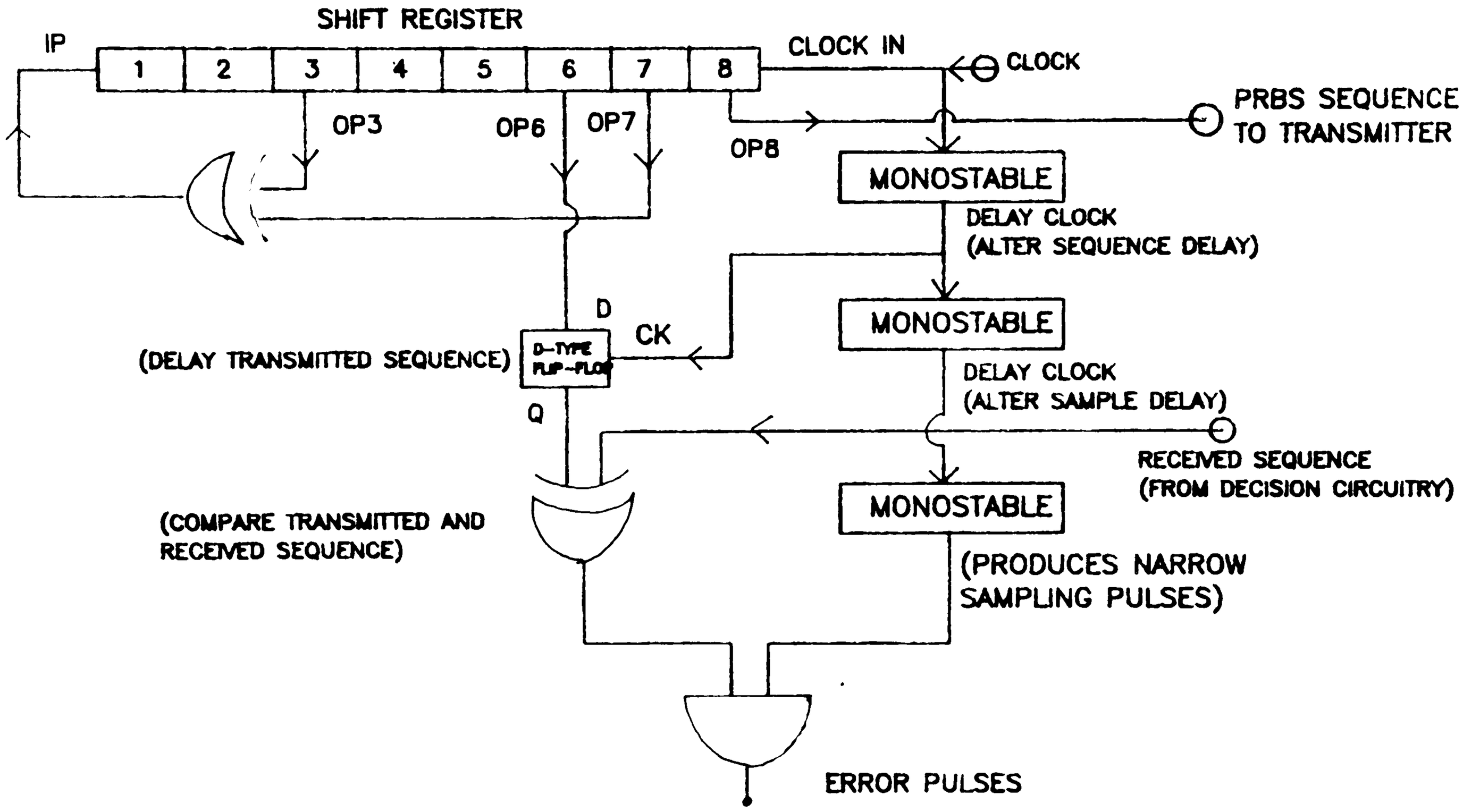

APPENDIX C

NORMALISATION OF SNR FOR BER MEASUREMENTS

Noise Density measured on a spectrum analyser = -125.85dBm in 1Hz

= Actual Noise Density + Analyser Noise Density.

Analyser Noise Density (measured with no input to the spectrum analyser)

= -139.39 dBm in 1Hz.

Actual Noise Density = $10\log_{10}\{10^{-(125.85/10)} - 10^{-(139.39/10)}\}$

= -126.05 dBm in 1Hz.

Actual Noise Density when taking the cable loss (0.48dB) into consideration

= -126.05 + 0.48

= -125.57dBm in 1Hz

$$\text{Normalised SNR} = \frac{\text{Signal Power}}{\text{Noise Power in 1Hz x Bit Rate}}$$

In dB's,

Normalised SNR = $10\log_{10}$(Signal Power) - $10\log_{10}$(Noise Power in Hz)

- $10\log_{10}$(bit rate)

= Signal Power(dBm) + 125.57 - $10\log_{10}$(bit rate)

APPENDIX D

PUBLISHED PAPERS

This paper is included at the end of this section.

Tharek, A.R., and McGeehan, J.P., "Propagation and Bit Error Rate Measurements within Buildings in the Millimetre Wave Band about 60GHz," 8th European Conf. on Electrotechnics, EUROCON 88, Stockholm, June 13-17, 1988, pp.318-321.

Also published by the author

1. Tharek. A.R., Kanso, A. and McGeehan, J.P., "Propagation measurements for 60GHz mobile radio," IEE Colloquium on Millimetre Wave Propagation, Digest No. 1986/17, January 1986.

2. Tharek, A.R., Kanso, A., McGeehan, J.P., "Initial propagation measurements for 60GHz microcellular mobile radio systems," Fourth International Conference on Radio Receivers and Associated Systems, Bangor, July 1986.

3. Tharek, A.R., and McGeehan, J.P., "Indoor Propagation and Bit Error Rate Measurements at 60GHz using Phase-Locked Oscillators," Vehicular Technology Conf. VTC - 88, Philadelphia, June 15 - 17, 1988.

4. Tharek, A.R., Mceehan, J.P., "Outdoor Propagation Measurements in the Millimetre Wave Band at 60GHz," Military Microwaves Conf., MM 88, London, July 5 - 7, 1988.

PROPAGATION AND BIT ERROR RATE MEASUREMENTS WITHIN BUILDINGS IN THE MILLIMETRE WAVE BAND ABOUT 60 GHz.

A.R. Tharek and J.P. McGeehan
Communication Research Group
Department of Electrical Engineering
University of Bristol
Bristol BS8 ITR

INTRODUCTION

Given the significant congestion in the mobile radio frequency bands below 1 GHz, there is currently significant interest in the millimetric waveband around 60 GHz for providing integrated personal communications and a wide range of digital services to mobile users and data terminals. Furthermore, with recent advances in GaAs technology, the use of 60GHz in broadband short-range point-to-point links is also the subject of much investigation at the moment. The work presented here is concerned with propagation and bit error rate measurements conducted within buildings using phase-locked oscillators at 60 GHz.

EQUIPMENT AND EXPERIMENTAL PROCEDURE.

The measurements were made with a 59.9GHz, 50mW phase-locked oscillator in the transmitter, and a 58.9GHz, 10mW phase-locked oscillator as the receiver local oscillator. Two omnidirectional 60GHz aerials were used for the measurements which had gains of approximately 7 dB, elevation beamwidths of about 20^0 and which were circularly polarised. These aerials were used for most of the propagation and BER measurements. For the edge diffraction measurements, a standard 20 dB gain horn aerial with a beamwidth of 18^0 was used for the receiver, and a high directivity horn-lens aerial was used for the transmitter. The horn-lens aerial had a gain of 37 dB, a beamwidth of 2.4^0, and sidelobes whose amplitudes were more than 27 dB below the main lobe. This type of aerial was used because the measurements had to be free of any significant reflected components.

The measurements were conducted within the Queen's Building of the University of Bristol, a substantial three storey brick and reinforced concrete building. For the majority of the measurements, the transmitter and the receiver were positioned 1.5 m above the floor. For the envelope distribution measurements, the signal coverage measurements and the BER measurements in fading, the transmitter was scanned over a small area to collect the data as detailed in reference [1]. Within the scanned locations, the mean signal strength was approximately constant so that the mean or median signal power, or the envelope distribution could be accurately determined.

ENVELOPE DISTRIBUTION MEASUREMENTS

Line-of-sight (LOS) and non-LOS measurements were made with the receiver stationary and the transmitter randomly moved in a horizontal plane. Figures 1 and 2 are graphs of the received signal power against time for both these cases, which illustrate the nature of the fast fading experienced within buildings. Figure 3 shows the cumulative distribution function (CDF) of the received signal envelope for both LOS and non-LOS conditions and also the theoretical Rayleigh CDF. When there was a LOS path between the transmitter and receiver, the envelope distribution significantly departed from the Rayleigh distribution and tended to follow a Rician distribution. It is interesting to note that when there was no LOS path, the distribution was approximately Rayleigh. The LOS result was as expected, since the signal was received via many reflections off nearby objects such as walls, furniture, ceiling and floor, and with no direct component, the envelope distribution should follow the Rayleigh distribution [2]. When a LOS path does exist, the signal so received is likely to be much stronger than the signal received via the reflected paths, so the distribution should depart from the Rayleigh distribution and become a Rician distribution [3].

When both the transmitter and receiver are stationary, the signal reaching the receiver is randomly affected by people or objects moving in the area. The results have shown that when a LOS path existed, the envelope distribution when a person was moving behind and in front of the receiver at a distance of 0.25m did not obey the Rayleigh distribution. However, when there was no LOS path the envelope distribution exhibited a near Rayleigh distribution as shown in figure 4.

MEDIAN RECEIVED SIGNAL POWER AGAINST DISTANCE DEPENDENCY MEASUREMENTS

These measurements were conducted under LOS conditions with the receiver stationary and the transmitter on a trolley pushed at a constant speed so that the time to distance conversion was linear. The received signal power was averaged over approximately 40 wavelengths. This distance was long enough to filter out most of the short term variations (fast fading), but short enough so that it did not significantly affect the variations in the median level [4]. In order to determine the propagation exponent, a straight line curve fit was performed on the median received signal power.

Different environments within buildings have different influences on the received signal power. Four areas have been examined: two types of corridor, a Laboratory, and an office. Details of these measurement areas and their influence on signal propagation are given below.

The first corridor was narrow with dimensions 18m x 1.8m x 2.7m (length x width x height) and had metal lockers along one side. The second corridor was wider with dimensions 18m x 3m x 2.5m (length x width x height) and had glass panelling on both sides. Both had 30cm thick plaster covered concrete walls and the floors were covered with varnished cork tiles. The median received signal power for the corridors decreased with distance as $1/d^{1.32}$ and $1/d^{1.20}$ respectively. The propagation laws for both corridors were therefore very similar, and the signal power fell more slowly than it would in free space. Theoretically, a $1/d^2$ law occurs in free-space, and this has been confirmed outdoors over short distances when reflections were minimised. The slow fall-off in signal power in the corridors was probably due to the smooth parallel walls, floor and ceiling which produced strong specular reflections which channelled the power to the receiver.

The laboratory was a 24m x 5.5m x 3.75m (length x width x height) room with 30cm thick plaster covered concrete walls and a floor covered with varnished cork tiles. There were many chairs and wooden benches in the room, and a large amount of electrical equipment. The median signal power decreased as $1/d^{1.71}$, which was a faster fall with distance compared to the

corridors but was still slower than it would be in free-space. Presumably, the channelling effect was still present, but to a smaller degree because the benches and equipment prevented strong specular reflections off the walls, although there could still be strong reflections off the floor and ceiling.

The office was a postgraduate work room, which was 15.5m x 3.5m x 5m (length x width x height) with plaster covered concrete walls and a carpeted floor. There were many desks, chairs and bookshelves in this room. The median signal power decreased as $1/d^{2.17}$, which was faster than the other areas tried and quite close to the $1/d^2$ free-space law. This was probably because the furniture and carpet prevented strong reflections off the walls and the floor. This was confirmed by the envelope fading which was less severe than in the two corridors and the laboratory.

SIGNAL COVERAGE MEASUREMENTS

Measurements have been conducted in an area with many offices separated by metal partitions. The transmitter was carried around the rooms and the signal was received at a fixed point in the middle of the room. The results have shown that, as expected, the 60 GHz signal is effectively screened by the metal partitions. However, when the transmitter and receiver were in the same room, a high signal power was maintained, although with severe multipath effects.

Measurements were also conducted within an area with corridors and rooms having concrete walls and wooden doors. A plan view of the area and the median received signal power at various points is shown in figure 5. The signal power when the transmitter and receiver were in different rooms was generally too small to be usable. There was, however, some leakage through the wooden doors, resulting in a high received signal power near them or when there was a LOS path through them, but it was insufficient to give adequate room to room coupling. This situation was illustrated by three median signal power measurements which were made at transmitter-receiver separation distances of about 11m. The first was a LOS measurement, the second was blocked by a 4cm thick wooden door made of oak, and the third was blocked by a 40cm thick plaster covered concrete wall. The losses relative to the LOS path were 7 dB for the path through the wooden door and 27 dB for the path through the concrete wall.

Median signal power measurements have been made with the receiver placed at ceiling height in the middle of a large room. The results have indicated that the signal power was at its lowest behind obstructions but was generally higher here compared to when the receiver was 1.5m above the floor. The signal could cover the whole room even though there was no LOS path between the transmitter and receiver at certain locations. It therefore seems that a suitable position for the radio ports is at ceiling height in the middle of the room.

RECEIVED POWER SPECTRUM MEASUREMENTS.

Measurements were also conducted to determine the spectrum of the received signal by down-converting the 1 GHz IF to an IF about 3kHz, and monitoring the spectrum on a digital spectrum analyser. This signal was centred on the analyser when there was no movement between the fixed transmitter and receiver. When the transmitter was moved away from the receiver at a constant speed of about 1 m/s, the IF shifted upwards by about 200 Hz, as shown in figure 6. Theoretically, for a mobile moving at a speed of about 1 m/s and a carrier of 60 GHz, the maximum doppler shift, fd, is 200 Hz.

The broad peak shifted by 600Hz (+3fd) could have been due to the signal reflecting back to the transmitter, which then reflected it to the receiver. The broad spectrum between -fd and +fd can be attributed to many reflections arriving from different angles, and therefore having doppler shifts between -fd and +fd.

KNIFE EDGE DIFFRACTION MEASUREMENTS

Knife edge diffraction measurements were made using an aluminium sheet as the knife edge. The experimental results were found to fit the theoretical curve [5] as shown in figure 7.

The loss at a diffracted angle of 11^0 (v=3) was 22 dB above the free-space loss, which is not excessively large. In practice though, obstructions cannot be considered to be knife edges of this form, so diffraction measurements were attempted around a metal covered wall. It was found, however, that even for a small diffraction angle of 3^0, the received signal was dominated by reflected signals. It is therefore likely that the diffraction around most obstructions will be small, and that reflections must be relied upon. Diffraction measurements outdoors are covered in another publication.[6]

BIT ERROR RATE (BER) MEASUREMENTS.

BER measurements were conducted for FSK modulation at 240 kbits/sec and 480 kbits/sec in both LOS and non-LOS conditions while moving the transmitter randomly in a horizontal plane in order to produce fading. The received signal envelope was recorded and analysed to obtain the mean signal power and the envelope distribution. The output noise power density was measured and the normalised SNR was calculated as the ratio of the average signal power to the noise power in a bandwidth equal to the bit rate. The SNR was varied by reducing the transmitted power with a variable attenuator. The results are shown in figure 8, where the BER varies as a function of the average, normalised SNR.

It is interesting to note that for non-LOS conditions, where the envelope was found to obey the Rayleigh distribution, the experimental curve for the probability of error was very close to the theoretical curve. Under Rayleigh fading conditions, in order to maintain an error rate of 1 in 10^3, an increase of 18 dB in the SNR was required compared with the required SNR in the absence of fading. However, when there was a LOS path between the transmitter and receiver, an error rate of 1 in 10^3 required an increase of about 13 dB in average SNR compared to that in the absence of fading.

Fig. 8 also shows that for the conditions of the experiments conducted in our laboratory, no irreducible error rate occurred for either bit rate under LOS and non-LOS propagation. This implies that the time delay spread was much less than the bit duration of the transmitted data and also that the random FM due to doppler shifts was much smaller than the FM of the FSK signal.

DISCUSSION AND CONCLUSIONS

This paper has presented the measured data for indoor 60GHz propagation characteristics and FSK BER measurements.

Generally, the non-LOS case causes the greatest difficulties since the median received signal power is at its lowest, the fast fading is more severe (Rayleigh) compared to that for LOS conditions (Rician), and the BER is at its highest. Attaching the radio transmitter near the middle of the ceiling can be expected to

improve the signal strength behind obstructions. An aerial which directs the radiation downwards and sideways would probably improve the signal strength even further.

The screening effect of concrete walls means that one radio transmitter would be required per room. The low attenuation of wooden doors suggests that if the walls are made of chipboard, the signal would perhaps cover several rooms.

Doppler spreading is small indoors compared to the transmitted signal bandwidth of FSK, so its effects are likely to be small. This is confirmed by lack of an irreducible error rate with the BER measurements. The results have also indicated that a relatively low attenuation of signal strength occurs with knife edge diffraction. However, practically occurring diffractors (obstacles) do not have knife edges, and the received signal power due to diffraction is generally small compared to that due to reflections.

Since no irreducible error rate occurred in the BER measurements at 480 kbits/sec, it is possible that a higher bit rate could be used without problems of intersymbol interference caused by time delay spread. However, in other areas, the time delay spread may be higher, so a lower bit rate would have to be used.

Acknowledgement

One of the authors (A.R. Tharek) would like to thank the University of Technology Malaysia and the Malaysian Government for their financial support.

REFERENCES

1. Cox, D.C., Murray, R.R., and Norris, A.W. " 800 MHz measurements in and around suburban houses," Bell Labs. Tech. J. pp 921-950, July-Aug, 1093

2. Clarke, R.H. "A statistical theory of mobile radio reception" Bell Sys. Tech. J. Vol 47, pp 957-1000, July 1968.

3. Rice, C.O., "Statistical properties of a sinewave plus random noise", Bell Sys. Tech J., Vol 27 pp 109-157, Jan. 1948.

4. Lee, W.C., "Estimate of local average power of mobile radio signal" IEEE Trans. on Vehicular Technology, Vol. VT-34, No. 1, February 1985.

5. Rokkos, N. Johnson, R. A. "Diffraction of millimeter wave communication signals into shadow region" CORADCOM-81-1, U.S. Army Communication Research and Developement Command, Fort Mormouth, NJ 07703 (1981)

6. Tharek, A.R., Kanso, A. and McGeehan, J.P., " Initial propagation measurements for 60GHz microcellular mobile radio systems" Forth International Conference on Radio Receivers and Associated Systems, Bangor, July 1986.

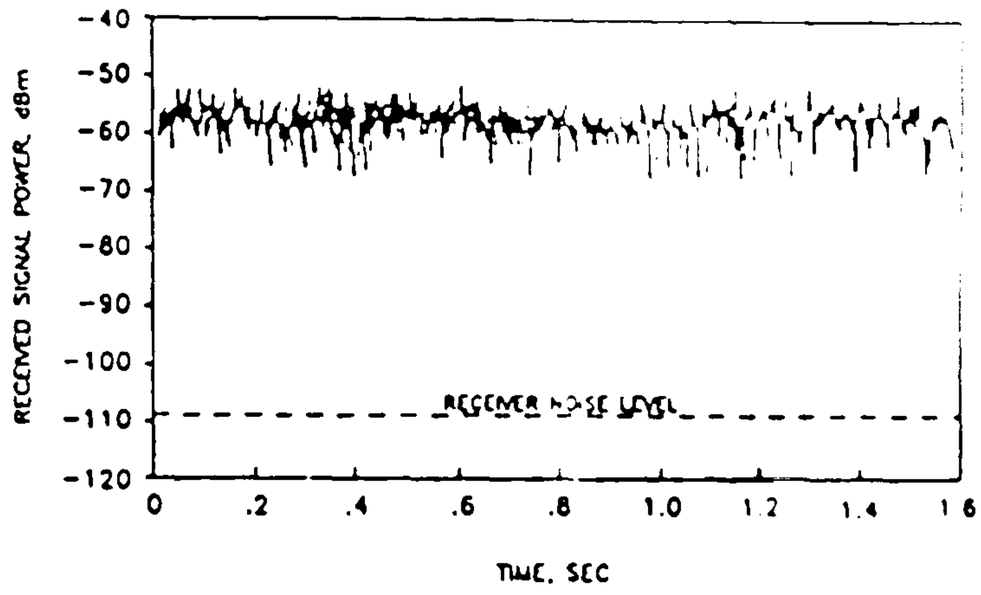

FIG. 1 RECEIVED SIGNAL POWER WHEN THERE WAS A LOS PATH BETWEEN TRANSMITTER AND RECEIVER FOR RANDOM SCANNING OF THE TRANSMITTER AT ABOUT 0.8m/sec

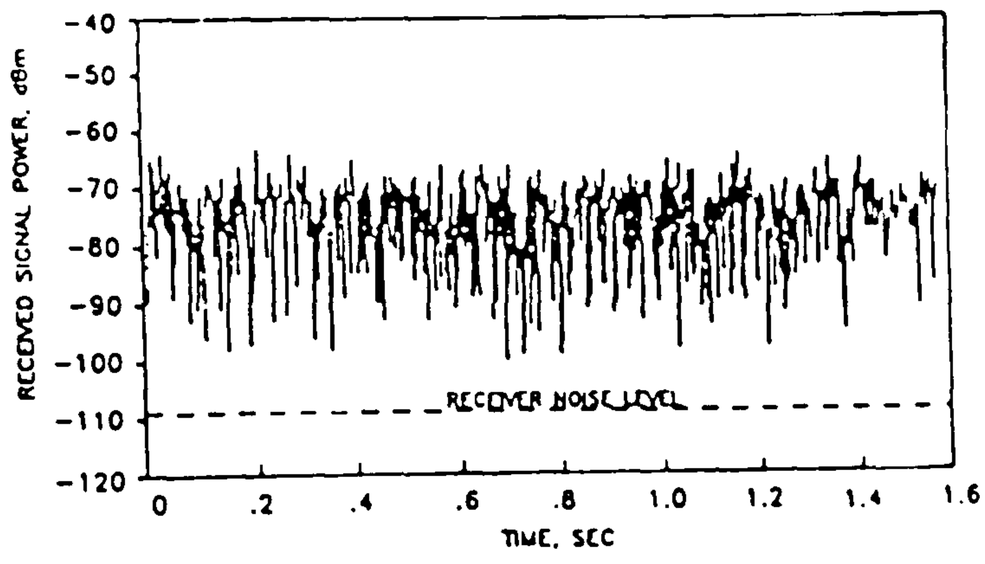

FIG. 2 RECEIVED SIGNAL POWER WHEN THERE WAS NO LOS PATH BETWEEN TRANSMITTER AND RECEIVER FOR RANDOM SCANNING OF THE TRANSMITTER AT ABOUT 0.8m/sec.

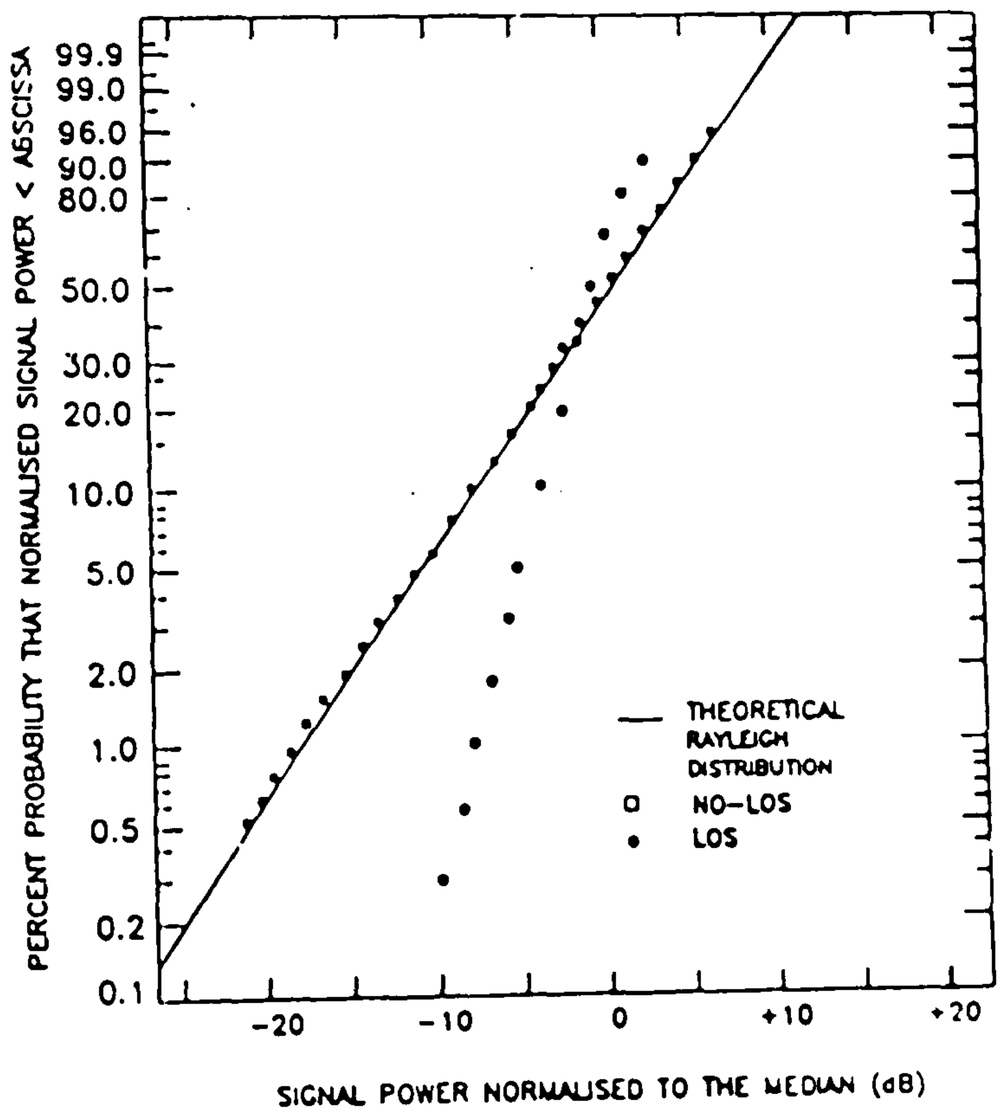

FIG. 3 CDF OF THE RECEIVED SIGNAL POWER FOR LOS AND NON-LOS CONDITIONS WITH THE TRANSMITTER MOVING.

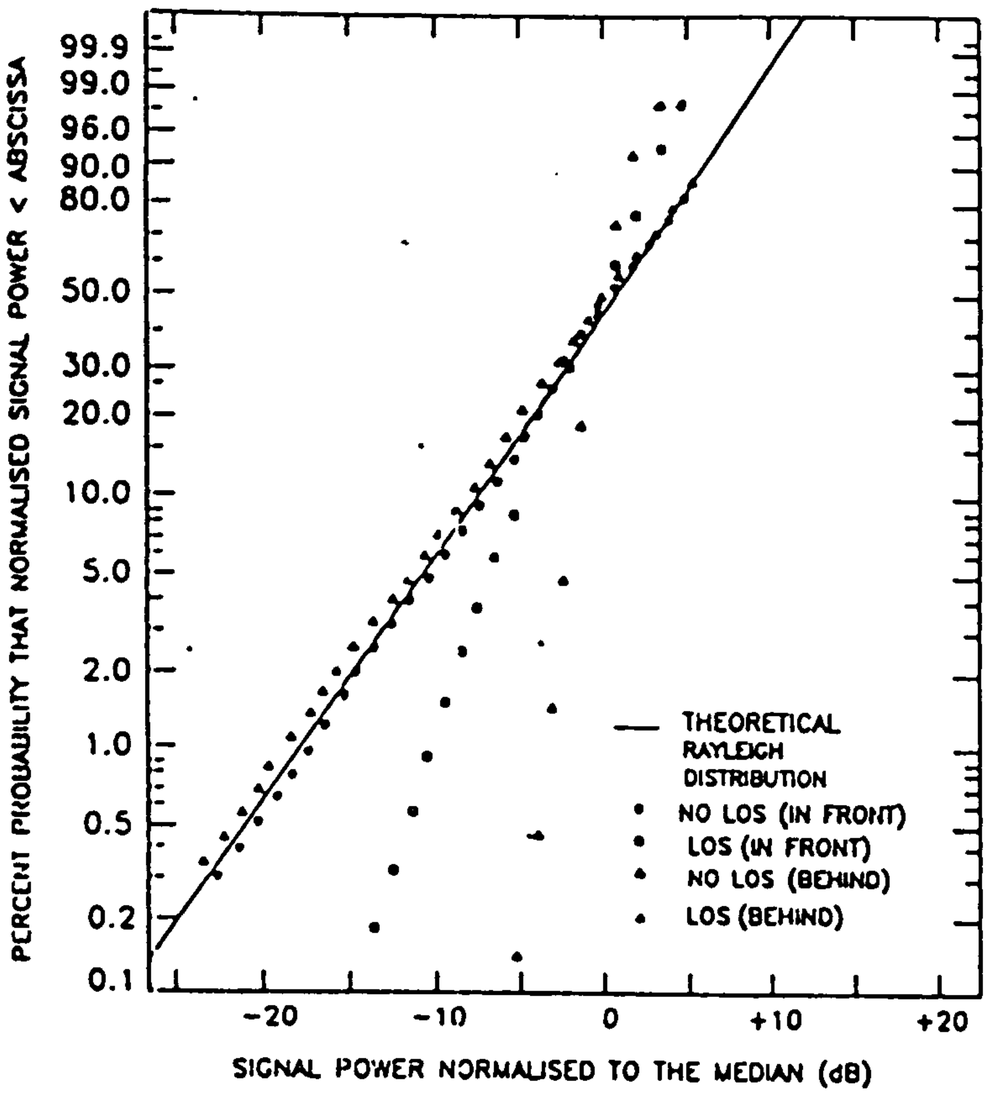

FIG. 4 CDF OF THE RECEIVED SIGNAL POWER FOR LOS AND NON-LOS CONDITIONS WITH A PERSON MOVING IN FRONT OF AND BEHIND THE RECEIVER

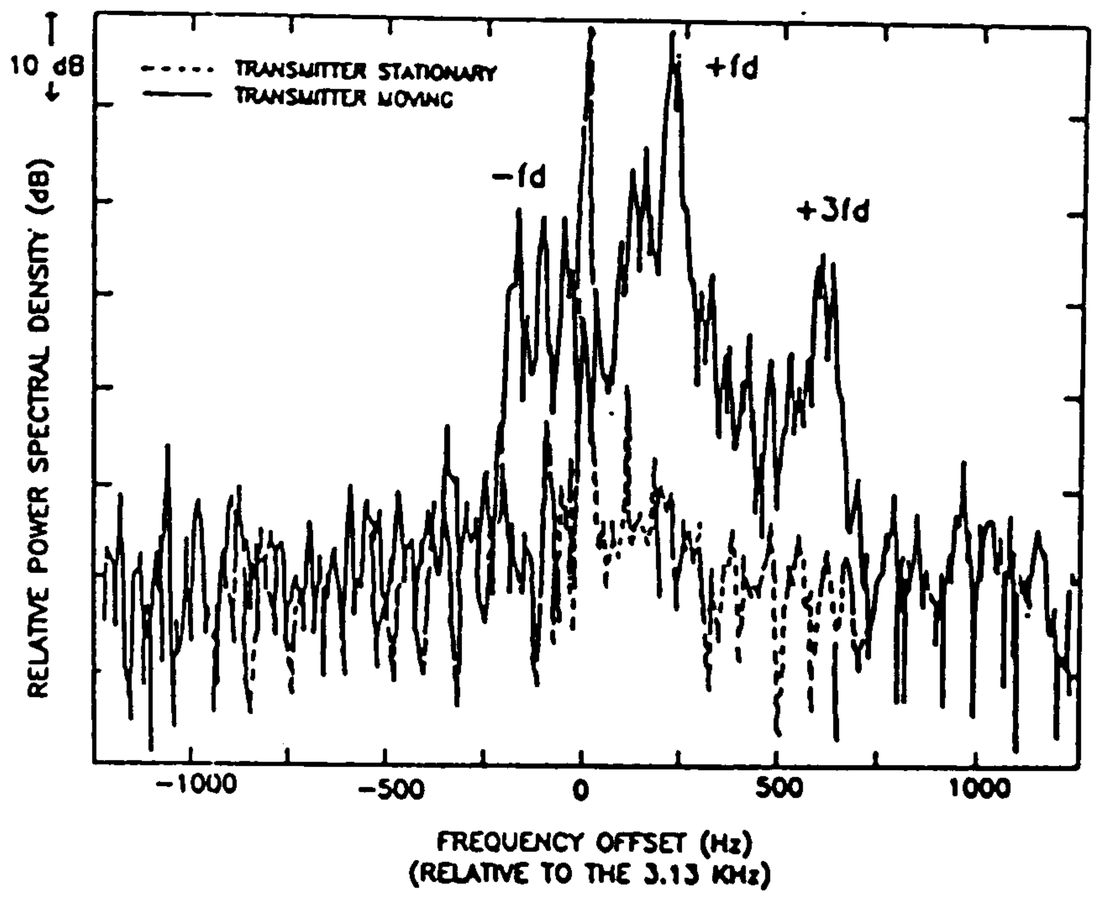

FIG. 6 POWER SPECTRUM OF RECEIVED SIGNAL

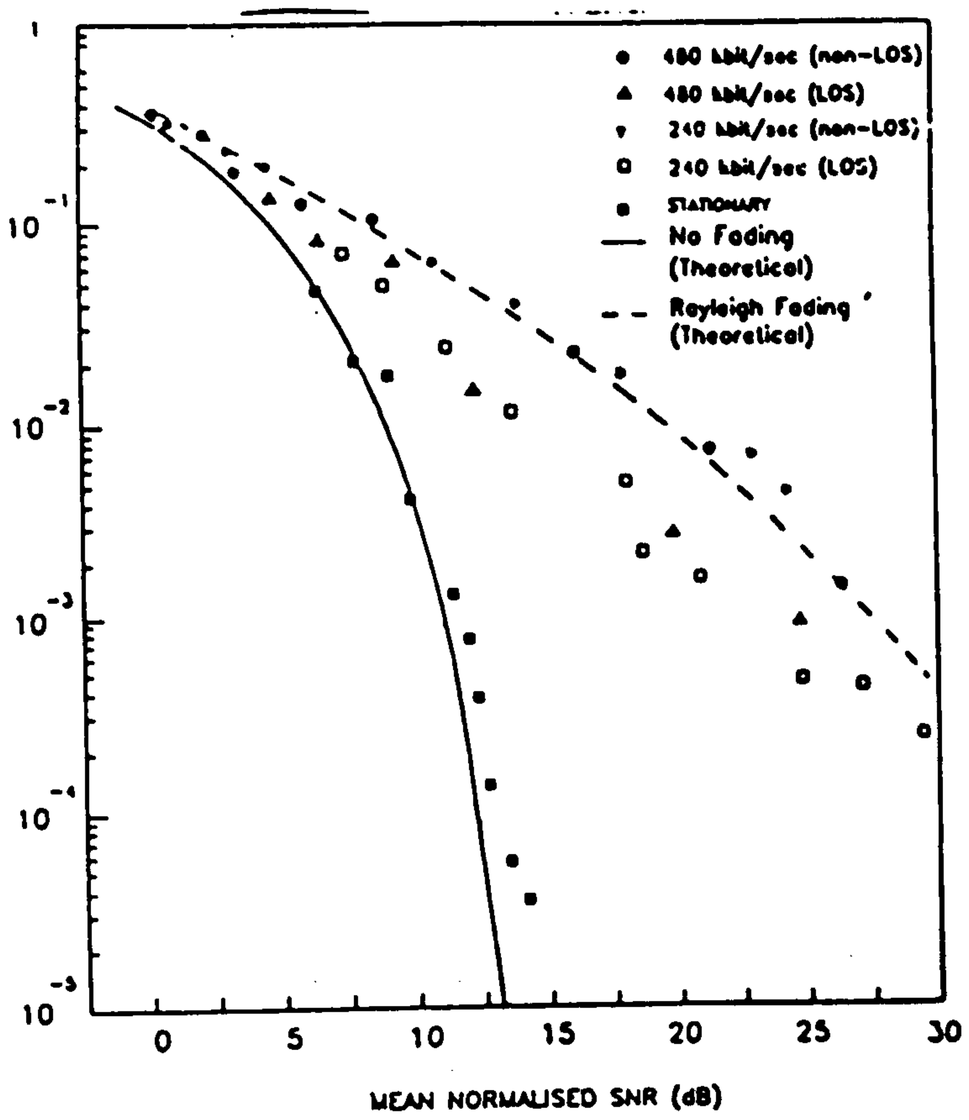

FIG. 8 BER IN FADING AND NON-FADING CONDITIONS FOR NON-COHERENT FSK.

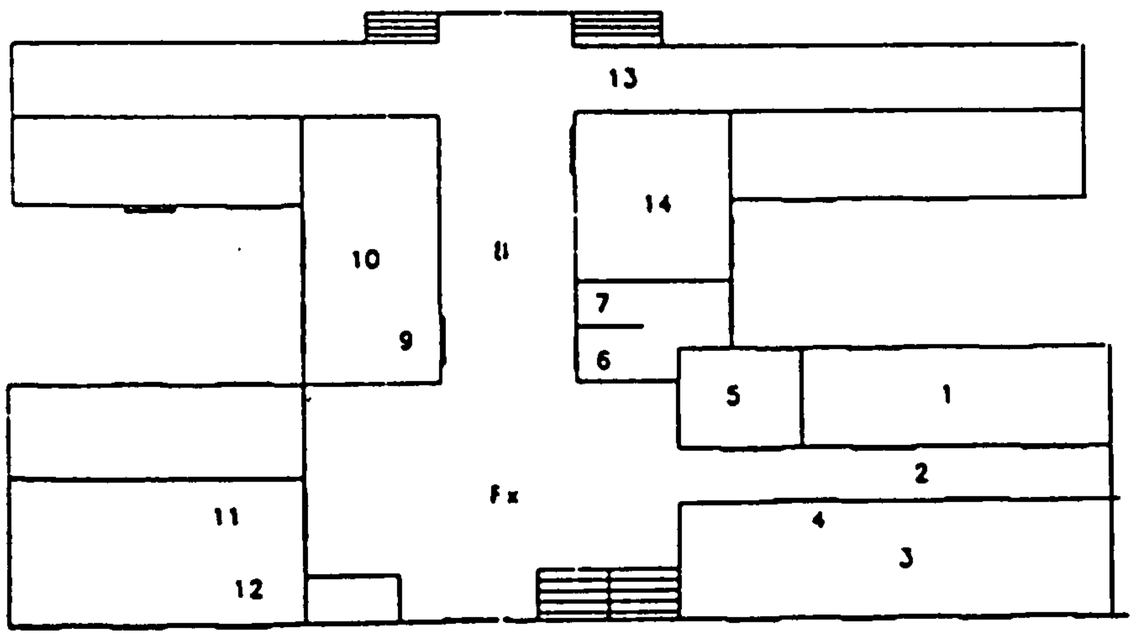

LOCATIONS	MEDIAN SIGNAL POWER, dBm
1	<-109
2	-68
3	<-109
4	-103
5	-91
6	-95
7	<-109
8	-82
9	-94
10	-98
11	-83
12	-85
13	<-109
14	-101

RECEIVER NOISE FLOOR = -109 dBm

FIG. 5 PLAN VIEW OF AN AREA WITH CORRIDORS AND ROOMS AT GROUND FLOOR OF THE BUILDING AND THE MEDIAN RECEIVED SIGNAL POWER AT VARIOUS LOCATIONS.

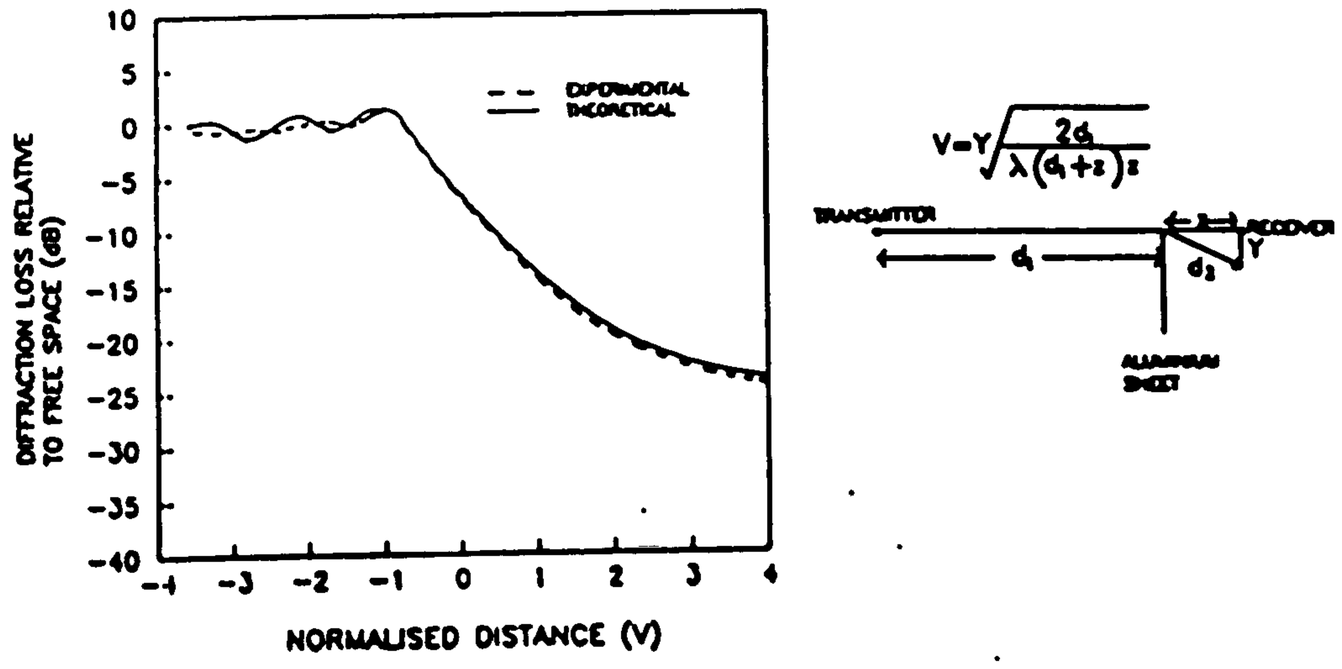

FIG. 7 KNIFE EDGE DIFFRACTION LOSS MEASUREMENTS.